Compacting and aging of powders : influence of the formulation

Shirin Enferad

THÈSE

Pour obtenir le grade de:

DOCTEUR DE L'UNIVERSITÉ DE LORRAINE

Mention: Énergie et Mécanique

École doctorale: SIMPPÉ

Présentée par:

Shirin ENFERAD

Intitulé:

Compactage et vieillissement des poudres: influence de la formulation

Préparé au LEMTA et au LIBio

Thèse soutenu à:

Nancy le 17/12/2020

Devant le jury composé de:

Christelle Turchuili	Maître de Conférences, Paris Saclay	Rapporteur
Blaise Nsom	Professeur, Bretagne Occidentale	Rapporteur
Sergiy Antonyuk	Professeur, TU Kaiserslautern	Examinateur
Geoffroy Lumay	Maître de Conférences, GRASP, Liège	Examinateur
Sébastien Kiesgen de Richter	Maître de Conférences, LEMTA, Nancy	Invité
Mathieu Jenny	Maître de Conférences, LEMTA, Nancy	Directeur de thèse
Claire Gaiani	Professeur, LIBio, Nancy	Co-directeur de thèse

Acknowledgments

This thesis is the result of my study at laboratories of LEMTA and LIBio in université de Lorraine. I would like first to thank Fabrice Lemoine and Pascal Boulet respectively ex-director and current directors of LEMTA for welcoming me to the laboratory. Many thanks for the warm welcoming and the good daily mood of people in LEMTA. I would also like to thanks to our project director in PowderReg project Sébastien Kiesgen de Richter that provided the opportunity of doing research in such a big project and cooperating with many universities and industry in different countries within the framework of project. Thank you for allowing me to discover other researchers in the field of granulars through the PowderReg project meetings, cooperation as well as the numerous conferences that I attended in France and other countries.

I would like to express my greatest appreciation and thanks to my thesis director Mathieu Jenny and co-director Claire Gaiani.

Mathieu, from the beginning of my thesis you gave me the complete autonomy over the management of my thesis. You were always respecting all the aspects relating to my time, my decisions and you were available when I needed to discuss. Your optimism and kindness was always giving me desire to move forward. Also, your attempts in lowering the stress and pressure of work by the sense of humor was really appreciating. Your great scientific qualities, listening skills and calm personality allowed me to grow and learn pleasantly.

Claire, I started the beginning of my thesis in LIBio with you. You were always present and very precise in the work. You were always answering my questions and even were organizing meetings between members of the powder group in LIBio to answer my questions related to my research. Your responsible personality and strong pedagogy are really appreciating. You provided opportunity of extending my skills in cooperation with many researchers as well as working in multi-disciplinary environment starting from LIBio. Many thanks for you both to supervising me during these three years of my PhD study in université de lorraine and for giving me a taste for research as well as supervising master students.

I would also like to thank to Jeremy Petit who helped me a lot in my study at LIBio. He was always positive, energetic and of course always very helpful, THANK YOU Jeremy for every things. I also would express my thanks to Nicolas Louvet from LEMTA. Many thanks to our project partners that welcomed me in their laboratory to perform experiments and cooperate in publishing common: thanks to Véronique Falk and Philippe Marchel from LRGP in France; to Rishab Handa and Jorge Edurado Fiscina from universitat saarlandes in Germany, to Robert Hesse and Sergiy Antonyuk from universität Kaiserslautern in Germany, to Salvatore Pillitteri, Geoffroy Lumay and Nicolas Vandewalle from universite de Liege in Belgium and Finally to Filip Franqui from Granutools in Belgium.

I take the opportunity to thank to our manager in “PowderReg” project Diana Righi to being always helpful, positive and friendly. A special thanks to the secretary of our team Valérie Reichhart for being super kind, always respectful and of course very helpful in organizing all my scientific travels that I did

to our project partner countries and conferences.

I would additionally like to thank to all PhD students and post-docs in LEMTA and LIBio which we shared good moments. Special thanks to my ex-colleague Morgan Sans which it was very nice to share office with him and of course thanks to Justine Noel and Ghita Marouazi which are my current Colleague. Thank you for all your supports.

Many thanks to all my friends which without them these three years of thesis would not have been so easy. I am not going to make a list because I am afraid to forget someone by mistake. I need to truly thank to two friends of mine Narmina Gasimova and Adeline Lambert for all the moments that we shared and for all their supports and helps.

Finally, I would like to express an immeasurable amount of gratitude to my parents and my brothers Ehsan and Erfan for their unconditional and endless love and support throughout my life.

"To My Dear Parents"

Contents

List of figures

List of tables

Abbreviations and Symbols

$\boldsymbol{A}$	Hamaker constant (J) (chapter 2)
	Projected contact area (nm^2) (chapter 3)
	Amplitude of vibration (m) (chapter 4)
$\boldsymbol{A_r}(nm^2)$	Residual sample area
$\boldsymbol{a}(m)$	Distance between particles
$\boldsymbol{C}(g/cm^3)$	Flow index (chapter 4 and 5)
$\boldsymbol{c}(Pa)$	Cohesion
$\boldsymbol{D}(m)$	Diameter of GranuCharge tube
$\boldsymbol{D_{10}}(\mu m)$	Diameters for which 10% of the volume of particle population has a lower size
$\boldsymbol{D_{50}}(\mu m)$	Median particle size
$\boldsymbol{D_{90}}(\mu m)$	Diameters for which 90% of the volume of particle population has a lower size
$\boldsymbol{d}(mm)$	Diameter of orifice of GranuFlow disc
$\boldsymbol{d_{min}}(mm)$	Minimum diameter of orifice of GranuFlow disc
$\boldsymbol{d_p}(mm)$	Particles diameter
$\boldsymbol{E_r}(GPa)$	Reduced young's modulus
$\boldsymbol{E_s}(GPa)$	Reduced Young's modulus of sample
$\boldsymbol{E_i}(GPa)$	Reduced Young's modulus of indentor
$\boldsymbol{E_v}(J)$	Mechanical vibration energy
$\boldsymbol{e}$	Euler number
$\boldsymbol{F_{cap}}$ (N)	Capillary force
$\boldsymbol{F_{cap_{max}}}(N)$	Maximum capillary force
$\boldsymbol{F_e}$ (N)	Electrostatic force
$\boldsymbol{F_{Waals}}$ (N)	Van der Waals force
$\boldsymbol{F_G}$ (N)	Gravity force
$\boldsymbol{F_p}$ (N)	Particles weight
$\boldsymbol{F_r}(g/s)$	Flow rate
$\boldsymbol{f_c}$ (Pa)	Maximum stress supported by the powder on a free surface (cohesive stress)
$\boldsymbol{g}(9.81\ m/s^2)$	Earth gravity acceleration
$\boldsymbol{H}$ (GPa)	Hardness
$\boldsymbol{Hr}$	Hausner index (ratio)

$\boldsymbol{h_e}$ (nm)	Displacement associated with elastic recovery during unloading
$\boldsymbol{h_{max}}$ (nm)	Indenter displacement at peak load
$\boldsymbol{h_p}$ (nm)	Depth of residual impression
$\boldsymbol{h_r}$ (nm)	Heap height
$\boldsymbol{K_\sigma}$	Stress calibration constant
$\boldsymbol{K_{\dot{\gamma}}}$	Shear rate calibration constant
$\boldsymbol{L}(m)$	Length
$\boldsymbol{l_{ch}}(m)$	Width of baffle
$\boldsymbol{m}(kg)$	Mass
$\boldsymbol{N}(N)$	Normal force
$\boldsymbol{n}$	Tap Number
$\boldsymbol{P_{max}}(GPa)$	Load at maximum indentation
$\boldsymbol{q_1}, \boldsymbol{q_2}(C)$	Electrostatic charges
$\boldsymbol{q}(nc/g)$	Charge density
$\boldsymbol{R}(m)$	Particle radius
$\boldsymbol{R_c}(m)$	External radius of the measuring cell
$\boldsymbol{R_e}(m)$	External radius of Couette cell
$\boldsymbol{R_i}(m)$	Internal radius of Couette cell
$\boldsymbol{r_1}(m)$	Radius of external bridge curvature
$\boldsymbol{r_2}(m)$	Radius of internal bridge curvature
$\boldsymbol{r}(m)$	Position in the air gap
$\boldsymbol{r^*}(m)$	Position in the air gap for the calculation of the calibration constants
$\boldsymbol{S}(GPa)$	Contact stiffness
$\boldsymbol{T}(N.m)$	Torque
$\boldsymbol{V_{medium}}(m^3)$	Total volume of medium
$\boldsymbol{V_p}(m^3)$	Volume occupied by the particles
$\boldsymbol{V_{pores}}(m^3)$	Volume of the inter-particles void
$\boldsymbol{V_{solid}}(m^3)$	Volume of the particles
$\boldsymbol{V_{tot}}(m^3)$	Total volume
$\boldsymbol{v}(m/s)$	Velocity
$\boldsymbol{v_{out}}$ (m/s)	Speed of the particles
$\boldsymbol{\rho_b}(kg/m^3)$	Apparent density of the granular medium
$\boldsymbol{\rho_p}(kg/m^3)$	Real density of the particles
$\boldsymbol{\rho_p}(kg/m^3)$	Density of the fluid that fills the pores
$\boldsymbol{\pi}$	Mathematical constant
$\boldsymbol{\Delta P}(Pa)$	Pressure difference on both sides of liquid bridges
$\boldsymbol{\gamma}(N/m)$	Surface tension of liquid
$\dot{\boldsymbol{\gamma}}$ (rad/s)	Shear rate

$\boldsymbol{\varepsilon}$	Porosity
$\boldsymbol{\epsilon_0}(8.854\ C^2/m^2N)$	Permittivity of vacuum
$\boldsymbol{\epsilon}$	Strain
$\boldsymbol{\theta}$	Maximum angle of pile
$\dot{\boldsymbol{\theta}}(rad/s)$	Angular velocity (chapter 4)
$\boldsymbol{\alpha}$	Freeze angle of flow
$\lvert\boldsymbol{N}\rvert(N)$	Normal component of the weight of particles
$\lvert\boldsymbol{T}\rvert(N)$	Tangential component of the weight of particles
$\boldsymbol{\mu}$	Coefficient of friction
$\boldsymbol{\mu_S}$	Coefficient of static friction
$\boldsymbol{\varphi}$	Internal angle of static friction
$\boldsymbol{\tau}(Pa)$	Shear stress (chapter 2)
$\boldsymbol{\tau}$	Asymptotic compaction characteristic time (chapter 4 and 5)
$\boldsymbol{\tau_c}(Pa)$	Shear stress at end point of yield locus curve
$\boldsymbol{\tau_s}$ (Pa)	Shear stress at powder bed breaking points
$\boldsymbol{\sigma}(Pa)$	Stress tensor
$\boldsymbol{\sigma_1}(Pa)$	Maximum principal stress
$\boldsymbol{\sigma_c}(Pa)$	Unconfined yield strength at end point of yield locus curve
$\boldsymbol{\sigma_f}$	Cohesive index (Granutools)
$\boldsymbol{\sigma_f}(Pa)$	Frictional stress (Discovrry HR3-rheometer)
$\boldsymbol{\sigma_N}(Pa)$	Normal stress
$\boldsymbol{\sigma_r}$	Static cohesion
$\boldsymbol{\sigma_s}(Pa)$	Unconfined yield strength at powder bed breaking points
$\boldsymbol{\sigma_v}(Pa)$	Mechanical vibration stress
$\boldsymbol{\rho_{bt}}(kg/m^3)$	Powder packed density
$\boldsymbol{\rho_b}(kg/m^3)$	Power bulk density
$\boldsymbol{\rho_t}(kg/m^3)$	True density
$\boldsymbol{\rho_0}(g/ml)$	Initial density
$\boldsymbol{\rho_{500}}(g/ml)$	Density after 500 taps
$\boldsymbol{\rho_s}(kg/m^3)$	Suspension density
$\boldsymbol{\rho_f}(kg/m^3)$	Density of the interstitial fluid
$\boldsymbol{\phi}$	internal friction
$\boldsymbol{\delta}$	Effective angle of friction
$\boldsymbol{ff}$	Flowing factor
$\boldsymbol{\nu}$	Poisson ratio
$\boldsymbol{\nu_s}$	Poisson ratio of sample
$\boldsymbol{\nu_s}$	Poisson ratio of indenter
$\boldsymbol{\beta}$	Free parameter

$\boldsymbol{\Omega}(rad/s)$	Rotating speed of GranuDrum
$\boldsymbol{\alpha_f}$	Rotating angle
$\boldsymbol{\alpha_r}$	Static angle of repose
$\boldsymbol{\Delta Z}(m)$	Displacement
$\boldsymbol{\eta_0}$	Initial packing fraction
$\boldsymbol{\eta_{500}}$	Packing fraction after 500 taps
$\boldsymbol{\eta(n)}$	Packing fraction after n tap
$\boldsymbol{\eta(\infty)}$	Asymptotic volume fraction
$\boldsymbol{\eta}(Pa.s)$	Viscosity
$f(Hz)$	Frequency of vibration
$\boldsymbol{\phi_v}$	Volume fraction of suspension
AE (mJ)	Aerated energy
AR	Aeration ratio
BFE (mJ)	Basic flowability energy
CBD (g/mL)	Conditioned bulk density
DVS	Dynamic water sorption
$\boldsymbol{IC}$	Carr index (ratio)
RH	Relative humidity
SE (mJ/g)	Specific energy
SEM	Scanning electron microscopy

Chapter 1

General introduction

Granular material is one of the most abundant material on the planet. In addition, many industries are dealing with handling and processing these materials. In each industries, they are three major actions called: storage, transport and mixing. Whereby, understanding the behavior of granular material during these actions are of crucial challenges of industries and researchers.

While, understanding the behavior of granular material is very complex, some problems related to the physical and mechanical properties of granular environments are affecting various industrial sectors: pharmaceutical, civil engineering, food,... . For improving the use of granular environments, science looks for solutions to overcome several obstacles that industries face per days. As an example, most production stages can be disrupted drastically by phenomena of flow blockage, consolidation and/or segregation of powders.

These problems are often solved empirically, while the precision and reproducibility of powder processes are crucial in most of these industries (i.e. pharmaceutical, fine chemicals industries,...).

Among these complex phenomena, this thesis will focus on powders flow. Powders flow arouses the fascination of many scientists and researchers. Thus, good powder flowability is essential to ensure the proper functioning of a process along a production line. However, to ensure a good powder flowability, it is first necessary to be able to evaluate this property in relation with the processes used.

Many researchers have tried to establish unified rheological models to predict the behavior of granular materials in flow. However, the complexity of the powder interactions and the variety of granular materials are still a barrier to obtain relevant rheological processes models adapted to the different processes and situations that they face in industries.

Up to date, to assess the flowability of a granular medium, the literature has mainly use experimental techniques.

Among the research teams, the powder research teams in Laboratory of Energies & Mechanics Theoretical and Applied (LEMTA) as well as Laboratory of Biomolecule Engineering (LIBio) have dedicated their activities to studying the behavior of powders and granular materials including the

identification of key factors that may affect the flow of powder media. Based on this goal, in 2017, LEMTA lunched a research in cooperation with the universities of Luxembourg, Saarland, Kaiserslautern and Liege. The study is conducted by LEMTA and it is in the framework of the "PowderReg" project, funded by the European program Interreg VA GR within the priority axis 4 "Strengthen the competitiveness and the attractiveness of the Grande Région / Groβregion". The aims are to better understand and control the flowability of granular media from their manufacture to their transport and storage and to set up an experimental demonstrator to simulate the different situations in which a granular medium faces during the different steps of a process.

In this context, this thesis is focused on the influence of the powder formulation on flowing properties. In addition, the influence of environmental conditions in their bulk behavior were studied. The results obtained from different equipments are evaluated in order to see if all types of granular materials can be characterized with these equipements or not. The manuscript is structured in five chapters as follow:

- The current chapter is an introduction of what has been done in the thesis and scientific valorization of this study has been presented.
- The second chapter provides a literature review about granular medium and powder flowability. Then, it presents the main characteristics of powders as well as factors that can influence the inter-particle interactions. At the final, the different techniques of evaluating flow behavior of powders have been presented.
- The chapter three is devoted to study the influence of different particle size and the powder surface formulation in flow behavior of powders. The flow behavior of powders have been studied with different protocols provided by FT4 rheometer.
- The chapter Four is a study dedicated to compare different measurement techniques on the characterization of the powder bulk behavior. The objective is to figure out the properties which are obtained by the different techniques.
- The chapter five is dedicated to study the influence of humidity on powders flowability.

The results obtained within the framework of this thesis have been the subject of the following publications and communications:

Publications in international journals :

- **S. Enferad**, J. Petit, C. Gaiani, V. Falk, J. Burgain, S. Kiesgen de Richter, M. Jenny, Effect of particle size and formulation on powder rheology, Particulate Science and Technology, (2020) 1-9.
- **S. Enferad**, S. Pillitteri, G. LumaY, C. Gaiani, S. Kiesgen De Richter, M. Marck, S. Umbetov, N. Vandewalle, M. Jenny, Powder flow behaviors governed by the surface properties of particles, submitted.
- **S. Enferad**, S. Pillitteri, G. LumaY, C. Gaiani, S. Kiesgen De Richter, M. Marck, S. Umbetov, N. Vandewalle, M. Jenny, Hydrophobic and raw glass beads flow behavior under different processing dynamics, submitted.

The list of oral communications and poster:

Oral communications

- **S. Enferad**, J. Petit, C. Gaiani, J. Burgain, V. Falk, P. Marchal, S. Antonyuk, S. Kiesgen de Richter, M. Jenny, Influence of surface treatment on the flow properties of powders, *9th International Conference for Conveying and Handling of Particulate Solids, CHoPS*, 2018, London, UK .
- R. Handa, J. Edurado Fiscina, **S. Enferad**, C. Wagner, Rheologically probing and predicting the non-linear behavior of functional powders, *9th International Conference for Conveying and Handling of Particulate Solids, CHoPS*, 2018, London, UK.
- P. Grohn, F. Krull, **S. Enferad**, C. Gaiani, M. Jenny, S. Antonyuk, Experimental investigation of the fluidization behaviour of fine particles with differently treated surfaces, *Meeting of the ProcessNet "Agglomeration and Powder Technology" and "Food Technology"*, Nestlé Research Lausanne, Lausanne, 2018, Switzerland.
- **S. Enferad**, J. Petit, C. Gaiani, J. Burgain, V. Falk, P. Marchal, S. Antonyuk, F. Krull, S. Kiesgen de Richter, M. Jenny, Particles surface formulation effects on powder rheological behavior, *12th European Congress of Chemical Engineering*, 2019, Florence, Italy.
- **S. Enferad**, C. Gaiani, J. Petit, J. Burgain, V. Falk, P. Marchal, S. Antonyuk,S. Kiesgen de Richter, M. Jenny, The link between particles surface formulation and flow properties, *Powtech, Leading Trade Fair for Powder & Bulk Solids Processing and Analytics*, 2019, Nuremberg, Germany.
- **S. Enferad**, C. Gaiani, J. Petit, J. Burgain, V. Falk, S. Kiesgen de Richter, M. Jenny, Influence of air humidity on flowability of various formulated powders, *Workshop on Powders and Granular Materials Challenges and Future Trends*, 2019, Montpellier, France.

- **S. Enferad**, J. Petit, C. Gaiani, J. Burgain, V. Falk, P. Marchal, S. Antonyuk, F. Krull, S. Kiesgen de Richter, M. Jenny, Particles surface formulation effects on powder rheological behavior, *Congrès Français de Mécanique*, 2019, Brest, France.
- **S. Enferad**, S. Pillitteri, G. LumaY, C. Gaiani, S. Kiesgen De Richter, M. Marck, S. Umbetov, N. Vandewalle, M. Jenny, Hydrophobic and raw glass beads flow behavior under different processing dynamics, submitted.

Poster

- R. Handa, J. Edurado Fiscina, **S. Enferad**, C. Wagner, Rheologically probing and predicting the non-linear behavior of functional powders, *Joint Symposium of the Belgian Group of Rheology German Rheological Society ProcessNet-Subject Division "Rheology" Rheology – 360*, 2017, Luxembourg.

Chapter 2

Literature Review

2.1 Introduction

Granular materials are widely used in plenty of industries (pharmaceutical, metallurgical, food, agricultural, ...). Ceramics, composites and polymers industries also use these materials. A deeper understanding of granular behaviors would allow evaluating powders flowability. Understanding the flow behavior of powders have a positive impact on many industrial techniques. For instance, it is an important factor when the powders are handling like as charge and discharge of silos or storage. Currently, several methods allow characterizing the mechanical behavior of a powder. The size of the particles and its distributions, angle of repose, apparent densities before and after settlement are all distinct measurable characteristics that define a powder. By using these characteristics, it is possible to predict up to a certain extent the behavior of the powder in motion thus to speculate on its flowability and its potential functionality on certain industrial processes.

2.2 General information on granular material

The granular material is a term used to define a broad category of materials. These materials exhibit a behavior between solid and liquid. If one pours a powder in a container, it behaves like a liquid and it takes the form of the container. However, if one tilts the container a few degrees, the powder does not move like a solid block. When this container tilted to the inclination, then a layer of grains from the free surface of the powder start to flow and the medium behaves like a liquid. This transition between liquid to solid behavior is one of the most remarkable properties of granular media.

The properties of granular media has a hybrid state of matter whose description is not fully understood yet, unlike simple liquids and solids whose properties and behavior are well modelized [1]. Up to date, we are unable to fully predict the influence of a change in particle size, shape or geometry on the outcome of an experiment or in an industrial process.

Granular materials are extent in size and shape and their particle sizes are larger than 100 µm [1–4]. Figure 2.1, illustrates classification of divided media based on particles size; particles with the size between 1 nm and 1 µm are in the category of colloids [1, 5] whereas particle sizes between 1 µm and 100 µm fall into the category of powders [1, 6]. Here in this thesis, we focused exclusively on granular material among the divided media presented in Figure 2.1.

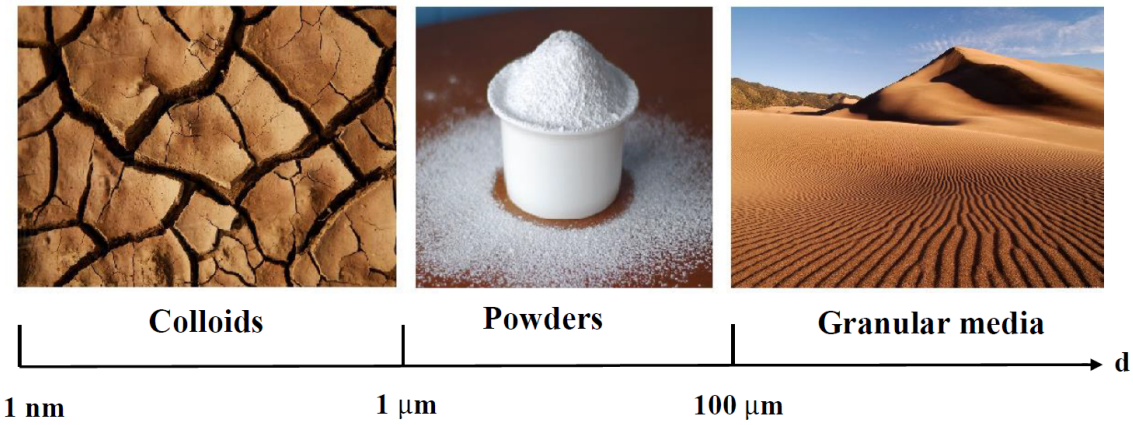

Figure 2.1 A classification of particulate matter as a function of the particle size: colloids (mud), powder (flour) and granular media (a sand dune) [1].

The granular material is the second most used material in the world after water [3]. The presence of granular materials in many natural phenomena (like as avalanche, landslide, sand dunes, etc) converted it as an important research topic in the science and industrial worlds. It is of great interest in civil engineering, chemical engineering, mining industry, pharmacy and agriculture. Whereby, it has been estimated that more than half of worldwide product markets are dealing with granular materials and their energy consumption during processing of this material is approximately 10 % of the energy resources used in the planet which is quite huge [3]. Therefore, any progress in understating the nature of granular material which could help to better predict the behavior of this material has considerable economic consequences.

Despite several researches on granular materials especially on glass beads as model powders there is no predictive unified structural model to describe the behavior of real granular media in an industrial process [7]. This issue rise from the fact that studying granular material is very complex since many factors govern their behavior that will be addressed in the following.

Figure 2.2 presents the list of possible factors to consider a granular material like a sand. As illustrated in sand, monitoring the individual movement of each particle during discharging sand in the silo is not possible. Since, the number of particles in a sand pile is numerous. In addition, the wide size distribution of particles is another factor that need to be taken into account since different particle sizes have their own particular behavior. In addition, one of the major characteristics of granular media lies in the fact that the volume properties of a set of grains are essentially derived from the surface properties at the particle

scale. Therefore, non-ergodic systems giving different varieties of possible configurations. Another reason is linked to the presence of inter-particle interactions. Influence of external environmental situation such as humidity and temperature is another factor needed to be taken into account. Furthermore, the powders under mechanical stress can behave like a solid or a liquid and put itself suspended like a gas. Consequently, it is difficult to figure out the behavior of granular material by considering the difficulty of obtaining experimentally reproducible results and then interpretation of these results.

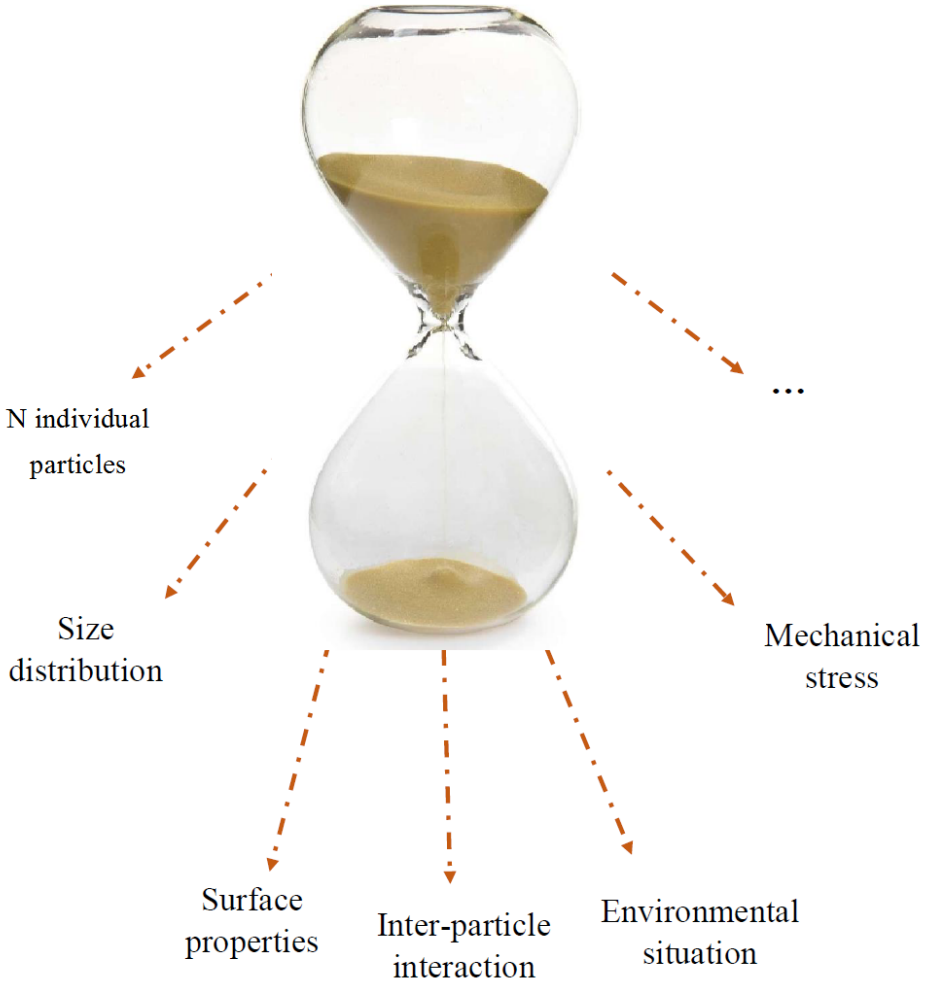

Figure 2.2 Some difficulties of studying the granular material posed by their complexity [8].

Generally, the characterization of a granular material can be achieved in two categories:

-**The individual physical properties:** consisting of particle size, size distribution, shape, surface porosity and roughness.

-**The overall physical-mechanical and hydraulic properties :** density, compaction, shear, cohesion, angle of repose, consolidation, friction and attraction forces.

These macroscopic properties are linked to the flowability of powder. In the literature, diverse definitions have been provided for powder flowability. In a study on powder metallurgy, flowability is expressed in number of seconds required to flow 50 g of powder (ISO 4490) [9]. In a research done on food industries, the "flow behavior" or "flowability" is defined as an essential property of powders, both for industrial user

as well as for the consumer. It depends on the origin of the powders, as well as their production methods that can be very diverse in food industry [10]. According to Henni-Kouadri's "Flowability is the ability of a granular material to acquire the specific behavior desired and sought in a given environment and for a specific use situation: it is the ability to flow, to handle, to storage, compression, settling,... » [11]. Saleh et al [12] defines the flowability as a property subject to many interpretations. Meaning that in order to converge towards a common definition of flowability in different domains, many deep researches are needed.

In the following, some parameters and properties of granular materials that influence the flow behavior of powders have been defined first. Then the methods of characterizing powder flowability have been presented.

2.3 Intrinsic and extrinsic factors of powders

Powders behavior can be impacted by a multitude of factors. Nevertheless, they are influenced by some intrinsic and extrinsic factors. The intrinsic factors are used to denote the specific properties of powders: morphology, porosity, size, size distribution, chemical surface composition, etc. While the extrinsic factors are linked to the process conditions which are mainly temperature and humidity. These extrinsic factors can influence particle generation process or the characteristics of the generated particles. The temperature has an effect on the molecular properties of the powder that can modify the structure of particles, especially their surface [13]. Also mechanical stresses applied to the powder, interactions of the powder with the equipment are extrinsic factors that influence powders behaviors.

2.3.1 Particle morphology

Particle morphology plays an important role in powder behavior such as filtration of suspensions, flowability of powders, compression, etc. It also influences the measured values of the particle size. Particles rarely come in a simple geometric form such as a sphere or a cube. A common way of classifying particles according to their physical appearance is through standardized descriptive terms presented in Table 2.1.

By considering that spherical particle with a smooth surface has fewer contact points and promote good flow behavior [14]. However, a non-spherical particle such as irregular and fibrous shape has a lower flow behavior and it is difficult to interpret their behavior. Meaning that more a particle is far from sphericity more its surface specific and complexity increases. In non-spherical particles, more inter-particle interaction come to play role in governing their behavior since it has more surface contac [15].

2.3.2 Particle surface roughness

In considering powder behavior, surface roughness is an important factors which can has substantial influence in inter-particle interaction. As an instance, in the particles with surface roughness the contact area of particles decrease as the result of increasing distance in contacting particles which it can lead to reduction of the attractive inter-particle interactions. The role of surface roughness has been studied extensively in the literature [16–20].

In overall, increasing surface roughness results in decreasing cohesion consequently powder flowability increases. However, other studies reported the incense of powder flow as a result of smoothing the rough surface of particles. Smoothing particles surface decreases the mechanical interlocking of particles which reduces the inter-particle friction [21–25]. Finally, a study conducted by Raula et al. indicated that the scale of surface roughness is an important factor to determine their effect on inter-particle interaction [26]. Whereby, they reported a decrease in the emission and dispersion due to the mechanical interlocking with increase in surface roughness size.

2.3.3 Particle porosity

A particle with a smooth or porous characteristic may greatly affect the collective properties of the granular medium. When a medium consists of porous particles the void fraction is much greater than if it consists of solid particles. In general, if the medium is dry, the air traps in void fraction corresponds to the inter-particle porosity. In wet medium like as suspension medium, the void fractions are filled with the liquid. With regard to an assembly of particles, the porosity (ε) is an important characteristic and defined as the ratio between the volume of the inter-particle void particles and the total volume occupied by the particles in a bed. It is independent of the absolute size of the particles [27].

$$\varepsilon = \frac{V_{pores}}{V_{pores} + V_{solid}} = \frac{V_{pores}}{V_{medium}} \tag{2.1}$$

However, the void of a granular medium can be divided into inter-granular (like as powder bed porosity) and intra-granular pores (such as powder surface porosity). In a random homogeneous medium, the surface porosity of the system is equal to the volume porosity. The density of the granular medium can therefore be calculated by the following expression:

$$\rho_b = (1 - \varepsilon)\rho_p + \varepsilon\rho_f \tag{2.2}$$

while:

ρ_b is the apparent density of the granular medium (kg/m^3),

ρ_p is the real density of the particle (kg/m^3),

ρ_f is the density of the fluid that fills the pores (kg/m^3).

Whereby, the dry granular medium is a set of particles, powders or grains with pores filled with a gaseous fluid. The components of this environment are always subject to the action of gravity but there are also interactions between them which are not negligible. Powders with a high porosity have high tendency to trap air and flow with difficulty, since the ability to release air is low [28].

2.3.4 Particle size and size distribution

The particle size has been reported extensively in the literature as a factor that influence the bulk behavior of powders [29–34]. Farley and Valentin [34] reported an empirical correlation between bulk cohesion and contact surface area of particle for inorganic materials. They have reported that cohesion increases with decreasing particle size and increasing surface area. Also, a study on milk powders conducted by Fitzpatrick et al. [35] showed that powder flow function increases as particle size increases. Therefore, particle size has a major influence on powder flow behavior. A powder is considered as having a good flowability with a particle size larger than 200 μm; between 200 and 100 μm it is a transition region and under 100 μm the flowability gets worse. One may not notice a major change in flowability as size is reduced from 80 to 60 μm while a noticeable decrease in flowability would be expected if the powder is reduced in size by an order of magnitude, (i.e. from 100 to 10 μm). This reduction in flowability at smaller particle size is due to the increased surface area of the powder. Meaning that in smaller particle size, the inter-particle force plays a significant role in comparing with gravity force.

The influence of particle size and size distributions on the flow behavior of a powder or a granular materials have been widely studied experimentally and numerically [36,37]. The flowability of powders is influenced by size distribution, particularly by the presence of fine particles. The presence of fine particles tend to block the flow. However, The numerical study, further validated with experimental findings, revealed that a fine size fraction could significantly affect positively the negatively during powder flow through a hopper [38]. In other words, the presence of fine particles into the size distribution may help to the flow behavior of powders. Meaning that the fine particles can fill the hollows at the surface of the particle, it decreases the surface friction force by increasing the inter-particle distance, and reduces the inter-particle forces where the powder flow behavior increases.

Table 2.1 Definition of the different terms used for the description of particle morphology [39].

Name	Description
Acicular	Needle-shaped
Angular	Quite sharp angled shape
Crystalline	Usual crystalline form
Dentritic	Crystal form with branches
Fibrous	Filamentous, regular or irregular shape
Granular	Irregular shape approximately one-dimensional
Irregular	Without any symmetry
Nodular	Round and irregular shape
Spherical	Round and regular shape

2.3.5 Particle surface chemical composition

In the literature, many studies reported the efficiency of surface chemical composition of powders in flow behavior. Different techniques were used for the surface composition of powders but the results were indicative of improved flowability in most of studies. A study conducted by Ehlers et al. [40] presented a thin-coating on pharmaceutics powder with improved flowability without affecting the particle size, shape and size by implementing fluidized bed coating technique. In another study by Genina et al. [22] the surface composition on drug particles reported a thin coating layer which was enough to decrease cohesion forces and to improve flow behavior of powders. In this case, the ultrasound-assisted fine polymeric mist deposition technique is utilized.

In an alternative research, the spray drying method is implemented for surface modification of particles, which result in reducing cohesion and improving bulk behavior of pharmaceutical powders [24, 41]. Also, sufficient amount of lipid coating on particles presented an strong efficiency in flow behavior of powders in drug delivery to the lunges, the coating reduced friction between particles by addition of a layer of lipid to particle surface [42]. In a study on food powders, using lecithin coating additive for milk powders improved their wettability [43]. Also it has been reported that adding small amounts of surface active additives to a lactose solution prior to spray drying can increase flowability of lactose powders [44]. Moreover, a study reported that a coating can be helpful in reducing the electrostatic charging of micronized powders [45]. Therefore, modifying the surface properties may significantly influence positively the flowability of powders.

2.3.6 Environmental conditions

Humidity is one of the major extrinsic factors that effects powder flow behavior by modifying inter-particle interaction and causes irregular flow behaviors. This phenomenon is function of the quantity

of water absorbed at the particle surface and is independent of the original water content of the powder. The water content is different from powder to powder and is influenced by factors like storage, temperature, relative humidity and/or exposed surface. Powder water absorption is therefore a problem of physico-chemical properties of the surface [46]. Based on the quantity of the water absorbed by the surface and on the particles structure, different results can appear as follow [14]:

(a) If the particle has capability of water intake, then absorption of moisture soften the surface and increases adhesion between particles.

(b) If the particle does not has water absorption ability, the moisture covers in a multi-molecular thick layer on the surface of particle.

Depending on the amount of air that remains between particles, at very low humidity, particles adhere to each other by electrostatic charge. Increasing humidity until a mono-molecular layer forms decreases in adhesion by removing electrostatic charges and increase the flow behavior of powder. While, too high relative humidity increases the surface area and the number of contact points between particles by appearing the capillary condensation. Therefore, there will be an increase in adhesion and cohesion between particles, consequently it lowers the flow behavior of the powder [47].

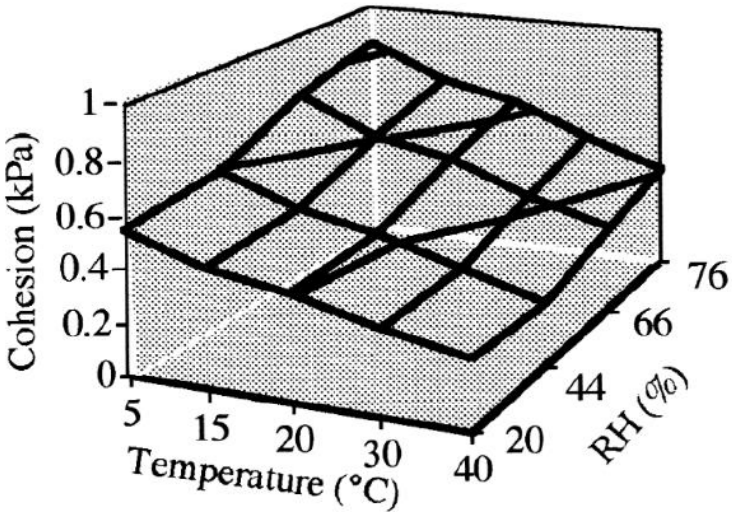

Figure 2.3 Evolution of cohesion as a function of temperature and relative humidity of flour particles [48].

Besides, temperature is another factor that can influence powders surface and their bulk behavior. According to Pilpel [49] and Teunou et al, [48], it is possible to improve the powder flow simply by lowering its temperature. However, the temperature can influence the flow behavior of powders in different ways. By increasing the temperature, the water content at the surface of the particle decrease which lowers the surface cohesion by lowering the liquid bridge between particles (Figure 2.3). Also an increase in

temperature can exceed the glass transition temperature of the material and therefore modify the texture of the latter [50].

2.3.7 Processing parameters

Apart from all aforementioned parameters, the attractive interaction of powders can lead to particle adhesion to the processing equipment and cause processing problems. Whereby, the electrostatic charge of particles induces adhesion of particles to the processing equipment surface. Thus, at the result of contacting particles with each other and with the equipment surface, the electrostatic charge exchange occurs meaning that the nature of contacting surface influences the electrostatic charge generation, consequently addition of adhesion [25].

Many studies in the literature reported this phenomena and its dependency to surface structure and material of processing equipements. Also porosity and roughness of process equipments have an impact in particle charging, while smooth stainless steel surface produced slightly higher charge than rough stainless steel [51]. Furthermore, the impurities present at the surface of particles affect the magnitude of generated electrostatic charges. In a study conducted by Eilbeck et al. [52], a decrease in the charging of lactose powders with the use of uncleaned stainless steel surfaces has been reported. The physicochemical properties of the interacting surface also play a vital role in particle adhesion to a surface. By implementing the scanning probe microscopy of gelatin capsules, it has been reported that the high surface heterogeneity and contrast friction caused increase in adhesion of lactose particles to the capsule surface [53].

In addition, the history of experiencing various stresses has impact in powder bulk dynamics. As an instance, the powder undergoes different stress during its handling, storage, transport, etc. Each one of the mentioned process affects powder behavior differently. During the transport, the powder undergoes vibrations that leads to reorganization of particles until they reach to a compact state [8]. This compact state is unfavorable to the powder flow [54]. However, a vibration can shake a pile of powder and re-aerate the powder then reduce the inter-particle forces by fluidizing the granular medium [55]. In this sense, it can also improve the flow behavior of powders. Therefore, it is important to be precise about using vibration in processes to enhance the flow behavior of powders by implementing convenient amplitude and frequency of vibration.

2.4 Particle interactions in granular media

As presented before, the study of granular medium can be carried out at two different scales: microscopic or macroscopic, depending on the interest. The microscopic scale is based on the study of contact phenomena between particles, and the macroscopic scale is the phenomena of a fraction of the medium or of the whole. Generally, the measurable properties of the granular medium are of the collective type

(i.e. the macroscopic scale) and their results are expressed by an average calculated per particle or per unit of mass, area or volume of the medium [56]. A granular medium is a collection of particles which are always subject to the action of gravity, but there are also interactions between particles which are not negligible. These interactions are very significant such that particles stack on top of each other can transfer stresses between them. If these interactions are no longer sufficient to keep the particles heap in the equilibrium then the heap will collapse. In the following, the main inter-particle interactions are presented.

2.5 Inter-particle forces between solid particles

The inter-particle interactions play a significant role in bulk behavior of powders like as powder flow, compaction, etc. The different types of inter-particle interaction forces are van der Waals force, electrostatic force, capillary force and solid bridge force [25]. Figure 2.4 depicts the corresponding inter-particle forces. In general, all particles are always subject to the gravity and inter-particle interaction. However, inter-particle interaction is more impressive in humid particles than dry particles [25]. This is due to the fact that in dry particles, the capillary force is negligible and the total force is mostly due to the van der Waals and electrostatic forces. However, strength of the electrostatic force is lower compared to van der Waals and capillary forces. Therefore, the van der Waals forces are the dominate forces in dry uncharged and small size range of powders [6]. The magnitude of the inter-particle forces can be measured by atomic force microscopy [25] which is detachment force of two particles between each other. In the following, the inter-particles forces are presented briefly (Figure 2.4).

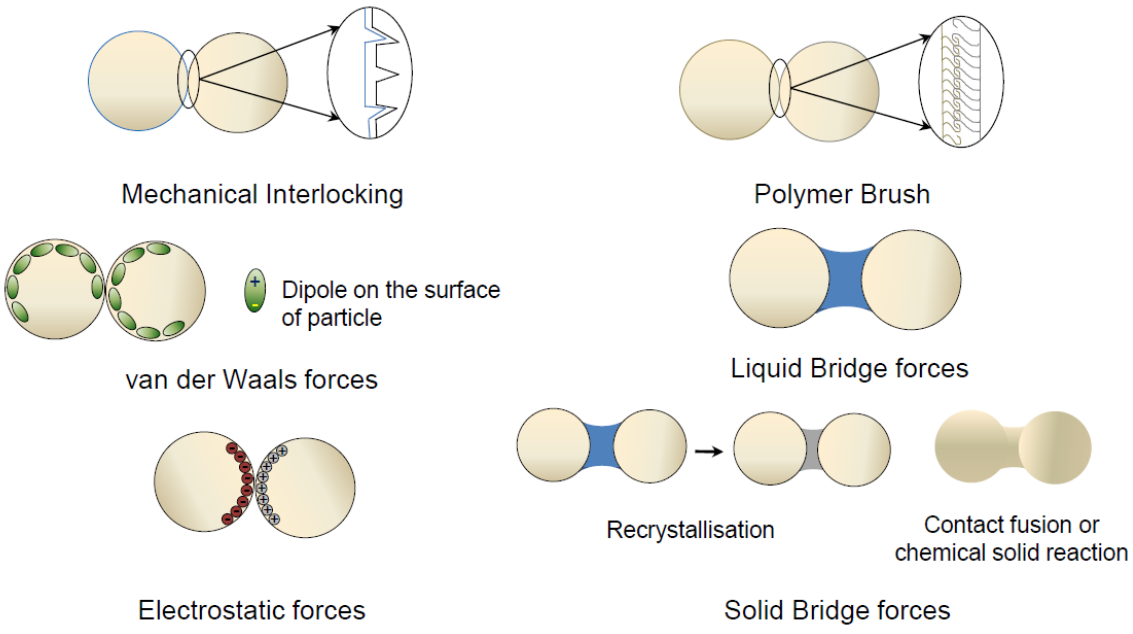

Figure 2.4 Different inter-particle interaction mechanisms [25].

2.5.1 Van der Waals forces

Van der Waals forces are attractive forces between particles, which decrease with distance according to a force law. These forces are weak in comparing to gravity force but it is not negligible for very fine particles [57,58]. The van der Waals forces are always present regardless of the nature of the interacting surfaces [59]. The Van der Waals force developed by two particles of the same diameter (d_p) is proportional to the size of the particles.

$$F_{Waals} = \frac{A}{12a^2}(\frac{d_p}{2}) \tag{2.3}$$

where F_{Waals} is the van der Waals force (N), A is the Hamaker constant (J), a the distance between particles (m), d_p is the particle diameter (m).

It should also be noted that the van der Waals force tends to infinity if the distance between the particles is $a = 0$. In addition, the powder acquires a cohesive behavior when the van der Waals forces become greater than their weight ($F_{Waals} \gg F_p$), this happen when the particles diameters are less than 100 µm. The order of magnitude of diameter of 100 µm has been estimated as the border between cohesive behavior and free flow [8].

$$F_p = \frac{4}{3}\rho_p g\pi(\frac{d_p}{2})^3 \tag{2.4}$$

here, F_p is the gravity force (N), g is the gravity acceleration (m/s^2) and ρ_p is particle density (Kg/m^3).

2.5.2 Capillary force

By apparition of certain amount of liquid around particles surface, the formation of liquid between contacting particles develop and consequently additional forces called capillary force appears. This force results in the formation of a bridge that binds two particles. The Equation 2.6 presents a maximum static liquid bridge or capillary force (F_{cap}) between two spherical particles [59],

$$F_{cap} = 2\pi r_2\gamma + \pi r_2^2\Delta P \tag{2.5}$$

,

$$\Delta P = \gamma(\frac{1}{r_1} - \frac{1}{r_2}) \tag{2.6}$$

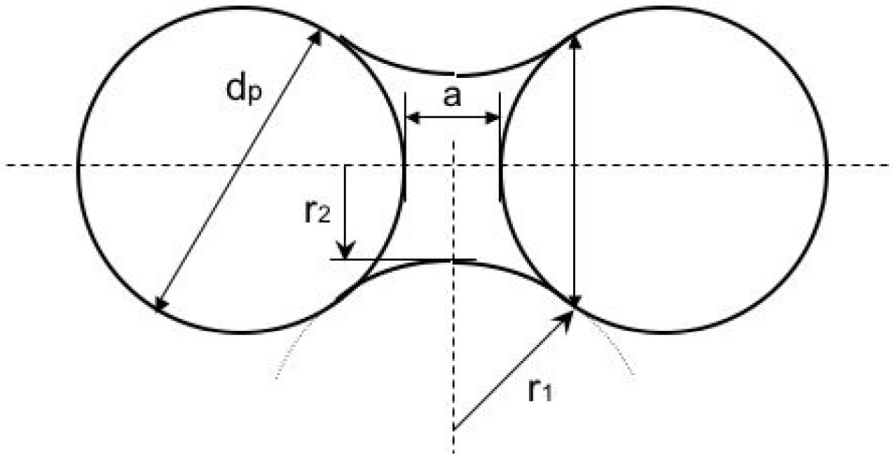

Figure 2.5 Liquid bridge between two identical spherical particles [59].

Where capillary force is function of surface tension of liquid γ (N/m), the pressure difference on both sides of the bridges ΔP (Pa) and the radius of curvature of the bridges with r_1(m) as radius of external curvature and r_2(m) the internal curvature of the bridges (see Figure 2.5). In addition, capillary forces are influenced by the particle properties like size, shape and surface roughness [60].
The maximum capillary force belongs to the smooth spheres that are in direct contact with completely wet surface. When the particles are in direct contact, the maximum capillary force in calculated as follow,

$$F_{cap_{max}} = \pi \gamma d_p \tag{2.7}$$

In the case of having one of the following conditions (i) a hydrophilic surface (ii) hygroscopic particles (iii) relative humidity higher than 60-70 %, the capillary force reaches to its maximum value [61]. Consequently, the capillary force dominates the Van der Waals force. It should be noted that, the capillary force increases at very high humidity condition and it results the formation of large agglomerations of particles and finally decreases the powder flow properties [62–65].

2.5.3 Electrostatic force

The particles can obtain electrostatic charges at the result of friction, collide with each other or with the wall of processing equipments. These electrostatic charges can lead to attractive or repulsive forces between the particles. The electrostatic force between two spherical particles of the same diameter, with the electric charge q_1 and q_2 (C) is defined as follow [61]:

$$F_e = \frac{q_1 q_2}{4\pi a^2 \epsilon_0} \tag{2.8}$$

where a is the distance between two particles (m), ϵ_0 is the permittivity of vacuum ($\epsilon_0 = 8.854 \times 10^{-12} C^2/m^2 N$).

The attractive force between two particles can cause particle agglomeration and adhesion of particles

to the surfaces of the equipment which it can lead to processing problems [25, 66]. Also, repulsive force can be problematic. As an instance, it can lead to the segregation of particles.

2.5.4 Gravity force

This force is proportional to the cube of the diameter of the particle (d_p) and is expressed according to the following equation:

$$F_G = \frac{\pi \rho_p g}{6} d_p^3 \tag{2.9}$$

where ρ_p represents the density of the particle (kg/m^3) and g is the acceleration of the gravity (m/s^2).

2.5.5 Relative importance of different forces

Figure 2.6 shows the comparative evolution of the Van der Waals, capillary, electrostatic and gravity forces as a function of the particle size [59]. In this figure, the larger the particle size is, the more the capillary and Van der Waals forces are predominant in comparision to electrostatic and the gravity forces. Moreover, this comparative study shows that, whatever the size of the particles, the capillary force has an action of greater intensity than the other forces in particular the Van der Waals force.

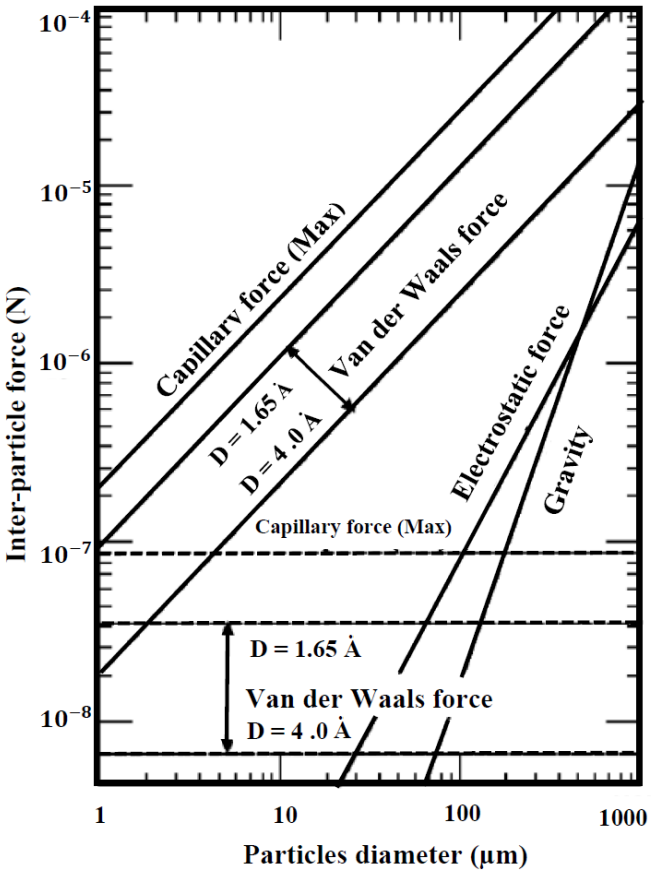

Figure 2.6 Evolution of inter-particle forces as a function of particle diameters [67].

Here the strength of capillarity is estimated at its maximum value, when the particles are in contact ($\gamma = 73 \times 10^{-3} N/m$, case of water). The electrostatic force is considered at its maximum intensity (charge of opposite sign) for a charge surface area of 10 $\mu C/m^2$. The weight is evaluated for the density of 3000 kg/m^3.

The Van der Waals force is determined for a Hamaker constant $A = 6.5 \times 10^{-20}$ J (case of quartz) and distances between particles varying between 1.65 and 4.0 angstroms.

2.6 Techniques to measure powder flowability

Flowability is often viewed as the ability of a powder to flow [68]. The powder flowability is highly dependent on the properties of the particles, meaning that the link between local interactions at the particle scale plays the major role in the overall behaviors of powder [8]. However, it is important to remind that understanding the flow behavior of powders is difficult because of their dissipative nature and unbalanced state, it constitute a complex system to be defined. It is well known that powder may flow well in one apparatus, but not in another [69]. This is why, a general behavioral law has not written to predict the powder flowability and the complexity of powders make them almost impossible to be fully understand with just one flowability measurement technique. There is many techniques of evaluating powder flowability based on the different processing dynamics that they undergo. But, in general the techniques are classified into two groups [8]:

-Direct methods are based on shear stress measurement of granular medium.

-Indirect method are based on measuring the parameters that are related to the powder flowability (like as repose angle, bulk density, etc.).

However, Krantz et al [70] in their study indicated that the flowability measurement techniques must be chosen according to the industrial application in use. Therefore, after testing different methodes, they recommended to measure the powder flowability based on the level of stress that it experiences during a process. In addition, Leturia et al [71] suggested a classification based on the level of stress applied by each technique. They classified powders into three categories, corresponding to different stress levels: (a) The conditions under which the powder is in a compact state under stress such as the measurement in shear cell. (b) Free surface conditions such as measurement in a rotating drum (c) Aerated conditions such as fluidization. Lumay et al, [72] defined granular material as a "complex system because its behavior depends on the applied stress".

They classified the measurement techniques into three categories.

- Static state: when a collection of particles form a pile in a container,

- Dynamic state: if the powder is in continues motion,

- Guasi-static state: between the static and dynamic states, a granular assembly can experience a quasi-static state. Indeed, if the pile of powder is gently vibrated, the grains rearrange themselves inside

the packing and the volume of the pile decreases slowly. In fact, in this state the power is temporarily experience stress.

Therefore, since the behavior of a powder is strongly dependent on the stress level that is subjected to, a classification of techniques according to this degree of stress is more logical than a classic classification by direct or indirect techniques. Therefore, in this thesis different measurement techniques were used to evaluate powder behavior, in static, dynamic and Guasi-static states.

In the following, powder characterization methods are discussed, also at the beginning of each chapter the equipments corresponding to the each measurements are detailed.

2.7 The repose angle

One of the most visible property of a granular medium is the characteristic angle of the pile that it forms, as an instance when pouring the powder from a funnel shown in Figure 2.7. This angle is called angle of repose and it can be measured easily.

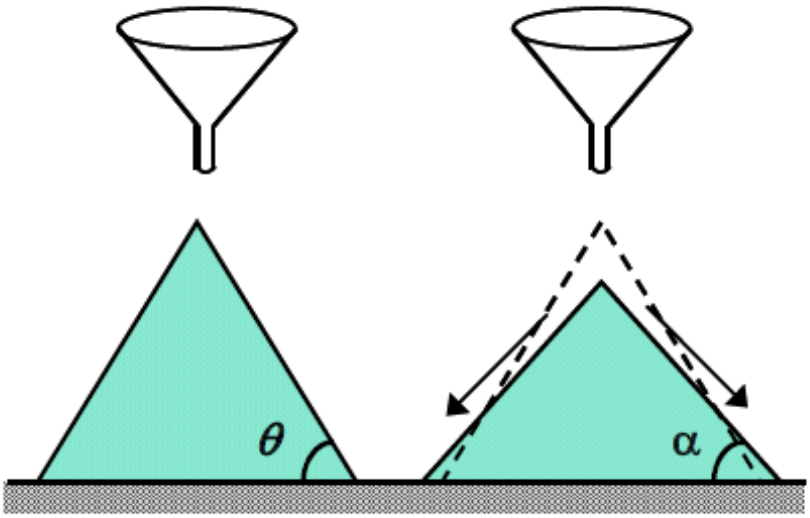

Figure 2.7 Pile of powder formed by flowing through a funnel. The angle θ is the maximum angle observed during the formation of the pile, and the angle α is the angle at which the flow freezes when the slope of the pile exceeds the angle θ [73].

Condotta [73] reported that by considering the formation of a heap in more detail, two critical slopes appears. He indicated that by adding more particles to a stable pile of powder, the particles accumulate for some time and the slope locally exceeds the angle of the pile. Once the slope becomes greater than a maximum angle θ, the particles start to move and slide down the slope. This is reduced to a minimum angle α at which the flow freezes (Figure 2.7). The construction of the slope is made by a series of such events, with a slope oscillation between two values.

Based on finding of Coulomb on slope differences for different materials, it is possible to relate this

maximum angle θ to a friction between particles [74].

Therefore, it can be expressed that the particles on the surface of the powder pile start to move when the static friction force is no longer sufficient to hold them. Figure 2.8 presents the sliding plane of solid bodies and between particles, the top layer is equivalent to a pad arranged on a inclined plane [73]. The force (P) is the weight of sliding particles on the pile surface and can be broken down into two components: the normal force ($|N| = P.\ cos\theta$) and the tangential force ($|T| = P.\ sin\theta$) at the sliding plane.

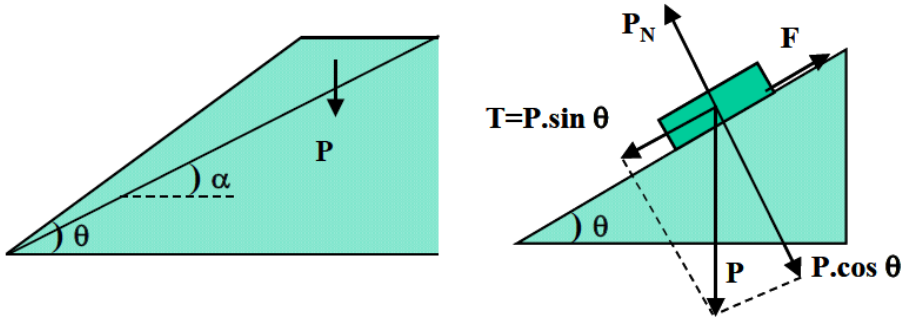

Figure 2.8 sliding plane of solid bodies and between grains [27].

The particles of powder will remain at rest as long as the tangential force is compensated by the friction force (F). According to Coulomb [73], the friction force has a relation with normal force as follow:

$$N\mu_S \geq F \tag{2.10}$$

where μ_S is the coefficient of static friction defined by Coulomb. Thus, the particles remain at equilibrium as long as the tangential force (T) does not exceed the maximum of the static friction force (F) as follow:

$$P.\ cos\theta\ \mu_S \geq P.\ sin\theta \tag{2.11}$$

which it leads to:

$$\mu_S \geq tan\theta \tag{2.12}$$

By defining the internal angle of static friction (φ) with $\tan\varphi = \mu_S$, the maximum angle of the free surface of the pile is then limited by:

$$\varphi \geq \theta \tag{2.13}$$

According to Coulomb [73], the aforementioned expression is valid for non-cohesive powders, where the only force of interaction between the particles is the force of friction. Coulomb's classical expression for the phenomenon of solid friction is usually written in the form of stress, dividing the force by the (hypothetical) sliding area.

$$\tau = \mu\sigma \tag{2.14}$$

For cohesive powders, where the attractive forces between grains add to the solid friction, Coulomb added a term (c) in Equation 2.14:

$$\tau = \mu\sigma + c \tag{2.15}$$

Cohesion (c) can also be interpreted as the resistance of the solid to shear under zero compressive stress.

Generally, cohesive powders form piles with high value and large irregularity in the shape of the resulting cone [75]. Also in literature there is different angle measuring devices that can be used to characterize the granular material [10, 76], these multitude techniques are presented in Figure 2.9 .

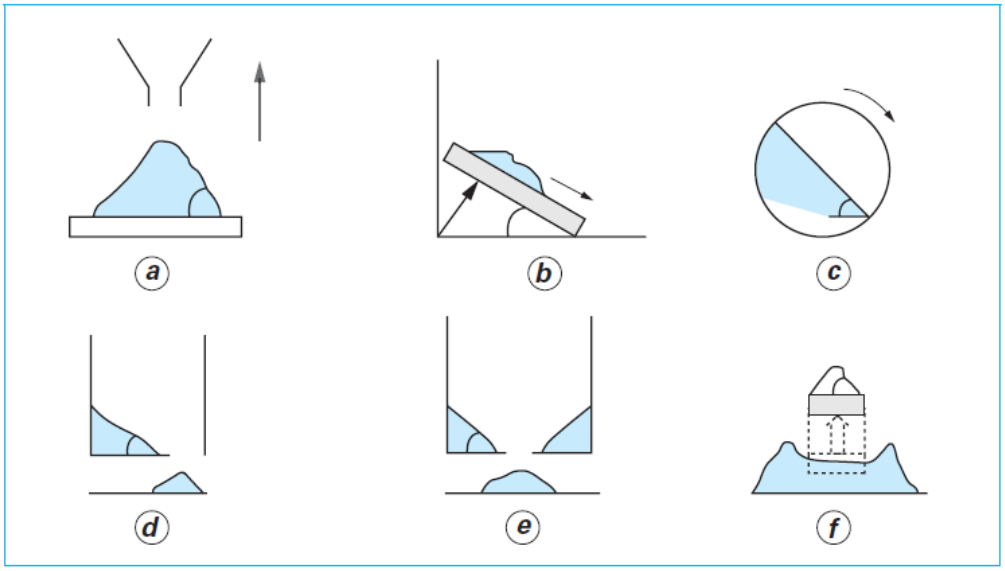

Figure 2.9 Schematic representation of the main angles measures [10]: **(a)** angle of repose by overturning (or angle of landslide, **(b)** sliding angle, **(c)** angle of rotation, **(d)** edge rest angle, **(e)** crater rest angle (or flow angle) **(f)** conical angle of repose (spatula angle) [10].

Different factors can impact the measurement of the angle of repose such as the surface roughness on which the pile is formed, the shape of the measuring equipment, the existence of segregation between the particles, the height that powder are filling, etc [8, 77]. Also this technique is used in many industrial sectors, transport and storage of granular materials, agricultural engineering, mining activity, but also in the study of natural phenomena such as dune formation, avalanches, to determine the angle necessary to avoid a landslide phenomena [8]. It should be taken into account that in this technique the powder is subjected to very low stresses and they simulate the behavior of powder during flow conditions therefore it should not be the only flowability characterization measurement.

2.8 Dynamic angle

One of the properties of powders is the ability to maintain a static (solid) state despite a certain inclination. Coulomb had previously find out that this ability is associated with frictional forces within the material [4]. However, the static state of powders can be broken under certain conditions, and the granular material may enter the phase of movement. As an example, when exceeding a critical value of the angle of inclination of the material, as defined in previous section. The particularity of this phenomenon is that only the particles belonging to the surface layer will be set in motion, the rest of the particles will remain in a static state, this is called the avalanche phenomenon. The dynamic angles have been widely studied in the literature [15, 78–80]. Because one of the ways to prevent this phenomena is to determine the angle which avalanche can happen. Daerr et al [81] reproduced avalanches by placing glass beads on an inclined plane. This assembly makes it possible to control the angle of inclination as well as the thickness of the layer of particles available for movement. The avalanche is created by inclining the plane at an angle greater than the angle of rest (the angle of repose in static state) and depositing then a few more particles. When the deviation from the angle of repose is small, the avalanche remains confined but when the plane angle is similar to the maximum angle of stability, the deposition of particles causes an avalanche downstream of the point and also drives the particles upstream in the downward motion. However, this type of operation does not quantify the importance of the avalanche. Here in this test, the roughness of inclined plane had influence in the result also other factors like as environmental parameters are important in this type of measurements.

Figure 2.10 illustrates the four geometries for studying of dynamic or avalanche angle of powders. In setup A, the grains are added one by one to the top of a heap formed on a circular tray placed on a balance interconnected to a computer. The total weight is detected at all times by the scale and recorded using the computer [82–84]. The main disadvantages are continuously adding the particles and the controling environmental condition which is almost impossible [83]. The slope changes for techniques B and C are obtained either by sprinkling particles randomly on the surface of a pile formed between three sides and an opening (B), or by very slow rotation of a half cylinder (C) [85–87]. In both cases, the falling grains are identified by a detector. Its response varies depending on the amount of grain that passes, and its resolution can detect the passage of a single particle. As with assembly A, the environmental factors are out of control. In addition, the amount of powder decreases with experience. With the technique D, avalanches are created inside a slowly rotating drum [88–90]. The analyzed powder is introduced into a transparent rotating drum. A light source is placed on the front. The rotation of the drum causes a gradual increase in the angle between the free surface of the grain stack and the horizontal. When the avalanche angle is reached, the surface destabilizes and an avalanche occurs [88–90]. The flow continues until the free surface stabilizes to give the fixed angle (angle of repose). The flow of the powder is

monitored via a camera and then the images are processed by using image analysis software to obtain the desired angle values. By comparing the technique D (rotating drum) with the previous techniques, the avalanche angle is interpreted in the same way, the powder is evaluated in free flow regime without external stress, and the environmental condition is better controlled. Nevertheless, it need to take into account that the result of rotating drum is influenced by particle and drum size as well as the roughness of drum wall.

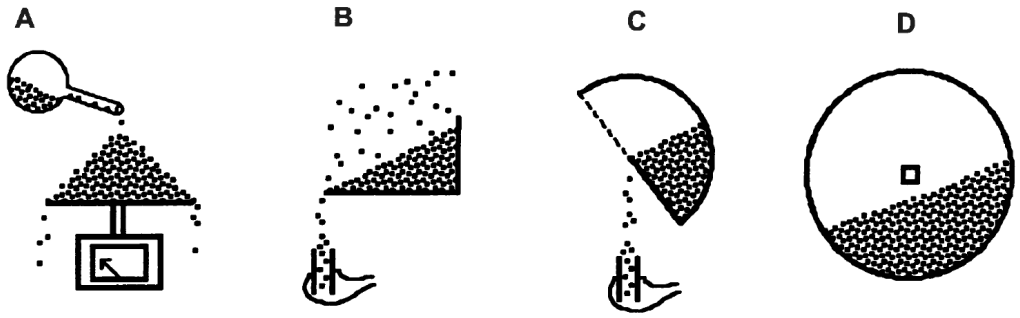

Figure 2.10 Four geometries diagrams for studying the dynamics angle of powders [91].

2.9 Powder settlement and compressibility tests

The values of the apparent densities before and after compaction are often required in pharmaceutical development processes and in the quality control of powders [14]. In addition, they are used through the notion of compressibility in civil engineering, in industry for discharge, transport and storage of the granular material. In fact, these measurements reflect the degree of particle stacking composing the powder. When the powder is put into a container, it eventually reaches a level of balance between gravity and the forces of cohesion and adhesion. When subjected to vibrations, the particles are put back into motion and when the vibrations stop, the powder bed returns to equilibrium. While, exhibiting a different volume due to a new spatial conformation of the particles [92]. There is no single value for any given powder [93]. The apparent density before settlement is obtained by dividing the mass by the volume occupied by the powder. It is difficult to measure, because a small disturbance of the medium produces a new free density caused by a spatial rearrangement of the particles [92]. The free density of the powder increases as the small particles move to the voids created by the larger ones and occupy them as a result of environmental disturbances. It has already been established that the shape [15, 94] and the particle size are factors influencing particles arrangement by offering a multitude of possibilities of spatial conformations [95]. It should be indicated that density and compactness measurements are used to define flow indices to assess the flowability of a powders. In fact, compressibility refers to the ability of a material to decrease in volume under the effect of stress [96]. Compressibility is determined from the loss of apparent volume of a mass of powder placed in a test specimen subjected to a series of shocks or vibrations. This property can be evaluated using two indices: the Hausner index [78] and the Carr

compressibility index [96].

The Hausner index (Hr) is always greater than unity and is expressed using the following equation:

$$Hr = \frac{\rho_{bt}}{\rho_b} \tag{2.16}$$

where ρ_{bt} is the packed density (kg/m^3), which corresponds to the maximum value that can have the density of a powder obtained by calculating the ratio between the mass of a set of particles and the total volume occupied by this packed set. ρ_b is the bulk density (kg/m^3), sometimes referees to unpacked or aerated. Which is defined by the ratio between the mass of powder and the total volume occupied by this non conditioned powder. This index makes it possible to classify the powders into different categories. According to the Hr index, the higher the Hr, the more the flowability deteriorates. Table 2.2 presents the powder classification based on Hr values; the detailed classification of Hausner values is presented in chapter 4.

Table 2.2 Interpretation of the Hausner compressibility index [78].

Hausner report	Powders
Hr $\leq$1.25	Sandy or granular
1.25 $<$ Hr $<$ 1.4	Fusante
Hr $\geq$ 1.4	Cohesive

Carr, used the values of aerated (ρ_b) and packed density (ρ_{bt}), defined a material compressibility index which is given by the following relation:

$$IC = \frac{\rho_{bt} - \rho_b}{\rho_b} \times 100 \tag{2.17}$$

According to this index, the more compact a powder becomes, the poorer the flowability. This implies that a powder with a high Carr ratio (IC) has a poor flowability. The interpretation of the results of the IC values is done in the same way as the Hr, i.e. the higher the IC, the higher the compressibility. In general, the compressibility of powders has inverse relation with their flow behavior.

Table 2.3 presents the quantative ranking of powders based on Carr compressibility ratios.

Table 2.3 Interpretation of the Carr compressibility ratios [96].

Particle size	Flowability	Powders
5-10	Excellent	Granules, sands, powder without fine particles or fibers
11-15	Good	
15-25	Fair	Powder with few fine particles and high density
25-30	Low	Powder containing fine particles
30-40	Very low	Cohesive powder
> 40	very very weak	Very cohesive powder

These indices are not intrinsic values of the powder and they are dependent on the methodology used, in particular the filling mode. Also, they depend on many other factors like the number of shocks applied to the powder, the stacking of particles may be in more complex configurations or less cowardly [97]. As well as, the frequency and amplitude of shocks are parameters set by standard settlement devices whose effect cannot be quantified. The state of powder configuration is also affected with many experimental parameters such as the diameter of the cylinder used and the mass of material analyzed. It is also recommended to weigh a defined volume of powder to increase accuracy [93]. However, it should be taken into account that it is difficult to measure the mass since a small disturbance of the environment can create a new special rearrangement of particles [93]. In addition, it was determined that the particle rearrangement is closely dependent of the particles shape [15,79] and the particle size [98,99]. Therefore, they can offer a variety of spatial configurations or not.

2.10 Flow measurements through a fluidized bed

One of the remarkable property of a powder is its ability to be fluidized. Fluidization is giving the property of a fluid to a solid by suspending it with a gas or a liquid. This property, which finds various industrial applications in many fields such as the treatment of gaseous or liquid effluents, chemistry, pneumatic transport, is the subject of numerous works, both experimental and theoretical [100–106]. During fluidization operation, the state of the particles will change depending on the speed of the gas stream. The particles are placed on a plate of the perforated sheet or porous plate type, thus forming a regular layer. In addition, if an ascending gas stream passes through the plate, a whole series of phenomena can be observed, ranging from non-fluidization during particle entrainment, depending on the speed of the gas stream. The fluidization operation is not feasible with all powders. In 1973, Geldart [101] presented the most popular powder classification up to date in fluidized bed material. As illustrated in Figure 2.11, he classified the powders into 4 groups, the classification is based on particle size and the difference in density between fluid and solid.

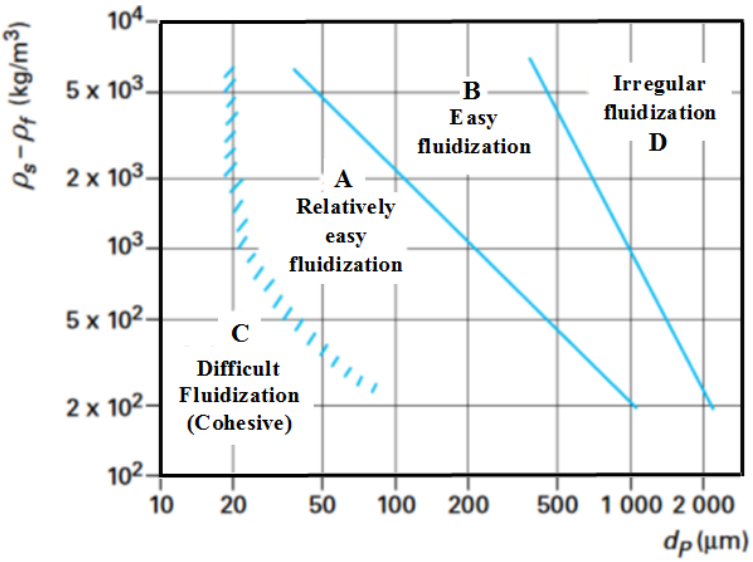

Figure 2.11 Classification of particles according to the Geldart empirical diagram [101].

Table 2.4 Types of powders and their fluidization characteristics [101].

Category	Type of powders	Fluidization	Characteristics
A	Fusantes	Easy	Fluidized particles, strong expansion of the bed,bubbling (fluid speed > minimum fluidization speed)
B	Sandblasters	Easy	Aggregative fluidization, low bed expansion (fluid speed < minimum fluidization speed)
C	Cohesive	Difficult	Difficult to fluidize, need for agitation or vibration,
D	Granular	Unstable	High fluidization speed, turbulent fluidization, bubble explosion on the surface

The physical characteristics of powders and inter-particle forces within the powder play important role in their fluidization. Based on mentioned characteristics of powders, the fluidization can be easy for certain powders and difficult for some others or sometime impossible. Table 2.4 is a classification proposed by Geldart [101] presenting powders according to their behavior towards fluidization. In the table, category A concerns granular media of small diameter, (d_p < 50 µm) and/or low densities (less than 1400 kg/m^3). Category B includes granular media with a diameter in the range of 40 µm < d_p < 500 µm. These two categories A and B relate to easily fluidizable powders. Category C is related to fine particles with a diameter d_p < 30 µm. These powders are cohesive and difficult to fluidize. Finally the last category, category D, concerns large particles d_p > 500 µm.

In order to fluidize nano or micro-powders (i.e. the powders that classified in group C), inter-particular forces need to be defeated. The literature proposes some activated fluidization processes: vibrating

bed fluidization [107, 108], fluidization under acoustic field [109], fluidization in mechanically agitated bed [28], etc. Fluidization is used in many and varied industrial applications such as chemistry, metallurgy, ceramics, food, pharmaceuticals, etc.

2.11 Flow measurement through an orifice

This test is based on the ability of a powder to flow through orifices of different diameters and in observing the flow regime (constant or discontinuous) and its flow rate [107]. The devices for this type of manipulation consist of a cylinder and a device which allows the lower opening of this cylinder to be varied, through which the powder must pass. This opening transition can be done using funnels or a plate. Figure 2.12 shows a schematic of this device. Special care is always necessary, as the way the operator fills the cylinder influences the results. This method is still a qualitative method which provides good results for comparison. For non-cohesive powders, where the action of gravity is much greater than the inter-particle forces of the powder, the flow proceeds smoothly. Beverloo [110] observed this phenomenon and studied the flow of several powders as a function of different opening diameters for small flat-bottomed silos. He found that the discharge mass flow rate remains only function of the discharge opening diameter. In this thesis we used the Granuflow equipement to measure the flowabilities of our powders and the details of measurement is presented in chapter 4.

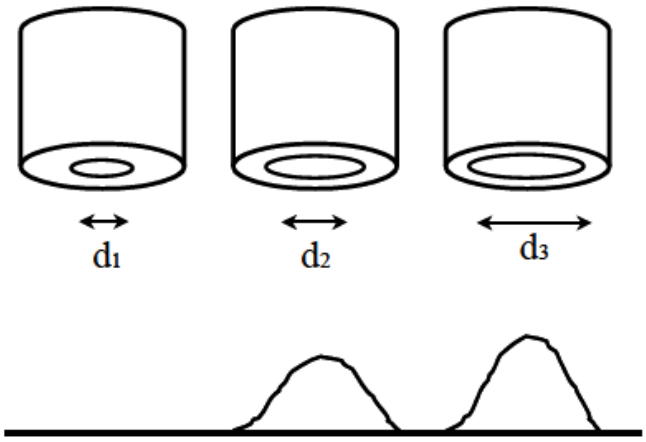

Figure 2.12 Diagram of a Flodex® device.

2.12 Flow measurement in shear cell

A more basic assessment of the powder flowability can be obtained by measuring the inter-particle friction under stress [92]. To measure the flowability of powder with this approach, the most used instrument is the shear cell. There are several types of shear cells such as: Jenike cell, Hiestand plateau-like cell and Can & Walker ring-like cell, to name a few that are used in industry [111]. In this among, Jenike's method is a standardized method which quantifies the flow properties of the granular medium by observing the

breaking point of powder bed under shearing, regardless of its compressibility [112]. In general, the shear is characterized by two quantities, the shear rate, ($\dot{\gamma}$), and the shear stress, (τ). The shear itself is defined as a movement between two flat surfaces, one stationary, the other animated by a movement parallel to the first. Throughout the flow, the layers slide over each other in a laminar (non-turbulent) motion. Jenike's method is based on determining the shear stress (τ) to be applied to a stack of powder that are initially consolidated and subjected to a normal stress (σ_N). The shear test should be repeated with several magnitudes of normal forces, (N) on identically prepared samples. The powder stack reaches a critical level of consolidation when the powder volume become constant. Once the status of critical consolidation is achieved, the breaking point can be determined. Therefore, the Jenike's method follow consolidation and the shearing cycle as presented in Figure 2.13.

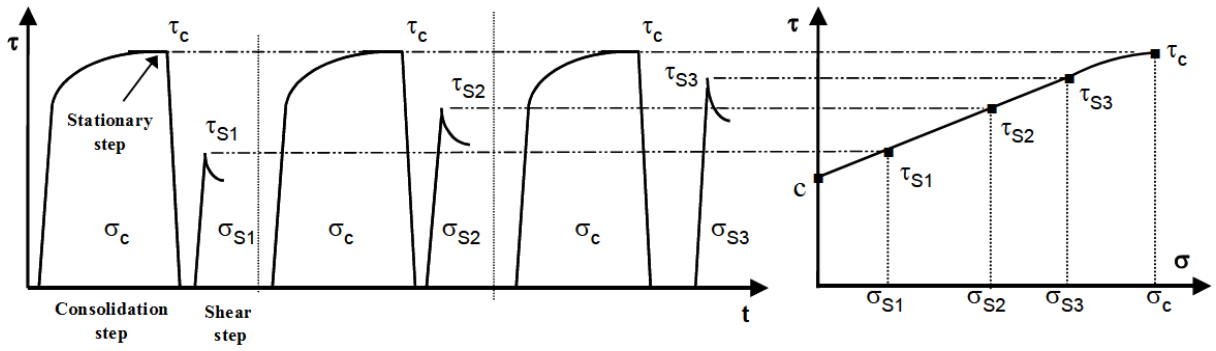

Figure 2.13 Determination of the flow steps by the Jenike shear test [27].

This curve is constructed from a number of powder break points, where obtaining each of these points is done through Jenike's procedure. This procedure is divided into two parts:

- **Critical consolidation**: this step is necessary to have reproducible results because the breakage of a powder sample depends on its consolidation. Here, a normal stress (σ_c) is first applied to the sample, then the powder is sheared. The shear stress increases until the medium begins to flow. The force necessary to maintain the shearing (τ_c) will then gradually stabilize and the critical state of consolidation is reached. This state coincides with the state of the critical density of the powder. The critical density state is defined as the state of the powder where its density no longer varies, compactness (constant).

- **The shear test**: once the consolidation step has been completed, the constraint of consolidation is removed and a new stress (σ_s) lower than σ_c is applied to general medium. The couple of (σ_s , τ_s) determines the breaking point. The achievement of several points of rupture allows the flow location to be traced Figure 2.13.

The complete procedure for obtaining the yield locus (powder bed breaking) curve consists in repeating these two experimental steps for different normal stress failure less than the consolidation stress [112]. The different pairs (σ_s , τ_s) obtained constitute the points of the yield locus of the powder for the

consolidation σ_c, and the pair (σ_c , τ_c) constitutes the end point of the curve of the yield locus Figure 2.13.

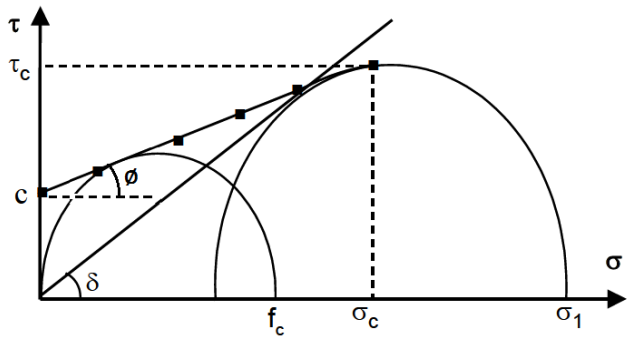

Figure 2.14 Diagramme (σ_s , τ_s), the flow point, cohesion (c), internal friction (ϕ), effective angle of friction (δ) as well as Mohr's circles. as well as Mohr's circles [27].

In this technique, the flowability of a powder (ff) is the ratio between the maximum principal stress (σ_1) that the powder can undergo without changing consolidation. Whereby, the maximum stress (f_c) supported by the powder on a free surface, developed for this state of consolidation.

As shown in Figure 2.14, the cohesion (c) of the medium is given by the intersection of the adjustment curve with the y-axis, the internal friction angle of the powder (ϕ) is given by the slope of the latter ($\mu = tan\phi$). Physically, this cohesion represents the constraint necessary to apply on an unconsolidated powder to make it flow. It is representative of inter-particle forces. Also based on Jenike's method the following information can be extracted:

-Cohesive stress (f_c): it represents the compressive stress to be applied to an arch to break it. An arch forming during the flow has a tangent plane to its free surface which is not subjected to any constraint, neither tangential nor normal. The Mohr circle is representative of this constraint condition and which goes through the origin. The cohesive stress is given by the major principal stress of the circle passing through the origin and tangent at the point of failure (see Figure 2.14).

- The major consolidation stress (σ_1): this is the maximum stress that could have been exerted on the powder for the given state of consolidation (maximum stress of the main plane). This stress is obtained by the Mohr circle tangent to the breaking point and passes through the end point of the breaking point with coordinates: σ_c , τ_c. The flow function of a powder is the ratio between the maximum principal stress, (σ_1), that the powder can undergo without changing consolidation and the maximum stress, (f_c), supported by the powder on a free surface, developed for this state of consolidation. The flow functions indicate the stress required to reset a flow based on the major stress that consolidated the powder. As we have seen previously, each breaking point makes it possible to determine a pair (f_c , σ_1), so it is necessary, to obtain a complete flow function, to carry out tests for different consolidation stresses. Thus, the powders can be classified into different categories according to the position of their flow function in the diagram of Figure 2.15. It defines different categories from the linear relationship

between f_c and σ_1 [112]. In Figure 2.15, we can see that the more the points obtained have values close to the x-axis, the powders present high flow function values. This technique is utilized in this thesis for powder classifications in chapters 3 and 4.

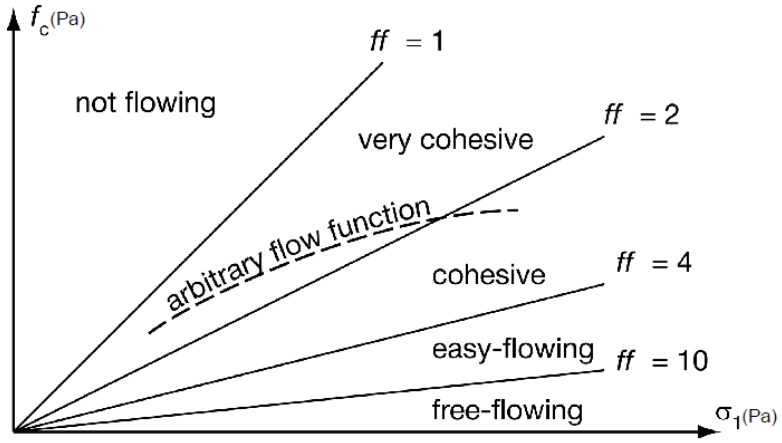

Figure 2.15 Classification of powders based on their flow factor *ff* [112].

2.13 Rheological measurements

There are different rheometers which can be used in order to study the rheological behavior. Mechanically stirred fluid-bed rheometer (msFBR) is a rheometer which has been developed at the University College of London to study the rheology of fluidized powders. In this equipment, a model was developed to estimate the state of stress at the impeller depth and to evaluate the torque at low consolidation stresses based on combining actions of material weight, aeration and impeller position within the powder bed [113].

Anton Paar MCR is another rheometers which measures the powder flow behavior by Anton Paar Powder Cell (APPC) [114]. This equipment measures the torque required to rotate an impeller immersed in a powder bed which can be aerated either below or above the minimum fluidization velocity. APPC is a automated testing without any operator involvement apart from sample preparation.

One of the most used techniques to study the flow behavior of powders is rheological measurements with a rheometer. This technique is in use widely for characterizing a large number of dry and saturated granular materials [115–118]. This equipment is an imposed stress rheometer which constitutes a dynamic analysis method; it has the advantage of highlighting the variations of dynamic quantities throughout the experiment. A certain number of measurable quantities (torque, force, displacement, angular speed) will be converted into rheological quantities (stress, strain, moduli, viscosity). This powder rheometer is capable to generate granular agitation within the powder samples by subjecting them to vertical vibrations [119, 120]. The cell where the powder sample is introduced is connected to a minivibrator connected to an amplifier. The frequency and amplitude of vibration are controlled by a function generator and a accelerometer, also connected to a measurement amplifier. Based on the collected data with mentioned rheometer we can intemperate about powder flowability. This rheometer has been explained

in more details in chapter 4.

In the chapter 4 and 5 of this thesis the Discovery-HR3 rheometer with a vane geometry has been used to characterize five powder samples (control, hydrophilic, hydrophobic, lactose coated glass beads and agglomerated lactose powder) with and without humidity control as well as powder characterizing at low and high shear rates.

Also, one of the mostly used and well known rheometer is FT4 eqipement which has been introduced by Freeman Technology [121–123]. This rheometer has wide applications in powder industries particularly food and pharmaceutic industries. It allows to achieve a wide range of standardized tests adapted to situations encountered in industry. In this thesis, powder flow behavior was measured with shear cell, compressibility, aeration and stability tests. The shear cell tests follows by powder consolidation and powder shearing and it measures the shear stress needed to obtain a failure of the powder, i.e. the powder particles start to move relative to one another, as function of the applied normal stress [124]. Based on impressibility test,the bulk density of the bulk solid are measured as function of normal stress. Based on reduction of flow energy upon powder fluidization caused by air circulation through the powder bed, powder fluidizability can be measured with aeration test. Furthermore, by stability test we can have access to the basic flowing energy, normally higher value of basic flowing energy shows low flow behavior. The FT4 rheometer has been discussed in more details in chapter 3.

2.14 Conclusion

According to the literature, in order to properly assess the powder behavior, it is crucial to have a good knowledge of powders physical characteristics. The behavior of powders is linked to the characteristics of particles that constituting powders as well as inter-particle interactions. Moreover, these characteristics should ideally be studied individually in order to understand the effect of each parameter without having any interference with the other influencing properties. It has also been shown that there is direct relationships between inter-particle forces and flow properties of a given powder. Therefore, the description of the behavior of a powder cannot be made without determining collective properties such as cohesion and apparent densities; but it also requires characterizing individual properties of particles such as size, shape, porosity, etc. Therefore, the parameters influencing the flow dynamic of powders including the influence of intrinsic as well as that of extrinsic parameters have been explained in the text.

The techniques allowing the evaluation of powder flow behavior based on different measurement techniques concerning the powder evaluation in static and dynamic states have been presented. The complex nature of the powders flowability requires to use different techniques for assessing the flowability in line with the intended application. Also, the flow indices used must be representative of the dynamics of the powder flow.

Chapter 3

Influence of surface formulation and particles size on powder flowability

3.1 Introduction

This chapter is dedicated to the influence of the formulation on powders behavior. Raw glass beads have been formulated with hydrophobic, hydrophilic and lactose surface coating to modify the surface properties of the particles. The two first treatments should modulate the sensitivity to humidity which is known to increase the cohesiveness between the particles. The lactose coating modifies the roughness and the cohesiveness of the powders. Indeed, the lactose coating increases both surface friction and sensitivity to the humidity. Furthermore, in this chapter the influence of powder size has been studied. With this objective, two different sizes (100 µm and 500 µm) have been used for the five formulations (i.e. control, hydrophilic, hydrophobic and lactose-coated glass beads, as well as agglomerated lactose powder). The powders have been characterized using the **FT4 rheometer** and their cohesiveness has been measured by **shear cell test**. Investigations at the particles scale have been performed. For instance, the surface friction and hardness of the beads are determined by **scanning electron microscopy** and **nanoindentation technique**.

3.2 Powder surface formulations

The following figs. 3.1 to 3.4 illustrate the formulation steps which have been performed in this thesis.

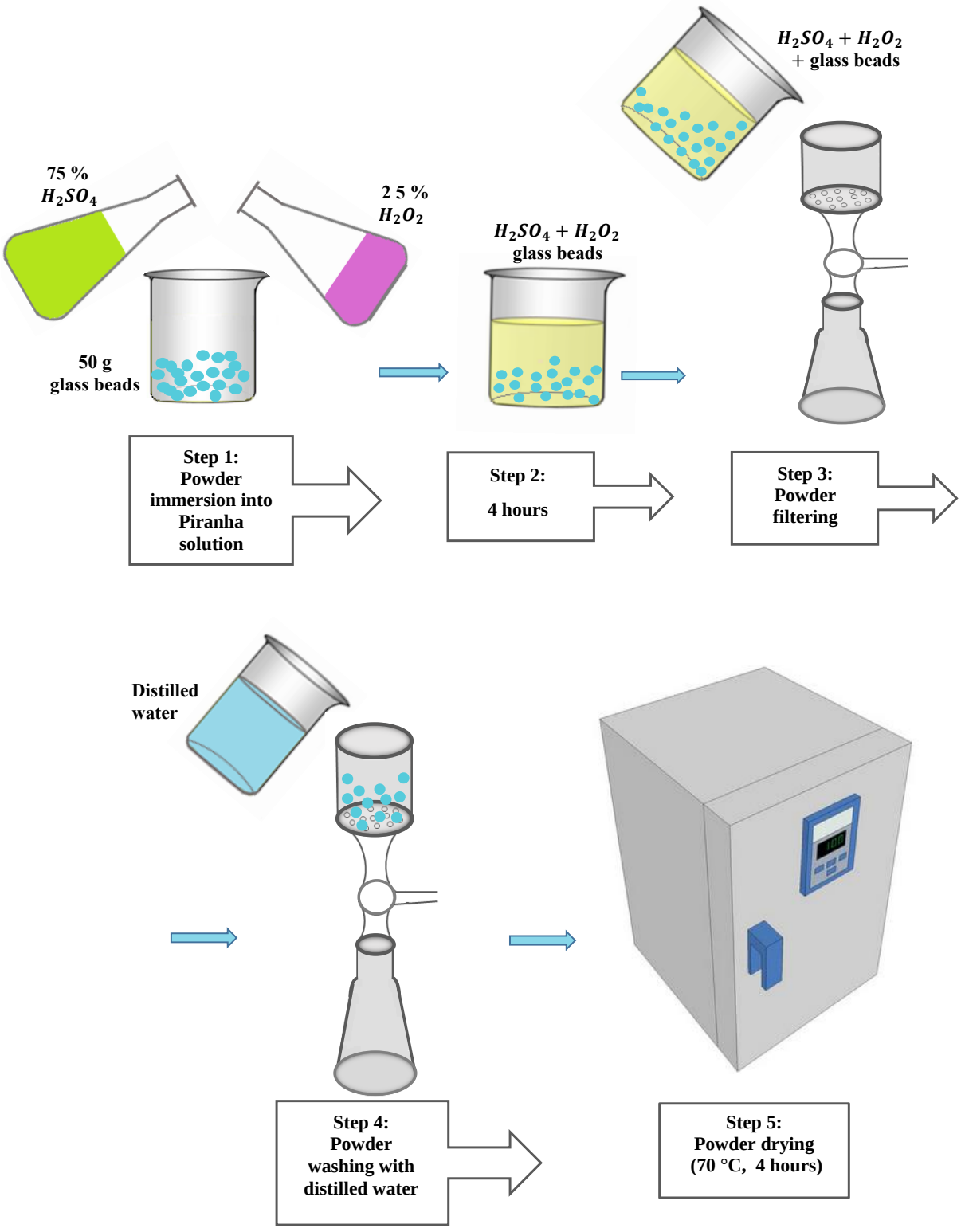

Figure 3.1 Hydrophilic surface formulation on glass beads.

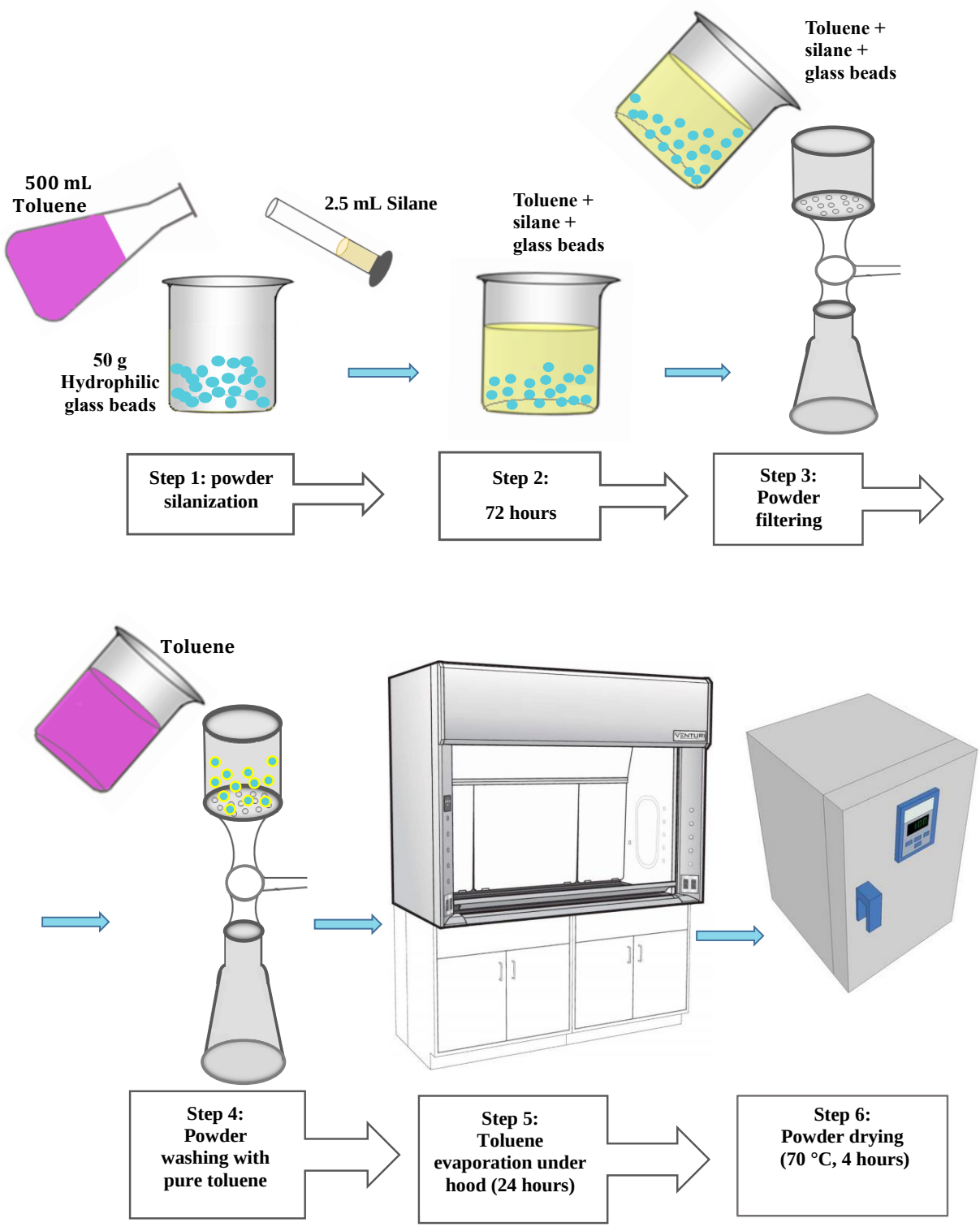

Figure 3.2 Hydrophobic surface formulation on glass beads.

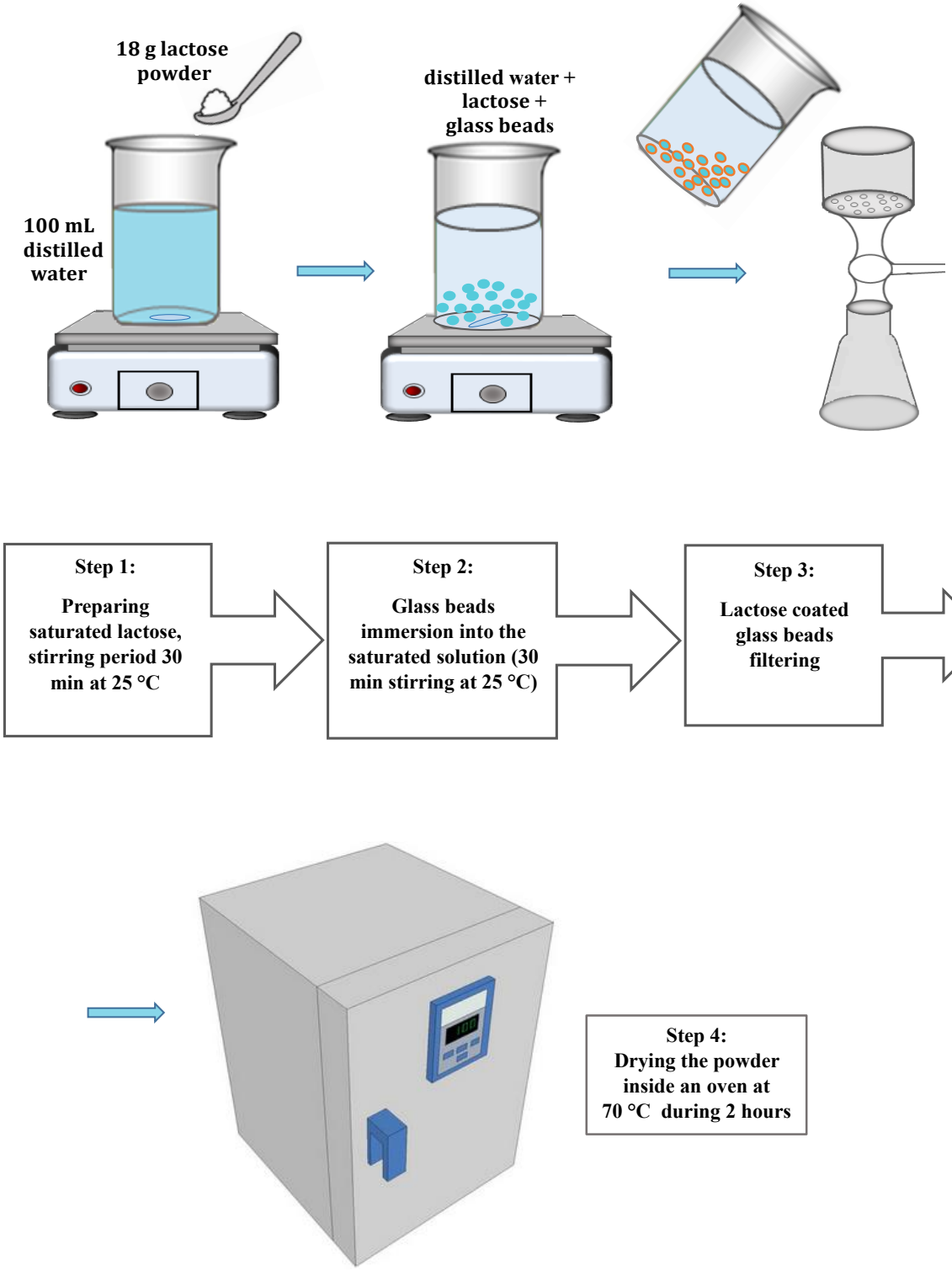

Figure 3.3 Lactose surface coating on glass beads.

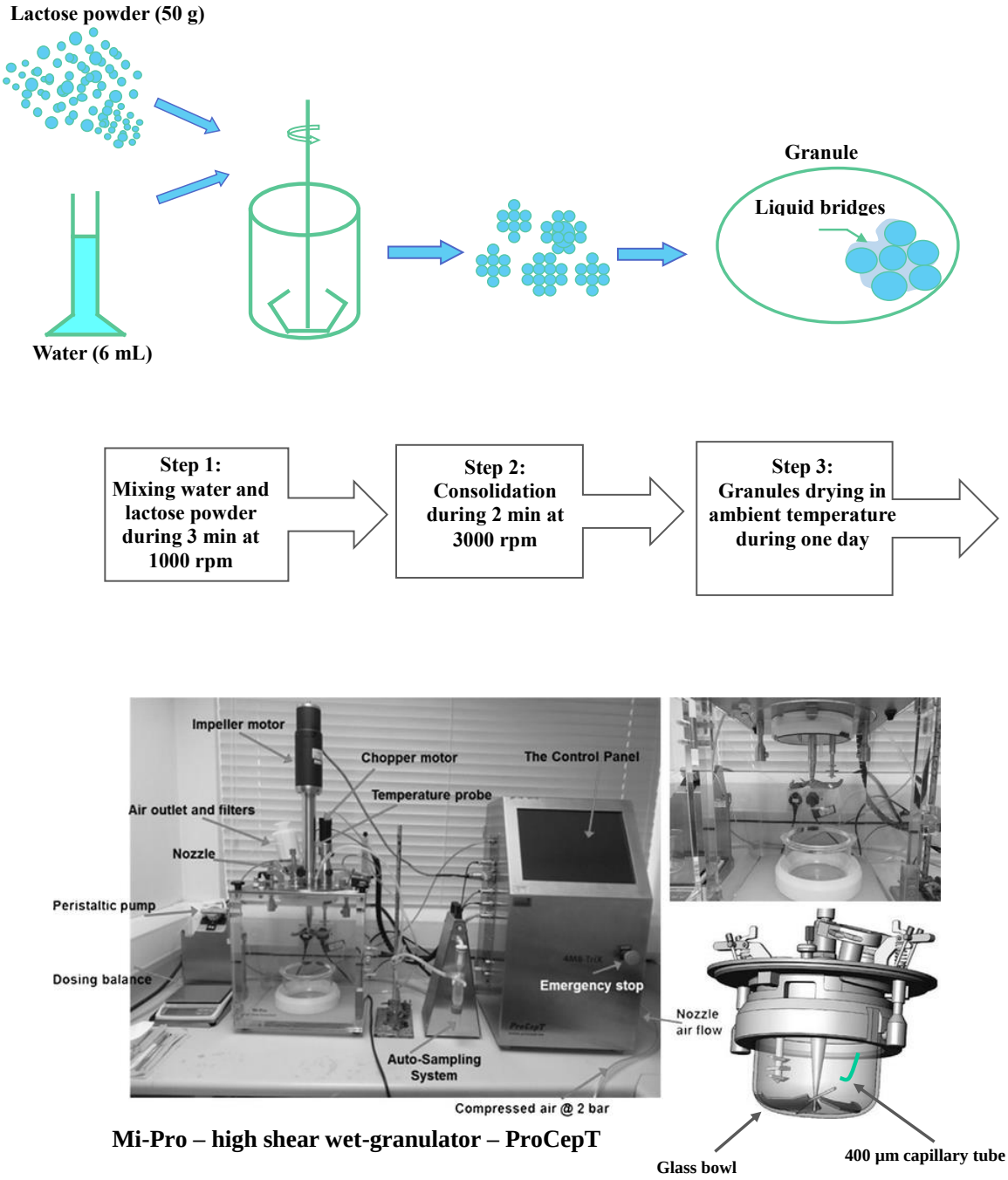

Figure 3.4 Granulation of lactose powder with a Mi-Pro 500 mL equipement (Pro-C-epT granulator) [125].

3.3 Powder flowability based on different particle sizes and surface treatement

The following part is copy of our scientific article presenting the results of the experimental study, entitled **Effect of particle size and formulation on powder rheology**, published in Particulate Science and Technology, DOI: 10.1080/02726351.2020.1738605.

Links between flow properties and formulation of powders of 100 and 500 µm mean particle sizes were investigated. To determine the influence of surface treatment, the flow properties of glass beads were analyzed after various surface treatments leading to hydrophilic, hydrophobic, and lactose- coated surfaces. Furthermore, to investigate the influence of powder core composition, agglomerated lactose powders of circa 100 and 500 µm mean particle size were also produced by high-shear wet granulation and characterized. Hydrophilic and hydrophobic surface treatments did not alter surface topography and particle size distribution, whereas lactose-coated glass beads and agglomerated lactose powders presented noticeable changes of surface structure and particle size increase. Furthermore, all 100 µm powders were classified as easy flowing; hydrophobic glass beads and agglomerated lactose presented the highest and lowest powder flowability, respectively. For 500 µm powders, hydrophilic glass beads and agglomerated lactose powders had the highest and lowest flowability, respectively. The poorer flowability of agglomerated lactose may arise from their angular shape, their higher width of particle size distribution, the lower core density and the higher cohesion of lactose-coated particles. Last, no significant difference of powder compressibility was observed and all studied powders were hardly fluidizable, due to their high particle weight.

3.3.1 Introduction

Flow properties of powders are of great interest, particularly in pharmaceutics, food, cosmetics and ceramic industries. Indeed, the flow behavior of powders is crucial for product design, conveying, packing or transport. Recently, the flowability of hard granular material has been widely considered; dry particulate tribology (theory, experiments and numerical simulations) has been reviewed [126]. The effect of vibration on the flowability of granular materials in an idealized system has been studied by Gaudel et al. [119]: in this system, the glass beads flow down a 40-cm long and 10-cm wide plane that can be inclined up to 35° and the flow is confined. It has been experimentall investigated that the flowability of spherical granular material on inclined plane is highly modified by the application of horizontal vibrations, especially in small angle declined plane where vibrations significantly improve powder flowability. Friction between particles is known to strongly influence the flowability of granular materials and dense suspensions [127, 128]. Dry cohesion and consequently frictional forces can deeply

affect flowability of cohesive particles, and thus, the triggering of the avalanching phenomenon which is known to have a prominent impact on granular flow behavior [129]. Also, as the Young's modulus of particles influences their collision behavior, thus an impact of particle core composition on flowability may be expected. Moreover, it is well-known that inter particle interactions are directly linked to particle surface structure and composition therefore the latter physicochemical characteristics may equally influence powder flowability [130].

The influence of formulation on powder flowability has often been investigated in the literature and it was evidenced that an hydrophobic particle surface enhances powder flowability [131]. This is why the present study intended to investigate the influence of surface treatments (hydrophilic, hydrophobic) and lactose coating on the flowability of glass beads. The influence of core composition (related to particle Young's modulus) was also investigated by comparing flowability of lactose-coated glass beads and agglomerated lactose powders of similar particle size distribution. Powder flowability is highly dependent on environmental conditions (i.e., temperature and relative humidity), as the macroscopic behavior of powders is determined by interparticle interactions. Thus, moisture content of particle surface is another factor to deal with in matter of powder flowability [132]. For instance, the phenomenon of interparticle liquid bridge formation due to moisture uptake from air humidity is known to decrease the flowability [48]. Therefore, hydrophilic and hydrophobic surface treatments as well as lactose coating are expected to interfere with moisture uptake by powders and thus modify powder flowability. Furthermore, particle size (more precisely, the surface-to-volume ratio of particles which generally decreases when increasing particle size) has a significant effect on moisture sorption and flowability of glass beads. In fact, small particles are more susceptible to moisture sorption, leading to poorer flow properties than large particles [132]. The presence of lactose at particle surface may also increase powder cohesion and decrease its flowability, owing to the phenomenon of glass transition, occurring near ambient temperature for lactose powders containing 5 % (w/w) moisture [133]. Indeed, when temperature is increased over the glass transition temperature of lactose, powders covered by amorphous lactose may become sticky, which can even result in powder caking [50, 129]. The main objective of this article is to study the influence of particle surface composition and structure on powder flowability. With this aim, hydrophilic and hydrophobic treatments as well as lactose coating were performed on glass beads of two mean particle sizes (100 and 500 µm). Particle size distributions of samples were checked by laser granulometry. Then, powder flowability was characterized by four standard FT4 rheometer tests (stability, compressibility, aeration, and shear cell tests). FT4 powder rheometer (Freeman Technology) [122, 123] is a universal powder rheometer which provides comprehensive series of methods that allows powder behavior to be characterized in various stress conditions. It has the capacity of providing classification of powder flowability by performing various standard tests [122, 123, 134]. This experimental setup also permitted to investigate if the impact of surface treatment on powder flowability is size dependent. To be able to uncouple the influence of particle surface and core on powder flowability, agglomerated lactose powders were produced by high-shear wet granulation and their granulometric characteristics and flow properties were compared to those

of lactose-coated glass beads.

3.3.2 Materials and methods

Material: glass beads, lactose and chemicals for surface treatment

Glass beads of types S 90–150 µm and S 400–600 µm as well as monohydrate milled lactose powders (200 M) of 32 µm mean size with the bulk density of 530 g/L and packed density of 820 g/L (Meggle group, Wasserburg, Germany) were used for this study. For surface treatments, sulfuric acid (H_2SO_4), 1H,1H,2H,2H-perfluorooctyltriethoxysilane (98 %; Sigma-Aldrich, Germany), hydrogen peroxide (H_2O_2), and toluene(VWR International SAS, France) were employed.

Surface treatment of glass beads

Three types of glass bead surface modifications consisting of hydrophilic and hydrophobic treatments as well as lactose coating have been performed. The hydrophilic treatment [135] was achieved with a 3:1 mixture of sulfuric acid and hydrogen peroxide. First, 50 g glass beads were put in a beaker and immersed in sulfuric acid then hydrogen peroxide was gently added. The mixture was kept 4 h at ambient temperature (20 °C) under extractor hood. After that, glass beads were washed with distilled water and dried during 4 h at 70 °C.

For the hydrophobic treatment [135], the procedure of hydrophilic treatment was first followed, then hydrophilic glass beads were put in 500 mL toluene containing 2.5 g 1H,1H,2H,2H-perfluorooctyltriethoxysilane and the mixture was kept 72 h at ambient temperature under extractor hood. After that, the beads were washed twice with pure toluene, filtered with 125 mL Pro. 4 funnel and finally put 24 h at ambient temperature under extractor hood for drying purposes. A saturated lactose solution (composed of 100 mL distilled water and 18 g lactose) was prepared for lactose coating. Lactose powder was rehydrated during about 30 min at 300 rpm with a magnetic stirrer (IKA RET basic IKAMAG,Sigma-Aldrich, Germany) at ambient temperature. Glass beads of 70 g were then put in the saturated lactose solution under stirring during 30 min. Finally, glass beads were recovered by filtering (125 mL Pro. 4 funnel), then dried in an air oven during 2 h at 70 °C.

Production of agglomerated lactose powder by high-shear wet granulation

Agglomeration of lactose powder [136] was carried out with a 500 mL Mi-Pro granulator vacuum dryer (ProCepT, Zelate, Belgium) and operating parameters were selected with the objective of obtaining powders ranging from 100 to 500 µm mean particle sizes: 6 mL water, 50 g lactose powder, stirring at 1000 rpm, water addition at 2 mL/min during 3 min, and 2 min consolidation time at 3000 rpm chopper speed. Particles were kept in ambient conditions for 1 d for drying purposes. Obtained agglomerated lactose powder was then sieved with mesh sizes of 80 and 180 µm to obtain the 100 µm sample and with mesh sizes of 400 and 600 µm for the 500 µm sample.

Physical properties

The particle size distributions of investigated powders were determined by laser granulometry with a Mastersizer 3000 (Malvern Instruments Ltd., Worcestershire, UK) supplied with an Aero S dry dispersion unit. Dispersion conditions were as follows: 1 bar, 100 % air pressure, 50 % feed rate, and 4 mm hopper length. The size estimator was the equivalent diameter in volume. The median particle size D_{50} and the span were determined. D_{50} is defined as the diameter for which half of the volume of particle population has a lower size. The span represents the width of the particle size distribution and was calculated with the following formula: Span = $(D_{90}$- $D_{10})/D_{50}$. D_{10} and D_{90} are defined as the diameters for which 10 and 90%, respectively, of the volume of particle population has a lower size. To check the efficiency of surface treatment and lactose agglomeration protocols, particle microstructure was imaged with a scanning electron microscope (SEM; S-240 Rustat Road, Cambridge, United Kingdom) operating at 3 kV acceleration voltage. Before analysis, samples were deposited on a carbon adhesive tab (EMSV®77825-12) at ambient temperature and coated with a mixture of gold/palladium for 100 sec in a sputter coater (Polaron SC7640, Thermo VG Scientific, East Grinstead, UK). The images were obtained at two magnifications differing according to powder mean particle size: × 100 and × 600 for 100 µm powders and × 35 and × 120 for 500 µm powders.

Flow properties

Powder rheology was evaluated with a FT4 powder rheometer by performing stability, compressibility, shear cell and aeration tests using 25-mm accessories. In order to observe the influence of hydrophobic treatment on capillary interactions between powders, the shear cell and aeration tests have also been performed on control and hydrophobic glass beads in wet conditions, obtained by adding 1 mL = water to 25 mL = powder. Each test has been replicated three times at ambient temperature with air relative humidity ranging between 30-40 %.

Stability test

The stability test performs a series of seven successive conditioning and test cycles [71, 123, 137, 138]. Conditioning was achieved by the gentle displacement of powder by the downward and upward moving of the rotating blade through the powder bed: it allowed erasing the previous stress history of the powder sample and removing entrapped air. Then, in each test cycle, the rotating blade moved faster through the powder bed contained in a 25 mL vessel and the total input energy required to make impeller flow in the powder bed was deduced from recorded axial force and torque. From these data, the software calculated basic flowability energy (BFE) and specific energy (SE). The BFE represents the total energy needed to displace the whole powder bed during the seventh test. The SE corresponds to the flow energy per mass of powder: it was calculated as the energy needed to displace the powder bed during the upward moving of the blade divided by the mass of analyzed powder sample.

Compressibility test

The compressibility test measures the evolution of powder bed density upon applied normal stress. In a single assay, the sampled powder mass is fixed, thus the evolution of density under compression can be evaluated by volume change. First, the powder was placed in the measurement vessel consisting of two overlaid glass cylinders of 25-mm diameter and 10-mL volume. Sample powder was conditioned, then vessel was split to obtain a precise volume (10 mL) of sampled powder which is compressed with a vented piston at 0.05 mm/sec from 0.50 to 15 kPa. Finally, the compressibility at x kPa was defined as the percentage change in sample volume after x kPa compression. Besides, the conditioned bulk density (CBD) was calculated as split mass of powder over split volume of powder.

Aeration test

The reduction of flow energy upon powder fluidization caused by air circulation through the powder bed can be measured with the aeration test. Before the aeration test begins, three conditioning cycles were performed with the powder sample placed in the measurement vessel fitted with a vented base. Flow energy required to displace the powder bed with the blade moving at 100 mm/sec tip speed was recorded at air velocities from 0 to 50 mm/sec by 10 mm/sec steps for 100 mm powders and from 0 to 100 mm/sec by 20 mm/sec steps for 500 µm powders (maximal air velocity achievable by the FT4 apparatus is 161.2 mm/sec). Aerated energy (AE) corresponded to the flow energy at maximal investigating air velocity and aeration ratio (AR) was calculated as the ratio between BFE and AE. Also, the minimum fluidization velocity was defined as the minimum air velocity required to fluidize the powder bed: it was determined graphically as the air velocity for which the measured flowability energy reached the AE.

Rotational shear cell test

By applying high shear stress with a rotational shear head, FT4 shear cell test evaluates the flowability of powders in confined environments. The shear cell itself was constituted by two overlaid glass cylinders of 10 mL volume. After conditioning, powder was preconsolidated at 9 kPa normal stress. Then, decreasing normal stresses from 7 to 3 kPa by 1 kPa steps were successively applied and the shear stresses (τ) required to make the powder flow (i.e. to induce preconsolidated powder bed failure) were recorded. Then, the software applied the yield locus approach to deduce the major principal stress (σ_1), the unconfined yield strength (σ_c) and powder cohesion (corresponding to the intercept of the yield locus, i.e. the equivalent shear stress causing powder bed failure at 0 kPa normal stress). The flowability index *ff*, characterizing powder flowability, was calculated with the following formula (Equation 3.1):

$$ff = \sigma_1/\sigma_c \tag{3.1}$$

According to the Jenike classification [127], powders were considered as not flowing for $ff < 1$, very cohesive for $1 < ff < 2$, cohesive for $2 < ff < 4$, easy-flowing for $4 < ff < 10$ and free-flowing for $ff > 10$.

The shear cell test has just been carried out with 100 µm powder samples, as 500 µm powders contained too large particles to be measured with the 25-mm vessel.

Statistical analysis

All analyses were triplicated to ensure a good analytical repeatability and presented values correspond to means ± standard deviations. The presence of significant differences between results was checked by one-way ANOVA performed with Excel software version 2016 and means were separated by Tukey's HSD test at $\rho < 0.05$ significance level using the DSAASTAT add-on.

3.3.3 Results and discussion

a. Physical properties

Granulometric characteristics

Figure 3.5 shows the particle size distributions of 100 (Figure 3.5 (A)) and 500 µm (Figure 3.5 (B)) powders. It shows that hydrophilic and hydrophobic surface treatments did not alter the particle size distributions of 100 and 500 µm powders, as granulometric characteristics of control, hydrophilic, and hydrophobic glass beads were similar (Table 3.1). However, agglomerated lactose powders and lactose-coated glass beads presented wider particle size distributions, which was reflected by their higher spans. Median particle size D_{50} of agglomerated lactose (113.0 ± 1.0 µm) was rather close to the target of about 136 µm (corresponding to the mean particle size of control glass beads of 100 µm) while being significantly lower, whereas lactose-coating induced a mean particle size increase up to 155.0 ± 3.0 mm owing to the addition of a lactose layer at the particle surface. It is similar for 500 mm powder samples. The refraction model used to deconvolute the light scattering in these measurements is Mie theory which assumes homogeneous materials characterized by a certain complex refractive index.

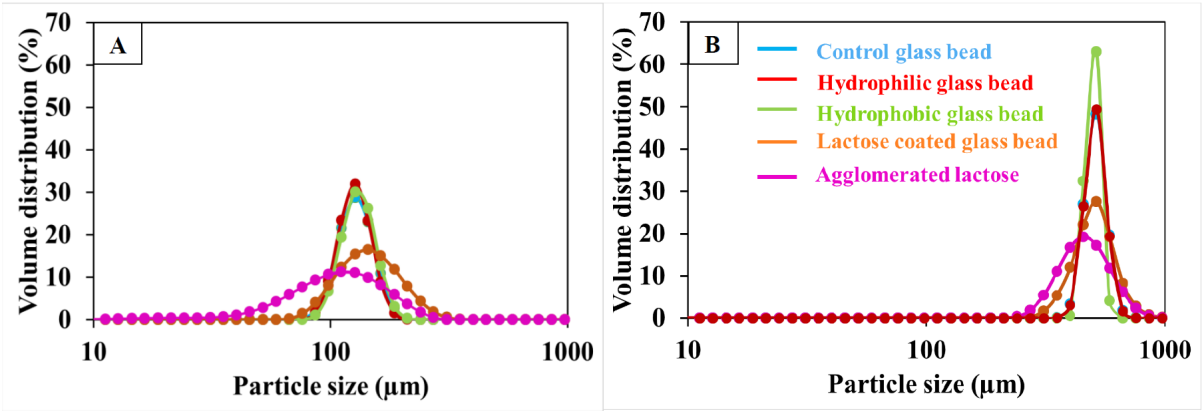

Figure 3.5 Particle size distributions of investigated powders with 100 (A) and 500 µm (B) mean sizes.

Table 3.1 Granulometric parameters of investigated powders.

Particle size	Powders	D_{50} µm	Span (-)
100 µm	Control glass beads	$136.66^{a} \pm 0.66$	$0.44^{b} \pm 0.02$
	Hydrophilic glass beads	$135.00^{a} \pm 0.57$	$0.40^{ab} \pm 0.01$
	Hydrophobic glass beads	$137.00^{a} \pm 1.00$	$0.41^{ab} \pm 0.01$
	Lactose coated glass beads	$155.00^{a} \pm 3.05$	$0.92^{d} \pm 0.09$
	Agglomerated lactose powders	$113.00^{a} \pm 1.00$	$1.18^{e} \pm 0.00$
500 µm	Control glass beads	$543.00^{c} \pm 3.76$	$0.92^{ab} \pm 0.03$
	Hydrophilic glass beads	$537.33^{c} \pm 1.27$	$0.23^{a} \pm 0.00$
	Hydrophobic glass beads	$543.33^{c} \pm 2.67$	$0.29^{ab} \pm 0.00$
	Lactose coated glass beads	$553.33^{c} \pm 29.50$	$0.45^{b} \pm 0.05$
	Agglomerated lactose powders	$476.00^{b} \pm 4.01$	$0.73^{c} \pm 0.01$

Means with different superscripted letters in the same column were significantly different according to Tukey's HSD test ($\rho < 0.05$; n = 3).

Particle appearance

Particle morphology and surface appearance after surface treatment were imaged by SEM (Figure 3.6). Whatever the mean particle size, surface structure of hydrophilic and hydrophobic glass beads was comparable to control glass beads meaning that chemical treatment did not modify surface structure, but lactose-coated glass beads were a little larger and their surface was wrinkled (similarly to agglomerated lactose). SEM permitted to confirm the heterogeneity of particle sizes of lactose-coated and agglomerated lactose samples previously evidenced by laser granulometry. The increase in span induced by lactose-coating or wet granulation has been already reported in the literature [137, 139, 140].

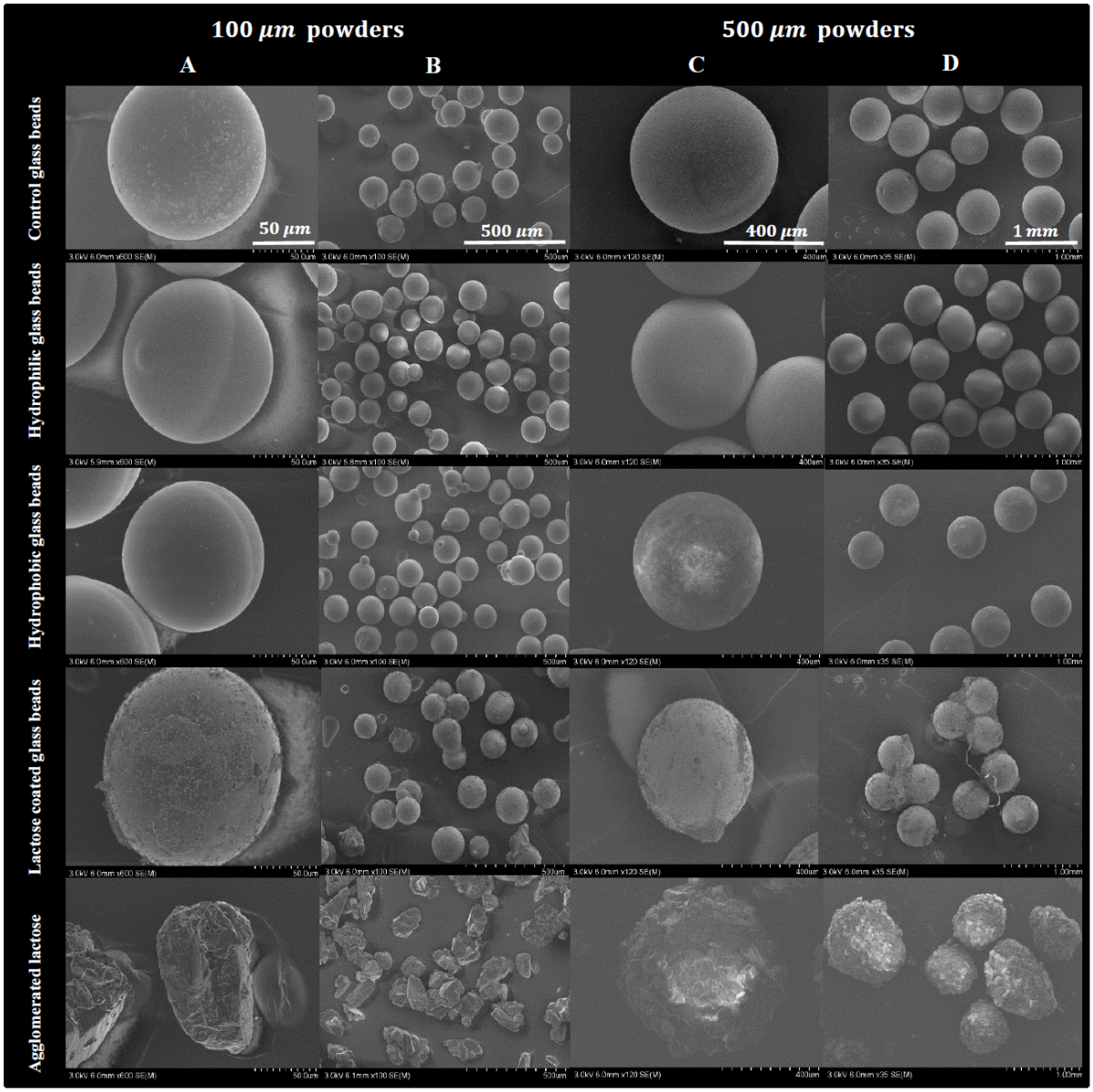

Figure 3.6 SEM images of investigated powders (magnification for 100 µm powders: × 600 (A) and × 100 (B); magnification for 500 µm powders: × 120 (C) and × 35 (D)).

b. Powder flow properties

Stability

Table 3.2 represents the mean flow parameters determined in stability and aeration tests for 100 and 500 µm powders. Based on BFE results, two groups of powders can be defined whatever the mean particle size: control, hydrophilic, and hydrophobic glass beads exhibited the lowest BFE, whereas lactose-coated glass beads and agglomerated lactose had the highest BFE. This denoted better flow properties of control, hydrophilic, and hydrophobic glass beads, which was logical owing to the spherical shape of these particles; indeed, lactose coated glass beads and agglomerated lactose were composed of wrinkled spherical particles and angular particles, respectively [137]. It is worth noting that BFE measures the energy required to put

in motion a given volume of powder bed: it is informative of powder flowability in low-stress conditions, but powder density has an important impact on BFE values. SE is generally more efficient to sort powders according to their flowability, as it corresponds to flow energy per mass of powder sample and it is a good indication of powder cohesion in low-stress conditions [137]. For 100 µm powders, three groups can be formed from SE results: first, control and hydrophilic glass beads had very low SE (under 2 mJ/g) indicating very good flowability, then hydrophobic and lactose-coated glass beads had low SE around 3 mJ/g showing a good flowability, last, agglomerated lactose had higher SE (about 5 mJ/g) which can be interpreted as correct powder flowability. For 500 µm powders, the same classification was obtained, except that hydrophobic glass beads had closer SE to control and hydrophilic glass beads (i.e. SE values led to the same powder classification as BFE for 500 mm powders). Then, hydrophobic surface treatment decreased flowability of 100 µm glass beads but not the one of 500 µm glass beads. This may due to the fact that the relative importance of cohesive forces was decreased when increasing the particle size. It should also be noticed that BFE and SE of 500 µm powders were generally lower than those of 100 µm powders, which was logical as large particles have lower contact points, then interparticle friction is decreased and powder flowability improved, in comparison with powder samples composed of small and/or irregular particles. The poorer flowability of lactose-coated glass beads and agglomerated lactose powder may be explained by their more irregular particle shape [137]. Similar results have been reported in the literature [121, 122, 140]. Also Table 3.2 displays the CBD values of all tested particles. All the particles with glass core logically showed higher density than agglomerated lactose. In general, a lower powder density is detrimental to powder flowability and CBD results were consistent with the lower flowability of agglomerated lactose in comparison with lactose-coated glass beads.

Aeration

Figure 3.7 shows the evolution of flow energy with air velocity: it appeared that 100 µm powders reached a fluidized state in the conditions of the aeration test, whereas 500 µm powders were not fluidized even when increasing the air velocity up to 100 mm/sec (the standard FT4 aeration test has a maximal air velocity of 10 mm/sec). This can easily be explained by the fact that 500 µm particles had a well higher weight than 100 µm particles, then making it more difficult to suspend them in the air. For 500 µm powders, only agglomerated lactose seemed significantly sensitive to aeration, as its flow energy markedly decreased with air velocity. This is in accordance with the fact that agglomerated lactose had the lowest density of studied powders. These observations were confirmed by AR and AE values reported in Figure 3.7. 100 µm powders had well lower AE and higher AR than 500 µm powders. Generally, powders with low AR values are cohesive and/or have a high weight; consequently, they require a higher air velocity for fluidization [134, 137]. Thus, according to the classification of powders based on AR values proposed by Freeman Technology, studied 100 µm powders fall in the category of average sensitivity to aeration.

Minimal fluidization velocities obtained for 100 µm powders ranged from about 16 to 31 mm/sec, which is rather high and can be explained both by the large size of 100 µm powders and the elevated true density of particles (close to glass density, i.e. about 2.5 g/cm^3, for control, hydrophilic, hydrophobic, and lactose-coated powders and close to lactose specific density, i.e. about 1.5 g/cm^3, for agglomerated lactose), leading to high particle mass. Minimal fluidization velocity of 500 µm agglomerated lactose was estimated at circa 126.5 ± 5.5 mm/sec by linear regression of the curve presented in Figure Figure 3.7 (B); this value is huge which illustrates the difficulty to fluidize 500 µm particles. Minimal fluidization velocities permitted to draw the general classification of 100 µm powders sensitivity to aeration as follow: control glass beads > hydrophobic glass beads > hydrophilic glass beads > agglomerated lactose powders > lactose-coated glass beads.

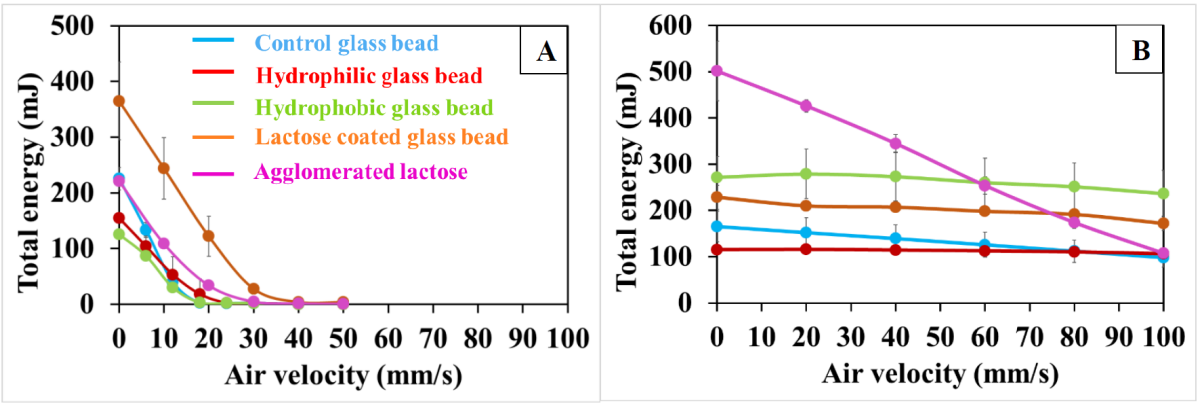

Figure 3.7 Evolution of flowability energy of the powder bed with air velocity during the aeration test for studied powders of 100 (A) and 500 (B) µm mean sizes. Error bars represent standard errors; some were not visible as their size was inferior to the marker size.

Table 3.2 Stability and aeration test results of 100- and 500-µm mean size powders.

Powders	BFE (mJ)	SE(mJ/g)	AE(mJ)	AR(-)	Minimum fluidization velocity (mm/sec)*	CBD (g/mL)
100 µm						
Control glass beads	$171.52^{ab} \pm 5.63$	$1.95^{a} \pm 0.00$	$1.75a^{a} \pm 0.14$	$129.92^{c} \pm 4.36$	$16.86^{a} \pm 0.02$	$1.46^{d} \pm 0.00$
Hydrophilic glass beads	$217.76^{bc} \pm 11.22$	$1.92^{a} \pm 0.01$	$1.60^{a} \pm 0.04$	$100.25^{b} \pm 3.10$	$20.47^{ab} \pm 3.15$	$1.46^{de} \pm 0.00$
Hydrophobic glass beads	$234.06^{bc} \pm 2.75$	$3.03^{b} \pm 0.05$	$1.45^{a} \pm 0.66$	$89.63^{b} \pm 1.35$	$17.67^{a} \pm 0.04$	$1.46^{de} \pm 0.00$
Lactose coated glass beads	$372.20^{d} \pm 6.88$	$3.13^{b} \pm 0.06$	$2.26^{a} \pm 0.23$	$160.63^{d} \pm 5.28$	$31.7^{b} \pm 0.82$	$1.29^{c} \pm 0.00$
Agglomerated lactose powders	$295.52^{cd} \pm 14.48$	$5.05^{c} \pm 0.18$	$0.89^{a} \pm 0.00$	$248.68^{e} \pm 0.75$	$22.98^{ab} \pm 0.26$	$0.59^{a} \pm 0.00$
500 µm						
Control glass beads	$158.76^{ab} \pm 5.13$	$1.82^{a} \pm 0.10$	$106.33b^{b} \pm 4.55$	$1.60^{a} \pm 0.05$	*n.a.*	$1.49^{ef} \pm 0.00$
Hydrophilic glass beads	$99.16^{a} \pm 2.24$	$1.25^{a} \pm 0.00$	$106.73^{b} \pm 0.00$	$1.09^{a} \pm 0.10$	*n.a.*	$1.50^{f} \pm 0.00$
Hydrophobic glass beads	$191.20^{b} \pm 12.61$	$2.10^{a} \pm 0.10$	$236.33^{d} \pm 29.05$	$1.15^{a} \pm 0.03$	*n.a.*	$1.47^{def} \pm 0.00$
Lactose coated glass beads	$353.39^{d} \pm 31.43$	$3.56^{b} \pm 0.16$	$172.00^{c} \pm 7.22$	$1.23^{a} \pm 0.02$	*n.a.*	$1.28^{c} \pm 0.00$
Agglomerated lactose powders	$351.62^{d} \pm 33.57$	$4.64^{c} \pm 0.50$	$107.00^{b} \pm 1.89$	$4.70^{b} \pm 0.41$	$125.56^{c} \pm 5.50$*	$0.67^{b} \pm 0.00$

n.a.: not applicable. Estimated by linear regression of corresponding curve in Figure Figure 3.7(B). Means with different superscripted letters in the same column were significantly different according to Tukey's HSD test ($\rho < 0.05$; n = 3).

Compressibility

The evolution of compressibility according to applied normal stress is displayed in Figure 3.8 for 100 and 500 µm powders. Compressibility of 100 µm powders increased from 1-2 % to 2-4 %, while for 500 µm powders it evolved from 0.5-2.5 % to 1-4 %, showing that the range of compressibility of investigated powders was not dependent on mean particle size. Compressibilities at 15 kPa were very low (inferior than 5%), meaning that very good flow properties may be expected for investigated powders, consistently with BFE and SE results. Indeed, compressible powders require higher flowability energy to be put in motion; when trying to displace them, the powder bed first undergoes compaction before it could move [123,136].

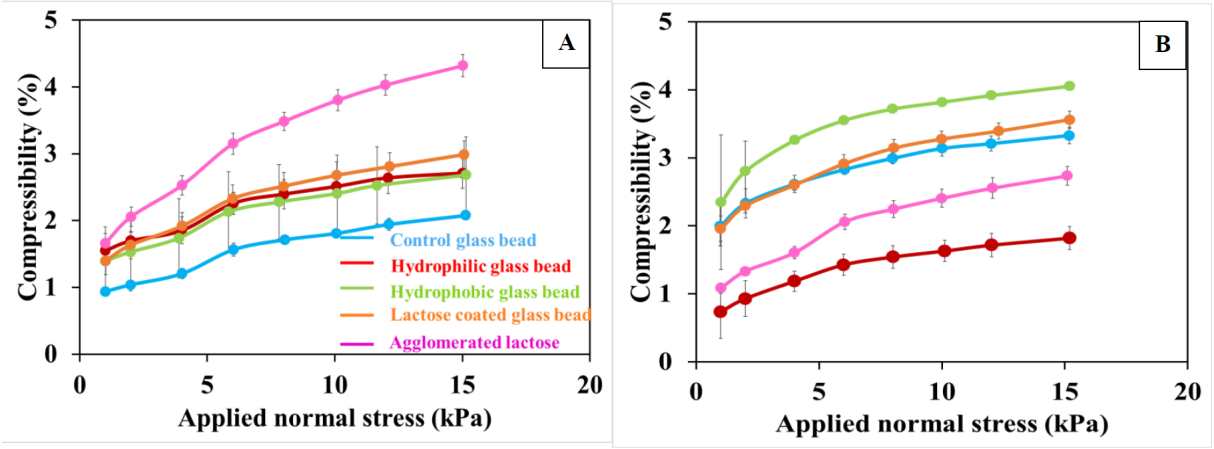

Figure 3.8 Evolution of powder compressibility with applied normal stress for studied powders of 100 (A) and 500 (B) µm mean sizes. Error bars represent standard errors; some were not visible as their size was inferior to the marker size.

Shear cell

Shear stress versus applied normal stress curves obtained during the shear cell test for 100 µm powders are presented in Figure 3.9 and flow characteristics (cohesion and flow factor) deduced from these curves following the yield locus approach which are listed in Table 3.3. A higher shear stress at a given applied normal stress denotes poorer powder flowability in high-stress conditions, as shear stress represents the force needed to induce consolidate powder bed failure, i.e. relative motion of particles within the powder bed. Following this, powder flowability in high-stress conditions increased in the following order: agglomerated lactose powders < lactose coated glass beads < hydrophilic glass beads ≈ ctrol glass beads ≈ hydrophobic glass beads. This is globally consistent with stability and compressibility results. Flow parameters deduced from the yield locus approach for 100 µm powders confirmed these observations (Table 3.3). All powders exhibited low cohesion ranging from 0.20 to 0.42 kPa, in agreement with the good flowing and aeration properties previously evidenced. Cohesion of investigated powders increased in the following order: hydrophobic glass beads ≈ control glass beads ≈ < hydrophilic glass beads ≈ lactose coated glass beads < agglomerated lactose powders. Also, ff values were found over 10 for all

100 µm powders, indicating that they were "free-flowing." Such excellent flow properties were expected for powders composed of large particles. On the basis of ff values, powder flowability in high-stress conditions increased as follow: agglomerated lactose powders < lactose-coated glass beads < hydrophilic glass beads ≈< hydrophobic glass beads ≈ control glass beads. The higher density and sphericity of lactose-coated glass beads in comparison with agglomerated lactose may explain the better flowability of the former. In order to clarify the influence of hydrophobic treatment on glass beads, the shear cell test was performed on control and hydrophobic glass beads after water addition. In wet conditions, control glass beads flowability was markedly decreased, as denoted by the increase in cohesion from 0.20 to 2.05 kPa and the decrease in flow factor from 19.70 to 2.43, whereas flowability of hydrophobic glass beads remained correct (cohesion increased from 0.20 to 0.30 kPa and flow factor decreased from 17.27 to 14.96). This "protecting" effect of the hydrophobic treatment against cohesion increase in wet state was also evidenced by the strong decrease of fluidizability of control glass beads, to be compared to the small decrease of fluidizability of hydrophobic glass beads (see Supporting Information presenting aeration test results for wet control and hydrophobic glass beads). The shear cell test could not be carried out on 500 µm powders, because some particles of 500 µm powder samples may be too large to be correctly analyzed with the FT4 25-mm vessel. Indeed, according to Freeman Technology support, the clearance gap (distance between blade and vessel wall) for 25-mm vessel is 750 µm. Consequently, particle trapping may occur for investigated samples (especially for lactose coated glass beads and agglomeration lactose that have maximal particle size of circa 900 µm), thus impairing result accuracy and reliability.

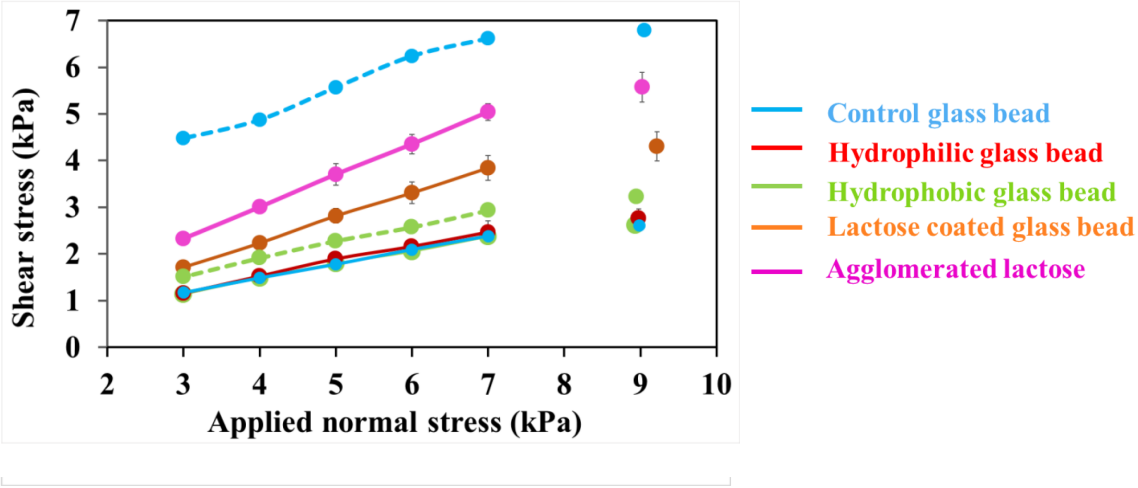

Figure 3.9 Evolution of shear stress with applied normal stress after preshear at 9 kPa for 100 µm powders. Error bars represent standard errors; some were not visible as their size was inferior to the marker size. Solid lines: dry powders, dash lines: wet powders.

Table 3.3 Flow parameters derived from shear cell test for 100 µm mean size powders.

Powders	Cohesion (kPa)	*ff* (-)
Control glass beads	$0.20^{a} \pm 0.00$	$19.70^{d} \pm 0.81$
Hydrophilic glass beads	$0.27^{ab} \pm 0.02$	$17.27^{cd} \pm 0.40$
Hydrophobic glass beads	$0.20^{a} \pm 0.01$	$19.74^{d} \pm 1.66$
Lactose coated glass beads	$0.31^{ab} \pm 0.03$	$13.44^{bc} \pm 1.21$
Agglomerated lactoses	$0.42^{b} \pm 0.06$	$10.01^{b} \pm 1.44$
Wet cnontrol glass beads	$2.05^{c} \pm 0.06$	$2.43^{a} \pm 0.07$
Wet hydrophobic glass bead	$0.30^{ab} \pm 0.00$	$14.96^{bcd} \pm 0.44$

Means with different superscripted letters in the same column were significantly different according to Tukey's HSD test ($\rho < 0.05$; n = 3).

3.3.4 Supplemental data

In order to put in evidence the influence of hydrophobic treatment on the flowability of glass beads, 1 mL distilled water was added to 25 mL of hydrophobic and control glass beads, separately, before performing the aeration test. As displayed in figure Figure 3.10, glass beads sensitivity to aeration was strongly impaired by the addition of water, presumably because capillary forces induced by the presence of water at the glass bead surface markedly increased interparticle cohesion, which is detrimental to powder fluidization. Wet and dry hydrophobic glass beads were fluidized between 0 and 100 mm/s, as reflected by the AE, AR and minimal fluidization velocity values. Also, control glass beads in dry state were fluidizable, but not wet control glass beads, consistently with the fact that the cohesion induced by the presence of water was well more important for control glass beads than for hydrophobic glass beads. Thus, hydrophobic treatment may help reducing cohesion caused by interparticle capillary forces.

Table 3.4 Aeration test results obtained for wet and dry hydrophobic and control glass beads (100 µm mean size).

Powders	AE (mJ)	AR(-)	Minimum fluidization velocity (mm/s)
Control glass beads	$1.75^{a} \pm 0.14$	$129.92^{c} \pm 4.36$	$16.86^{a} \pm 0.02$
Hydrophobic glass beads	$1.45^{a} \pm 0.66$	$89.63^{b} \pm 1.35$	$17.67^{a} \pm 0.04$
Wet control glass beads	$184.16^{b} \pm 3.89$	$1.08^{a} \pm 0.02$	$523.08^{b} \pm 99.08$
Wet hydrophobic glass beads	$2.21^{a} \pm 0.30$	$147.48^{d} \pm 4.00$	$41.78^{a} \pm 0.18$

Means with different superscripted letters in the same column were significantly different according to Tukey's HSD test ($\rho < 0.05$; n = 3).

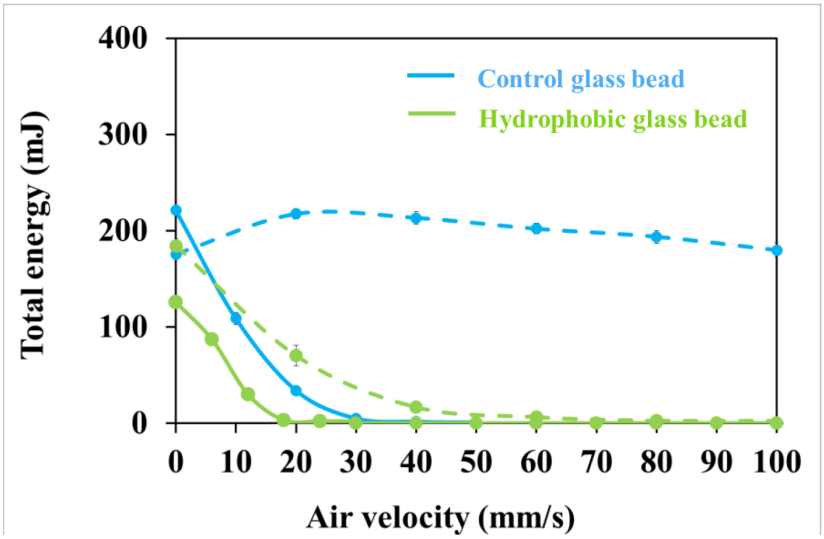

Figure 3.10 Evolution of flowability energy of 100 µm mean size powders with air velocity during the aeration test. Error bars represent standard errors; some were not visible as their size was inferior to the marker size. Solid line: dry powders; dash line: wet powders.

3.3.5 Conclusion

The objective of this study was to evaluate the influence of particle size, chemical surface treatment, and core composition on powder flowability. Therefore, control glass beads were compared with surface-treated glass beads (hydrophilic, hydrophobic, lactose-coated) and agglomerated lactose powders with mean particle sizes of 100 and 500 µm. Whatever the mean particle size, the particle size distribution of investigated powders was not modified by hydrophobic and hydrophilic surface-treatments, whereas agglomerated lactose and lactose-coated glass beads had close mean particle sizes and wider particle size distributions. These results were confirmed by SEM which showed that surface of hydrophilic, hydrophobic, and control glass beads had the same appearance. Lactose-coated glass beads were a little larger and less monodisperse and presented a more wrinkled surface, whereas agglomerated lactose particles were a little smaller and had a rather irregular and angular shape. Furthermore, FT4 rheological tests permitted to obtain a general classification of powders according to flowability: in decreasing order, hydrophobic glass beads $\approx$ control glass beads $\approx$ hydrophilic glass beads $>$ lactose coated glass beads>agglomerated lactose. The higher cohesion and wider spans of lactose-coated glass beads and agglomerated lactose, as well as the more irregular shape and lower density of agglomerated lactose particles were likely responsible for their poorer flowability. All powders were hardly fluidized, owing to their high weight (resulting from their high density and/or size): 100 µm powders only reached a fluidized state between 16 and 31 mm/sec air velocity. For 100 µm powders, the hydrophobic treatment was rather effective in preserving the fluidisability of wet hydrophobic glass beads, whereas wet control glass beads became hardly fluidizable, as denoted by the minimum fluidization velocities of wet control and hydrophobic glass beads: 523 and 41 mm/sec, respectively.

3.4 Surface hardness and elasticity of formulated powders

The indentation was developed in early 1670 as characterization technique to measure the hardness value and elastic properties of samples [141–143], normally the depth-sensing indentation is used to extract the elastic properties by knowing indenter geometry and material properties [144].

For our experiments the nanoindentation experiments were conducted using the Berkovich indenter (Bruker Hysitron TI premier) with diamond tip. Appropriate load function (loading time 14 s, holding time 5 s and unloading time 15 s) was used for all the samples. The hardness (H (GPa)) and Young's modulus (E_r (GPa)) were obtained as a function of load (or penetration depth).

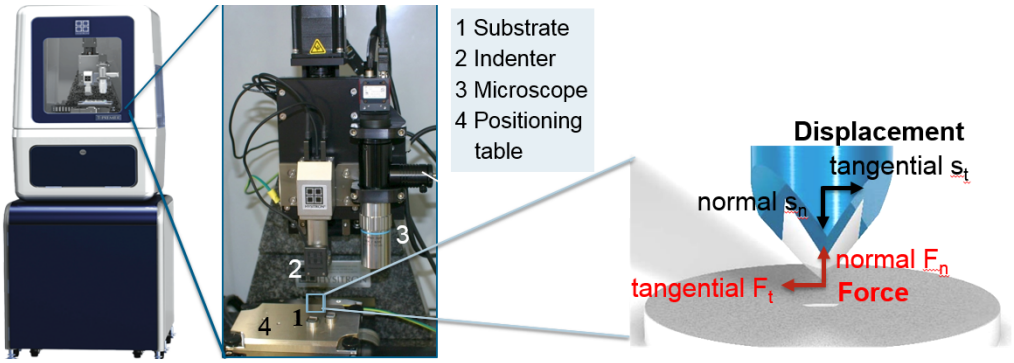

Figure 3.11 Schematic of Nano/Tribo-Indenter (Hysitron).

In an indentation test a hard tip is presses onto a sample surface and then the load placed on the indenter tip increases as the tip penetrates further into the sample until to reache a pre-defined value. At this point, the load holds constant for a period. The area of the residual indentation in the sample gets measured and the hardness H (GPa) is defined as the maximum load $P_{max}(\mu N)$ divided by the residual sample area $A_r(nm^2)$:

$$H = P_{max}/A_r \tag{3.2}$$

Figure 3.12 shows an example of typical force-displacement curve obtained by nanindentation test. The size of impression is calculated indirectly by relating the projected area to the penetration depth.

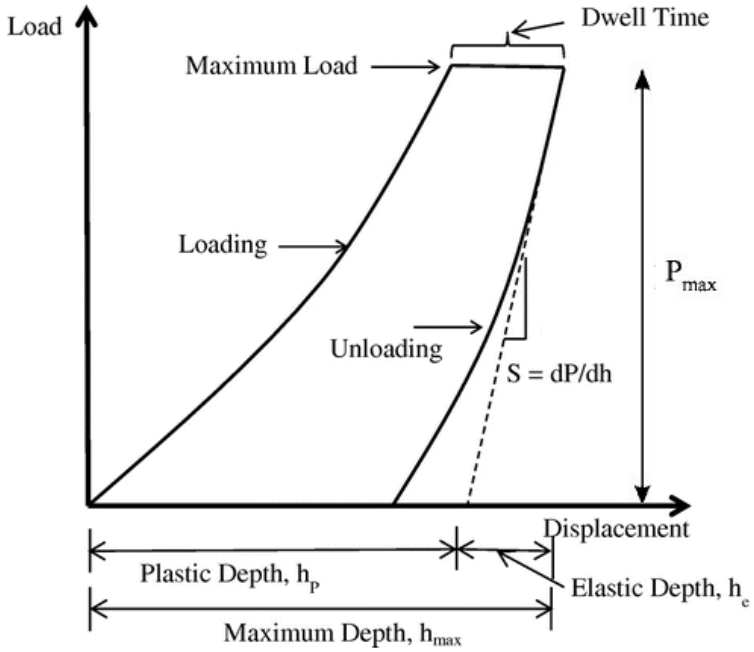

Figure 3.12 Schematic representation of loading-unloading curve for a nanoindentation measurement; $P_{max}(GPa)$ is the load at maximum indentation, $h_{max}(nm)$ is the indenter displacement at peak load. $h_p(nm)$, $h_e(nm)$, dp/dh ($\mu N/nm$) are depth of residual impression, displacement associated with elastic recovery during unloading and contact stiffness, respectively [145, 146].

Young's modulus, E (GPa), is a measure of the stiffness of a material and is defined as the ratio of stress σ (GPa) to strain ϵ $(-)$ as follow,

$$E = \frac{\sigma}{\epsilon} \tag{3.3}$$

In an indentation, the stiffness of the contact is used to calculate the reduced Young's modulus E_r,

$$E_r = \frac{\sqrt{\pi}}{2}\frac{S}{\sqrt{A}} \tag{3.4}$$

where S (GPa) is the contact stiffness and A is the projected contact area between the indenter and the particle (see Figure 3.11). The reduced modulus of the contact is function of Young's modulus $E_r(GPa)$ and poisson ratio ν (-) of the sample and indenter as follow,

$$\frac{1}{E_r} = \frac{1-\nu_s^2}{E_s} + \frac{1-\nu_i^2}{E_i} \tag{3.5}$$

where subscripts s and i refer to the sample and indenter, respectively.

The minimum particle size that can be measured with nanoindenter TIPremier is 200 nm, the force range applied by indenter is ranged as 70 nN-70 N by displacement limit of 0.2 nm-7 μm and with the resolution of 1 nN/0.1 nm. The nanoindenter TIPremier is used already to measure the Young's modulus [147], stiffness of particle during loading/unloading [147], plastic displacement [148] and Rolling, sliding friction

coefficient [149]. In our study, the nanoindentation tests have been done for measuring the hardness of our four formulations: control, hydrophilic, hydrophobic and lactose coated glass beads with the size of 500 µm. Here, all the measurements as well as all figures except Figure 3.12 have been realized by our project partner in university of Kaiserslautern in Germany. The measurements have been carried out in ambient temperature at room humidity.

Figure 3.13 presents the indentation load-displacement curve for our four formulations: control, hydrophilic, hydrophobic and lactose coated glass beads. 10 different particles for each treatment were measured. As mentioned before, the maximal load was 10 mN by a loading time of 15 sec, a hold time of 5 sec and an unloading time of 15 sec were used for this measurement. Because of the hold time, it can be seen a plateau at the maximum force in each curve. This plateau results from the thermal drift during the measurement.

Figure 3.14 presents reduced modulus measured for control, hydrophilic, hydrophobic and lactose coated glass beads. The reduced elastic/Young's modulus and hardness are more or less the same. Control, hydrophilic and hydrophobic glass bead presented more or less similar hardness and lactose coated glass bead showed less hardness than aforementioned three powder samples. This lower hardness can be due to the addition of lactose coating around glass bead surface. This lower hardness has been confirmed with the more displacement of lactose coated glass bead under load of indenter in Figure 3.13. It should be indicated that performing measurement on lactose coated glass bead was very complicated due to capillary forces therefore the measurement on agglomerated lactose powder has not been performed.

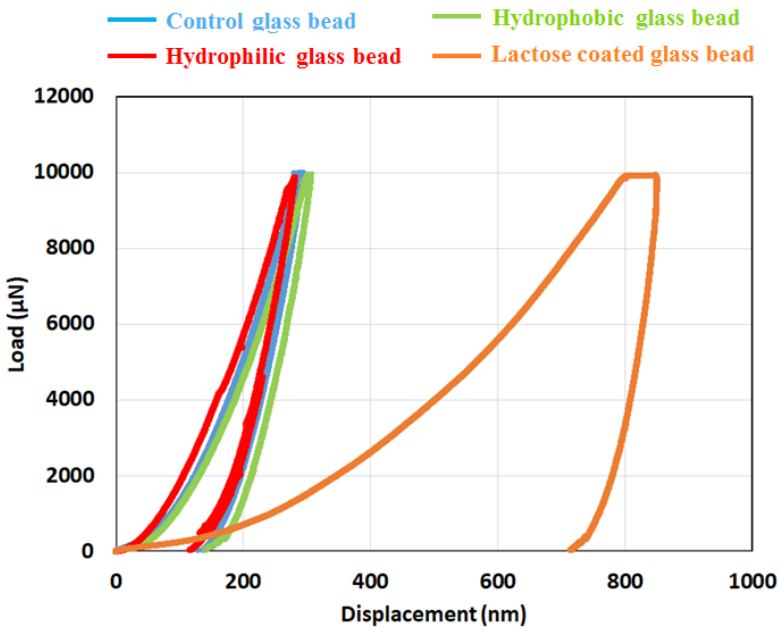

Figure 3.13 Indentation load-displacement curves of control, hydrophilic, hydrophobic and lactose coated glass beads with the size of 500 µm.

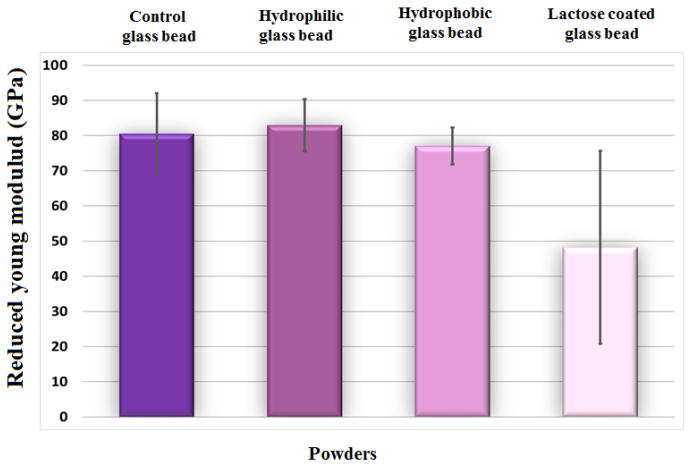

Figure 3.14 Reduced modulus measured for control, hydrophilic, hydrophobic and lactose coated glass beads by nanoindentation with the size of 100 µm.

Mechanical properties of powders play an important role in powder research & development including powder dosage form design and manufacturing in pharmaceutical sector, particle size control and compaction behavior as well as chemical sector, food industry, etc [150–154]. Whereby, better understanding of structure-mechanical property relationships saves the industries from huge economic loss [155]. Nanoindentation provides valuable information on the mechanical properties of powders. Especially, it allows indentation measurements to be conducted on individual particles or crystals [156].

In a research conducted by Cao, et al. [154] on hardness of pharmaceutical powders, they found out that the powders with very low or high particle hardness are most likely to exhibit poor compaction, while the materials with medium particle hardness are expected to have a good compaction behavior [157]. They have classified the powders hardness as follow: (a) low hardness $H < 1$ GPa (b) medium hardness 1 GPa $< H < 5$ GPa (c) high hardness $H > 5$ GPa.

In our measurements, the obtained hardness values for control, hydrophilic, hydrophobic and lactose coated glass beads are respectively as follow: 7.50 ± 2.15, 7.57 ± 1.19, 6.98 ± 1.4 and 4.68 ± 2.30 GPa.

It was not possible to find the technique applied to systems similar as ours. But, based on a nanoinditation measurement performed on pharmaceutical powders, the lactose powder presented a hardness value between 0.18 and 0.51 GPa [154, 157].

Therefore, considering the classification presented in Ref [157], our four formulations have high hardness value, which is proof of good flowing behavior. Except, the lactose coated glass bead that has presented a lower value of hardness (reduced modulus) in compare with other three powders. That is may due to the lactose coating on glass bead surface. The large standard deviation corresponding to lactose coated glass bead can be due to the inhomogeneous nature of lactose on glass bead surface.

In addition, concerning the effect of temperature on cohesive powders, nanoindentation revealed an increase in surface hardness as a result of storing powder at high temperature [158]. The effect of

humidity on five powder formulations will be discussed in the following chapters.

3.5 Concluding diagram

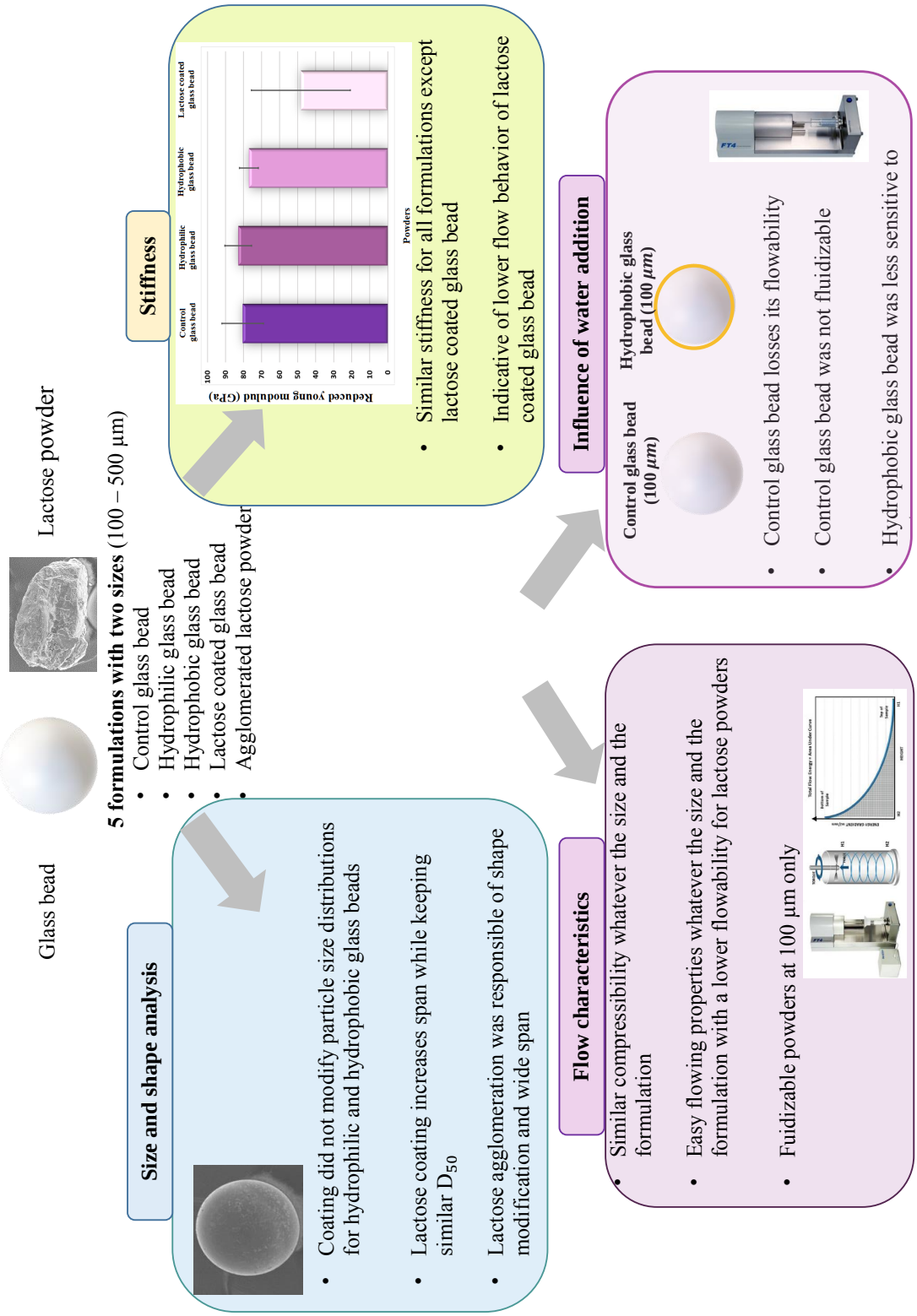

Figure 3.15 Concluding diagram.

Chapter 4

Comparison of different flow measurement techniques

4.1 Introduction

Many factors influence the powder behavior like surface formulation and roughness, particles size, environmental situation (humidity,temperature, aging, etc). All these factors may modify the mechanical properties of the particles and their interactions during the flow, such as the friction and the cohesion. Because of this complexity, it may be difficult to characterize the flowability of a powder. Any difference in the flow conditions may modify the result.

To evaluate the reliability of different techniques, powders ranking was done in terms of flowability by using different measurement equipements. Three types of equipements have been compared in this study: FT4 Rheometer, Granutools and Rheometer Discovery-HR3. The FT4 rheometer has been used with the five formulations and the following tests: stability, shear cell, compressibility and aeration. The Granutools equipment was used to perform GranuFlow, GranuDrum, GranuPack, GranuCharge and GranuHeap. Each test provided different factors and indexes like as flow index, Hausner ratio, charge density, etc to provide a better understanding of powder behavior. The third equipment is the Discovery-HR3 Rheometer utilized for powder characterization. This rheometer measures the powder flow by imposing a wide range of shear rate or shear stress and at the result measures the viscosity curve.

At the final, the powder behavior has been analyzed by controlling external conditions. In this case, the powders are kept in a humid chamber (at 50 % RH) with the fixed temperature (20 °C). Then their flow behavior has been studied and compared with the bahvior of dry powders. Two rheometers have been implemented for the characterization: FT4 and Discovery-HR3 with a cylindrical Couette cell (vane geometry).

4.2 Powder characterisation with Granutools equipement

4.2.1 Granutools methodology

GranuFlow

By the different diameter orifices, it is possible to assess the powder flowability by measuring the powder fall through these orifices. This technique is based on a study conducted by Berverloo et al [110] they found out that the discharge mass flowrate is depending only on the opening diameter which powders fall through.

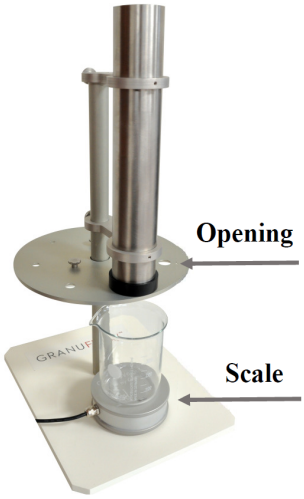

Figure 4.1 Schematic of GranuFlow® equipment.

The GranuFlow equipment in Figure 4.1 is a relatively simple device based on Beverloo law to draw flow curves as a function of different opening diameters. It is equipped with a cylindrical stainless steel tube with a capacity of 500 mL and a disk with 7 different diameter size openings from d = 2 mm to d = 28 mm, through which the powder pass from each opening one by one. The powder is introduce inside the tube by a glass funnel and at the base of the device a container collects the quantity of powder passed through the orifice. A scale placed under container measures continuously the powder mass. The instrument is connected to a software which allows to record the evolution of the flow rate depending on the opening diameter then the obtained data are expressed as a function of collected powder mass and the flow time of powder. The mass flow rate (F) through a circular orifice of diameter (d) is function of the mean speed of the particles ($< v_{out} >$), the aperture diameter and the bulk density (ρ_b) as follow:

$$F = \rho_b < v_{out} > \pi \frac{d^2}{4} \tag{4.1}$$

By taking into account that the Beverloo's law is based on two hypotheses:

- The powder flow blocks if the orifice diameter is below a threshold d_{min}.

- The powder fall free passing through the orifice meaning that $v_{out} = \sqrt{2gd\beta}$.

This equation comes from the idea that the jamming mechanism is due to the formation of a semi-spherical arch before the orifice. The value of β is as $\beta = 0.5$, in the case of having proportional size between this arch and orifice. In general, the parameter β can be a free parameter.

Finally, the mass flow rate expression becomes as follow which is representation of Berverloo law:

$$F = \frac{\sqrt{2\beta\rho_b}\pi}{4}\sqrt{g}(d - d_{min})^{2.5} = C\sqrt{g}(d - d_{min})^{2.5} \tag{4.2}$$

Where, by measuring the flow rate F depending on the orifices size d, the flow index C can be obtained by using the Beverloo model (Equation 4.2). The flow index C, expressed in g/ml can be interpreted as the ability of a powder to flow, here g is the gravity of earth (9.81 m/s).

It has to indicate that his method is recommended to measure the flowability of powders with a minimum free flow while for the powders with high cohesion it is not practical since the powder flow through the orifices of GranuFlow is not possible in this case [159].

GranuDrum

The powders can keep their static state despite a certain inclination, however if this static state breaks, only the particles belonging to the surface layer will be set in motion and the rest will keep the static state, this phenomenon is called avalanche. Determining the angle in which this phenomenon happens allow to prevent it. This Dynamic angle has widely studied in literature for cohesive [79, 80] and non-cohesive powders [15, 78].

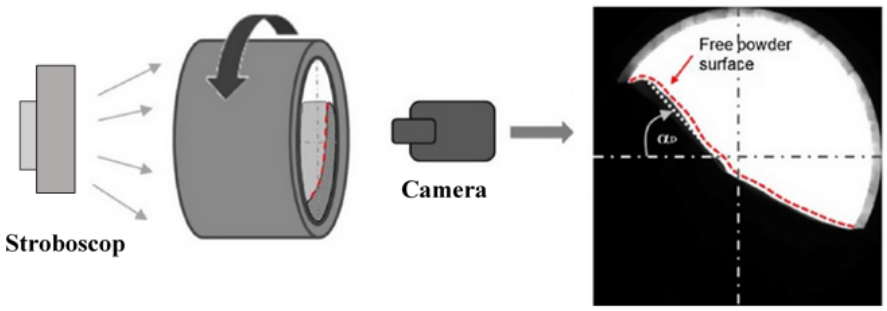

Figure 4.2 Experimental set-up in GranuDrum [160].

The GranuDrum is used in this thesis to measure the flow properties of powders under different rotating speed Ω of drum. GranuDrum evaluates the flow properties of powders in a free flow regime and the only stress applied to the powder here is due to their own weight [78, 98]. The experimental set-up is consists of a vertically positioned drum rotating around its central axis. The dimension of the drum is 84 and 10 mm in diameter and the cylinder length, respectively. The similar experimental set-up was previously used by Castellanos et al [161]. During the measurements, by using stroboscope, the half filled rotating drum (55 g of powder) is back-illuminated and a CCD camera is recorded the granular flow. For each

given angular velocity, 50 images of drum that separated by 0.5 s are recorded. After monitoring the flow of powders via a camera then the images are processed by using image-processing algorithm. In the images, the granular material appears in black and the air appears in white, whereby the position of the air/powder interface gets determined by an edge detection.

The average interface position and the fluctuations around this average position are computed. Also, the standard deviation calculated from the fluctuations of the interface, this parameter is directly linked to the cohesion inside the drum σ_f . In fact, in the range of considered rotating speed Ω, the cohesive granular material leads to irregular flow and non-cohesive granular material leads to a continuous flow (see Figure 4.3). From the average interface position, the flowing angle α_f is measured in the center of the flow.

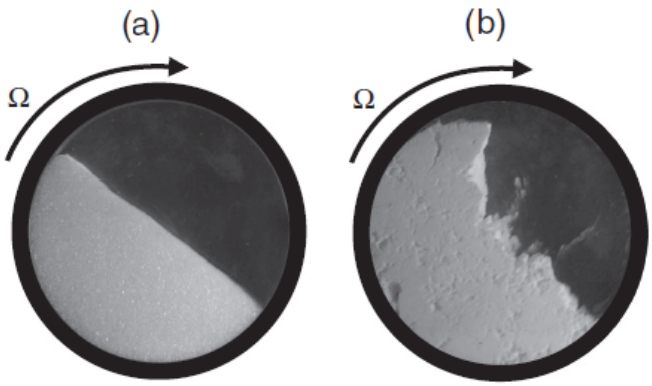

Figure 4.3 Two typical flow in GranuDrum: (a) regular flow obtained with a non-cohesive granular and (b) irregular flow of a cohesive granular material [72].

Figure 4.4 shows an example of typical picture obtained by GranuDrum during an experiment. It shows the average position of the interface calculated over 50 pictures in gray line and two white lines are correspond to the standard deviation of the interface. An average of this deviation of the interface calculated to obtain the estimation of fluctuation around interface σ_f. The dynamic angle of repose α_f is measured in the center of average interface. In general, lower the angle of repose is indicative of better flowability. However, the angle measurement obtained by rotating drum is closely influenced with the geometric characteristics of the drum, the roughness of the flow surface (drum walls) [160] and of course with environmental situation which need to keep controlled and constant always.

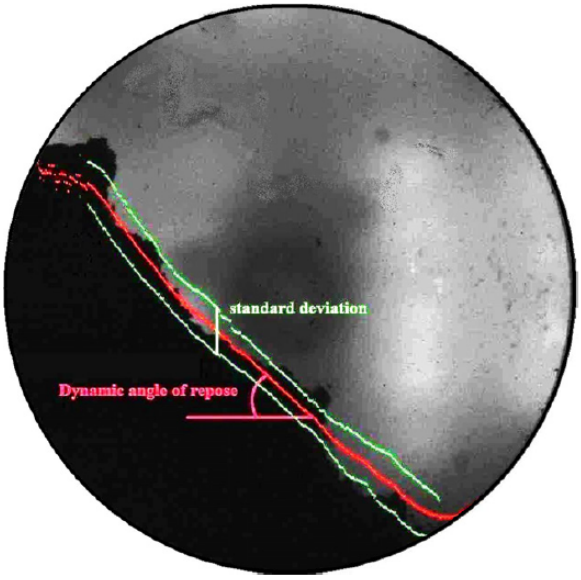

Figure 4.4 Dynamic angle of repose and standard deviation of the bed free surface [80].

GranuPack

Figure 4.5 shows the automated device GranuPack develped by Granutools to measure precisely the compaction dynamics of the powder submitted to successive taps. In order to prevent the accumulation of electric charges during the measurement process, all parts of device are connected to the earth also the metallic tube is used for the measurements.

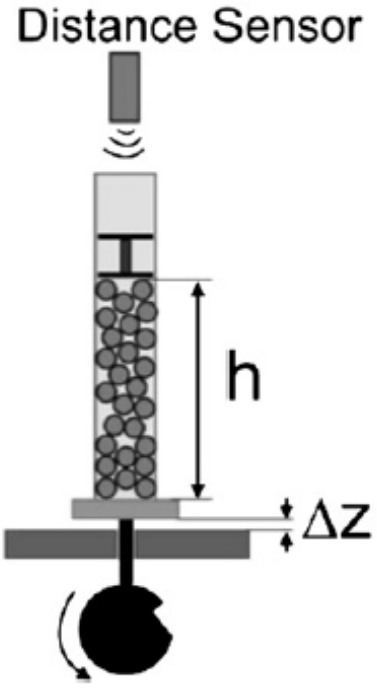

Figure 4.5 Schematic of GranuPack device [72].

The measurement starts with initialization protocol meaning that at the beginning of each test a

bottomless tube is inserted into the measurement tube then the initialization tube is filled with 35 mL of powder that supposed to be packed. Then, the initialization tube moves upward with very low velocity v = 1 mm/s and let the powders to rearrange themselves in the measurement tube. In order to keep the powder surface flat during packing measurement, a very light (11.5 g) hollow cylinder is placed on the top of powder. Then the tube containing the powder sample goes up to a height of $\Delta Z = 3$ mm and performs a free fall.

From this distance, the height and the volume of the powder bed are computed allowing to obtain the evolution of bulk density and packing fraction as function of the number of taps N. Where the bulk density is mass of powder m over the volume V of the powder and packing fraction η is obtained by dividing the bulk density ρ_b bulk over the true density ρ_t of the powders. The fraction η itself is the ratio between the volume occupied by the grains inside the tube and the volume of the pile. Here the Hausner ratio is obtained as $Hr = \frac{\rho_{500}}{\rho_0}$,

where ρ_0 is the initial density and η_{500} is density after 500 taps [162]. Based on the study conducted by Lumay et al [72], the Hausner ratio is not adequate to conclude about powder behavior. The reason has been presented in Figure 4.6, as one can see the two curves show the same Hausner ratio despite having different packing dynamics. They proposes the characteristic number of taps to quantify the compaction speed in front of the Hausner ratio that quantifies the compaction ratio [72]. In the following two methods are presented to perform the mentioned analysis.

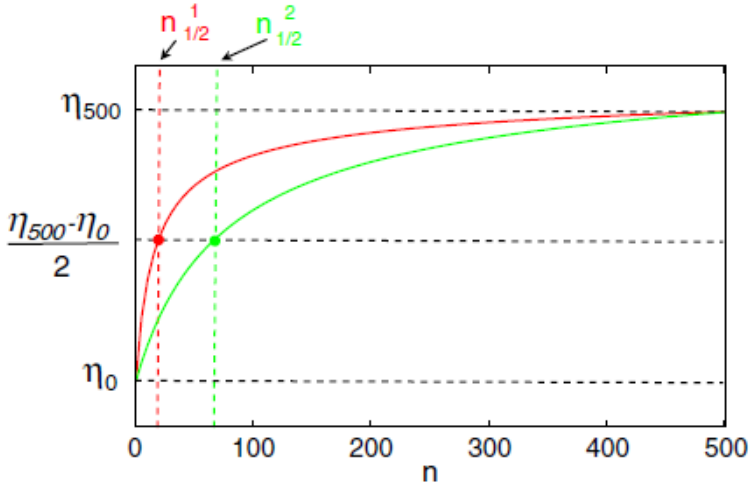

Figure 4.6 Evolution of the packing fraction (η) as a function of the tap number (n) in two compaction curves. The two curves have the same Hausner ration meaning the same initial packing fraction (η_0) and final packing fraction (η_{500}). The only difference between the two curves is their compaction characteristic time (τ) (see Equation 4.3) [72].

- Geometrical method: Based on this method the number of taps $n_{1/2}$ that need the powder reaches the middle of the packing process is measured from the compaction curve ($\eta = (\eta_{500} + \eta_0)/2$).

- Fitting with physical model [163, 164]:

$$\eta(n) = \eta(\infty) - \frac{\eta(\infty) - \eta(0)}{1 + ln(1 + \frac{n}{\tau})} \tag{4.3}$$

Where the fitting parameters $\eta(\infty)$ and τ are the asymptotic volume fraction and the compaction characteristic time, respectively. $\eta(\infty)$ is representative of maximal packing fraction achieved by tapping the powders also the compaction characteristic time is expressed in number of tap as well.

By considering that the characteristic time τ and characteristic tap number $n_{1/2}$ are informative of packing speed. It should be indicated that from the packing curve one can easily obtain $(n_{1/2})$ however (τ) is the result of the fit by a theoretical law. Thus, the parameter *tau* is independent of number of tap applied in packing dynamic, if experimental data and theoretical law fit. These two parameters are linked together as following equation $n_{1/2} = (e-1)\tau$.

GranuCharge

The triboelectric effect takes place at the contact between the powders and at the contact between the powders with device (mixer, silo, ...); during their flow. To measure the electrostatic charge of powders the GranuCharge equipment has been used here. Figure 4.7 (A) illustrates the experimental set-up of GranuCharge to measure the total electrostatic charge created inside powder during a flow in contact with a selected material and Figure 4.7 (B) shows the Faraday cup where the powders fall down to measure their electrostatic charge after flow.

The GranuCharge equipment consists of two parts: a V tube and a Faraday cup. The V tube itself composed of assembly of two tubes (Tube1 and Tube2) the lengths and the diameter of tubes are L = 350 mm , D = 47 mm; respectively. These two tubes connect each other with the angle of 90° forming a V shape. The tube material can be selected form different materials as follow: stainless steel 316L, aluminum 6063-T6, borosilicate glass, ABS, PVC and HDPE which the Stainless Steel 316L has been used in this study. At the end of V tube the faraday cup is placed and this cup connected to a customized electrometer able to measure electrostatic charges ranging from 0.1 nC to 1 μC.

At the end of the flow, the total value of the electrostatic charge Q and the charge density q = Q/m are measured, where m is the sample mass. In each samples, we checked the electrostatic charge present in the powder before the flow inside the V-tube. The V-tube geometry has been selected to combine different mechanisms leading to tribo-electrification: (a) friction between the particles (b) friction between the particles and the wall and (c) impacts of the particles on the wall at the connection between the two tubes since V-tube charges the powder more in comparison to a single tube geometry [165].

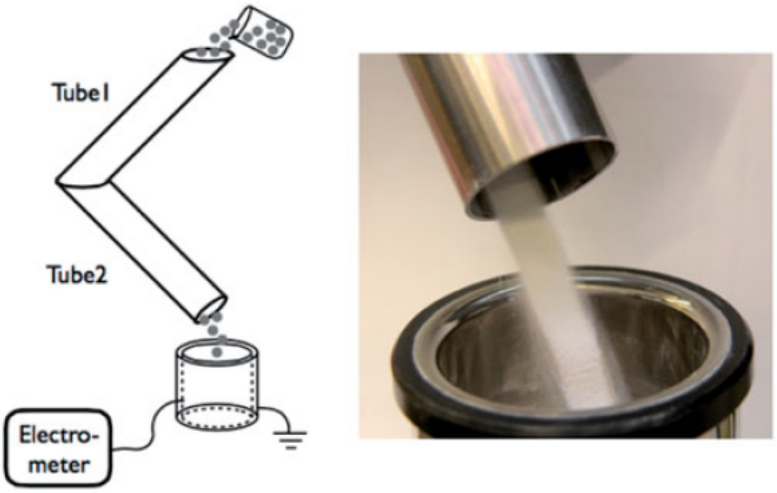

Figure 4.7 (A) Schematic diagram of GranuCharge used to measure the electrostatic charge created inside a powder after flow in contact with a selected material. (B) Picture of the powder flowing from the Tube 2 into the Faraday Cup measuring the electrostatic charge [166].

GranuHeap

The powder forms a heap when it is poured on a surface. It is known that the heap angle and the heap shape are function of powder properties. In general, a cohesive powder forms an irregular heap while a non-cohesive powder forms a regular conical heap also a cohesive powder gives a high value of the repose angle and strong deviations from the conical shape [75]. Figure 4.8 shows example of heap measurement, two typical heap shapes for granular sugar with regular heap with very low cohesion and powdered sugar with irregular heap and high cohesion. Thus, a precise measurement of the heap shape can provide beneficial information about the powders physical properties.

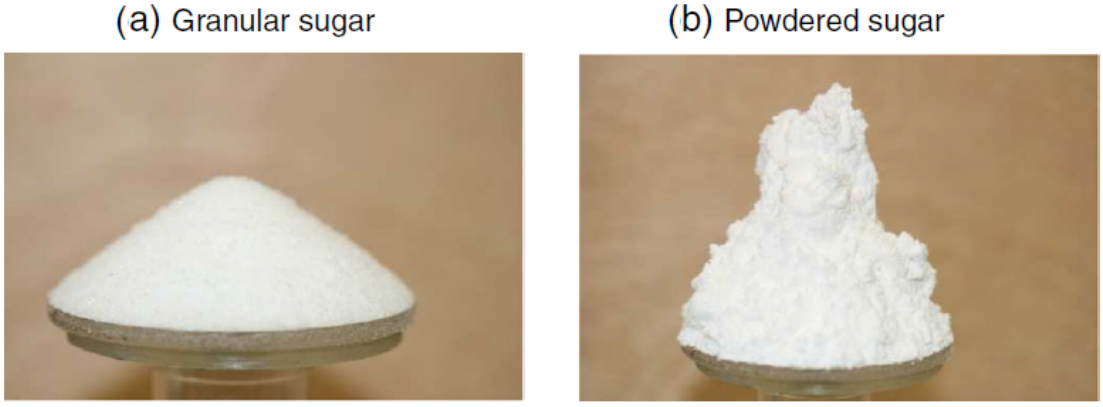

Figure 4.8 Two typical heap shapes: regular conical heap shape obtained with a non cohesive granular sugar (A) and irregular heap of powdered sugar which is a cohesive granular material (B) [72].

Figure 4.9 illustrates GranuHeap, an automatic device developed by Granutools to measure angle of repose also measuring the static powder cohesiveness from an analysis of the heap shape. For the

measurement, first an initialization tube with an internal diameter equal to the support diameter is placed on the support then the tube fills manually with the powder sample. After, initialization tube goes up at a constant speed of 5 mm/s and lets the powder flows from the tube to form a heap on the cylindrical support.

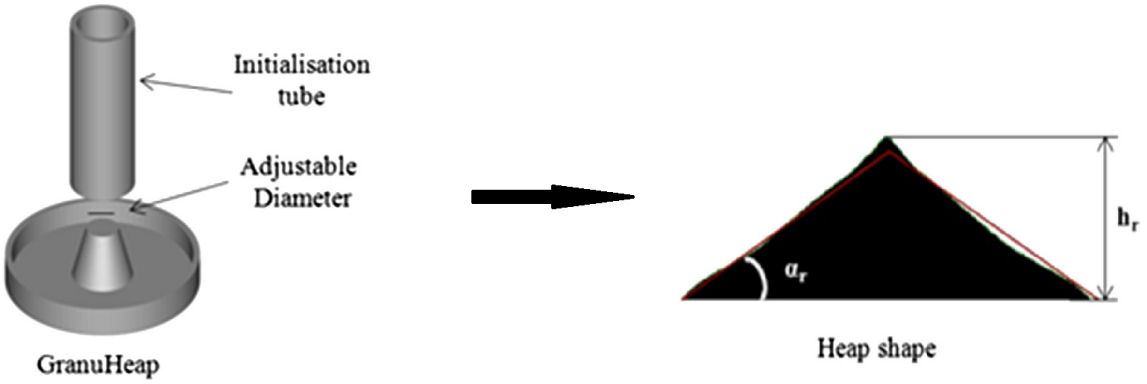

Figure 4.9 Illustration of the GranuHeap measurement [167].

Then, a CCD camera takes pictures of the heap from different orientations and a dedicated algorithm finds powder/air interface position by image analyzing of each pictures. The software extract all the geometrical information even if the heap shape is complex and asymmetric even if the heap shape is complex. The repose angle α_r refers to the angle of the isosceles triangle with the same surface than the powder heap projected image and the isosceles triangle corresponds to the ideal heap shape. Furthermore, from the deviation between heap interface and ideal heap shape the index σ_r calculated that is corresponds to the cohesive index of the powder sample.

In the following Table 4.1 presents the relation of powder flowability with repose angle and Hausner ratio. These two simple and experimental relations are used commonly to figure out the macroscopic properties of powders.

Table 4.1 Empirical relation between the flow properties and the results obtained with two well known powder tests; repose angle and Hausner ratio measurements [72].

Flow property	Angle of repose (-)	Haunser ratio
Excellent	25-30	1.00-1.11
Good	31-35	1.12-1.18
Fair	36-40	1.19-1.25
Passable	41-45	1.26-1.34
Poor	46-55	1.35-1.45
Very poor	56-65	1.46-1.59
Very very poor	>66	>1.60

4.2.2 Granutools measurement results and discussions

GranuFlow

Figure 4.10 presentes the flowability curves of the five formulations: control glass bead, hydrophilic glass bead, hydrophobic glass bead, lactose coated glass bead and agglomerated lactose powder. In the GranuFlow equipment room, the relative humidity and temperature of the experimental room were controlled at 37-44 % and 22 °C, respectively. The flow rate of each powder has been measured for several aperture, from 2 to 16 mm. Then, the obtained raw data were fitted with Beverloo law (Equation 4.2). As one can see in Figure 4.10, the powders flowrate is classified in decreasing order as follow: control glass bead ≈ hydrophilic glass bead ≈ hydrophobic glass bead > lactose coated glass bead > agglomerated lactose powder. We can interpreter that the high and very close flowrate of control, hydrophilic and hydrophobic glass beads can be due to the similar and smooth surface properties of these powders. While, by doing lactose coating on glass bead, the powder surface is not smooth anymore which it explains why it has lower flowrate than aforementioned three powders. In addition, the low density of agglomerated lactose powder as well as its surface roughness are explaining well its lowest flowrate. The flow index (C) obtained by Beverloo model for the five formulations are collected in Table 4.2. Based on flow index, the powders have the same classification as presented just before for flow rate. It has been reported that the optimal quantity of additives to be added to improve the flow of pharmaceutical powders were successfully determined by GranuFlow technique [159].

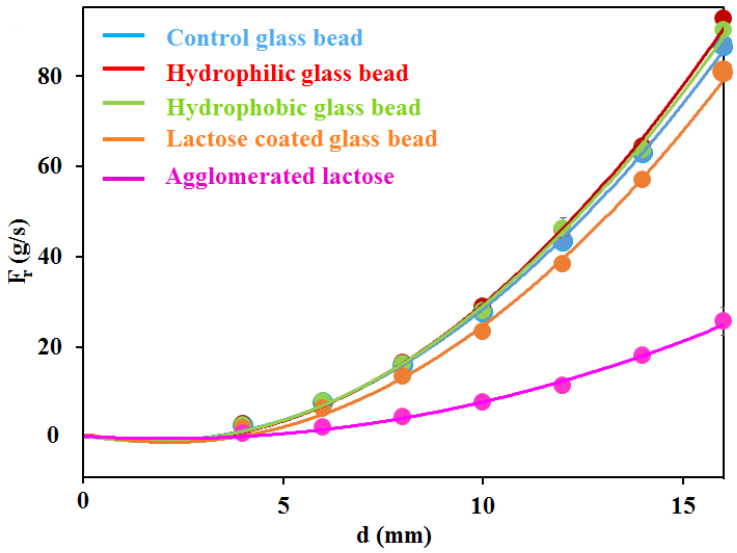

Figure 4.10 Powders flowability classification based on GranuFlow measurements, the experimental data are fitted with the Beverloo law (Equation 4.2). The experimental room humidity and temperature values were 37-44 % and 22 °C, respectively.

GranuCharge

The powders electrostatic charge measurements were performed with a GranuCharge equipment. All powders were analyzed in the relative humidity and temperature range of 37-44 % and 22 °C, respectively. In each measurements 70 g of powder were introduced into Faraday cup and the initial charge density of each powder samples q_i (nC/g) has been measured. Then, the powder were poured inside the rotating feeder and after it fall freely inside Fraday cup. The final charge density of powder q_f and $\triangle q = q_f - q_i$ (nC/g) were measured with electrometer at the end of each experiments.

Figure 4.11 shows the electrostatic charge measurement on control, hydrophilic, hydrophobic and lactose coated glass beads as well as agglomerated lactose powder. It has been observed that the initial charge density in all powder samples are almost zero while after free fall into V-tube all powders get charged which is due to the powder interaction with each other and with V-tube. The control, hydrophilic and hydrophobic glass beads obtained negative charge with this clear difference that the final electrostatic charge of hydrophilic and hydrophobic glass beads were almost the same and having more negative charge than control glass bead. The more negative charge of hydrophilic and hydrophobic glass beads can be due to the performed surface formulations.

Indeed, in the literature it has been reported that the surface formulation or additive can change the sign of particle charge or modify the quantity of charge [168]. As an instance, they noticed that by adding syloid 244FP to the lactose powder it gets negative final charge, while by addition syloid XDP 3050 to lactose powder it gets positive charge. Whereby in our study, the glass bead with hydrophilic and hydrophobic surface formulations presented negative final charge. While, the same bead with lactose coating showed positive final charge. Also, the different quantity of additive can modify the particle charge differently [169].

Therefore, in our study we have noticed that agglomerated lactose powder presents more positive electrostatic charge than lactose coated glass bead. The lower charge of lactose coated glass bead may due to the less layer of lactose around its surface. In general, during flow process, the powders can obtain and loss electrical charge based on their tendency to obtain or loss electron.

Humidity is another undeniable factor that interplays with the powder electrostatic charge [170]. In fact, humidity influences both particles surface conductivity and capillary bridges formation. As it presented by Lumay, et al. [168], at low relative humidity the particles electrical conductivity necessary for charge dissipation decrease. For high relative air humidity, the electrical conductivity increases and liquid bridges may be formed at the contacts between the particles, resulting in sticking. Therefore, the electrical charges dissipate more easily. However, apparition of the liquid bridges induce cohesive forces between particles. While at intermediate relative humidity, the cohesion is expected to be lower.

In our study, in order to have same measuring condition for all power samples and avoiding the influence of humidity on powder electrostatic charge, all measurements have been performed at the constant humidity (37-44 %) and temperature (22 °C) to have same measuring condition for all power samples.

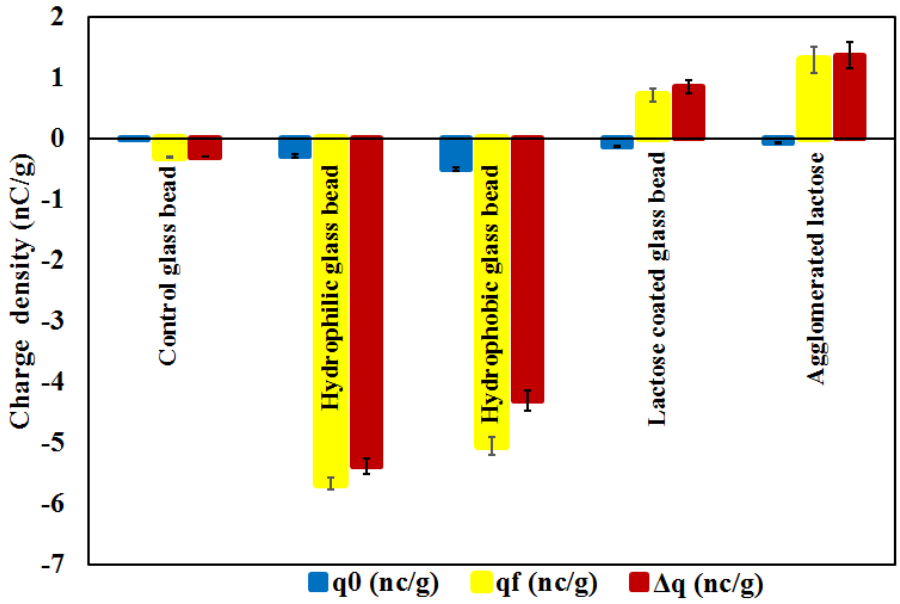

Figure 4.11 The electrostatic charge evolution of powders before and after flowing inside V-tube. Measurements have been done with GranuCharge equipment. The experimental room humidity and temperature values were controlled at 37-44 % and 22 °C, respectively.

GranuDrum

Figure 4.12 shows the evolution of the macroscopic parameters obtained with GranuDrum measurement. The flowing angle α_f and the fluctuations of the powder-air interface σ_f have been collected for different rotating speed from 2 to 30 rpm. The cohesive index σ_f is linked to the cohesion of powder inside drum. Figure 4.12 has been plotted based the data collected for cohesive index σ_f and flowing angle α_f by GranuDrum. One can see that almost all the powders have increasing tendency in both cohesive index and flowing angle, meaning that the flowability of all powder samples decrease under motion. This tendency has been proofed already in the studies on lactose powder and granular material [80, 168]. Thy have reported that rotating angle of repose for granular powders generally increases by increasing rotational speed, except in the case of rheofluidizing granular flow. Rheofluidization represents an improvement in the flowability when the shear rate increases. It should be indicated that the dynamic angle of repose has direct relation with the powder cohesion.

We have observed that control, hydrophilic and hydrophobic glass beads have very close values of rotating angle α_f and cohesive index σ_f, while lactose coated glass bead has slightly higher values. In addition, the highest cohesion and rotating angle belong to agglomerated lactose powder. Based on the cohesion measurement performed by FT4 shear cell in chapter 3, we have seen that lactose powder has more cohesion in compare with glass bead. It may presents why lactose coated glass bead presented more cohesion than control, hydrophilic and hydrophobic glass beads. In addition, agglomerated lactose powder (pure lactose) appears as highest cohesive powder in between powder samples.

It should be taken into account that the particles morphological properties have significant influence

on powder behavior also. In a research which was done on flow behavior of different lactose powders with GranuDrum, the lactose powders with angular surface showed a higher angle of rotation and cohesion [72,171]. Which it explain the higher flowing angle of lactose coated glass bead and agglomerated lactose powder in compare with control, hydrophilic and hydrophobic glass beads. The scanning electron microscopy (SEM) has been reported smooth surface for control, hydrophilic and hydrophobic glass beads in chapter 3.

Furthermore, powder behavior can highly depend on the air relative humidity. However, humidity can play a role in different ways on the different cohesive powders, meaning that the effect is not identical from one powder to the other. While, it has been reported that the best condition for conducting granular experiments with glass beads corresponds to a relative humidity of about 45%, where the cohesion is minimum in this humidity value [170]. Our experiments have been carried out in a humid range of 37-44 % which is the lowest sensitivity range for glass bead. Also, for the agglomerated lactose powder and lactose coated glass bead we proofed that they are not sensitive to the humidity in the mentioned range (they were already crystallized during formulation process). The corresponding measurements have been performed with DVS and they have been presented in the following.

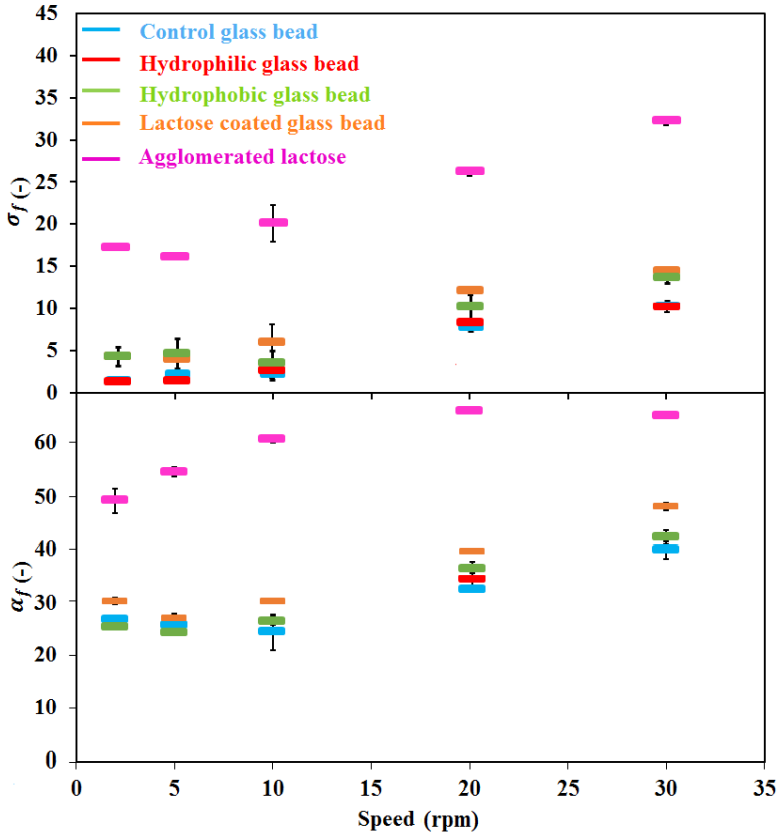

Figure 4.12 Evolution of the flowing angle (α_f) and cohesive index (σ_f) under different rotational speed. The measurements performed with GranuDrum on control glass bead, hydrophilic glass bead, hydrophobic glass bead, lactose coated glass bead and agglomerated lactose powder. The experimental room humidity and temperature values were controlled at 37-44 % and 22 °C, respectively.

GranuPack

The evolution of the powders packing dynamic as a function of number of taps are presented in linear and logarithmic scales in Figure 4.13 and Figure 4.14, respectively. The curves correspond to each powder samples are fitted with theoretical model (Equation 4.3). As one can see, the experimental data are in good agreement with theoretical model. The compaction increases by increasing number of taps in all powder samples. In addition, the monitoring of compaction as a function of tap number shows that the powders reached to the steady state both in linear and logarithmic scale.

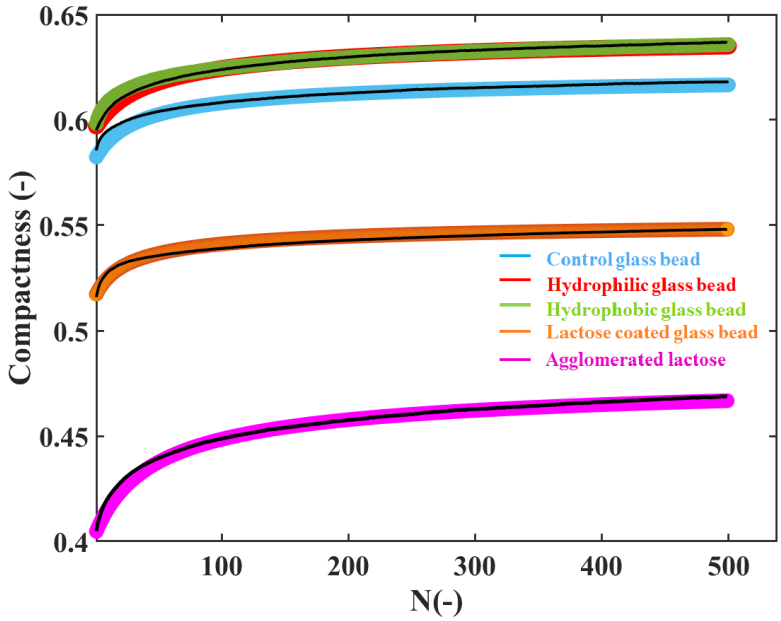

Figure 4.13 Evolution of powders compressibility as a function of tap numbers; measurements performed with GranuPack and the experimental data are fitted to theoretical model (black line) Equation 4.3; figure is in linear scale. The experimental room humidity and temperature values were controlled at 37-44 % and 22 °C, respectively.

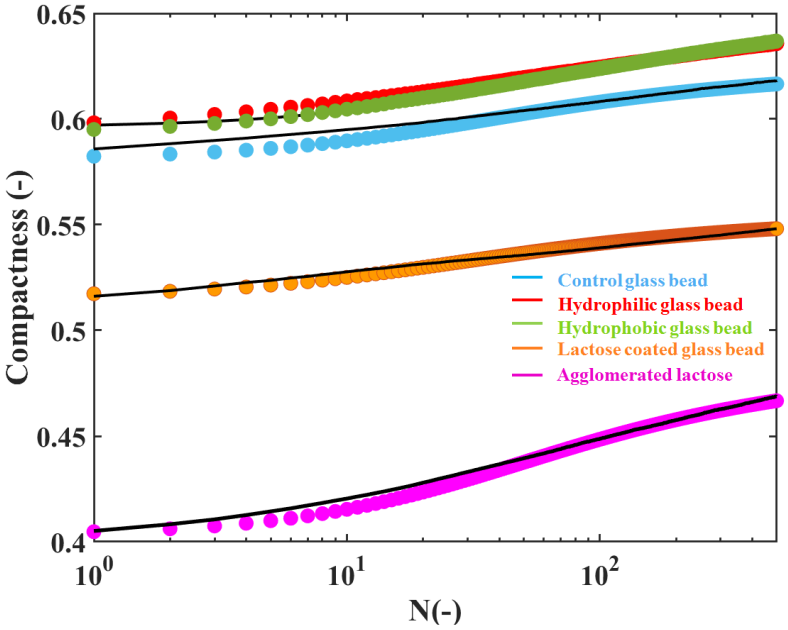

Figure 4.14 Evolution of powders compressibility as a function of tap numbers; measurements performed with GranuPack and the experimental data are fitted to theoretical model Equation 4.3(black line); figure is in logarithmic scale. The experimental room humidity and temperature values were controlled at 37-44 % and 22 °C, respectively.

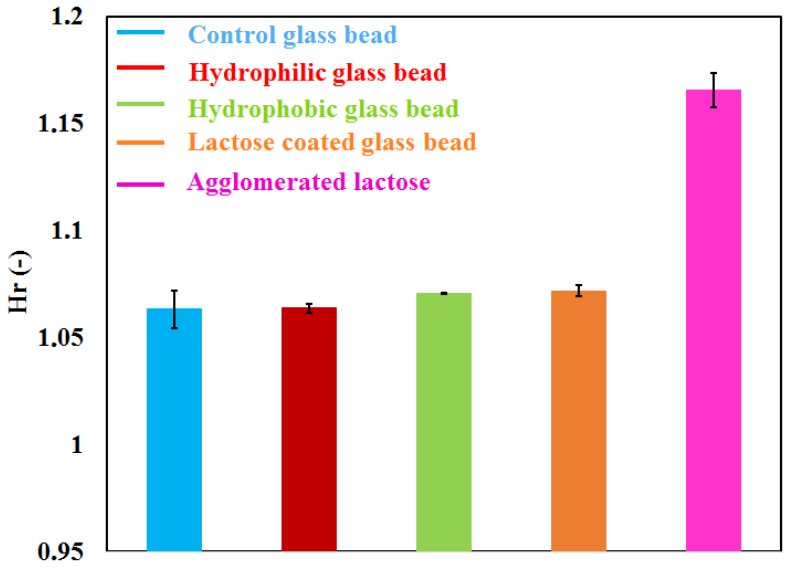

Figure 4.15 Haunser ratio of powders measured by GranuPack. The experimental room humidity and temperature values were controlled at 37-44 % and 22 °C, respectively.

The Table 4.2 presents the raw data collected from GranuPack measurement consisting of initial packing fraction at zero tap (η_0), final packing fraction at 500 taps (η_{500}), maximum packing fraction (η_∞) and Hausner ratio (Hr). According to the collected Hausner ratio (Hr) and based on the classification of Granutools in Table 4.1, the powders are classified in two groups (see Figure 4.15).

(a) Control, hydrophilic, hydrophobic and lactose coated glass beads are excellent flowable powders with Hr values as: 1.06, 1.07, 1.07 and 1.06; respectively.

(b) Agglomerated lactose powder with higher Hr ratio is in the category of good flowable powders. Indeed, for the particle diameter inferior to 50 µm , the macroscopic properties of powders are mainly related to the cohesive force between particles [122]. The cohesion strongly decreases the packing fraction and increase the Hausner ratio Hr. For the particles larger than 50 µm , the particle shape become an important factor. As an instance, elongation of the particles decreases the packing fraction [172]. Our five formulations have larger particle size than 50 µm , it seems that compaction of powders here is related to the shape and surface roughness of particles.

Besides, higher Hr value of agglomerated lactose powder can be due to the lower density of this powder in compare to the powders with glass core. Normally, powders with lower density present low flow behavior. By knowing that, higher the Hr ratio means higher compressibility. Therefore, one can conclude that agglomerated lactose powder is more compressible. The obtained results are in coherent with GranuFlow results.

GranuHeap

Figure 4.16 depicts the evolution of macroscopic parameters obtained with GranuHeap measurement. The repose angle α_r and the deviation σ_r from the ideal heap were measured for control, hydrophilic,

hydrophobic, lactose coated glass beads and agglomerated lactose powder. It has been observed that both parameters (α_r , σ_r) are almost the same for control, hydrophilic and hydrophobic glass beads, while lactose coated glass bead has slightly higher value. Moreover, agglomerated lactose powder shows highest values of repose angle and deviation from ideal heap (see table Table 4.2 for more details).

As we know, the higher value of σ_r and α_r is representative of powder lowe flowability. In addition, the heap shape strongly depends on the particles properties. The cohesive powders present a high value of repose angle and irregular heap shape [75]. It needed to remind that, this criteria is true for small particles. For larger particles $>$ 50 µm, the particle shape becomes an important parameter. Whereby, the particles with angular surface present higher heap height.

The measured values for the heap height of our five formulations are ranked in decreasing order as follow: agglomerated lactose powder $>$ lactose coated glass bead $>$ control glass bead $\approx>$ hydrophobic glass bead $\approx>$ hydrophilic glass bead. Which higher heap height of agglomerated lactose powder can be due to the irregular surface properties of this powder. Also by returning back to the Table 4.1 that presents Granutools powder flow ranking based on repose angle measurement, the powders are classified as follow: control, hydrophilic and hydrophobic glass beads are excellent flowable powders while lactose coated and agglomerated lactose powders ranked as good and poor flowable powders; respectively. Therefore, what has been obtained from heap height measurement, the repose angle α_r and the deviation σ_r from the ideal heap are in good agreement with our powders characteristics. Furthermore, the same behaviors are observed with the dynamic measurements (σ_f, α_f) performed with GranuDrum.

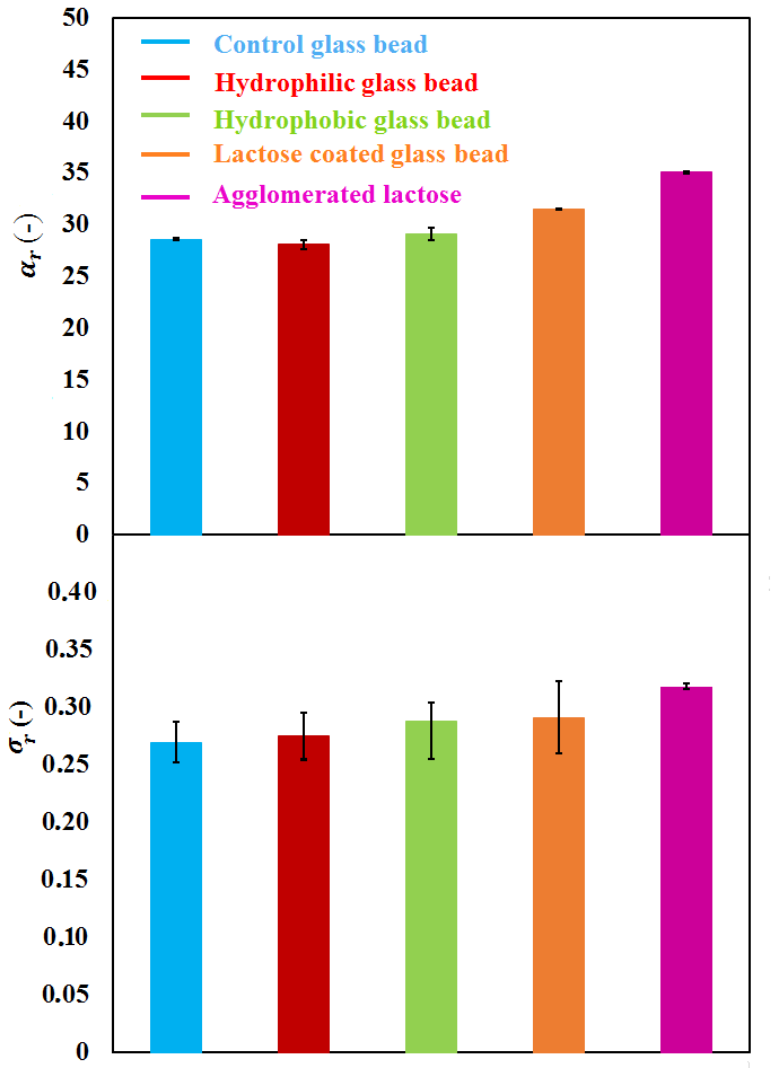

Figure 4.16 The repose angle (α_r) and the deviation (σ_r) from the ideal heap measured for powder samples with GranuHeap instrument. The experimental room humidity and temperature values were controlled at 37-44 % and 22 °C, respectively.

Table 4.2 Raw data collected from GranuFlow, GranuPack, GranuCharge, GranuDrum and GranuHeap measurements.

	Control glass beads	Hydrophilic glass beads	Hydrophobic glass beads	Lactose coated glass beads	Agglomerated lactose powder
α_r (-)	28.53 ± 0.08	27.99 ± 0.39	29.04 ± 0.59	31.43 ± 0.09	34.98 ± 0.10
σ_r (-)	0.27 ± 0.01	0.27 ± 0.04	0.28 ± 0.04	0.28 ± 0.07	0.32 ± 0.03
h_r(mm)	9.90 ± 0.04	9.10 ± 0.08	9.83 ± 0.11	10.82 ± 0.02	21.39 ± 0.19
C (g/s)	0.86 ± 0.01	0.89 ± 0.01	0.88 ± 0.01	0.84 ± 0.01	0.25 ± 0.01
$\Delta q(nC/g)$	-0.30 ± 0.00	-5.38 ± 0.17	-4.55 ± 0.12	0.84 ± 0.20	1.37 ± 0.10
$\alpha_f(-)(30rpm)$	39.73 ± 0.96	42.20 ± 0.83	42.13 ± 3.34	48.10 ± 0.20	65.03 ± 0.00
$\sigma_f(-)(30rpm)$	9.98 ± 0.21	9.96 ± 0.31	13.80 ± 0.43	14.40 ± 0.70	32.20 ± 0.00
$\rho_0(g/ml)$	1.45 ± 0.01	1.48 ± 0.01	1.48 ± 0.01	1.28 ± 0.01	0.66 ± 0.01
$\rho_{500}(g/ml)$	1.54 ± 0.01	1.58 ± 0.01	1.59 ± 0.01	1.37 ± 0.01	0.76 ± 0.01
$\rho_\infty(g/ml)$	1.58 ± 0.01	1.63 ± 0.01	1.64 ± 0.01	1.40 ± 0.01	0.74 ± 0.01
$\eta_0(-)$	0.58 ± 0.01	0.59 ± 0.01	0.59 ± 0.01	0.51 ± 0.01	0.39 ± 0.01
$\eta_{500}(-)$	0.62 ± 0.01	0.63 ± 0.01	0.64 ± 0.01	0.55 ± 0.01	0.46 ± 0.01
$\eta_\infty(-)$	0.63 ± 0.01	0.65 ± 0.01	0.66 ± 0.01	0.56 ± 0.01	0.49 ± 0.01
Hr (-)	1.06 ± 0.01	1.06 ± 0.01	1.07 ± 0.01	1.07 ± 0.01	1.16 ± 0.01

4.3 Powder characterization with the Discovery-HR3 Rheometer

Here, the macroscopic rheological behavior of powders have been studied with the Discovery-HR3 Rheometer. The rheological study was carried out by a shear imposed protocol in a cylindrical Couette cell using a vane for the rotating inner cylinder. The objective is to observe the behavior of powders under shear imposed system and to compare with the Granutools and FT4 rheometer results (the whole system consists of a cell containing sample and a measurement geometry, the used geometry is a vane geometry analogous of Couette geometry). The rheometer is capable of generating granular agitation within the samples by subjecting the measurement cell to vertical vibrations from the bottom of the measurement cell. The vibration is controlled with an amplifier and an accelerometer attached to the base of the measurement cell. The vibrational rheology induces the apparent yield stress to trigger the flow, it allows to explore the flow at low shear rates. The rheological measurements in this chapter has been done without vibration and the vibrational rheology is studied in chapter 5.

4.3.1 Methodology

In this section, the methodology of the Discovery-HR3 rheometer has been taken from references [115–117, 120, 173]. The powder rheometer has been already widely used to characterize a large number of dry or saturated granular media [117, 118, 120, 173]. The rheological study has been done both with and without vibration, in both cases vane geometry analogous to a Couette geometry was utilized.

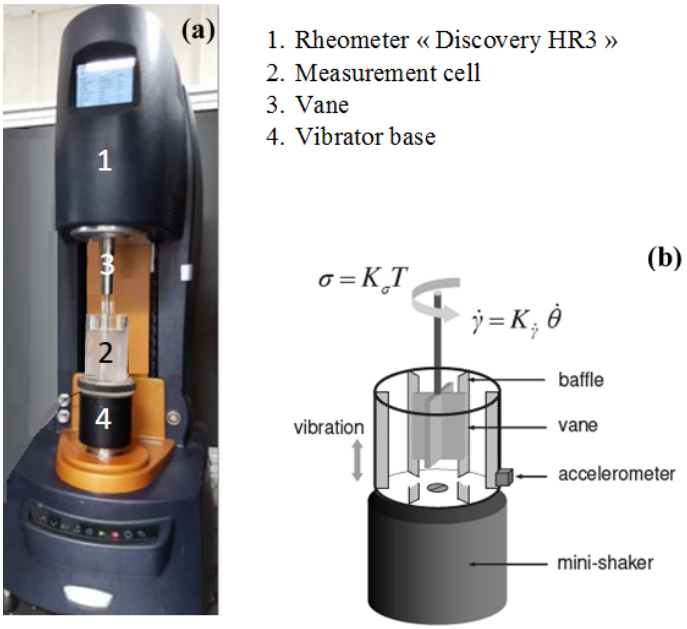

Figure 4.17 (a) Rheometer discovery (b) Schematics of Couette type cell connected to vibrator [115].

Figure 4.17 (a) and (b) present the experimental device. The measuring device uses a conventional stress imposed protocol. The sample to be studied is placed in a cylindrical measurement cell with the radius (R_c = 25 mm), fitted with baffles of width (l_{ch} = 5 mm) which prevents the sliding of sample on the wall of cell [174] and the external radius of cylinder (cell) is defined as (R_e = R_c - l_{ch} = 20 mm). The rheometric measurement is carried out with 4-blade or "vane" (3), of height (h_v = 50 mm) which describes a fictitious cylinder when it rotates about its axis of radius (R_i = 7.5 mm). The sheared sample is thus confined between two formed cylinders of the sample itself, similar to a Couette cell gap, of radius (R_e-R_i = 12.5 mm). The inner cylinder is set in motion under the action by imposing a constant torque and the device measures the angular velocity of rotation $\dot{\theta}$ of the vane. Shear stress and the shear rate are linked to the torque and to the angular velocity by calibration constants K_σ and $K_{\dot{\gamma}}$ whereby $\sigma = K_\sigma T$ and $\dot{\gamma} = K_{\dot{\gamma}}\dot{\theta}$. To determine the expression of these constants, a cylindrical coordinate system needed to be considered $(\vec{e_r}, \vec{e_\theta}, \vec{e_z})$. The flow velocity is as $v_\theta = v_\theta(r)$ with the reasons of symmetry and in the absence of an axial pressure gradient. Therefore, non-zero components of the stress and shear rate tensors are $\sigma_{r\theta} = \sigma$ and $\dot{\gamma}_{r\theta} = \dot{\gamma}$, respectively. The calibration constants are then determined by solving the momentum conservation equation with the following boundary conditions $v_\theta(r = R_i) = \dot{\theta}R_i$ and $v_\theta(r = R_e) = 0$ and by postulating that the stress and shear rate of deformation are linked by a behavior

law like Ostwald de Waele's law defined by $\sigma = k\dot{\gamma}^n$ where k is the consistency index and n the flow index. For n = 1, the fluid is Newtonian. For 0 < n <1, the fluid has a fluid-thinning behavior. For n > 1, the fluid is thickening. The solution of this problem leads to the following equations:

$$K_\sigma = \frac{1}{2\pi h_v r^2} \quad \text{and} \quad K_{\dot{\gamma}} = \left(\frac{2}{n}\right)\frac{(R_e/r)^{2/n}}{(R_e/R_i)^{2/n} - 1} \tag{4.4}$$

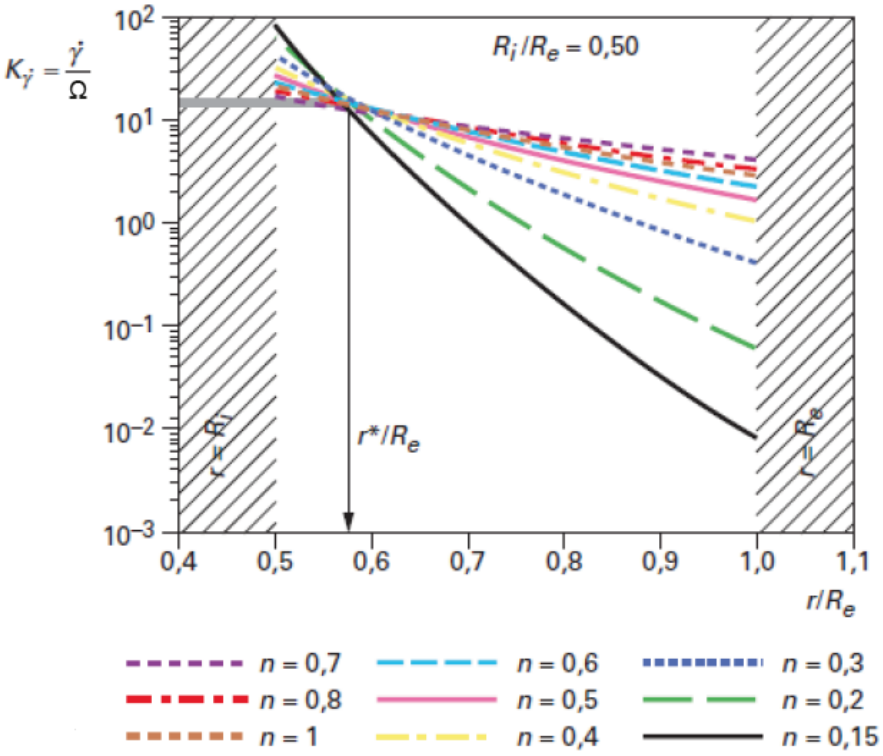

Figure 4.18 For a Couette like cell with $R_i/R_e = 0.50$: the calibration constant $K_{\dot{\gamma}}$ as a function of position r in the gap for different values of the flow index n, according to Choplin et al. [175]. The curves intersect at a point, defined as $r = r^*$.

r represents the radial position in the air gap and the value of n remains unknown and depends on the fluid, according to Aït Kadi et al [176]. It has been shown that there is a region in the air gap located at r^* for which the constant $K_{\dot{\gamma}}$ is independent of n (see Figure 4.18). Therefore, the analytical expression of r^* by considering the intersection of the curves K are defined as follow: $K_{\dot{\gamma}}(r, n)$ and $K_{\dot{\gamma}}(r, n')$, where n = 1 and $n' = 0.15$ are two extreme values of flow index:

$$r^* = \left(\frac{n'}{n}\frac{(R_e/R_i)^{2/n'} - 1}{(R_e/R_i)^{2/n} - 1} R_e^{2/n-2/n'}\right)^{(2/n-2/n')^{-1}} \tag{4.5}$$

This means that in the region near r^*/R_e, the sample will always be sheared regardless of value of n (see Figure 4.19). The rheological values determined by the rheometer are therefore implicitly calculated in $r = r^*$ from experimental measurements of the torque T and the angular velocity of rotation $\dot{\theta}$.

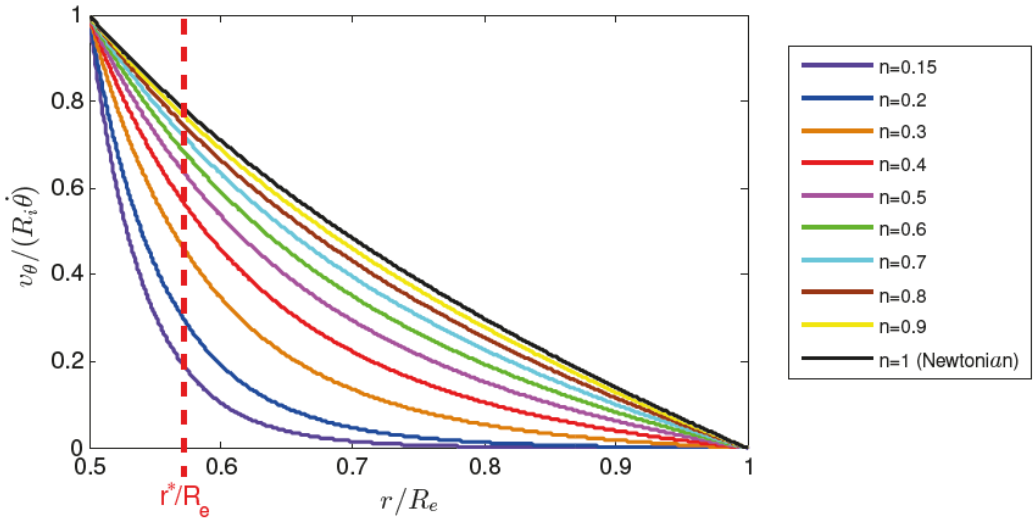

Figure 4.19 For a Couette like cell with $R_i/R_e = 0.50$: Dimensional theoretical velocity profiles $v_\theta/(R_i\dot{\theta})$ as a function of the position in the gap r/R_e, according to Hanotin [120].

The measuring cell is connected to a mini electromagnetic vibrator (type 4840, Brüel & Kjaer) which imposes vertical and sinusoidal vibrations. A closed loop system allows the control of vibrations by an amplifier and an accelerometer fixed to the base of the measuring cell (see Figure 4.17). The work carried out by C. Hanotin [120] on vibrated granular suspensions has shown that the value of the plateau viscosity depends on the speed of vibrations through the control parameter σ_v, which is the mechanical vibration stress, defined as:

$$\sigma_v = \frac{1}{2}\rho_s A^2 (2\pi f)^2 \tag{4.6}$$

In general ρ_s is the density of the suspension which depends on ρ_f and ρ_p, densities of the fluid (in suspension) and the particles, respectively. It is defined by $\rho_s = \rho_p\phi_v + (1-\phi_v)\rho_f$, here we used dry powders therefore ($\rho_f = 0$) and $\rho_s = \rho_p\phi_v$, where ϕ_v is the initial volume fraction of the suspension such that $\phi_v = \dfrac{V_p}{V_{tot}}$, with V_p the volume occupied by the particles and V_{tot} the total volume. This vibration stress can be interpreted as volume energy of vibrations $\sigma_v = E_v/V$. Where, V is the volume of the sample and $E_v = 1/2m(2\pi f)^2 A^2$ is the vibration energy. What has been presented here are all required elements to perform rheology with vibration but at the same time it is possible to perform rheology without vibration in the same system just by disconnecting accelerator attached to vibrator base.

4.3.2 Newtonian and Frictional regimes

Figure 4.20 depicts a typical rheological result obtained with a Discovery-HR3 rheometer on glass bead. As it can be seen, the profile consist of two zones:

(a) Low shear rate zone appears with constancy of viscosity, in fact the slow rotational movement of the vane allows the system to reorganize faster under the modification made by vane which yields a

Newtonian behavior (Newtonian regime).

(b) High shear rate zone, if the imposed modifications are too fast compared to the reorganization time, the viscosity tends to drop rapidly within the limit of the high shear stresses and the behavior is no longer Newtonian and the regime becomes frictional. In general, vibrational rheology imposed low shear rate condition on measuring samples. Then, it removes the yield stress at the beginning of the flow curve and consequently the viscosity plateau appears where the main interaction between particles are related to their surface cohesion. While, in higher shear stress the frictional regime appears, where the main interactions between particles are function of the inter-particle frictions.

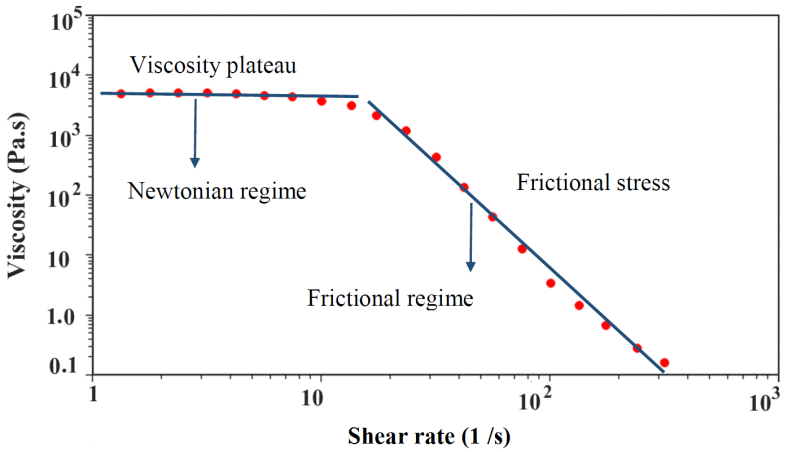

Figure 4.20 Example of flow curve obtained for glass bead with Discovery-HR3 rheometer (www.rheologylab.com).

Figure 4.21 presents the result of study done by Caroline Hanotin's in her thesis [120], the study was carried out in LEMTA with the powder rheometer (Couette type cell) coupled to the vibrating cell. Dry glass beads of 100 µm were measured in imposed shear stress test under sinusoidal vibration and date points are collected in steady state. Figure 4.21 presents evolution of glass beads viscosity as a function of applied shear stress for different values of σ_v, for the $\sigma_v = 0$ (filled symbols in the figure), σ remains constant for all imposed shear stress. This regime is a Coulombian frictional [173] and for $\sigma_v > \sigma_f$, all viscosity curves follow the non vibrated case whatever the mechanical vibration energy. However, the behavior observed for $\sigma_v < \sigma_f$ the powder loses its yield stress and a viscosity plateau appears, Newtonian regime. This results clearly evidenced influence of vibration in rheological measurements. In the following, the rheological measurement has been done on powder samples studied in this thesis without vibration to observe the classification of powder under shear imposed rheology with rheometer discovery-HR3 and the results corresponding to vibrational rheology are presented with detail in chapter 5.

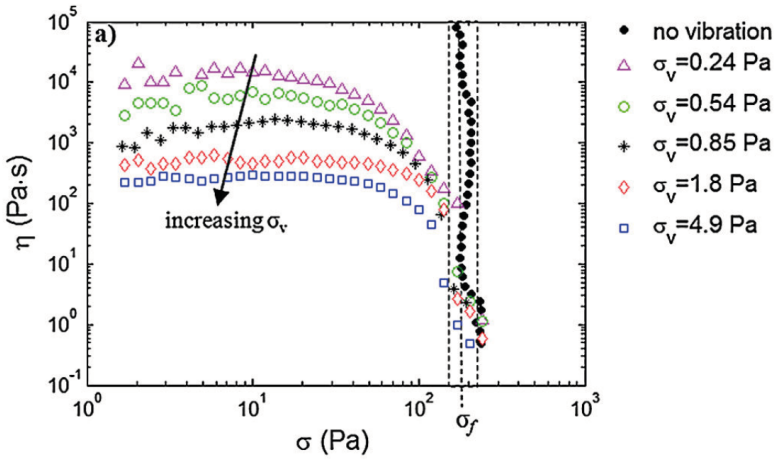

Figure 4.21 Viscosity (η) versus shear stress (σ), for various values of vibration stress (σ_v) applied for glass beads, $\phi_v = 0.62$ [120].

Figure 4.22 presents the rheological measurement performed by Discovery-HR3 without vibration on the five formulations. The vane geometry has been utilized. The figure presents evolution of shear stress versus shear rate for each formulation. The experiments have been carried out by imposing steady angular velocity 11-30 rad/s. Enough time has been waited for each value of the angular velocity to confirm reaching stationary state. During measurement, only 1/3 of height of vane has been immersed inside the powder sample since by filling full height, the vane was not able to turn inside the powders in low angular velocities. This is because of the high value of the stationary torque. In general, higher the curve means higher shear stress required to let the powder to be in motion; consequently less flowability [127]. So, based on this criteria agglomerated lactose powder and lactose coated glass bead showed less flowability and at the same time similar flowabilities. However, hydrophilic glass bead, hydrophobic glass bead and control glass bead evidenced very close flowability to each other and better flowing behavior than lactose coated glass bead and agglomertaed lactose powder. As it has been indicated previously, in non vibrational rheology we catch the frictional regime at high shear rates, therefore by starting from this point it is clear that similarity of flow behavior of lactose coated glass bead and agglomerated lactose powder are coming from their almost same surface structure (friction). By considering that hydrophilic and hydrophobic surface formulation did not alter the surface friction of glass beads in compare with control glass bead (see Figure 3.6), therefore they showed similar flowability in shear imposed rheology. Based on Figure 4.22, the flowability of powders decease in the following order: Hydrophilic glass bead > Hydrophobic glass bead > control glass bead > lactose coated glass bead ≈ agglomerated lactose powder. In overall, control, hydrophilic and hydrophobic glass beads showed better flowability than lactose coated glass bead and agglomerated lactose powder. This is due to the lower surface friction of mentioned three powders in compare with the surface friction of lactose coated and agglomerated lactose powder.

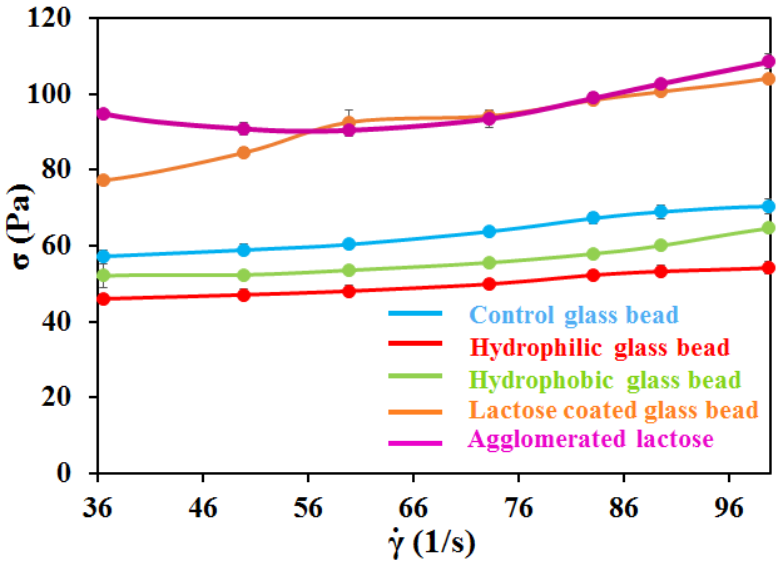

Figure 4.22 Evolution of shear stress versus shear rate, measurements performed with rheometer Discover-HR3 in high shear stress condition.

4.4 Powders behavior at a controlled temperature and humidity conditions

The behavior of five formulations at controlled humidity and temperature was studied. Powders humidity is controlled with a humid chamber and for the preliminary study 50 % RH is regarded. Before each measurements, the powders are kept inside the humid chamber at 20 °C. The duration of storage before analysis for control, hydrophilic and hydrophobic glass beads was 48 h, while lactose coated glass bead and agglomerated lactose powder were kept around one week inside the humid chamber to reach an equilibrium. The reason of time difference in maintaining powders inside humid chamber arise from the difference between their humidity intake abilities; lactose powder needed longer time to intake sufficient amount of humidity. Powders water activites (aw) have been confirmed by using thermoconstanter TH200 (Novasina, Switzerland) at a temperature of 25 °C; after taking them from humid chamber. This apparatus has a measuring range comprised between 0.05 to 1.00 and an accuracy of ± 0.01 over a temperature range between 0 and 50 °C. More precisely, 1 g of sample is introduced into a polypropylene cup deposited in the sealed enclosure of the apparatus. Then the aw is measured using an electrolytic sensor. After humid control, powders rheology has been studied with the Discovery-HR3 rheometer and FT4. The obtained results have been compared with the similar results obtained for the same powders without humid control.

4.4.1 The powders flow behavior after 50 % humid control

Table 4.3 collects the mean flow parameters determined in stability and aeration tests for 100 µm powders after 50 % of humid control. Here, according to the collected BFE values, two groups of powders can be defined: control, hydrophilic, and hydrophobic glass beads presented the lowest BFE, while lactose coated glass bead and agglomerated lactose powder had the higher BFE. This is indicative of better flow properties for control, hydrophilic and hydrophobic glass beads in comparison with lactose coated and agglomerated lactose powder.

Table 4.3 Stability and aeration tests results for samples with 100 µm mean sizes at 50 % RH.

Powders	BFE (mJ)	SE(mJ/g)	AE (mJ)	AR (-)	Minimum fluidization velocity (mm/s)	CBD (g/mL)
Control glass beads	206.22±8.66	1.93±0.06	1.57±0.29	133.48±0.52	18.01±0.15	1.47±0.02
Hydrophilic glass beads	179.50±1.14	1.89±0.01	1.90±0.14	153.75±0.25	19.87±0.02	1.47±0.00
Hydrophobic glass beads	252.91±6.45	3.09±0.00	1.44±0.10	104.59±8.72	22.32±0.07	1.47±0.00
Lactose coated glass beads	357.90±6.41	3.00±0.06	2.34±0.25	218.24±2.37	34.61±2.45	1.31 ± 0.22
Agglomerated lactose powder	300.33±3.15	5.31±0.18	1.09±0.14	250.85±0.09	27.99±0.25	0.60±0.01

As mentioned already, BFE measures the required energy to put a given volume of powder bed in motion while the powder density has an important effect on BFE values. By knowing that generally SE is more efficient to classify powders according to their flowability, as it corresponds to flow energy per mass of powder sample. Based on obtained SE values after 50 % of humid control, three groups of powders formed as follow: first, control and hydrophilic glass beads had very low SE (under 2 mJ/g) indicating very good flowability, after hydrophobic and lactose coated glass beads had slightly higher SE around 3 mJ/g showing a good flowability, and last, agglomerated lactose powder had highest SE (about 5 mJ/g) which can be interpreted as correct powder flowability. In the case of without humid control, the similar BFE has been obtained for the same powder samples and the BFE in both cases had very close values. By comparing the BFE and SE values obtained for five powder samples before and after 50 % humidity (see Table 3.2 and Table 4.3), it has been denoted that powders have same flowing ranking with similar BFE and SE values. Furthermore, the CBD values of all tested particles in aforementioned both tables displayed that all the powders with glass core logically have higher density than agglomerated lactose powder. Generally, a lower powder density results a lower powder flowability, therefore the CBD results were consistent with the lower flowability of agglomerated lactose powder in comparison with powders with glass core.

Figure 4.23 shows the evolution of flow energy with air velocity for 100 µm control glass bead, hydrophilic

glass bead, hydrophobic glass bead, lactose coated glass bead and agglomerated lactose powders after 50 % of humid control. The measurements performed with aeration test and the corresponding AR and AE values collected in Table 4.3. All powders reached a fluidized state in the conditions of the aeration test. Minimal fluidization velocities obtained for these powders ranged from about 18 to 34 mm/sec which is slightly higher than the minimum fluidization velocity for the powder samples before humid control with the value of 16 to 31 mm/sec. Similarly, AE values reported the similar increase in each powder samples after humid control. The increase in mentioned values are very low and by comparing the AE and AR values of before and after humid control we can interpret that the results are comparable and the increase of mentioned values do not have significant meaning. Only AE value of agglomerated lactose powder has increased in compare with the AE value of the powders with glass core for after and before humid control. This value has increased from 0.89 mJ to 1.09 mJ in agglomerated lactose powder which it may be due to the humid intake ability of agglomerated lactose, but still it is not an impressive increase. The minimal fluidization velocities permitted to draw the general classification of 100 µm powders sensitivity to aeration classified as follow: control glass beads > hydrophobic glass beads > hydrophilic glass beads > agglomerated lactose powders > lactose coated glass beads. The classification is the same as before humid control.

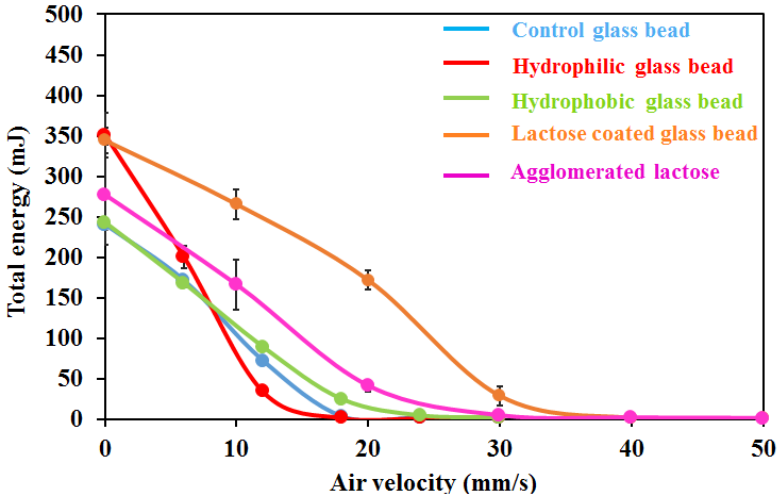

Figure 4.23 Evolution of flowability energy of the powder bed with air velocity during the aeration test for studied powders of 100 µm after 50 % of humid control during 48 h. Error bars represent standard errors; some were not visible as their size was inferior to the marker size.

The evolution of compressibility according to the applied normal stress is displayed in Figure 4.24 for 100 µm powders after 50 % of humid control. Before humid control the compressibility of powders increased from 1-2 % to 2-4 % (see Compressibility (A)) while after 50 % of humid control, the control, hydrophilic, hydrophobic and lactose coated powders kept the same compressibility range (1-2 % to 2-3 %) however agglomerated lactose powder showed slight increase in its compressibility (see Figure 4.24). At the beginning of compressibility at 1 kPa the compressibility of agglomerated lactose has increased

from 1 % to 4 % and at 15 kPa of applied normal stress, it showed an increase from 4 % to 7 %. However, this increase is not impressive but it can be due to the different rearrengements of particles during copmressibility measurement. Regarding to the compressibility of powders at 15 kPa that is very low, therefore very good flowability of investigated powders is expected consistently with BF and SE results. In general, compressible powders require higher flowability energy to be put in motion [123].

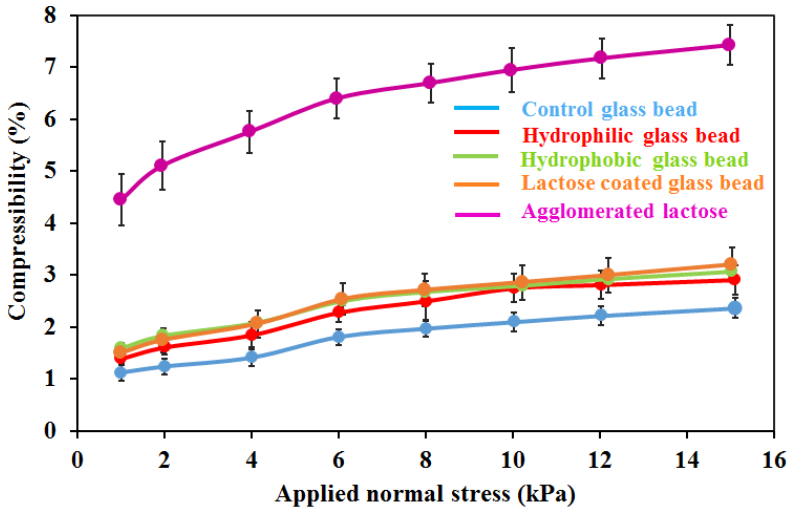

Figure 4.24 Evolution of powder compressibility with applied normal stress for studied powders of 100 µm mean sizes after 50 % of humid control. Error bars represent standard errors; some were not visible as their size was inferior to the marker size.

The shear cell test performed on 100 µm five powder samples after 50 % of humid control and the related curves of shear stress versus normal stress obtained accordingly in Figure 4.25. Also the flow characteristics of powders consisting of cohesion and flow factor deduced from their curves following the yield locus approach which are listed in Table 4.4. Shear stress represents the force needed to induce consolidate powder bed failure, i.e. relative motion of particles within the powder bed, therefore higher shear stress at a given applied normal stress presents poorer powder flowability in high stress condition. By starting from this point, powder flowability in high stress condition ranked in increasing order as follow: agglomerated lactose < lactose coated glass beads < hydrophobic glass beads ≈ control glass beads ≈ hydrophilic glass beads. The obtained results are in consistent with stability and compressibility results also the classification of powders are consistent with the classification before humid control (see Figure 3.9). All the powders exhibited low cohesion ranging from 0.20 to 0.44 kPa. The cohesion values before humid control was ranging from 0.20 to 0.41 kPa, only agglomerated lactose powder presents slight increase in cohesion which it previously appeared in compressibility increase of this powder sample. In both case the cohesion values are in agreement with the good flowing and aeration properties previously evidenced. Cohesion of investigated powders increased in the following order: hydrophilic glass beads ≈ control glass beads ≈< hydrophobic glass beads ≈ lactose-coated glass beads < agglomerated lactose.

In addition, *ff* values are almost all over 10 for all powders which is indicating of “free-flowing”

characteristics of these powders. It should be indicated that only the *ff* value of agglomerated lactose has slightly decreased which it confirmed by cohesion value increase (0.44 kPa) in compare with dry agglomerated lactose powder (0.41 kPa). However, based on *ff* value classification by Jenik [127] the powders with *ff*> 10 are free flowing therefore the humidity has not effected the flowability of powders and they still have almost the same flowability than before humid control (see Table 3.3). On the basis of *ff* values, powder flowability in high stress condition increased as follow: agglomerated lactose < lactose-coated glass beads < hydrophobic glass beads < control glass beads ≈ < hydrophilic glass beads. The sphericity and higher density of lactose coated glass beads in compare with agglomerated lactose powder may explain its better flowability.

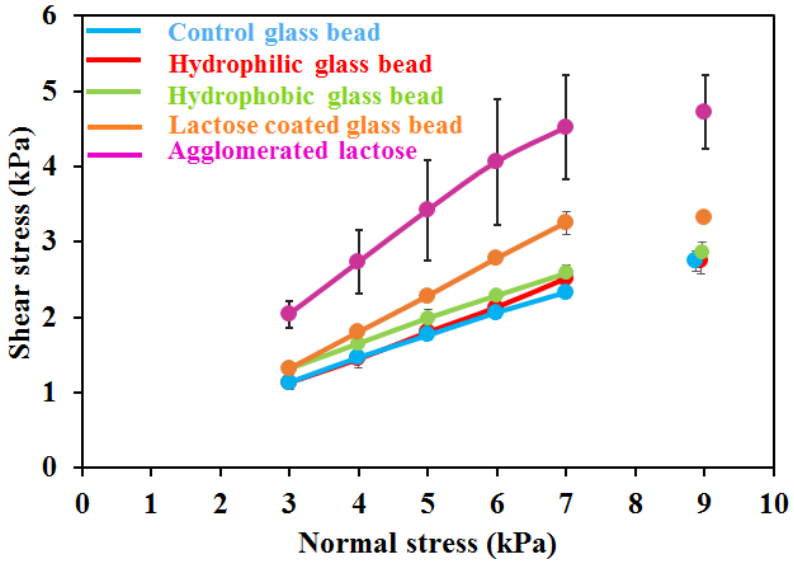

Figure 4.25 Evolution of shear stress with applied normal stress after pre-shear at 9 kPa for 100 µm powders after 50 % of humid control. Error bars represent standard errors; some were not visible as their size was inferior to the marker size.

Table 4.4 Flow parameters derived from shear cell test for powder samples with 100 µm mean sizes after 50 % of humid control.

Powders	Cohesion (kPa)	*ff* (-)
Control glass beads	0.20 ± 0.03	20.84 ± 0.40
Hydrophilic glass beads	0.20 ± 0.02	20.41 ± 0.86
Hydrophobic glass beads	0.26 ± 0.05	18.21 ± 1.43
Lactose coated glass beads	0.31 ± 0.00	13.62 ± 1.41
Agglomerated lactose powder	0.44 ± 0.04	9.88 ± 0.37

The Discovery-HR3 rheometer is the second equipment used in this chapter to characterize the five powder samples after 50 % of humid control. Here, this rheometer is utilized in stationary state. The

objective was to see the behavior of powders under different measurement condition. The powders humidity control followed like as previous measurements. Then the rheology performed by imposing angular velocity between 11-30 rad/s consequently shear stress, shear rate and torque have been measured. Enough time has been waited for each value of the angular velocity to confirm reaching steady state. During measurement, only 1/3 of height of vane has been immersed inside the powder sample. In the following, Figure 4.26 presents the result of measurement performed with rheometer discover after 50% humid control. The two groups of powders are evidenced, control, hydrophilic and hydrophobic glass beads showed similar flowability while lactose coated glass bead and agglomerated lactose powder have almost same flowing behavior. The powders after humid control have the same ranking than before humid control. In addition the shear stress value for control, hydrophilic and hydrophobic glass beads are between 40-60 Pa and for lactose coated and agglomerated lactose powder are between 80-100 Pa; for both before and after 50 % of humid control. Normally, powders with good flowability need lower shear stress to be put in motion therefore based on this criteria, control, hydrophilic and hydrophobic glass beads have better flowability than lactose coated glass bead and agglomerated lactose powder. As it has been indicated already, this is due to the similarity of surface structure of mentioned two groups of powders. By taking into account that in stationary rheology the measurement is in frictional regime and friction between particles play role in their rheology therefore powders with similar surface structures show the similar flow behavior.

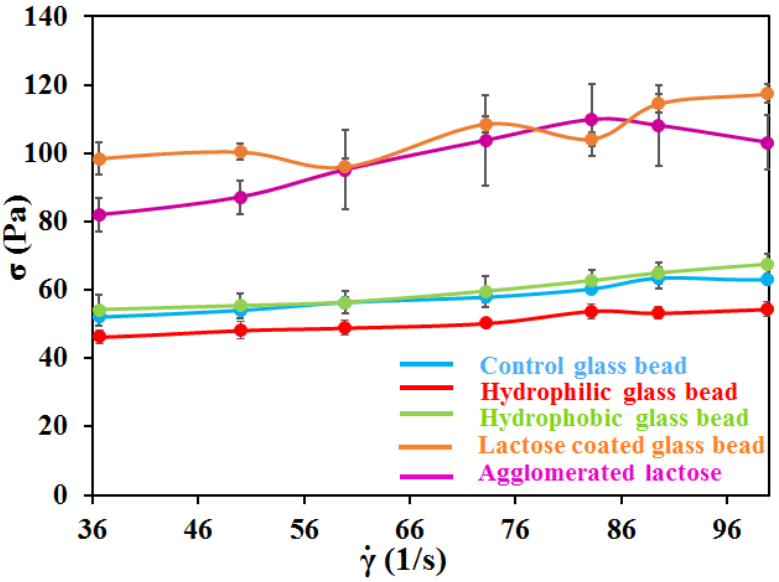

Figure 4.26 Evolution of shear stress versus shear rate based on measurements done with the Discover rheometer on five powder samples after 50 % of humid control.

4.4.2 Dynamic water sorption (DVS) of formulated powders

Dynamic vapor sorption or DVS (Surface Measurement Systems, London, UK), is an automated gravimetrical, rapid and accurate equipment to measure moisture sorption capacities of the powder during

storage in a large temperature range, using dynamic environment control and ultrasensitive recording microbalance [177, 178]. A small quantity of samples is required for analysis. It monitors evolution of the sample's weight over time at preselected temperature and relative humidity (RH), between 0-100 %. Here, we loaded about 100 mg of sample onto the quartz sample Pan and the program was set to measure during one week. The period was taken long enough to be sure about reaching the steady state in each humidity steps. The program was set to control humidity from 0 % to 100 % by 10 % of RH increasing steps. The mass change (m) has plotted against RH in Figure 4.27. One can see that there is no mass change in any powder samples. It is logical that glass beads do not have the ability of humid intake and since this equipment prevents condensation effect as well so no mass change has been recorded to the powders will glass core. However, agglomerated lactose powder has capability of humid intake while we did not observe any mass increase in this case. This is because during granulation of lactose, a small quantity of water was used to obtain agglomerated lactose. Thus the power was saturated with water and consequently crystalized already and after granulation it does not has tendency to intake more water. We confirmed the crystallization of lactose by microscope. The DVS measurement has not been performed on lactose coated glass bead since it has glass core with almost the same surface structure than agglomerated lactose powder.

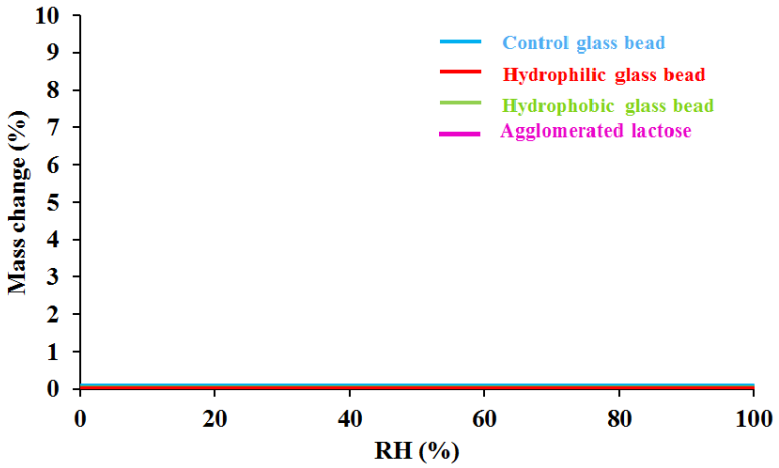

Figure 4.27 Evolution of powder mass in wide range of humidity, measurement performed with DVS.

4.5 Conclusion

a. Comparison between equipements: FT4-Granutools-Rheometer

In this chapter, the powders behavior have been studied with different equipments. The Discovery-HR3 rheometer and Granutools series of tests including GranuFlow, GranuPack, GranuCharge, GranuDrum and GranuHeap have been implemented in this chapter. The objective was to figure out the behavior of our powder samples under different processing dynamic, therefore all measurement performed in this chapter compared with the result obtained by **FT4-rheometer in chapter 3**.

The powder properties was measured with three different measuring methods as follow: in free fall condition with GranuFlow, in confined bed condition by shear cell test (FT4) and in shear imposed condition with rheometer discovery. Based on flowability measurement results with GranuFlow and FT4, the powders were classified into three groups: (a) control, hydrophilic, and hydrophobic glass beads presented higher flowabilities with very close flowability values (b) lactose coated glass bead showed lower flowability than previous three formulations and (c) agglomerated lactose powder had the lowest flowability. Previously, higher cohesion (Table 3.3, Table 4.2), more irregular shape (Figure 3.6) as well as lower density for lactose coated glass bead and agglomerated lactose powders have been measured (Table 3.2,Table 4.2). Particularly, agglomerated lactose powder presented lowest density which all aforementioned factors can explain the lower flowability of these two powders. Based on Dicovery-HR3 rheometer measurement results, the powder flowability were classified into two groups: (a) control, hydrophilic and hydrophobic glass beads with higher flowability and (b) lactose coated glass bead as well as agglomerated lactose powder with lower flowability. Lactose coated glass bead and agglomerated lactose powder presented the same flowability in the measurement performed with Dicovery-HR3 rheometer. This is because the measurement with Dicovery-HR3 rheometer has been done in high shear rate condition, where the powders are in frictional regime and the friction between particles govern their behaviors. Thus, by considering the similarity of surface friction of lactose coated glass bead and agglomerated lactose powder they fall into the same flowing category.

From the other side, the powder compressibility has been measured with FT4, to interpret powder flowability based on their compression ability. It measures powder compressibility by applying different values of normal stress (1-15 kPa) in a confined bed. In addition, the Haunser ratios has been obtained with GranuPack to be compared with the compressibility results from FT4. The Haunser ratio is a number that is linked to the powder flowability (see Table 4.1) and this value is measured during increasing tapping applied on powders in GranuPack measurements. The obtained Haunser ratio from GranuPack measurements and FT4 compressibility test results are in good agreement with the results obtained from flowability measurements. Control, hydrophilic, hydrophobic and lactose coated glass beads are presented lower compressibilities than agglomerated lactose powder. Furthermore, the powders showed similar classification in Haunser ratio with higher value for agglomerated lactose powder.

To figure out the flow behavior of powders under motion, the GranuDrum has been implemented. Powders flowability under different rotation velocity was monitored, it showed that powder cohesion increases under motion. In other words, powders flowability lower under motion while an increase in powder cohesion can be linked to apparition of electrostatic charge. To proof this idea, powders electrostatic charge has been measured with GranuCharge. It indicated that after flow, control glass bead had almost zero electrostatic charge while hydrophilic and hydrophobic glass beads obtained

negative charge after motion with slightly more negative charge for hydrophilic glass bead. Besides, lactose coated glass bead and agglomerated lactose powder obtained positive charge with more positive charge for agglomerated lactose powder. Based on GranuDrum measurement, agglomerated lactose powder and then lactose coated glass bead had higher cohesion evolution under rotation of drum. This can be due to the nature of lactose powder itself which is more cohesive in comparison to glass beads also the electrostatic charge apparition under motion evidenced by GranuCharge test.

Besides, hydrophobic glass bead presented higher cohesion in compare to control and hydrophilic glass beads. While, hydrophilic glass bead has more electrostatic charge than control glass bead therefore logically it is expected to observe higher cohesion for hydrophilic glass bead however, the contrary is observed. The fact is that the GranuCharge performs measurement in few seconds (2-3 s) and powder flow was very rapid in this measurement. While in GranuDrum, the measurement time was around 10 min and there was no humid control inside drum. Therefore, during GranuDrum measurement, hydrophilic glass bead lost its charge in encounter with air humidity (37-40 % of room humidity) while hydrophobic glass bead retained its electrostatic charge. It can be explained with the tendency of hydrophobic formulation to repel the humidity. Therefore, the low sensitivity of hydrophobic glass bead to humidity resulted in retaining its electrostatic charge. The evolution of flow behavior of hydrophobic glass bead with wide range of humid control will be explained in detail in chapter 5.

By using GranuHeap, we collected information about behavior of powders based on their heap height in static state. The heap height measurement are ranked in decreasing order as follow: agglomerated lactose powder > lactose coated glass bead > hydrophobic glass bead > control glass bead ≈> hydrophilic glass beads. Normally, higher the heap height means higher cohesion and lower flowability. The GranuHeap results are in well agreement with the result obtained by GranuDrum.
Finally, the powders fluidizability were measured with Aeration test. The powder bed was fluidized with an air tube. It has been observed that all powders were hardly fluidized. This can be due to their high weight resulting from their high density and/or size.

Therefore, by performing different measurement techniques, we have seen that we can collected more information about powders behavior which allows us to understand more about their behavior. Like as their behavior in static state, under rotation, compressibility, electrostatic charge, etc.

b. Comparison of powder behavior before and after environmental control

The influence of 50 % of humid control on five powder samples have been analyzed. All powders kept inside humid chamber during 24 hours at 20°C and their flow behavior has been studied with two rheometers: FT4 and Discovery-HR3. The obtained results were compared with the results of dry case that already evaluated with FT4 (in chapter 3) and Rheometer discovery (in current chapter). The reported results from FT4 in stability test evidenced that the powder BFE and SE were in consistent

with the results obtained without humid control. However, the minimum aeration velocity reported with aeration test evidenced slight incensement of minimum fluidization velocity for lactose coated glass bead and agglomerated lactose powder which it can be due to the humid intake ability in lactose powder. The compressibility test result showed that agglomerated lactose powder after 50 % of humid control presents slight incense on compressing ability while the other four powder samples had the same compressibility range than before humid control. The cohesion values reported in shear cell test indicated almost the same cohesion value at before and after humid control except a slight higher cohesion value for agglomerated lactose powder that is in consistent with the result of compressibility test explained before. By considering powder flowing value *ff* ranking based on classification proposed by Jenik [127], almost all the powders fall into free flowing powders category. Meaning that the powders have the same flow behavior before and after 50 % of humid control. Then measurement performed by rheometer discovery evidenced the same flowing behavior for before and after humid control too. In general the both rheometer presented same classification for these five powder samples. It has been noticed that at 50 % of humidity the flowability of studied powders did not modified also the performed tests all were in frictional regime meaning that for measuring influence of humidity on powder behavior it is needed to perform test in lower shear stress condition, where the cohesion between particles has the major effect in powders flowability. Therefore, in the following chapter, wide range of humidity in lower shear stress condition has been studied. Only control glass bead and hydrophobic glass bead are utilized to study, since the surface characteristics of hydrophilic glass bead is similar to control glass bead. In addition, humid control of lactose coated glass bead and agglomerated lactose powder in wide range of humidity was not practical, since they were crystalized already during formulation process. Therefore, they have not implemented in the following chapter.

c. Concluding diagram

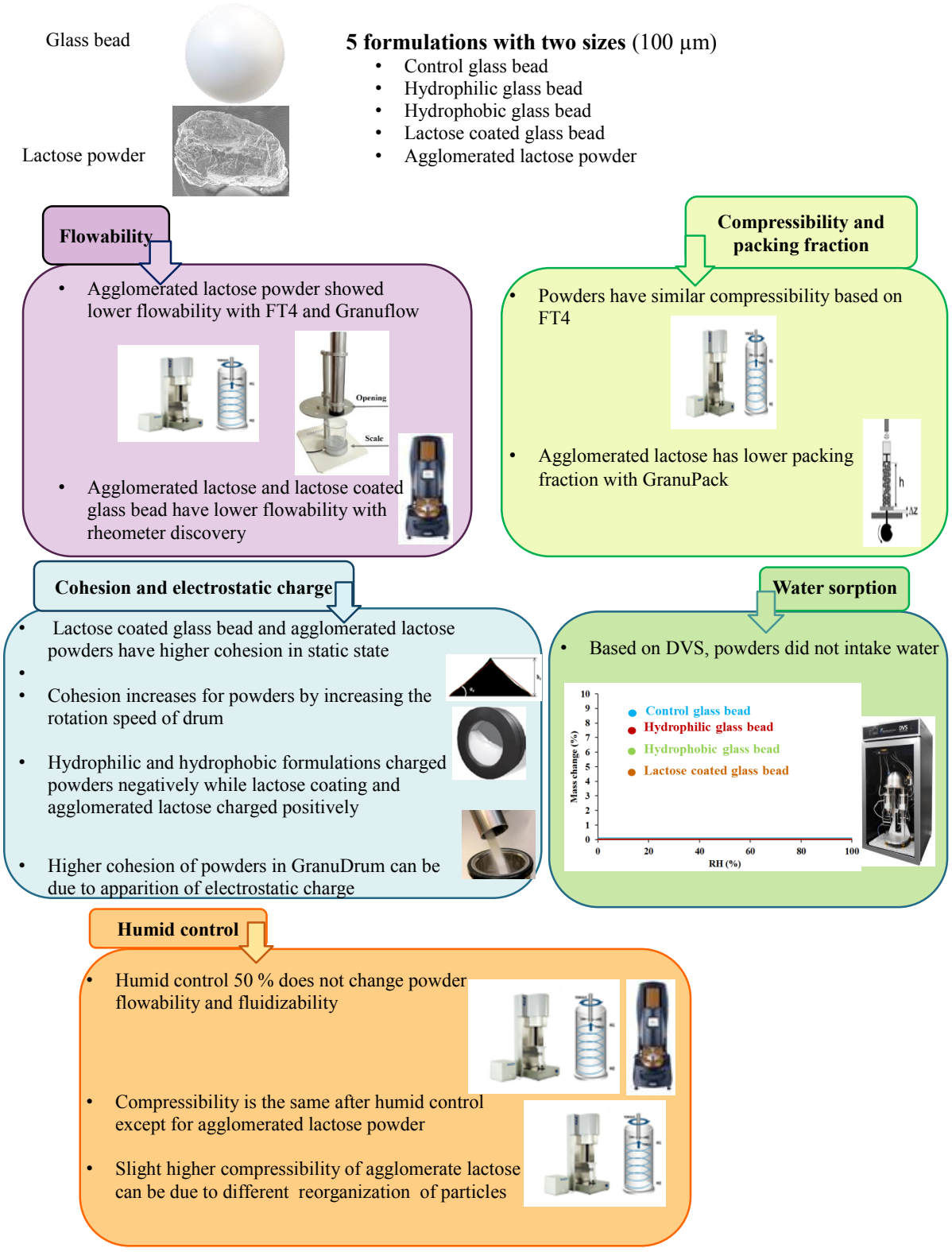

Figure 4.28 Concluding diagram.

Chapter 5

Influence of humidity and water addition on powder behavior

5.1 Introduction

In this chapter, influence of humidity and water addition on powder behavior has been studied. With this purpose, first the powders are kept inside humid chamber in preselected humidity during 48 h and then their rheology has ben measured with Discovery-HR3 rheometer at low shear rate. The protocol of rheology at low shear rate is explained with detail in chapter 4. Two powder samples; control and hydrophobic glass beads are utilized in this chapter. As mentioned previously, agglomerated lactose powder and lactose coated glass bead get crystallized during formulation process. Therefore, they are not used here since controlling their humidity in humid chamber was not practical. Moreover, hydrophilic glass bead has almost the same surface tendency to humidity in compare with control glass bead thus only control glass bead is used here.

First, the flow behavior of 100 μm control glass bead has been studied at 35-90 % humid control. The rheology of control glass bead has been measured by three series of measurement with different vibrational frequency at 40, 50 and 60 Hz and the amplitude 100 μm. The objective in performing test with three different frequencies was to obtain the optimum frequency for the theological measurements of control and hydrophobic glass beads at low shear rate.

Then, the rheology of control glass bead with two different sizes (40 and 100 μm) has been compared to figure out the link between particle size and flow behavior at low shear rate with humid control. In addition, the flowability of 100 μm hydrophobic and control glass beads are compared under humid control. At the end of this chapter, influence of addition of water in rheology of control glass bead has been studied. in this case an small step of powder preparation by vortex has been added to homogenize powder before measurement.

5.2 The powder preparation and rheology protocol

Humid control

Before perfoming measurement, each powder has been kept in humid chamber in order to reach the selected humidity value. The humid value which has been imposed was from 35 up to 90 % at 20 °C during 48 h. The relative humidity of powders have been confirmed by using thermoconstanter TH200 (Novasina, Switzerland) at a temperature of 25 °C; after taking them from humid chamber. This apparatus has a measuring range comprised between 0.05 to 1.00 with an accuracy of ± 0.01 over a temperature range between 0-50 °C. More precisely, 1 g sample is introduced into a polypropylene cup deposited in the sealed enclosure of the apparatus. The free water moistens or dries the air inside the enclosure until the balance is reached. The relative humidity is measured using an electrolytic sensor. The powder which prepared by humid control with the aforementioned protocol have been used in vibrational rheology measurements with Discovery HR3-Rheometer.

Discovery HR3-Rheometer

The rheology of powder subject to vibration has been studied with Discovery-HR3. Pre-vibration applied at 70 Hz during 10 min for removing any packing history before each measurements then the measurements have been performed by inducing the vibration at the frequency 60 Hz . The volume fraction of glass bead is $\phi_{glass} \approx 0.61$ [118,179] ($\rho_{glass} = 2500\ kg/m^3$). All tests have been carried out at imposed shear stress with the range of 4.5-188 Pa and the measured shear rate ranged as $3 \times 10^{-3} - 1\ s^{-1}$.

5.3 Influence of a wide range of humidity on powder behavior

In the following, rheology of 100 µm control glass bead has been considered at low shear rate with discovery-HR3 rheometer in a vane geometry. After preparing powder with aforementioned protocol, the measurements have been performed on each preselected humid values by vibrational rheology. The measurements have been carried out on control glass bead by inducing three different frequencies (40, 50 and 60 Hz) during separate tests at each controlled humidity. The objective was to find out the best frequency that allows us to differentiate viscosity curves of studied powder based one various humid control.

Figure 5.1, Figure 5.2 and Figure 5.3 present the evolution of viscosity versus shear rate at 40, 50 and 60 Hz vibration frequencies, respectively. The corresponding shear stresses have been normalized with the immersed length of the vane (2.1 cm) in order to have comparable results. With the purpose of keeping the unites of shear stress and shear rate unchanged, the normalization of shear stress has been done as ($\tau^* = \frac{\tau}{h} = \frac{1\ cm}{h}\tau$), where τ is the shear stress (Pa), τ^* is normalized shear stress (Pa) and h is the immersed length of vane (cm). As it is evident, at each three vibrational frequency, the yield stress has been disappeared; consequently the viscosity plateau has been appeared. While at 40 and 50 Hz of

vibrational frequencies, glass bead presented almost the same value of viscosity for any value of humid control. Thus, it is not easy to differentiate the powder viscosities (at 40 and 50 Hz vibrational rheology) based on different values of humidity. However, at 60 Hz of vibrational frequency, we noticed a clear difference in viscosity plateau in control glass bead with lower and higher values of humidity. Meaning that control glass bead showed higher viscosity plateau at humidity rage 85-90 % and the viscosity values are lower between 35-75 % humidity. Consequently, rheology at 60 Hz of vibrational stress permitted us to differentiate the powders based on their surface humidity values.

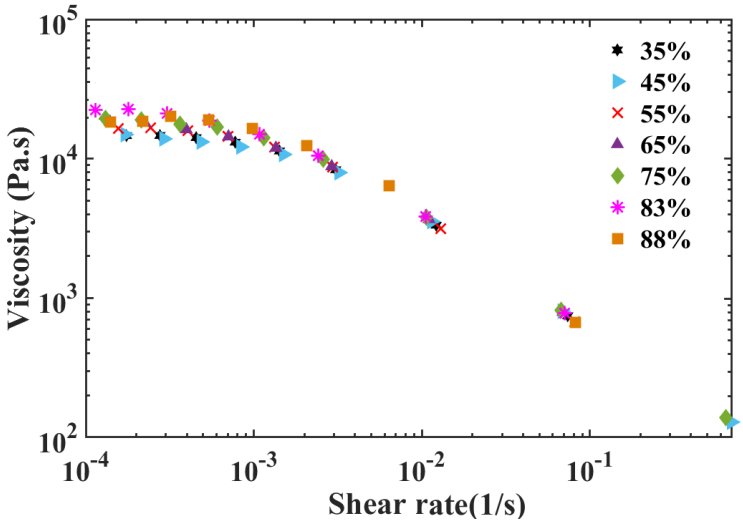

Figure 5.1 Flow curve of 100 µm glass bead for different values of humidity 35-90 % under 40 Hz of vibration stress. The amplitude of vibration is 100 µm.

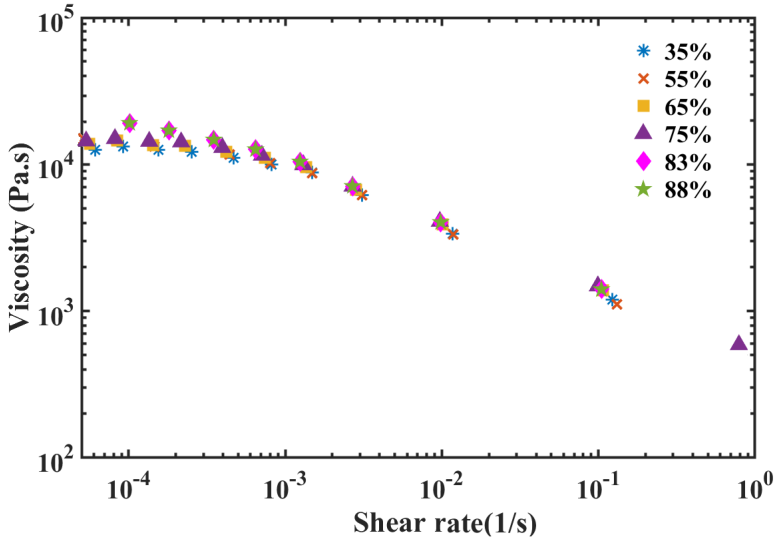

Figure 5.2 Flow curve of 100 µm glass bead for different humidity rage 35-90 % under 50 Hz of vibration stress. The amplitude of vibration is 100 µm.

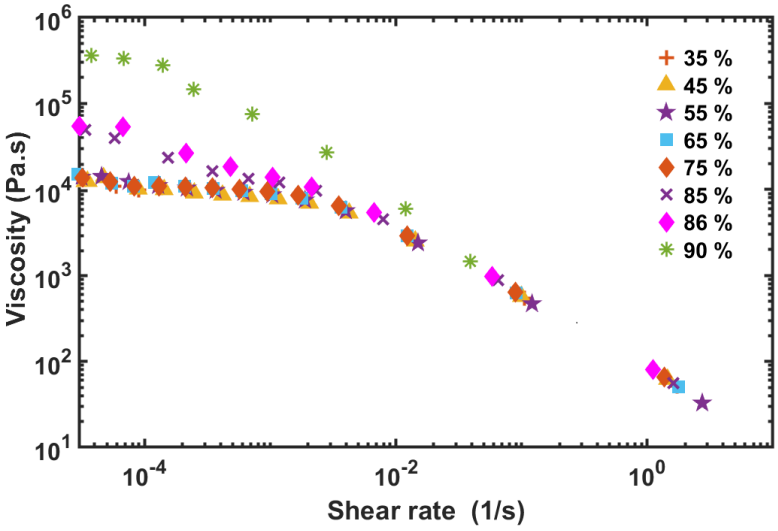

Figure 5.3 Flow curve of 100 µm glass bead for different values of humidity 35-90 % under 60 Hz of vibration stress. The amplitude of vibration is 100 µm.

5.3.1 Comparison of influence of humidity on flowability of control glass bead with two different sizes

The influence of humidity in flow behavior of control glass bead with two difference sizes of 40 and 100 µm has been considered. The goal was to understand the functionality of powders flowability according to their size, under humid control. Figure 5.3 and Figure 5.4 show the curves corresponding to 40 and 100 µm powders under 60 Hz of vibrational stress. It has been evidenced that in lower shear stress range, viscosity plateau appears in both powders. In fact, the viscosity plateau appears where the yield stress vanishes. Because at lower shear rates, the slow movement of vane allows the system to reorganize itself with the vibration faster than the modification is imposed by vane. This viscosity reaches a constant value. The viscosity plateau observed at $3 * 10^{-5}s^{-1} < \dot{\gamma} < 1.5 * 10^{-3}s^{-1}$ for 100 µm powder and for 40 µm powder it appeared at $10^{-5}s^{-1} < \dot{\gamma} < 1.5 * 10^{-4}s^{-1}$. While, powders are in frictional regime between $1.5 * 10^{-3} < \dot{\gamma} < 10$ for 100 µm and $1.5 * 10^{-4}s^{-1} < \dot{\gamma} < 1s^{-1}$ for 40 µm powders.

In order to simplify the comparison of these powder samples, their viscosity curves have been plotted versus corresponding humidity at given shear stress $\dot{\gamma} = 3 * 10^{-5}s^{-1}$. The mentioned shear rate has been selected since both powders are in viscosity plateau in this value. Figure 5.5 presents evolution of viscosity of control glass beads with 40 and 100 µm size as a function of different humidity values. It has been observed that both powders have constant viscosity almost up to 80 % of humidity. Meaning that their flowability is not influenced a lot up to this range of humidity. However, after 80 % of humidity, the viscosity curve has shifted in both case which is indicative of losing their flowability at higher humidity range. This viscosity shift is due to the higher number of surface contact in small diameter particle.

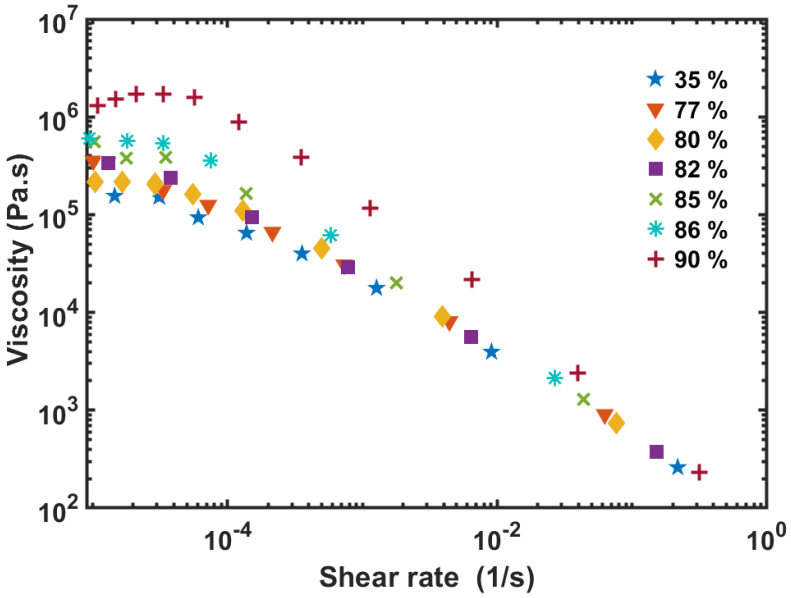

Figure 5.4 Flow curve of 40 µm glass bead for different values of humidity 35-90 % at 60 Hz of vibration stress. The amplitude of vibration is 100 µm.

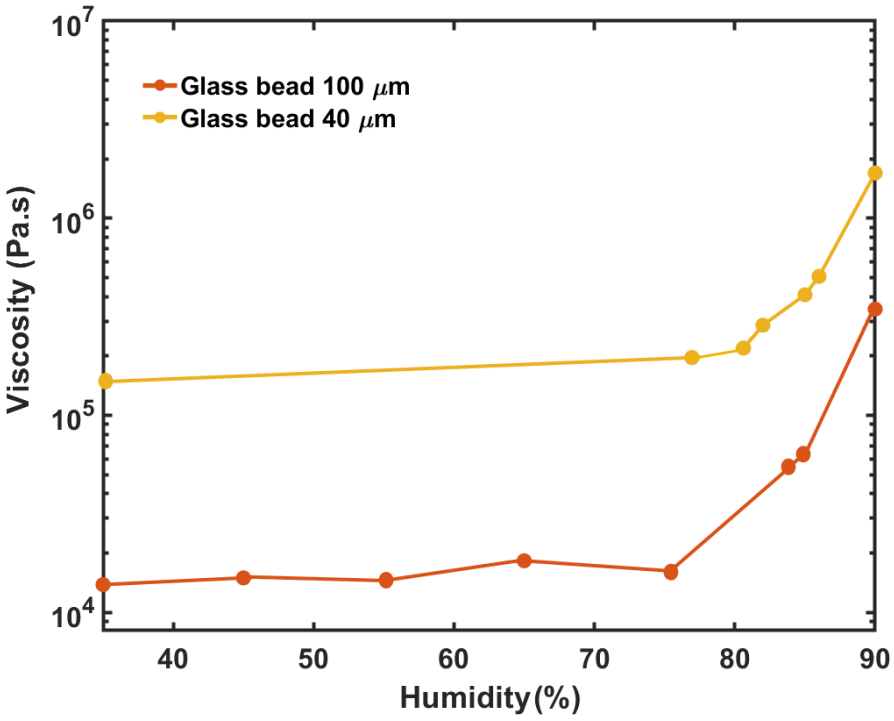

Figure 5.5 Comparison of evolution of viscosity of 100 and 40 µm glass beads in different range of humidity 35-90 % at 60 Hz of vibration frequency and 100 µm the amplitude of vibration. The curves are plotted in given shear rate at $\dot{\gamma} = 3 * 10^{-5} s^{-1}$.

5.3.2 Influence of humidity on flowablity of hydrophobic glass beads

Influence of humidity on flow behavior of hydrophobic glass bead has been considered in this section. Like as control glass bead, the hydrophobic glass bead has been kept in humid chamber during 48 h at preselected humid range and its flow behavior has been considered with rheometer discovery under 60 Hz of vibration stress. Figure 5.6 presents the evolution of viscosity of hydrophobic glass bead as a function of shear rate. The viscosity plateau appeared at $5 * 10^{-5} s^{-1} < \dot{\gamma} < 1.5 * 10^{-4} s^{-1}$ while after this range the powder falls into frictional regime at $1.5 * 10^{-4} s^{-1} < \dot{\gamma} < 10 s^{-1}$. Based on results presented in Figure 5.6 it has been seen that hydrophobic glass bead is less sensitive to the humidity even in higher range of humidity. If we compared the viscosity curve obtained for 100 µm control glass bead in Figure 5.3 with the same curve for hydrophobic glass bead of same size in Figure 5.6, one can see that in higher range of humidity, the viscosity of control glass bead increases; however we have not seen this behavior here for hydrophobic glass bead. In the following section, the behavior of control glass bead with hydrophobic glass bead has been studied in more detail. The next section is the reproduction of our submitted paper. The paper has been written in cooperation with our project partners in university of Liege, Belgium.

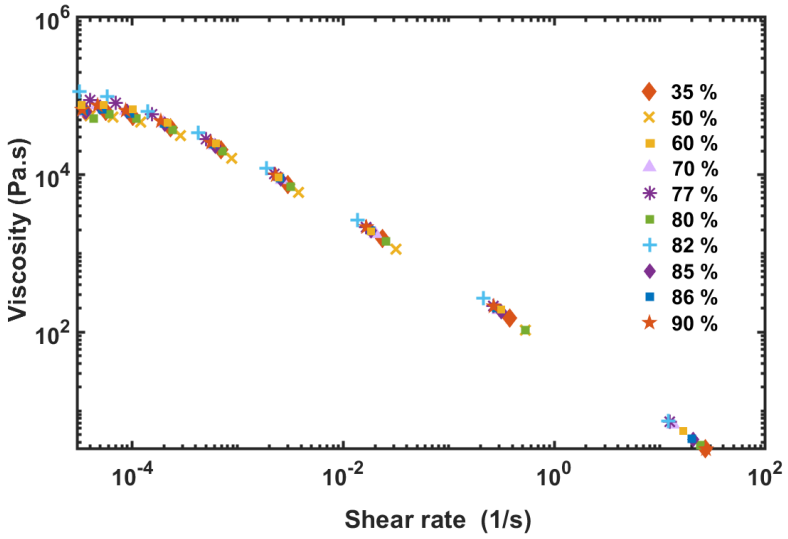

Figure 5.6 Flow curve of 100 µm hydrophobic glass bead for different values of humidity 35-90 % under 60 Hz of vibration stress. The amplitude of vibration is 100 µm.

5.4 Powder flow behaviors governed by the surface properties of particles

Tuning powder rheology and its sensitivity to surrounding environmental condition by controlling the surface properties of the particles is one of the major challenges of the powder industry. Indeed, handling large quantities needs powders with good flowability, adequate compressibility and few electric charges. We have performed a chemical treatment in order to obtain hydrophobic glass beads and their bulk

behaviors have been compared with control glass beads depending on the humidity. We characterized flow properties with various equipments. By performing hydrophobic surface treatment, the sensitivity of glass beads to the humidity is reduced. Furthermore, the influence of the electrostatic charges was not a deniable factor in increasing the viscosity of hydrophobic glass beads and consequently lowering its flowability in front of control glass beads, at low shear rate. At high shear rate, the powders showed similar behaviors.

5.4.1 Introduction

Powders are omnipresent in our daily life and they are extensively used in various industries such as pharmaceutical, cosmetics, chemical, food and construction. Despite numerous studies on powder rheology [72, 180–184], the behavior of powders is not fully understood, due to their complexity. In fact, the flow behavior of a powder depends on many factors consisting of surface properties, size, shape of particles [6] and environmental situation such as humidity [132].

However, understanding the powder's flowability is one the most important objectives in powder industries. Indeed, it can allow them to anticipate the powders' characteristics by knowing the condition that they encounter during process. In order to identifying the pertinent parameters governing the powder's flow, using different methods are always very beneficial approach. They can provide different point of view and indexes to assess powder flowability with several mechanical and dynamical conditions explained in the following.

It is well known that the Hausner ratio is an efficient and rapid method to estimate the powder behavior, based on bulk density [185]. Hausner ratio correlated to the ratio between settled bulk density and tapped bulk density. It has been reported that low compressible powders have the best flowability [96]. Similarly, a study on copper powder indicated that the Hausner ratio can be representative of friction condition between particles [78].

Particle-particle interaction and powders interaction with manipulating equipment during the process in industries result with apparition of electrostatic charges which is quite known phenomena whereby the increasing of powder charge lowers the powder flowability [186, 187]. Powder characterization based on this factor is of great interest [188, 189].

Also the free fall test is one of the inexpensive, efficient and rapid method to measure powder behavior without imposing any external force. The measurement is just based on the powder free fall due to the gravity. The flowability of powder is measured only by averaging time for which the constant volume of the powder pass through the measuring equipment [190].

In this among the rotating drum is a method to characterize the macroscopic properties of powders under aeration condition, it fluidize the powder and it reports the cohesion under rotation [72]; this technique measures in high shear stress. Furthermore, one of the most used methods in industry is applying vibration during process that it measures powder flowability in low shear rate condition. This

technique optimizes powder flowability and consequently enhance the saving of energy. Furthermore, this method is convenient to control the different steps of industrial process consisting of feeding, conveying and even parts of the equipment like as hopper, etc [118, 191].

From the other side, studying and understating the influence of environmental condition like as humidity on powder behavior is very significant and of great interest [170, 192, 193].

This paper focuses on studying influence of formulation on powder flowability and sensitivity of powder flowability to the external condition. Therefore, first influence of surface formulation on behavior of control and hydrophobic glass beads have been studied in ambient temperature and without humid control. Different methods utilized here to figure out the macroscopic flow and the rheology of powders. Then, influence of humidity on powder behavior has been studied and two different method of humid control and powder rheology utilized to characterize the powders and finally the results are compared.

First, to control the powders environmental condition, they have been kept in humid chamber 48 h at 20 °C in a given humidity ranging from 35 % up to 90 %; the humid control time kept long enough to reach the selected relative humidity and the humidity value confirmed by thermoconstanter TH200, at the end of humid control. Then the rheology of powders have been performed in a dry room in ambient temperature during maximum 30 min of measurement time. The apparent viscosity of powders are measured with HR3- Rheometer Discovery. The rheometer measurement cell is put on vibration in order to homogenize the system. All results have been collected by imposing shear stress.

A second experiment on humidity was conducted at the same time, in collaboration with another laboratory in order to compare and to link the dependency of the humidity on the shear stress with the electrostatic charge of powders and their cohesion. However, as the material was different, in this case the humid control has been done with a rotating drum with humid-air controlled flow. The powders have been kept 1 h in each selected humid range to reach the required humid equilibrium.

5.4.2 Materials and Methods

In the following, the materials and the different methods which are implemented here for characterizing powders are explained. The purpose of using different methods is to characterize the powders under different external conditions and to observe the influence of formulation and mainly effect of humidity on powders flowability. Therefore, two series of tests have been performed on control and hydrophobic glass beads. First, the characterization measurements have been done by implementing Granutools equipments. The packing dynamics of powders has been measured with GranuPack, the powder electrostatics charge studied with GranuCharge and the powder flowability measured with Granuflow and GranuDrum equipments. During performing Granutools measurements the humidity and temperature kept constant at, 37-44 % and 22 °C, respectively.

Then the study of influence of wide range of humidity has been done on powders under vibrational

rheology with Discovery HR3-Rheometer which provides possibility to be in low shear rate; where the cohesion of powders play role in their powder flowability. These result were confronted with the measurements of the GranuDrum and the GranuCharge. The goal here was to observe clearly the effect of humidity on powders behaviors based on the strength of their surface cohesion depending on their surface formulation.

Powders preparation and conditioning

In this study glass beads of types S 90-150 μm has been used. Hydrophobic surface treatment has been done on glass beads. With the purpose of preparing hydrophobic surface formulation on glass bead [135, 194], first the hydrophilic surface treatment has been performed (for hydrophilic formulation see [194]), then it has been followed with silanization. The silanization of glass beads with mixture of toluene (500 mL) and 1H,1H,2H,2H-perfluorooctyltriethoxysilane (2.5 g) has been performed, this mixture has been kept maximum 48 h under extractor hood at ambient temperature. Then, the powder filtered and washed with pure toluene and finally they kept about 24 h under extractor hood for evaporating the toluene inside the powder. Finally, with the purpose of completely drying process of the powder, it has been kept in an oven, maximum 4 h at 70 °C.

GranuFlow

The GranuFlow is an instrument that measures the flowability of a granular material. Figure 4.1 illustrated the diagram of GranuFlow equipment. The powder to analyze is poured in a steel tube to avoid electrostatic charges accumulation. The opening of the bottom is obstructed with a hole-pierced disk. Each hole of the disc has a different diameter aperture d. Below, a scale is placed and it measures the flow rate of the powder through the opening. By measuring the different mass flow rates F depending of the size aperture d, one can obtain the flow index C using the Beverloo model

$$F = C\sqrt{g}(d - d_{min})^{2.5}. \tag{5.1}$$

The flow index C, expressed in g/cm^3 can be interpreted as the ability of a powder to flow and g is the gravity of earth (9.81 m/s^2).

GranuDrum/Rheometer

The rotating drum is one of the most extensively used practical geometry to study the flow behavior of granular material [72, 195–197]; especially non cohesive powders [72]. The experimental set up in this study presented in figure 5.7 consists of a drum with two glass walls which rotates around its central axis with the angular velocity Ω. The flowing dynamics of powders inside the drum is function of this rotating angular velocity. The drum is generally half filled with the powder, whereas the length and the diameter of the drum are respectively 20 mm and 84 mm. During rotation, the drum is backlighted and a CCD camera takes pictures of the powder interface position inside the drum. For each imposed angular velocity, 50 pictures are taken, separated by 0.5 s. The average powder-air interface position is computed

by image processing analysis. From this analysis, two measures are extracted: the cohesion index σ_f, which is the fluctuations of the powder-air interface and is representative of the cohesion of granule inside the drum, and the flowing angle α_f, which is the angle between the horizontal and the average interface. In this study, the rotating angular velocity has been selected between 2-30 rpm.

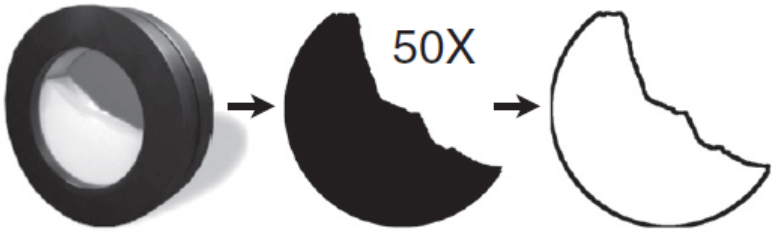

Figure 5.7 Sketch of the GranuDrum equipment. A cylinder is half-filled with the powder and rotates around its axis. For each rotating speed, a CCD camera takes 50 successive images of the flow. A dedicated algorithm enables to measure the flowing angle α_f and the fluctuations σ_f of the flow from the shape of the powder/air interface [72].

GranuPack

Measuring the tapped density and packing dynamic of powder are very popular in powder characterization [72,185]. Also, Hausner ratio is an efficient and widely used methode to interprated powder flow behavior [185]. It can be calculated based on the initial density and the final density extracted from compaction curve. The Hausner ratio is correlated to the powder flowability whereby high value of Hr corresponds to low flowability. Also, as it has been mentioned already, it can be representative of friction condition between particles [78]. The GranuPack equipment presented in figure Figure 4.5 has been developed to automate the procedure of compressibility measurement since it is usually realized with naked eyes. The analyzing cell is made of a tube with $D = 26$ mm in diameter and $L = 100$ mm in length. This tube is metallic to avoid the accumulation of electric charges during the measurement. A narrower and bottomless tube is inserted into this measurement tube and filled with the powder to analyze. Afterward, it is slowly removed upward at the velocity $v = 1$mm/s. This initialization procedure avoids human intervention and then increases the reproducibility.

A light hollow cylinder is placed on the top of the pile to keep it flat during the compaction process. The tube goes up and down over a height of $\Delta z = 3$ mm in order to compact the granular pile. A distance sensor measures the position of the hollow cylinder after each tap and computes the bulk volume V of the pile. As the introduced mass of powder is known, the evolution of bulk density ρ_b as a function of the tap number t is calculated. The bulk density is the ratio between the mass m and the volume V of the powder. The packing fraction η is calculated by dividing the bulk density ρ_b by the true density of the particles ρ_t, $(\eta = \rho_b/\rho_t)$. After recording the packing fraction for each tap, the compaction curve is

fitted with the classical logarithmic model [163],

$$\eta(t) = \eta_\infty - \frac{\eta_\infty - \eta_0}{1 + \ln(1 + t/\tau_t)}. \tag{5.2}$$

Then, one obtains the final packing fraction η_∞ and consequently the more common parameter, the Hausner ratio $\mathrm{Hr} = \frac{\eta_{500}}{\eta_0}$ [72, 162, 198]. η_0 is initial packing fraction and η_{500} is packing fraction after 500 taps.

GranuCharge

Electrostatic charges are created due to the triboelectric effect inside a powder during a flow; meaning that the particles charge exchange at the result of contact with the other particles and devices wall. GranuCharge equipment is illustrated in Figure 4.7, it is a very useful equipment to measure the ability of a flowing powder to be charged electrostatically. It measures electrostatic charge of the powders by putting them on motion under the influence of gravity. In this measurement, the experimental set up is consist of three parts: a stainless-steel pipe, V-tube and a Faraday cup. The stainless-steel pipe is for feeding the V-tube by automatic rotation inside the tube.

In general, the V-tube material can be selected between following list: stainless steel 316L, aluminum 6063-T6, borosilicate glass, ABS, PVC and HDPE which the Stainless Steel 316L has been used in this study. The V-tube itself consist of two tubes with the length of L = 350 mm and diameter D = 47 mm; the two parts are connect together with the angle of 90°. After feeding the tube by the stainless-steel pipe the powder flow inside V-tube and at the end it fall into the faraday cup which is connected to an electrometer to measure the powder charge obtained during flow; before starting each test the whole assembly has been connected to the earth to be sure that they are discharged. The electrometer is capable of measuring charge ranging 0.1 nC - 1 µC. The powder charge density is computed by dividing calculated charge by the mass of powders. The charge density unit is Coulomb per kilogram. The powders can obtain negative or positive charge after flow, based on their tendency to obtain or loss electron at the result of contact with measuring equipments [186].

The rheology measurements

The rheology of powder subject to vibration has been carried out with discovery-HR3 rheometer. The protocol of measurement has been explained at the beginning of this chapter and with more detail in chapter 4. The powder prepared by controlling its humidity in a humid chamber then after performing pre-vibration at 70 Hz, the rheology of powder has been performed at 60 Hz of vibration stress. The powder humid control assessed with two methods and the results have been compared. The first method carried out by a humid chamber which its procedure has been explained before in this chapter. In second method, humid control has been performed with GranuDrum and GranuCharge to study the effect of humidity, where the powder prepared with another conditioning method. The powder to analyze was placed in a rotating drum at 1 rpm with a controlled humid air flow during 1 h. As the powder was

continuously mixed and rotated, the humidity absorption is assumed to be efficient. With this method, the accessible range for humidity is RH $= 35 - 95\% \pm 5\%$ inside the drum.

5.4.3 Results

Influence of surface treatment

Flowability

The flowability of control and hydrophobic glass beads have been studied with the GranuFlow. Each powder flow rate has been measured for several aperture, from 2 to 16 mm in standard conditions of temperature and pressure. The results are shown on Figure 5.8. As one can see, the flow properties of hydrophobic and control glass beads are similar. The flowing index obtained from the fit of Equation 5.1 are respectively $C = 8.62\ 10^{-4} \pm 3.6\ 10^{-6}\ (g/cm^3)$ and $C = 8.89\ 10^{-4} \pm 4.5\ 10^{-6}\ (g/cm^3)$.

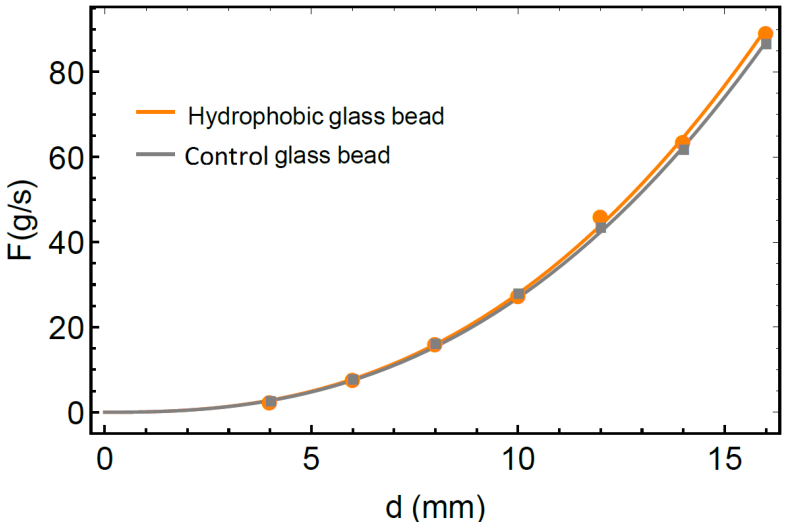

raw

Figure 5.8 Fit of the Equation 5.1 on the data for respectively control beads, in grey, and hydrophobic beads, in orange. The humidity range is 37-44 % and temperature is 22 °C, respectively.

Charge

The electrostatic charge measurement of control and hydrophobic glass beads have been performed with GranuCharge equipment with the humidity and temperature range at 37-44 % and 22 °C, respectively. Figure 5.9 represents the results corresponding to this test. Three values have been collected for each samples, these values are consisting of initial charge q_0, final charge q_f and $\Delta q = q_f\text{-}q_0$. The initial charge has been measured before performing test by directly introducing powder inside Faraday cup and final charge is a measurement after powder flow through V-tube. The obtained results show that both powder had almost zero electrical charge as initial charge. After flow inside stainless steel V-tube, control glass bead kept this tendency to having almost zero charge however hydrophobic glass bead obtained negative charge. The quantity of each sample was 50 mL during measurement.

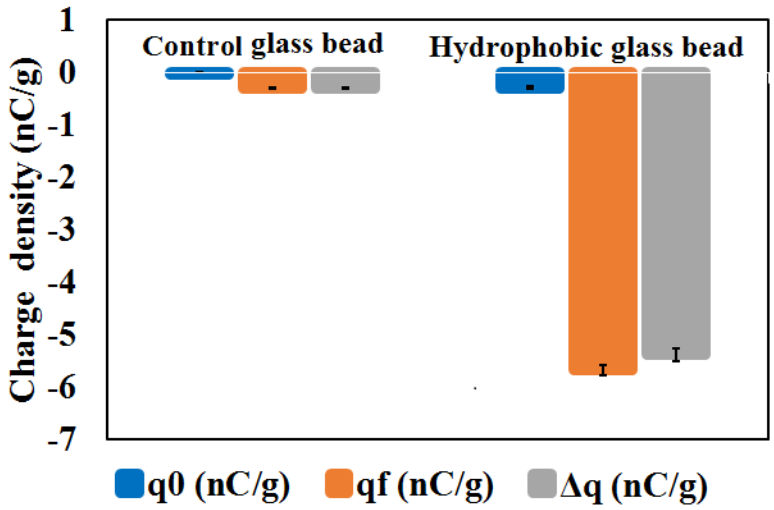

Figure 5.9 The electrical charge evolution of control and hydrophobic glass beads before and after flowing inside V-tube. The measurement performed by GranuCharge equipment. The humidity range is 37-44 % and temperature is 22 °C, respectively.

Cohesion

Figure 5.10 shows evolution of the cohesion σ_f and the flowing angle α_f of control and hydrophobic glass beads. It has been observed that cohesion of both samples have been enhanced by increasing rotating speed of the drum, meaning that their flowability decreases under motion, particularly after 10 rpm. Hydrophobic glass bead showed slightly more cohesion than control glass bead. This could be explained with the GranuCharge measurements. Hydrophobic glass beads have more electrical charge than control glass beads. This can lead to higher cohesion of hydrophobic glass bead under motion (see Figure 5.9).

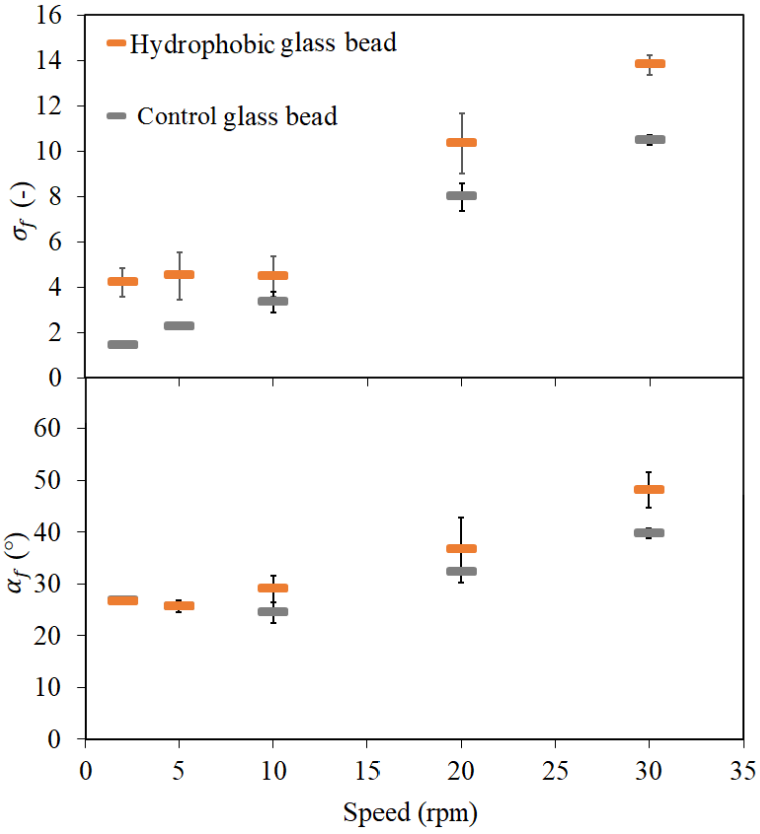

Figure 5.10 Evolution of the flowing angle α_f and cohesion σ_f of control glass glass bead and hydrophobic glass bead under different rotational speed with the measurements performed by GranuDrum. The humidity range is 37-44 % and temperature is 22 °C, respectively.

Packing dynamics

The compaction curves of control glass bead and hydrophobic glass beads have been recorded with the GranuPack in standard conditions of temperature and humidity and are presented on the Figure 5.11. One observe the difference of density between two powder at the beginning and at the end of the compaction process. Figure 5.12 presents the Hausner ratio Hr, where the packing density before tapping η_0, after 500 taps η_{500} and the asymptotic packing fraction after an infinite number of taps η_∞ obtained from the equation Equation 5.2. The Hausner ratio Hr in our powder samples is comparable and the difference is not meaningful. In the other word, the cohesion is not strong enough to modify the final state of compaction. It seems that compaction of powders here related to the shape and surface roughness of particles.

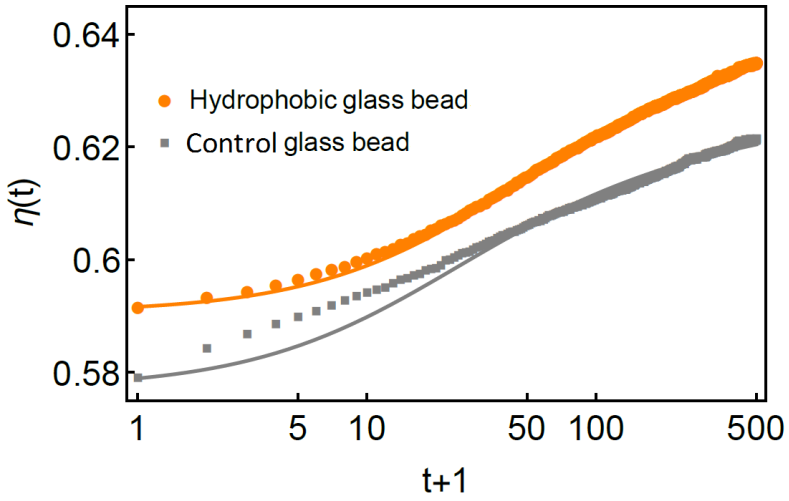

Figure 5.11 Experimental compaction curves for respectively control glass beads, represented by grey squares, and hydrophobic glass beads, represented by orange dots. Both are fitted with the logarithmic model (Equation 5.2), represented by plain curves of the same color. The humidity range is 37-44 % and temperature is 22 °C, respectively.

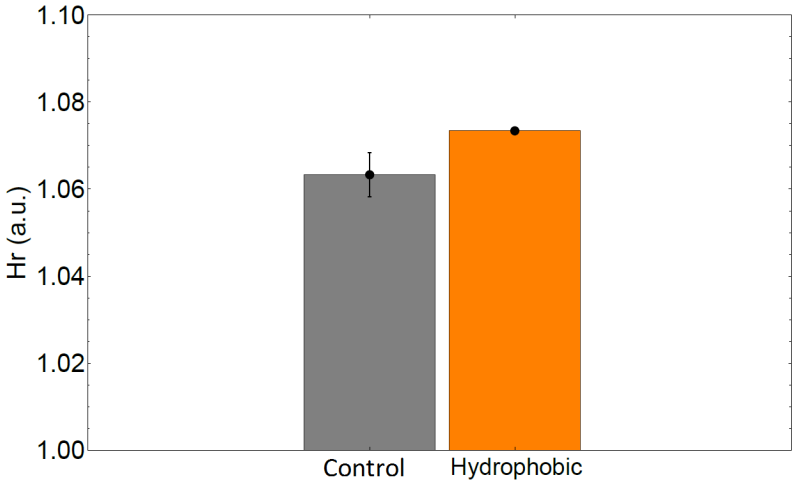

Figure 5.12 Comparison between the Hausner ratio $Hr = \frac{\eta_{500}}{\eta_0}$ of control glass beads, in grey, and the hydrophobic glass beads, in orange.

Impact of humidity

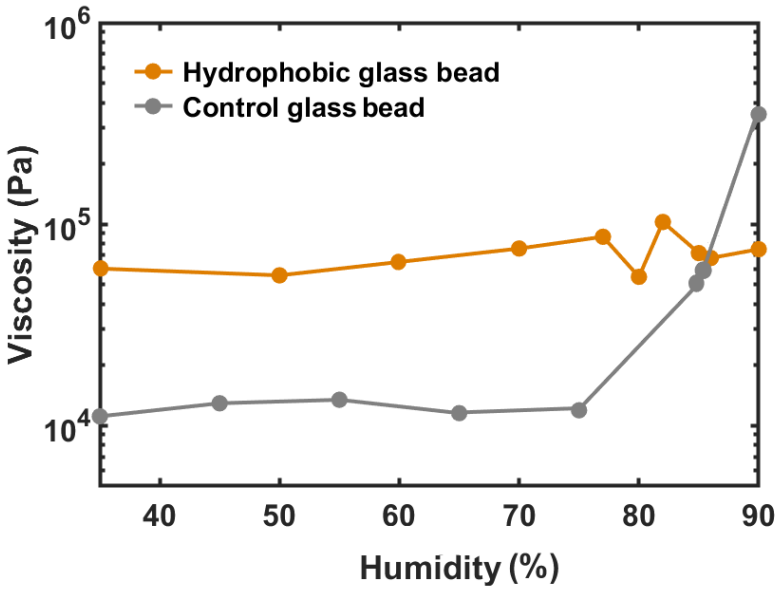

Figure 5.13 The evolution of viscosity of control and hydrophobic glass bead under humid control from 35-90 % and in given shear rate $\dot{\gamma} = 5 * 10^{-5} s^{-1}$.

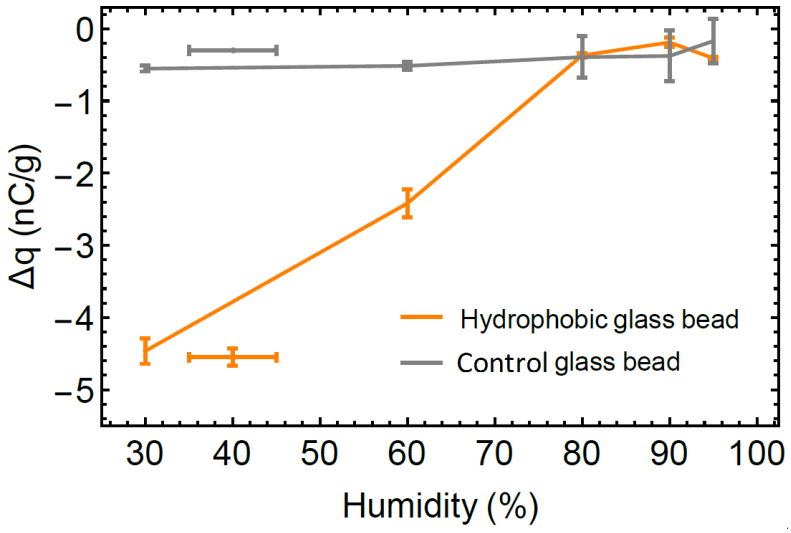

Figure 5.14 The evolution of the charge difference of control and hydrophobic glass beads based on humid control from 35-95 % ± 5 %. Both supplementary points out of the lines represents data from normal environmental conditions.

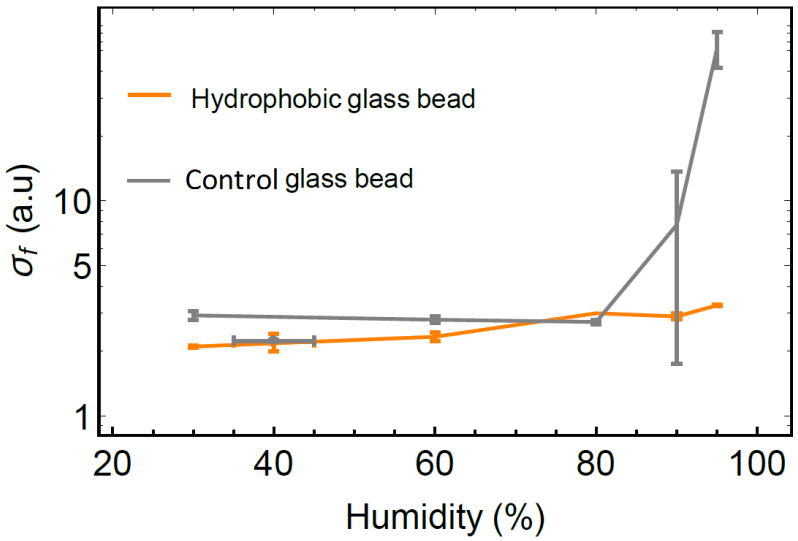

Figure 5.15 The evolution of the cohesion index of control and hydrophobic glass beads based on humid control 35-95 % ± 5 %. Both supplementary points out of the lines represents data from normal environmental conditions.

The influence of humidity on flowability of control glass bead and hydrophobic glass bead has been studied. HR3-Rheometer Discovery has been used for these measurements (see Figure 5.13). The measurements done in an experimental room in ambient temperature and the humidity of room was not controlled during performing rheological measurements but by using Thermoconstanter TH200 it has been proofed that control glass bead keeps its humidity value by the end of test; the powders humidity were controlled before each measurement in humid chamber. Furthermore, the powders cohesion and electrostatic charge have been measurement as complementary test with the objective of understanding the link between powders viscosity with their cohesion and electrostatic charge in different range of humidity. Indeed, it has been proved that the humidity can change the charging of a powder [186] which can induce variation of the cohesion. These measurements have been done with GranuDrum and GranuCharge equipments by adding the humid control step ranging 35-95 % ±5%. The humid control in this step has been done with a rotating drum with humid-air controlled flow. The powders have been kept 1 h in each selected humid range to reach the required humid equilibrium.

Figure 5.13 presents the evolution of viscosity of control and hydrophobic glass beads as a function of humidity ranging from 35-90 %; the measurement has been done with HR3-Rheometer Discovery in low shear rate condition and the related curves have been plotted in given shear rate at $\gamma = 5 * 10^{-5} s^{-1}$. Based on viscosity curves, the hydrophobic glass bead showed higher viscosity than control glass bead. It can be due to the fact that hydrophobic glass bead presented more electrostatic charge than control glass bead under vibration in the humid range of 35-80 % (see Figure 5.14). On the contrary, the viscosity curve of hydrophobic glass bead kept always constant trend and continued to show the same tendency even after 80 % of humidity. This is due to willingness of hydrophobic glass bead to repeal water and even in 90 % of humidity it does not keep humidity around surface. By taking into account that the rheology measurement has been done in dry room. Then, the slight amount of presented water in high humidity

range on hydrophobic glass bead evaporated rapidly. The rheology measurement time was between 20-30 min which was enough for evaporating the slight surface water and getting the powder charged again. It should be mentioned that the charge measurement time in Figure 5.14 which has been done with GranuCharge is few seconds and the powders do not have time to present charge evolution during this short time; against the case of rheology measurements.

In general, the control glass bead showed lower viscosity than the hydrophobic glass bead since it has lower electrostatics charge. However after 80 % of humidity the viscosity of control glass bead has dramatically increased which is due to the sensitivity of control glass bead to water which resulted with high cohesion. In addition, this increasing shift of viscosity in control glass bead can be due to the condensation effect while for the hydrophobic glass bead evolution of viscosity was not recorded for the same range of humidity. This sensitivity of control glass bead for humidity has been confirmed with the cohesion index measurement by GranuDrum equipment with the speed of 4 rpm with standard conditions, measuring 50 frames with 0.5 s between two frames. Figure 5.15 presents that the cohesion index of control glass bead increases after 80 % of humidity while the cohesion index curve of hydrophobic glass bead does not evolve even in higher value of humidity. Here the measurement performed with GranuDrum is in high shear rate condition.

5.4.4 Discussion

The flowability and the compressibility tests performed by the equipments of Granutools showed that the control glass bead and hydrophobic glass bead have similar behaviors in the case of flowability and compressibility, they both are in the category of easy flowing powders and hydrophobic surface formulation did not modify the flowability of glass bead in high shear rate condition. Despite of the GranuCharge measurement which reported negative charges for hydrophobic glass bead and almost zero charge for control glass bead, but it has not affected the powder flowability based on GranuFlow measurement. However, what it has been observed based on vibrational rheology with Discovery HR3-rheometer is indicative of the fact that hydrophobic glass bead showed higher viscosity than control glass bead at low shear rate condition. Applying vibration allows the powder to flow at low shear rates which in this range the influence of cohesion between particles is the most important factor in governing the behavior of the flow. Meaning that by considering the electrostatic charge of hydrophobic glass bead which was more than control glass bead, higher viscosity has been observed for hydrophobic glass bead which is due to its higher cohesion coming from its electrostatic charge. Furthermore, based on rheological measurements done after humid control it has been proofed that hydrophobic surface formulation decrease sensitivity of glass bead to the humidity which it evidenced in higher humidity range. Whereby, in high humid range, the flowability of control glass bead decreased impressively in compare with the flowability of same glass bead with hydrophobic surface. In the following the collected data from different set of measurements has been presented in Table 5.1.

Table 5.1 Recapitulation of the different values measured with the set of instruments; the humidity and temperature range are 37-44 % and 22 °C, respectively.

Measure	Control glass bead	Hydrophobic glass bead
C (g/cm^3)	0.86 ± 0.00	0.88 ± 0.00
Δ q (nC/g)	-0.30 ± 0.00	-4.55 ± 0.12
σ_f (a.u.) (30 rpm)	10.46 ± 0.21	13.80 ± 0.43
α_f (a.u.) (30 rpm)	39.73 ± 0.10	48.13 ± 3.43
η_0 (a.u.)	0.58 ± 0.00	0.59 ± 0.00
η_{500} (a.u.)	0.62 ± 0.00	0.64 ± 0.00
η_∞ (a.u.)	0.63 ± 0.00	0.66 ± 0.00
Hr (a.u.)	1.06 ± 0.00	1.07 ± 0.00

5.4.5 Conclusion

This paper presented a study on flow behaviors of two types of powders consisting of control glass bead and hydrophobic surface treated glass bead. The objective was to explore the behavior of hydrophobic formulated glass beads under different types of measurements and compare it with the same measurements done on control glass bead. Therefore, the behaviors of these two powders have been studied under different conditions consisting of free flow test, rotating drum test, charge and compressibility tests. The Granutools equipments allowed us to study all these. Based on GranuPack and GranuFlow measurements it has been observed that the powders have similar flowability. However, the GranuCharge measurement represented a charge difference between hydrophobic and control glass beads, it reported negative charge for hydrophobic glass bead and almost zero charge for control glass bead which was expected to has influence on their behavior. This issue has been confirmed with the cohesion increase of the hydrophobic glass bead under motion by measurement done with GranuDrum equipment which is indicative of decreasing the flowability of hydrophobic glass bead under motion due to the tendency of this powder to be more charged under motion. Also the influence of air humidity on utilized powders has been studied. In order to homogenize the powder sample, the vibrations are applied to the samples. The obtained results evidenced that hydrophobic glass bead under vibrational rheology is less flowable than control glass bead which is in agreement with what measured by GranuCharge measurement. Since hydrophobic glass bead was obtaining charge under motion by taking into account that at high shear rate the GranuFlow reported same flowing behavior for both control and hydrophobic glass beads. This is because the powders are in frictional regime meaning that the friction between particle-particle governs the powder flowability. Control glass and hydrophobic glass beads have similar surfaces; therefore they showed similar flowability in frictional regime. At low shear rate, the flowability of powders are linked to their surface cohesion. Furthermore, it has been indicated that by doing hydrophobic formulation on

control glass bead the sensitivity of powder to the humidity has decreased even in high humidity range and it kept its flowability as in low humidity. However, control glass bead lost dramatically its flowability in higher value of humidity.

5.5 Influence of water addition on powder behavior

In this section, the flow behavior of control glass bead has been considered by adding different quantities of water. The quantities of water that we added to the sample are 0.5-4 mL with 0.5 mL of steps. The measurement has been done in high and low shear rate conditions with Discovery-HR3 rheometer, which was attached to vertical vibration. For the measurements at low shear rate, before performing each test a pre-vibration at 70 Hz applied for each powder samples during 5 min. Then the measurement performed at 60 Hz of vibration frequency with the amplitude of 130 µm, during 30 min. Figure 5.16 presents the evolution of viscosity curve of control glass bead versus shear rate as a function of different quantity of water. Generally, it has been observed that in low shear rate, the yield stress disappeared and viscosity plateau appeared, in contrary in high shear rate condition the powders are in frictional regime. In addition, if we compare the obtained wet glass bead curves with dry glass bead curve (at low rate), one can see that the viscosity of wet glass bead with 1 to 4 mL of water is higher than dry case. This may be due to the fact that by adding water the liquid bridges between particles appear, consequently the inter-particle cohesion increases which it results on viscosity increase in wet powders. However, the glass bead with 4 mL of water presented lower viscosity than the rest of powders wet powders at high and low shear rate rheology. This may due to the apparition of clusters of glass bead in presence of 4 mL water inside sample. Meaning that by adding 4 mL of water to control glass bead, the particles joint together to make big clusters of particles. Therefore, the clusters behave like large particles, as we know the big particles have less surface contact in compare with small particles therefore they can have better flowability. Nevertheless, it should be mentioned that during measurement we noticed that the pre-vibration was not enough to fully homogenize the powder samples since big air gaps were evident inside sample. Therefore, an extra step of homogenization has been added after samples preparation. In this step the vessel containing the powder was kept on a vortex during few minutes to reach the homogeneous structure with less air gap between particles.

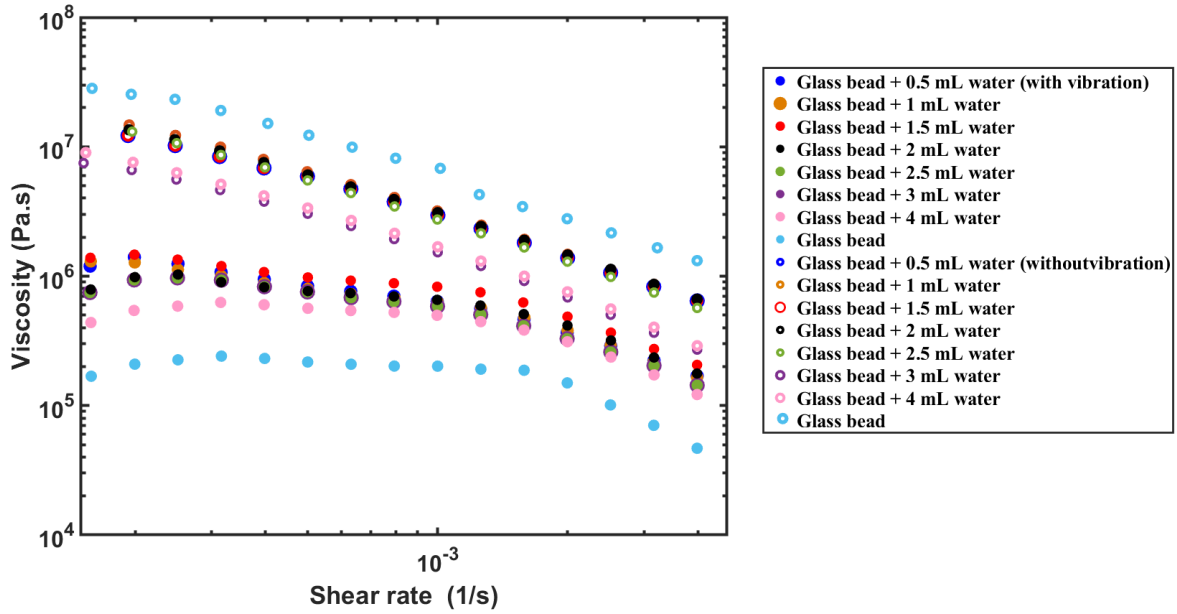

Figure 5.16 Evolution of viscosity of 100 µm glass bead by addition of different quantity of water with and without vibration stress. In vibration stress condition, the frequency of vibration is 60 Hz the amplitude is 130 µm. In these measurements, the samples vibrated by a vortex before each tests both in vibrational and non-vibrational rheology.

Figure 5.17 and Figure 5.18 show the evolution of viscosity of the control glass bead as a function of water quantity in glass bead at low and high shear rate conditions, respectively. The viscosity curves are plotted in given shear rate at $\dot{\gamma} = 2 * 10^{-4} s^{-1}$. In high shear rate condition, the powders present higher viscosity than in low shear rate condition. This is due to the fact that in low shear rate condition the yield stress vanishes and viscosity plateau appears.

Generally, by adding water inside powder, the liquid bridges appear between particles. By increasing the number of liquid bridges, the size of water curvature between particles increases and it results in increasing of viscosity. In general, there is an equilibrium between liquid bridges and inter-particle cohesion. Whereby, if the size of liquid bridges grow too much then a big curvature will be formed. In this case, the liquid bridges become strong enough and the inter-particle cohesion will decreases.

Therefore, at low shear rate measurement in the control glass bead with 4 mL of water, it may the particles surface started to saturate with the water. Consequently, tension on particles surface is not present anymore, since having surface tension means having water and air around particle surface. Thus, it results in losing the cohesion in this sample. Also the powder with 0.5,1 and 1.5 mL of water quantities have slightly higher viscosity than the rest of samples. This may because in this case there is an equivalent between inter-particles air and liquid bridges.

In addition, the powders with the water quantities of 2, 2.5 and 3 mL have almost similar viscosity but lower than the previous samples. It can be deduced that in these cases the inter-particle liquid brides have similar quantities. But, the inter-particle air has been started to get lower than liquid bridge. Therefore,

the viscosity of powders with 2, 2.5 and 3 mL of water is lower than the powders with 0.5, 1 and 1.5 mL of water.

In the case of high shear rate measurements, all wet powders presented lower viscosity than dry powder. This is because of shear band flow based on digging hole by the rotation of vane at high shear rate condition.

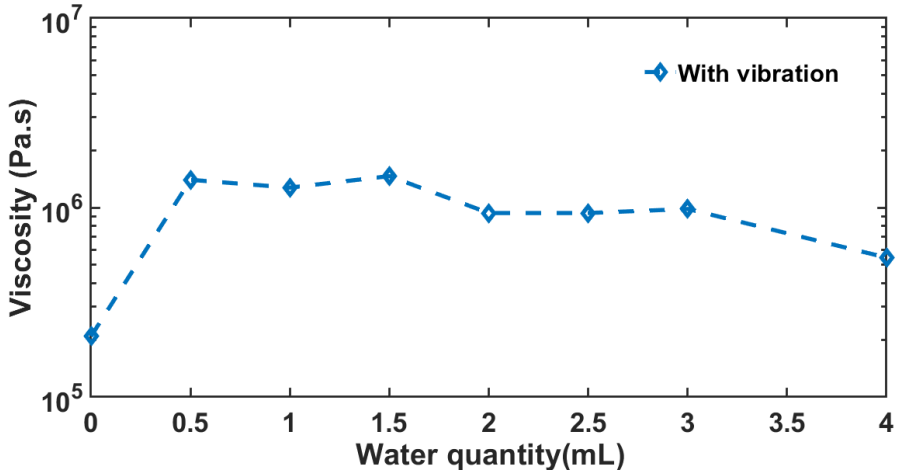

Figure 5.17 Evolution of viscosity of 100 µm glass bead by addition of different quantity of water with vibration stress and with extra vortex vibration step. The curve is plotted in given shear rate at $\dot{\gamma} = 2 * 10^{-4} s^{-1}$, based on the data collected in Figure 5.16.

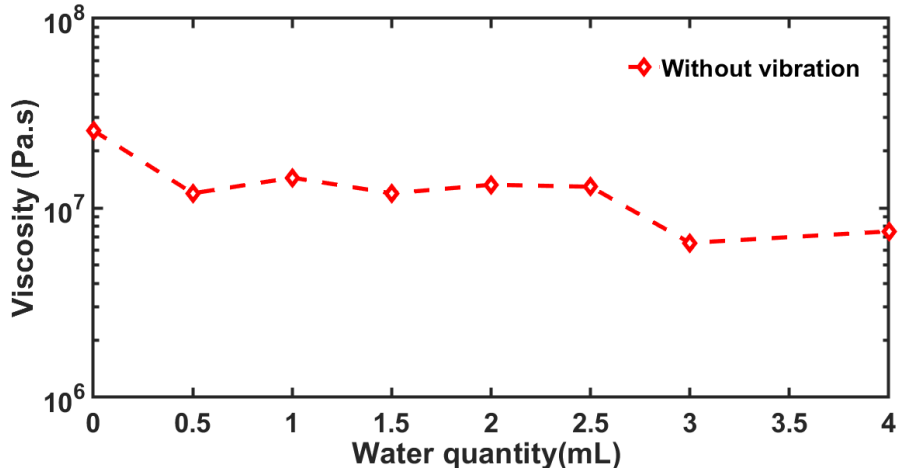

Figure 5.18 Evolution of viscosity of 100 µm glass bead by addition of different quantity of water without vibration stress and with extra vortex vibration step. The curve is plotted in given shear rate at $\dot{\gamma} = 2 * 10^{-4} s^{-1}$, based on the data collected in Figure 5.16.

5.6 Conclusion of the chapter

This chapter was dedicated to study the effect of humidity and water addition on flow behavior of powders. The control glass bead with two sizes of 100 and 40 µm as well as 100 µm hydrophobic glass bead have

been utilized. The powders humidity controlled in a humid chamber between 35-90 % and their flow behaviors have been measured at low shear rate with rheometer discovery. The comparison of rheology results of control glass beads with two different size evident that particle with small diameter has higher viscosity. This is due to the more surface contact of small diameter particles. In addition, the viscosity curve showed that sensitivity of these two powder samples increases drastically after 80 % of humidity. Furthermore, the flowability of 100 µm hydrophobic formulated glass bead has been compared with control glass bead of same size. Firstly, their flow behavior has been studied without humid control with Granutool equipments at high shear stress condition. Based on the collected data, it has been evidenced that these powders have similar flow behavior before humid control. Nevertheless, the GranuCharge equipment presented more negative charge for hydrophobic glass bead but it did not make difference in flow behavior of hydrophobic glass bead in compare with control glass bead, at high shear rate condition.

Then these two powder considered under humid control with two different method. Once the cohesion measurement of powders have been measured under rotation of powder inside drum at high shear stress. Then, another measurement has been done at low shear rate by rheometer discovery subject to vibration. In both measurements, glass bead showed high sensitivity when the humidity was higher than 80 % . While, hydrophobic glass bead was not very sensitive to humidity and it kept its viscosity as before humid control. Also, it should be mentioned that in low shear rate condition, the hydrophobic glass bead showed more viscosity or in the other word more cohesion than control glass bead. This was expected at low shear rate condition due to the higher electrical charge of hydrophobic glass bead.

In the last part of study, the effect of water addition on powder flowability has been considered. In this case only 100 µm control glass bead has been implemented. The quantity of added water to the powder was 0.5-4 mL. Based on the rheological measurement performed at low shear rate, we observed that all the wet powders have higher viscosity than dry glass bead. While the powder with 4 mL of water had lower viscosity than the rest of powders with lower quantity of water. We interpreted that it can be due to the apparition of big powder clusters at the result of joining 100 µm glass beads by saturation with water.

At high shear rate, dry powder presented higher viscosity than wet powders. It may because at high shear rates, the stress is orders of magnitudes over the cohesive force between particles.

In the following Figure 5.19 summarized the main results of this chapter in a diagram.

Concluding diagram

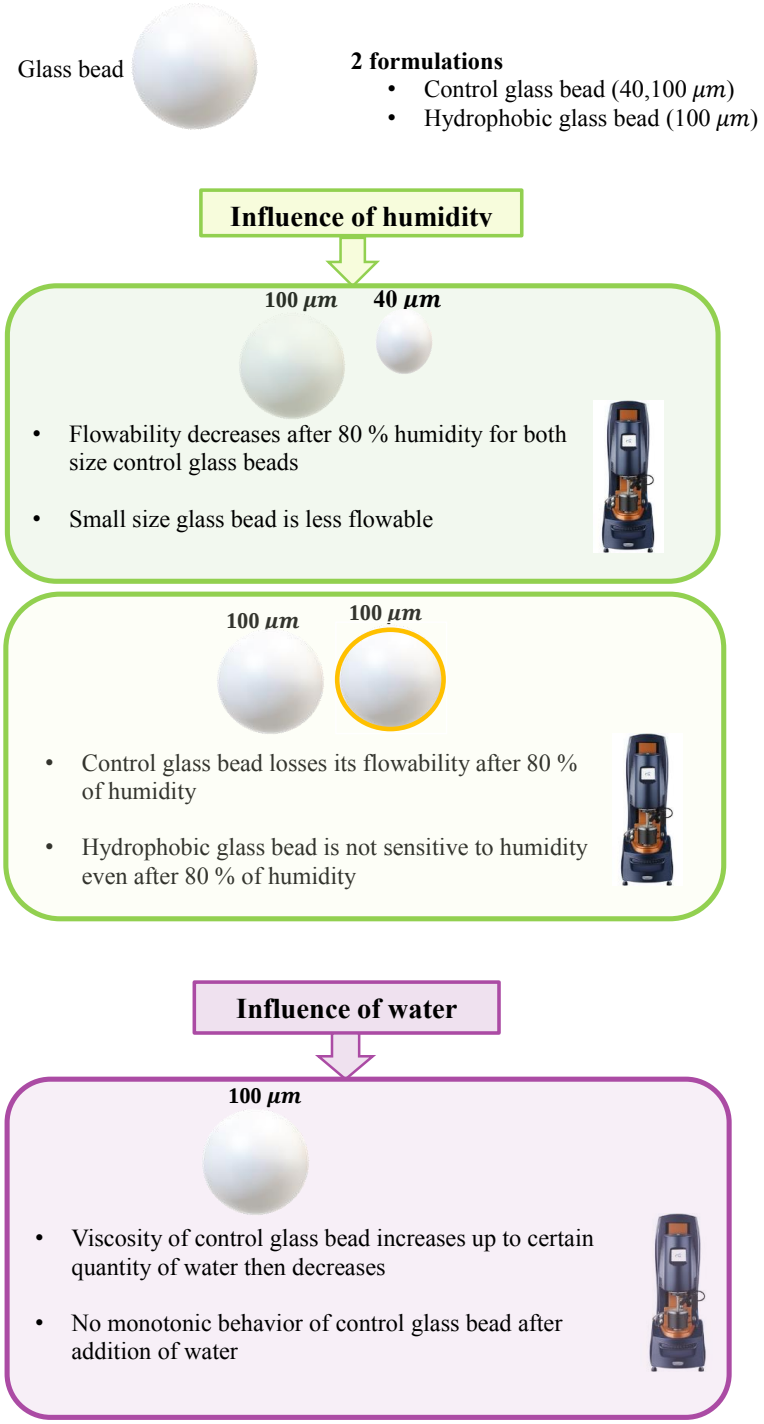

Figure 5.19 Concluding diagram.

General conclusion and perspectives

During this thesis, we have experimentally studied the flowability of powders by using several experimental equipments with different techniques. The powders omnipresence in our daily life makes their study essential to meet industrial, environmental and fundamental challenges. The objective of our study was to assess the flowability of powders by different flow measurement techniques to simulate the different processing dynamics that the powder can undergo. We were seeking the interpretation of the physical meaning of the different technique but also the meaning given by each flow values obtained by different techniques. In addition, we were interested to evaluate the influence of different formulations such as surface composition, different particle size, cohesion as well as the influence of environmental condition like as humidity on powders flow behavior. Therefore, in order to carry out our study, this work has been separated into different distinct sections as follow:

First, the bibliographic study has been carried out which allowed us to have a general view related to the powder intrinsic and extrinsic characteristics as well as the complexities that we can encounter in studying powder flow behavior. The bibliographical synthesis also clarified the necessity of having good knowledge of the physical characteristics of powders that depend on the particles which make them as well as interactions between particles. It has been also shown that the physical characteristics of powders are linked to their inter-particle forces. At the final of bibliography, the characterization and classification techniques have been presented. Based on the current knowledge that we have identified in the literature, we have used several experimental techniques allowing us to assess the information necessary for evaluating and quantification of the flowability via experimental techniques. Different factors and indexes have been assessed by the measurements like angle of repose, compressibility, rheology, shear cell, cohesion, etc. We have used control glass beads as model powder, since it does not has complex structure and was less complicated to control it under different conditions. We prepared four types of powder formulations: hydrophilic glass bead, hydrophobic glass bead, lactose coated glass bead as well as agglomerated lactose powder.

We have analyzed the influence of particle size, chemical surface treatment and core composition on powder flowability. Control glass bead was compared with surface-formulated glass beads (hydrophilic, hydrophobic, lactose-coated) as well as agglomerated lactose powders with two mean particle sizes of 100 and 500 μm. We have seen that whatever the mean particle size, the particle size distribution of

investigated powders was not modified by hydrophobic and hydrophilic surface-formulations, whereas agglomerated lactose and lactose-coated glass bead had close mean particle sizes and wider particle size distributions.

Base on FT4 flowability measurements with shear cell test and the SE values collected from stability test, the powders flowability have been classified into three groups (whatever the particle size): control, hydrophilic and hydrophobic glass beads showed higher flowability while lactose coated glass bead presented lower flow behavior than previous three formulations also agglomerated lactose powder showed lowest flow behavior. The higher cohesion and wider spans of lactose-coated glass bead and agglomerated lactose powder, as well as the more irregular shape and lower density of agglomerated lactose powder were the reason for their poorer flowability. Furthermore, based on compressibility test, the powders presented very low compressibility even at 15 kPa (inferior than 5 %), meaning that very good flow properties may be expected for investigated powders, consistently with *ff* value obtained from shear cell test showing the easy flowing properties of all powder samples. All powders were hardly fluidized, because of their high weight (resulting from their high density and/or size): 100 µm powders only reached a fluidized state.

In the next step of our study, we were interested to figure out the behavior of our five formulations under different processing dynamics. We were seeking the physical influence of different equipments on powders as well as the meaning of the different flow indexes and link between the results provided with several equipments. With this objective, we implemented Granutools equipments and Discovery-HR3 rheometer to characterize our powders under different processing conditions and the collected results have been compared with the results obtained from FT4. In the FT4, the flow was derived from shear cell, stability, compressibility and aeration tests. With Discover-HR3 rheometer, the powder flow was collected under experiencing wide range of shear rates. In addition, by Granutools equipment we assessed the flow behavior of powders by measuring the angle of repose in stationary state & under rotation, heap height, powder flow through different size of orifices and Hausner ratio.

We observed that switching from one evaluation technique to another can modify the classification of powders. Indeed, according to the different measurement techniques the powders are subject to different mechanical stress. We measured the powders flow at free flow condition with GranuFlow, confined bed condition with shear cell test and in a wide range of shear imposed condition with rheometer Discovery-HR3. Based on FT4 and GranuFlow techniques we obtained almost the same flow classification that has been presented above (three group of powder flow). However, in the flow classification obtained from Discovery-HR3 rheomter, the powders have been classified into two groups: control, hydrophilic and hydrophobic glass beads presented higher flowability, while lactose coated glass bead and agglomerated lactose powder showed lower flowability. In Discovery-HR3 rheometer, we performed the measurement in high shear rate condition, where the powder surface friction governs their flow behavior. Therefore, the powders flow classified based on their surface properties (friction). The result of electrostatic charge measurements with GranuCharge reported more negative charges to hydrophilic and hydrophobic glass

beads and almost zero charge for control glass bead, as well as positive charges for lactose coated glass bead and agglomerated lactose powder (with more positive charge for agglomerated lactose powder). In general, high electrostatic charge lowers the powder flow behavior. We were expecting to observe this effect on flowability of five formulations, while it has not been seen in the above mentioned flow measurements. Based on the cohesion measurement under motion with GranuDrum, an increase in powder cohesion has been observed under rotation. Meaning that the powders flowability decreased under motion that it can be linked to the apparition of powders electrostatic charge under motion. The cohesion ranking of five formulation under rotation in decreasing order has been reported as agglomerated lactose powder > lactose coated glass bead > hydrophobic glass bead ≈ hydrophilic glass bead ≈ control glass bead. Furthermore, based on the Haunser ratio corresponding to the GranuPack measurement we have seen that the powders with glass core have lower compressibility than agglomerated lactose powder, these results was in agreement with the compressibility measurement performed by FT4.

At the final, the influence of 50 % RH control on flow behavior of five formulations were compared with the same formulation without any humid control. The powders presented the same behavior based on the measurements performed with FT4 and rheometer Discovery-HR3. Therefore, another study has been carried out at low shear rate condition in a wide range of humidity control to figure out the influence of humid control in powder flow more precisely.

Therefore, influence of humid control 35-90 % RH on powders flow behavior has been considered. Only control and hydrophobic glass beads were utilized since hydrophilic glass bead had almost the same surface characteristic than control glass bead also controlling the humidity of lactose coated glass bead and agglomerated lactose powder was not practical because they crystallized already during formulation. The flow behavior has been studied with Discovery-HR3 rheometer subject to the vibration. Comparison of two sizes of control glass bead after humid control (40 µm and 100 µm) confirmed the sensitivity of small particles to the humidity which is due to the more surface contact consequently more cohesion of small diameter particles.

At low shear rate measurements with rheometer Discovery, the hydrophobic and control glass beads (size 100 µm) presented difference in their viscosity with higher viscosity in hydrophobic glass bead even in lower humidity value than 50 %. While these two formulations presented same flow behavior in the measurements performed without vibration. Indeed, we have seen influence of vibration in characterizing our powders, the control glass bead showed high sensitivity to the humidity after 80 % of humidity while hydrophobic glass bead kept constant tendency from the beginning of humid control up to maximum value of humidity value. In fact, at low shear rate the powders flow is mainly governed by inter-particle cohesion therefore we have observed influence of hydrophobic formulation in this shear rate range by reporting lower sensitivity to the humidity. In addition, the electrostatic charge of hydrophobic glass bead showed its influence at low shear rate, meaning that the higher value of viscosity in hydrophobic glass bead comes from its tendency to repel humidity and be recharged again. Finally, a preliminary study of influence of water addition in control glass bead showed that at high shear rate condition the

wet glass bead has lower viscosity than dry case. This is may due to the digging hole with vane inside wet powders during rotation of vane which it results in reporting lower apparent viscosity. While at low shear rate condition, the wet powder had higher cohesion. By considering that the powder with 4 mL of water had lower viscosity than the rest of wet powders both at low and high shear rate conditions, as mentioned already it may because of apparition of big clusters as a result of joining small wet particles.

In general, in this thesis we utilized three main equipments (FT4, Granutools and Discovery HR3-Rheometer) with different set of tests to characterize our five formulations. We have seen that the measurement techniques needed to be selected based on industrial use. In food since and pharmaceutical industries, FT4 rheometer is a well know and suitable for powder characterization to measure powder flowability, compressibility, fluidizability, cohesion, etc. However, powder electrostatic charge measurement can be done with GranuCharge equipment from Granutool equipment, this measurement can provide complementary information concerning powder flow after contacting with different processing equipment, as we know powder electrostatic charge appear as a result of contact with the wall of processing equipment which it decrease powder flow. Also, FT4 rheometer provides cohesion value of powder based on shear cell measurement in confined bed and we can obtain this value based on repose angle collected from GranuHeap in this case the powder cohesion is measured in stationary state with out applying any force. While, the powder cohesion can be collected under different rotating speed with GranuDrum which provides evolution of cohesion under motion with different speed which is quiet significant since the powders are mostly in motion in industrial process and their cohesion is evolving. Powder fluidizability has been collected by FT4 rheometer which it can provide useful information concerning fulidization velocity of powders in silo charge and discharge. Concerning measuring powder compressiblity, FT4 rheometer is a suitable choice, furthermore the evolution of powder packing can be measured with GranuPack. In our study, we have seen that FT4 rheometer and GranuFlow are not sensitive to measure flowability of cohesive powders. Therefore, by switching to Vibrational rheology with Discivery HR3-Rheometer the powders yield stress have been removed and their classification has been obtained based on their viscosity. We have seen the effectiveness of vibrational rheology to measure the flow behavior of cohesive powders. However, the information collected from GranuCharge was truly significant to figure out the reason for higher cohesion of formulated glass bead (hydrophobic glass bead) in compare with non-formulated glass bead. We have seen that it is not possible to conclude the flow behavior of powders based on one measurement technique and as explained previously, various tests are required based on different industrial use as well as different mechanical stress that the power can face during process.

In sum up, in order to complete this experimental study, other experimental studies could be carried out:

- It would be very relevant to continue the study of powder flowability with the polydisperse distribution of particle size. As well as the wide category of granular materials that are no longer model but industrial powders (e.g. pharmaceutical powders, milk powders, etc) with different sizes. These "real" powders exhibit properties like as different shapes, wide size distribution and the cohesion inter-particles which can influence widely their bulk behavior.
- Influence of other surface chemical compositions and addition of different types of additives in powders can be studied in order to carry out a comparative study with the results obtained in this work to tune the cohesion.
- Visualization of the dynamics of particles in 3D can permit to figure out the reorganization of powders under vibrations. In this context, X-ray tomography seems perfectly suites to analyze the evolution of the mobility of particles under vibration. Particularly, after addition of water inside powder samples it is of great interest to monitor powder behavior in 3D.
- the experimental work presented here could also be supplemented by numerical simulations.

This study is part of the European "PowderReg" project. The final objective of the project is to provide a demonstrator for the transport, storage and compaction of powders. This is why in this thesis we were interested on studying the flowability of powders under different processing dynamics.

Résumé étendu en français

La matière granulaire est l'une des plus abondantes de la planète. La mise en écoulement ou en mouvement des matériaux granulaires est observée dans de nombreux phénomènes naturels, tels que les avalanches, le déplacement des dunes de sable, les glissements de terrain, etc (Figure 5.20).

En outre, de nombreuses industries sont impliquées dans la manipulation et le traitement de ces matériaux. Par conséquent, la compréhension du comportement des matériaux granulaires est très importante pour les procédés industriels. Tout progrès dans ce domaine peut avoir de grandes conséquences économiques et écologiques pour l' industrie, notamment en réduisant la consommation énergétique et les pertes. Pour les procédés impliquant des poudres, il y a trois actions principales, le stockage, le transport et le mélange. Les conditions de stockage des poudres, en termes de température et d'humidité essentiellement, modifient leur vieillissement et donc leur fluidité lors du transport ou du mélange. La sensibilité des poudres aux conditions de stockage dépend de leur formulation.

Figure 5.20 Quelques exemples de phénomènes naturels que des matériaux granulaires sont présents (www.pinterest.fr; www.derbytelegraph.co.uk; www.pinterest.fr).

C'est pourquoi au cours de cette thèse, nous nous sommes intéressés à l'étude expérimentale de l'influence de la formulation et de l'humidité sur la fluidité des poudres. Différentes formulations ont

été testées en contrôlant la composition de la surface pour modifier sa rugosité et sa mouillabilité. Nous avons déterminé expérimentalement la fluidité des poudres en utilisant plusieurs équipements utilisant différentes techniques. Les différentes techniques ont été évaluées et les résultats obtenus avec les différentes formulations de poudre ont été confrontés.

Afin de mener à bien notre étude, ce travail a été séparé en différentes sections distinctes comme suit: Tout d'abord, l'étude bibliographique a été réalisée, ce qui nous a permis d'avoir une vue générale des caractéristiques intrinsèques et extrinsèques de la poudre ainsi que de la complexité du comportement de l'écoulement de la poudre. L'étude bibliographique a montré qu'en examinant le comportement de la poudre, de nombreux facteurs doivent être pris en compte, tels que la taille des particules, la distribution de la taille, la rugosité de surface, la porosité, les forces interparticulaires comme les forces électrostatiques et capillaires, l'influence des conditions environnementales comme l'humidité et la température, l'effet des différentes contraintes mécaniques auxquelles la poudre peut être soumise pendant le processus dans l'industrie et de nombreux autres facteurs. En outre, la synthèse bibliographique a clarifié la nécessité d'avoir une bonne connaissance des caractéristiques physiques des poudres qui dépendent des particules qui les composent ainsi que des interactions entre les particules.

En fin de bibliographie, les techniques de caractérisation et de classification ont été présentées. Sur la base des connaissances actuelles que nous avons identifiées dans la littérature, nous avons utilisé plusieurs techniques expérimentales nous permettant de mesurer la fluidité , la cohésion et la compressibilité. Pour notre étude, nous avons utilisé des billes de verre comme poudre modèle. Ce type de poudre n'a pas de structure complexe et se retrouve largement étudié dans la littérature scientifique. Nous avons préparé trois types de formulations de poudre: des billes de verre hydrophiles, des billes de verre hydrophobes et enfindes billes de verre revêtues de lactose. En outre, des poudres de lactose agglomérées ont été utilisées afin de s'apporcher des poudres utilisées dans les industries agroalimentaires et pharmaceutiques. L'objectif était de comparer le comportement de ces quatre poudres formulées avec la poudre constituée de billes de verre ne subissant aucun traitement.

Nous avons donc analysé l'influence de la taille des particules, du traitement chimique de surface et de la composition du noyau sur la fluidité de la poudre. Les billes de verre témoins ont été comparées à celles formulées en surface (hydrophiles, hydrophobes, revêtues de lactose) ainsi qu'à des poudres de lactose agglomérées avec deux tailles moyennes de particules de 100 et 500 µm. Nous avons vu que, quelle que soit la taille moyenne des particules, la distribution granulométrique des poudres étudiées n'était pas modifiée par les formulations de surface hydrophobes et hydrophiles, alors que le lactose aggloméré et les perles de verre revêtues de lactose avaient des tailles moyennes de particules similaires et des distributions granulométriques plus larges. Sur la base des mesures réalisées avec un rhéomètre à poudre FT4 utilisant la cellule de cisaillement, les valeurs de SE recueillies lors du test de

stabilitépermettent de classerles poudres en trois groupes en terme de fluidité (quelle que soit la taille des particules). Les billes de verre témoins, hydrophiles et hydrophobes ont montré une fluidité plus élevée tandis que les billes de verre revêtues de lactose ont présenté une capacité d'écoulement plus faible que les trois formulations précédentes. La poudre de lactose agglomérée a également montré une fluidité plus faible.

En outre, d'après le test de compressibilité, les poudres présentaient une très faible compressibilité même à 15 kPa (inférieure à 5 %), ce qui signifie que l'on peut s'attendre à de très bonnes propriétés d'écoulement pour les poudres étudiées, conformément à la valeur *ff* obtenue par le test de cisaillement en cellule montrant les propriétés d'écoulement facile de tous les échantillons de poudre. À la fin de cette section, afin de voir l'influence de la formulation de la surface hydrophobe, 1 ml d'eau est ajouté à 25 mg de poudres sèches. Sur la base de la valeur de cohésion rapportée par le test en cellule de cisaillement, nous avons vu que la bille de verre témoin humide a une valeur de cohésion plus élevée que la bille de verre hydrophobe humide.

En général, en comparant les échantillons humides et secs, la valeur de cohésion a augmenté considérablement pour les billesde verre témoins humides, mais pour les billes de verre hydrophobes humides, il s'agissait d'une augmentation négligeable montrant une plus faible sensibilité à l'eau. Ainsi, la poudre témoin de billes de verre a perdu sa fluidité après l'ajout contrairement à l'échantillon hydrophobe. Dans l'étape suivante de notre étude, nous avons voulu évaluer les informations obtenus par différents équipements sur l'écoulement des poudres ainsi que la signification des différents indices d'écoulement obtenus et le lien entre les résultats fournis par ces équipements.

Avec cet objectif, nous avons utilisé différents appareils de mesure Granutools, le rhéomètre Discovery-HR3 et le rhéomètre à poudresFT4 pour caractériser nos poudres. Avec le FT4, les mesures ont été obtenues à partir de tests de cisaillement, de stabilité, de compressibilité et d'aération. Avec le rhéomètre Discover-HR3, la rhéométrie de la poudre a été déterminée dans une large gamme de contraintes et de taux de cisaillement . Grâce à l'équipement de Granutools, nous avons mesuré l'angle de repos à l'état stationnaire et sous rotation, la hauteur d'un tas de poudre, le débit d'écoulement de la poudre à travers des orifices de différentes tailles et le rapport de Hausner.

Nous avons observé que le passage d'une technique d'évaluation à une autre peut modifier la classification des poudres. En effet, les différentes techniques de mesure ne déterminent pas les mêmes caractéristiques et soumettent les poudresà des contraintes mécaniques différentes dans différentes configurations. Sur la base des techniques FT4 et GranuFlow, nous avons obtenu pratiquement la même classification d'écoulement que celle présentée ci-dessus (trois groupes d'écoulement de poudre). Cependant avec le rhéomètre Discovery-HR3, les poudres ont été classées en deux groupes: les billes de

verre témoins, hydrophiles et hydrophobes, présentaient une fluidité plus élevée, tandis que les billes de verre revêtues de lactose et la poudre de lactose agglomérée présentaient une fluidité plus faible. Dans le rhéomètre Discovery-HR3, nous avons effectué la mesure dans des conditions de taux de cisaillement élevé, où la friction de la surface de la poudre régit leur comportement d'écoulement. Par conséquent, les poudres s'écoulent en fonction de leurs propriétés de surface (frottement). En outre, la poudre de lactose agglomérée présentait un comportement non monotone au début de la mesure, ce que nous ne nous attendions pas à observer. Nous soupçonnons que les poudres de lactose se brisaient pendant la rotation de la palette à l'intérieur de la cellule de mesure.

Le résultat des mesures de charges électrostatiques avec GranuCharge a fait état de plus de charges négatives pour les billes de verre hydrophiles et hydrophobes et d'une charge presque nulle pour la bille de verre de contrôle, ainsi que de charges positives pour la bille de verre revêtue de lactose et la poudre de lactose agglomérée (avec plus de charge positive pour la poudre de lactose agglomérée). Il semble que les formulations de surface hydrophiles et hydrophobes induisent une charge négative alors que la poudre de lactose enrobée était chargée positivement.

En général, une charge électrostatique élevée réduit la fluidité de la poudre. Nous nous attendions à observer cet effet sur nos poudres formulées, alors qu'il n'a pas été observé avec les équipements comme le FT4, le rhéomètre Discover et le GranuFlow. En se basant sur la mesure de la cohésion sous mouvement avec le GranuDrum, une augmentation de la cohésion de la poudre a bien été observée sous rotation.L'apparition de la charge électrostatique des poudres en mouvement explique l'augmentation de la cohésion avec la vitesse de rotation du tambour. Le classement suivant leur cohésion des cinq formulations de poudre par ordre décroissant a été obtenu comme suit: poudre de lactose agglomérée $>$ bille de verre revêtue de lactose $>$ bille de verre hydrophobe $\approx$ bille de verre hydrophile $\approx$ bille de verre de contrôle.

En outre, sur la base du rapport de Haunser obtenu avec l'équipement GranuPack, nous avons vu que les poudres à noyau de verre ont une compressibilité plus faible que la poudre de lactose agglomérée, ces résultats étaient en accord avec la mesure de compressibilité effectuée par le FT4.

Les résultats obtenus avec les cinq formulations de poudre, soumises à une humidité relative contrôlée de 50 %, a été comparée à ceux obtenus dans les conditions ambiantes de la pièce de mesure sans control. Les poudres ont présenté le même comportement d'après les mesures effectuées avec le FT4 et le rhéomètre Discovery-HR3. Sur la base des mesures de compressibilité, toutes les poudres ont montré une compressibilité similaire avant et après le contrôle de l'humidité, à l'exception de la poudre de lactose agglomérée qui a montré une compressibilité plus élevée après un contrôle de 50 % d'humidité relative.

Afin de déterminer l'influence de l'humidité relative, nous avons fait varier sa valeur de 35 à 90 %. Seules les billes de verre de contrôle et hydrophobes ont été utilisées car les billes de verre hydrophiles avaient presque les mêmes caractéristiques de surface que les billes de verre de contrôle. Les billes de verre revêtues de lactose et la poudre de lactose agglomérée n'ont pas été incluses dans l'étude car la cristallisation du lactose modifie sa sensibilité à l'humidité. La rhéométrie sous vibrations avec le rhéomètre Discovery-HR3 permet de travailler avec des contraintes de cisaillement faibles. La comparaison de deux tailles de billes de verre de contrôle après contrôle de l'humidité (40 µm et 100 µm) a confirmé que les billes de verre de contrôle de petite taille ont une fluidité plus faible que les billes de verre de contrôle de grande taille, ce qui peut être dû au fait que la surface de contact est plus importante dans les petites billes de verre.

Quelles que soient les tailles des billes de verre de contrôle, leur fluidité diminue considérablement lorsque l'humidité relative dépasse 80 %. La poudre constituée de billes de verre n'est donc pas sensible à une humidité inférieure à 80 %. Cela explique que l'absence de contrôle de l'humidité n'avait pas modifié nos résultats par rapport ceux obtenu à une humidité de 50 %. Cependant les billes de verre hydrophobes ont maintenu une viscosité apparente constante sur toute la gamme d'humidité testée. Nous avons donc observé l'influenceque la formulation hydrophobe rend la poudre insensible à l'humidité.

Lors de mesures à faible taux de cisaillement avec le rhéomètre Discovery, les perles de verre hydrophobes et de contrôle (taille 100 µm) présentaient une différence de viscosité avec une viscosité plus élevée dans la perle de verre hydrophobe même à une valeur d'humidité inférieure à 50 %. Pourtant, ces deux formulations présentaient le même comportementdans les mesures effectuées sans vibration. En fait, à faibles contraintes de cisaillement, l'écoulement des poudres est sensible par aux forces de cohésion interparticulaire. Les billes hydrophobes ont montré une charge électrostatique forte qui pourrait être à l'origine d'une cohésion plus importante et donc à une plus grande viscosité à un faible taux de cisaillement.

Enfin, une étude préliminaire de l'influence de l'ajout d'eau dans la bille de verre témoin a montré qu'à un taux de cisaillement élevé, la bille de verre humide a une viscosité plus faible que la bille sèche. Cela peut être dû au fait que la pale creuse un trou à l'intérieur des poudres humides pendant la rotation de la pale, ce qui fait que la viscosité apparente est plus faible. La poudre humide a une plus grande cohésion. En considérant que la poudre avec 4 mL d'eau avait une viscosité plus faible que le reste des poudres humides à la fois dans des conditions de taux de cisaillement faible et élevé, comme cela a déjà été mentionné, cela peut être dû à l'apparition de gros agrégats résultant de la jonction de petites particules humides. L'influence d'une quantité différente d'eau ajoutée dans le comportement d'écoulement de la bille de verre n'était pas monotone puisque dans des conditions de faible taux de cisaillement, la viscosité de la bille de verre a été augmentée jusqu'à environ 1,5 mL de teneur en eau alors qu'après, en augmentant

la quantité d'eau, la viscosité a diminué.

References

[1] Bruno Andreotti, Yoël Forterre, and Olivier Pouliquen. *Les milieux granulaires-entre fluide et solide: Entre fluide et solide*. EDP sciences, 2012.

[2] Robert Leslie Brown and John Colin Richards. *Principles of powder mechanics: essays on the packing and flow of powders and bulk solids*, volume 10. Elsevier, 2016.

[3] Jacques Duran. *Sables, poudres et grains*. Number BOOK. Eyrolles, 1997.

[4] Ronald Midgley Nedderman. *Statics and kinematics of granular materials*. Cambridge University Press, 2005.

[5] William Bailey Russel, WB Russel, Dudley A Saville, and William Raymond Schowalter. *Colloidal dispersions*. Cambridge university press, 1991.

[6] Antonio Castellanos. The relationship between attractive interparticle forces and bulk behaviour in dry and uncharged fine powders. *Advances in physics*, 54(4):263–376, 2005.

[7] CA Daerr. *Dynamique des Avalanches*. PhD thesis, Université Denis Diderot, 2000.

[8] Assia Saker. *Étude critique de quelques techniques expérimentales d'évaluation de la coulabilité des poudres*. PhD thesis, Université de Lorraine, 2018.

[9] Gérard Puente and Philippe François. *Métallurgie des poudres - Appliquée aux pièces mécaniques*. Techniques de l'ingénieur, 2011.

[10] Joël Scher. Rhéologie, texture et texturation des produits alimentaires. *Techniques de l'Ingénieur-F3300V2*, 1998.

[11] Afia Kouadri-Henni. *Contribution à l'étude des propriétés physiques des produits pulvérulents. Corrélation coulabilité-granularité. Application: produits alimentaires*. PhD thesis, Montpellier 2, 2002.

[12] Khashayar SALEH and Pierre GUIGON. Caractérisation et analyse des poudres: Propriétés physiques des solides divisés. *Techniques de l'ingénieur. Génie des procédés*, (J2251), 2009.

[13] E Teunou, JJ Fitzpatrick, and EC Synnott. Characterisation of food powder flowability. *Journal of Food Engineering*, 39(1):31–37, 1999.

[14] François Lavoie. Écoulements granulaires par avalanches: indices de fluidité, fractales et multifractales. 2005.

[15] K Ridgway, C Lazarou, and JB Scotton. The effect of granule shape on bulk density, shear properties

and tablet weight variation. *Journal of Pharmacy and Pharmacology*, 23(S1):213S–213S, 1971.

[16] Santoso Adi, Handoko Adi, Hak-Kim Chan, Zhenbo Tong, Runyu Yang, and Aibing Yu. Effects of mechanical impaction on aerosol performance of particles with different surface roughness. *Powder technology*, 236:164–170, 2013.

[17] Martin J Donovan and Hugh DC Smyth. Influence of size and surface roughness of large lactose carrier particles in dry powder inhaler formulations. *International journal of pharmaceutics*, 402(1-2):1–9, 2010.

[18] Marie-Pierre Flament, Pierre Leterme, and Anne Gayot. The influence of carrier roughness on adhesion, content uniformity and the in vitro deposition of terbutaline sulphate from dry powder inhalers. *International journal of pharmaceutics*, 275(1-2):201–209, 2004.

[19] Fridrun Podczeck. The influence of particle size distribution and surface roughness of carrier particles on the in vitro properties of dry powder inhalations. *Aerosol Science & Technology*, 31(4):301–321, 1999.

[20] Bernice Mei Jin Tan, Lai Wah Chan, and Paul Wan Sia Heng. Improving dry powder inhaler performance by surface roughening of lactose carrier particles. *Pharmaceutical research*, 33(8):1923–1935, 2016.

[21] Franca Ferrari, Daniela Cocconi, Ruggero Bettini, Ferdinando Giordano, Patrizia Santi, Michael Tobyn, Robert Price, Paul Young, Carla Caramella, and Paolo Colombo. The surface roughness of lactose particles can be modulated by wet-smoothing using a high-shear mixer. *Aaps Pharmscitech*, 5(4):69–74, 2004.

[22] Natalja Genina, Heikki Räikkönen, Henrik Ehlers, Jyrki Heinämäki, Peep Veski, and Jouko Yliruusi. Thin-coating as an alternative approach to improve flow properties of ibuprofen powder. *International journal of pharmaceutics*, 387(1-2):65–70, 2010.

[23] Limin Shi, Yushi Feng, and Changquan Calvin Sun. Origin of profound changes in powder properties during wetting and nucleation stages of high-shear wet granulation of microcrystalline cellulose. *Powder technology*, 208(3):663–668, 2011.

[24] Limin Shi and Changquan Calvin Sun. Overcoming poor tabletability of pharmaceutical crystals by surface modification. *Pharmaceutical research*, 28(12):3248–3255, 2011.

[25] Umang V Shah, Vikram Karde, Chinmay Ghoroi, and Jerry YY Heng. Influence of particle properties on powder bulk behaviour and processability. *International journal of pharmaceutics*, 518(1-2):138–154, 2017.

[26] Janne Raula, Anna Lähde, and Esko I Kauppinen. Aerosolization behavior of carrier-free l-leucine coated salbutamol sulphate powders. *International journal of pharmaceutics*, 365(1-2):18–25, 2009.

[27] Rodrigo Condotta. *Coulabilité des poudres cohésives: mesures aux faibles contraintes, granulaires humides et application à une poudre industrielle.* PhD thesis, 2005.

[28] Federica Raganati, Riccardo Chirone, and Paola Ammendola. Gas–solid fluidization of cohesive powders. *Chemical Engineering Research and Design*, 133:347–387, 2018.

[29] Frauke Fichtner, Denny Mahlin, Ken Welch, Simon Gaisford, and Göran Alderborn. Effect of surface energy on powder compactibility. *Pharmaceutical research*, 25(12):2750–2759, 2008.

[30] J Sebastian Kaerger, Stephen Edge, and Robert Price. Influence of particle size and shape on flowability and compactibility of binary mixtures of paracetamol and microcrystalline cellulose. *European journal of pharmaceutical sciences*, 22(2-3):173–179, 2004.

[31] KK Lam and JM Newton. Influence of particle size on the adhesion behaviour of powders, after application of an initial press-on force. *Powder technology*, 73(2):117–125, 1992.

[32] Fridrun Podczeck and Yasmin Mia. The influence of particle size and shape on the angle of internal friction and the flow factor of unlubricated and lubricated powders. *International Journal of Pharmaceutics*, 144(2):187–194, 1996.

[33] Norbert Rasenack and Bernd W Müller. Crystal habit and tableting behavior. *International journal of pharmaceutics*, 244(1-2):45–57, 2002.

[34] LW Wong and N Pilpel. The effect of particle shape on the mechanical properties of powders. *International journal of pharmaceutics*, 59(2):145–154, 1990.

[35] JJ Fitzpatrick, T Iqbal, C Delaney, T Twomey, and MK Keogh. Effect of powder properties and storage conditions on the flowability of milk powders with different fat contents. *Journal of food Engineering*, 64(4):435–444, 2004.

[36] Y Guo, C-Y Wu, KD Kafui, and C Thornton. 3d dem/cfd analysis of size-induced segregation during die filling. *Powder Technology*, 206(1-2):177–188, 2011.

[37] Aibing Yu. A numerical and experimental study of the angle of repose of granular particles. *Powder Technology*, 2002.

[38] William R Ketterhagen, Jennifer S Curtis, Carl R Wassgren, Angela Kong, Padma J Narayan, and Bruno C Hancock. Granular segregation in discharging cylindrical hoppers: a discrete element and experimental study. *Chemical Engineering Science*, 62(22):6423–6439, 2007.

[39] Antoine Cournoyer. Développement d'une technique optique ayant pour but l'analyse de procédés en ligne de comprimés pharmaceutiques. 2009.

[40] Henrik Ehlers, Heikki Räikkönen, Osmo Antikainen, Jyrki Heinämäki, and Jouko Yliruusi. Improving flow properties of ibuprofen by fluidized bed particle thin-coating. *International Journal of Pharmaceutics*, 368(1-2):165–170, 2009.

[41] Valérie Vanhoorne, Elisabeth Peeters, Bernd Van Snick, Jean Paul Remon, and Chris Vervaet. Crystal coating via spray drying to improve powder tabletability. *European journal of pharmaceutics and biopharmaceutics*, 88(3):939–944, 2014.

[42] Gabrielle Pilcer, Thami Sebti, and Karim Amighi. Formulation and characterization of lipid-coated tobramycin particles for dry powder inhalation. *Pharmaceutical research*, 23(5):931–940, 2006.

[43] Anna Millqvist-Fureby and Paul Smith. In-situ lecithination of dairy powders in spray-drying for confectionery applications. *Food Hydrocolloids*, 21(5-6):920–927, 2007.

[44] Michael Brech, Justin J Nijdam, David Pearce, and Payel Bagga. Improved lactose powder

properties by in-situ coating with additives during spray drying. *Journal of Medical and Bioengineering Vol*, 2(3), 2013.

[45] Laila J Jallo and Rajesh N Dave. Explaining electrostatic charging and flow of surface-modified acetaminophen powders as a function of relative humidity through surface energetics. *Journal of pharmaceutical sciences*, 104(7):2225–2232, 2015.

[46] X Pepin, SJR Simons, S Blanchon, D Rossetti, and G Couarraze. Hardness of moist agglomerates in relation to interparticle friction, granule liquid content and nature. *Powder Technology*, 117(1-2):123–138, 2001.

[47] N Fraysse, H Thomé, and L Petit. Humidity effects on the stability of a sandpile. *The European Physical Journal B-Condensed Matter and Complex Systems*, 11(4):615–619, 1999.

[48] E Teunou and JJ Fitzpatrick. Effect of relative humidity and temperature on food powder flowability. *Journal of Food Engineering*, 42(2):109–116, 1999.

[49] N Pilpe. Cool powders runfast. *New Scientist*, 29(4):313–315, 1981.

[50] JJ Fitzpatrick, M Hodnett, M Twomey, PSM Cerqueira, J O'flynn, and YH Roos. Glass transition and the flowability and caking of powders containing amorphous lactose. *Powder Technology*, 178(2):119–128, 2007.

[51] J Eilbeck, G Rowley, PA Carter, and EJ Fletcher. Effect of materials of construction of pharmaceutical processing equipment and drug delivery devices on the triboelectrification of size-fractionated lactose. *Pharmacy and pharmacology communications*, 5(7):429–433, 1999.

[52] J Eilbeck, G Rowley, PA Carter, and EJ Fletcher. Effect of contamination of pharmaceutical equipment on powder triboelectrification. *International journal of pharmaceutics*, 195(1-2):7–11, 2000.

[53] TH Ibrahim, TR Burk, FM Etzler, and RD Neuman. Direct adhesion measurements of pharmaceutical particles to gelatin capsule surfaces. *Journal of adhesion science and technology*, 14(10):1225–1242, 2000.

[54] Ahmed Raihane, Olivier Bonnefoy, J-M Chaix, J-L Gelet, and Gérard Thomas. Analysis of the densification of a vibrated sand packing. *Powder technology*, 208(2):289–295, 2011.

[55] Thomas Kollmann. *The influence of vibrations on flow prop-erties of cohesive powders*. PhD thesis, The Otto-von-Guericke-University, 2001.

[56] E Guyon. et jp troadec: Du sac de billes au tas de sables, editions odile jacob. *Sciences*, 1994.

[57] JP Seville, Ugammaur Tüzün, and Roland Clift. *Processing of particulate solids*, volume 9. Springer Science & Business Media, 2012.

[58] Jacob N Israelachvili. *Intermolecular and surface forces*. Academic press, 2011.

[59] JPK Seville, CD Willett, and PC Knight. Interparticle forces in fluidisation: a review. *Powder Technology*, 113(3):261–268, 2000.

[60] Hans-Jürgen Butt and Michael Kappl. Normal capillary forces. *Advances in colloid and interface science*, 146(1-2):48–60, 2009.

[61] William C Hinds. *Aerosol technology: properties, behavior, and measurement of airborne particles*. John Wiley & Sons, 1999.

[62] Gregory E Amidon and Michael E Houghton. The effect of moisture on the mechanical and powder flow properties of microcrystalline cellulose. *Pharmaceutical research*, 12(6):923–929, 1995.

[63] Vikram Karde and Chinmay Ghoroi. Fine powder flow under humid environmental conditions from the perspective of surface energy. *International Journal of Pharmaceutics*, 485(1-2):192–201, 2015.

[64] Matthew J Mollan and Metin Celik. The effects of humidity and storage time on the behavior of maltodextrins for direct compression. *International journal of pharmaceutics*, 114(1):23–32, 1995.

[65] Kaiming He, Xiangyu Zhang, Shaoqing Ren, and Jian Sun. Identity mappings in deep residual networks. In *European conference on computer vision*, pages 630–645. Springer, 2016.

[66] Philip Chi Lip Kwok and Hak-Kim Chan. Electrostatic charge in pharmaceutical systems. *Encyclopedia of Pharmaceutical Science and Technology (4th ed.)*, 2013.

[67] Marjorie Jacquelin. *Etude de la mise en suspension de particules par chute de poudre*. PhD thesis, Paris 12, 2007.

[68] James K Prescott and Roger A Barnum. On powder flowability. *Pharmaceutical technology*, 24(10):60–85, 2000.

[69] Austin T Sutton, Caitlin S Kriewall, Ming C Leu, and Joseph W Newkirk. Powder characterisation techniques and effects of powder characteristics on part properties in powder-bed fusion processes. *Virtual and physical prototyping*, 12(1):3–29, 2017.

[70] Matthew Krantz, Hui Zhang, and Jesse Zhu. Characterization of powder flow: Static and dynamic testing. *Powder Technology*, 194(3):239–245, 2009.

[71] Mikel Leturia, M Benali, S Lagarde, I Ronga, and K Saleh. Characterization of flow properties of cohesive powders: A comparative study of traditional and new testing methods. *Powder Technology*, 253:406–423, 2014.

[72] Geoffroy Lumay, Frédéric Boschini, Karl Traina, Sébastien Bontempi, J-C Remy, R Cloots, and N Vandewalle. Measuring the flowing properties of powders and grains. *Powder technology*, 224:19–27, 2012.

[73] RM Nedderman. Statics and kinematics of granuular materials cambridge univ. *Press, Cambridge*, 1992.

[74] R Brown. L., and richards, j. c. *Principles of Powder Mechanics*, pages 18–21, 1970.

[75] Alain de Ryck, Rodrigo Condotta, and John A Dodds. Shape of a cohesive granular heap. *Powder technology*, 157(1-3):72–78, 2005.

[76] Olivier LE BRUN, Jean-Philippe FASQUEL, Joël SCHER, and Joël HARDY. Caractérisation physicochimique et rhéologique des systèmes pulvérulents. *Industries des céréales*, (134):15–26, 2003.

[77] Wei Wang, Hongwei Yin, Dong Jia, Zhenyun Wu, Chuang Wu, and Peng Zhou. Calculating detachment depth and dip angle in sedimentary wedges using the area–depth graph. *Journal of*

Structural Geology, 107:1–11, 2018.

[78] Henry H Hausner. Friction conditions in a mass of metal powder. Technical report, Polytechnic Inst. of Brooklyn. Univ. of California, Los Angeles, 1967.

[79] K Ridgway and R Rupp. The effect of particle shape on powder properties. *Journal of Pharmacy and Pharmacology*, 21(S1):30S–39S, 1969.

[80] Sophie L Pirard, Geoffroy Lumay, Nicolas Vandewalle, and Jean-Paul Pirard. Motion of carbon nanotubes in a rotating drum: The dynamic angle of repose and a bed behavior diagram. *Chemical Engineering Journal*, 146(1):143–147, 2009.

[81] Adrian Daerr and Stéphane Douady. Two types of avalanche behaviour in granular media. *Nature*, 399(6733):241–243, 1999.

[82] Vidar Frette, Kim Christensen, Anders Malthe-Sørenssen, Jens Feder, Torstein Jøssang, and Paul Meakin. Avalanche dynamics in a pile of rice. *Nature*, 379(6560):49–52, 1996.

[83] Saurabh Rastogi and George E Klingzing. Characterizing the rheology of powders by studying dynamic avalanching of the powder. *Particle & particle systems characterization*, 11(6):453–456, 1994.

[84] Glenn A Held, DH Solina, H Solina, DT Keane, WJ Haag, PM Horn, and G Grinstein. Experimental study of critical-mass fluctuations in an evolving sandpile. *Physical Review Letters*, 65(9):1120, 1990.

[85] MA Aguirre, N Nerone, I Ippolito, A Calvo, and D Bideau. Granular packing: influence of different parameters on its stability. *Granular Matter*, 3(1-2):75–77, 2001.

[86] HM Jaeger, Chu-heng Liu, and Sidney R Nagel. Relaxation at the angle of repose. *Physical Review Letters*, 62(1):40, 1989.

[87] P Evesque, D Fargeix, P Habib, MP Luong, and P Porion. Pile density is a control parameter of sand avalanches. *Physical Review E*, 47(4):2326, 1993.

[88] Timothy M Crowder and Anthony J Hickey. The physics of powder flow: Applied to pharmaceutical solids. *Pharmaceutical technology*, 24(2):50–58, 2000.

[89] Yvonne SL Lee, Richard Poynter, Fridrun Podczeck, and J Michael Newton. Development of a dual approach to assess powder flow from avalanching behavior. *AAPS PharmSciTech*, 1(3):44–52, 2000.

[90] Michael K Taylor, Jeri Ginsburg, Anthony J Hickey, and Ferdous Gheyas. Composite method to quantify powder flow as a screening method in early tablet or capsule formulation development. *AAPS PharmSciTech*, 1(3):20–30, 2000.

[91] Heinrich M Jaeger and Sidney R Nagel. Physics of the granular state. *Science*, 255(5051):1523–1531, 1992.

[92] James C Boylan and James Swarbrick. *Encyclopedia of pharmaceutical technology*. Marcel Dekker, 2001.

[93] Ezzat Chan Abdullah and Derek Geldart. The use of bulk density measurements as flowability indicators. *Powder technology*, 102(2):151–165, 1999.

[94] Kazumi DANJO, Kazutoshi KINOSHITA, Kazutaka KITAGAWA, Kotaro IIDA, Hisakazu SUNADA, and Akinobu OTSUKA. Effect of particle shape on the compaction and flow properties of powders. *Chemical and pharmaceutical bulletin*, 37(11):3070–3073, 1989.

[95] Courtney Pitkin and JT Carstensen. Effect of particle shape on some bulk solids properties. *Drug Development and Industrial Pharmacy*, 16(1):1–12, 1990.

[96] Ralph L Carr. Evaluating flow properties of solids. *Chem. Eng.*, 18:163–168, 1965.

[97] Osborne Reynolds. Lvii. on the dilatancy of media composed of rigid particles in contact. with experimental illustrations. *The London, Edinburgh, and Dublin Philosophical Magazine and Journal of Science*, 20(127):469–481, 1885.

[98] S Chikosha, TC Shabalala, and HK Chikwanda. Effect of particle morphology and size on roll compaction of ti-based powders. *Powder technology*, 264:310–319, 2014.

[99] LA Mills and IC Sinka. Effect of particle size and density on the die fill of powders. *European Journal of Pharmaceutics and Biopharmaceutics*, 84(3):642–652, 2013.

[100] D Geldart and RR Cranfield. The gas fluidisation of large particles. *The Chemical Engineering Journal*, 3:211–231, 1972.

[101] Derek Geldart. Types of gas fluidization. *Powder technology*, 7(5):285–292, 1973.

[102] O Molerus. Interpretation of geldart's type a, b, c and d powders by taking into account interparticle cohesion forces. *Powder technology*, 33(1):81–87, 1982.

[103] GK Batchelor. A new theory of the instability of a uniform fluidized bed. *Journal of Fluid Mechanics*, 193:75–110, 1988.

[104] GK Batchelor. Secondary instability of a gas-fluidized bed. *Journal of Fluid Mechanics*, 257:359–371, 1993.

[105] Khalil Shakourzadeh. *Techniques de fluidisation*. Ed. Techniques Ingénieur, 2002.

[106] John Grace, Said SEH Elnashaie, and C Jim Lim. Hydrogen production in fluidized beds with in-situ membranes. *International Journal of Chemical Reactor Engineering*, 3(1), 2005.

[107] Mylène Lubert. *Aptitude à l'écoulement d'un milieu granulaire: exploitation des instabilités de cisaillement et évaluation du vieillissement*. PhD thesis, Atelier national de reproduction des thèses, 2008.

[108] Hamzah M Beakawi Al-Hashemi and Omar S Baghabra Al-Amoudi. A review on the angle of repose of granular materials. *Powder Technology*, 330:397–417, 2018.

[109] P Ammendola, R Chirone, and F Raganati. Fluidization of binary mixtures of nanoparticles under the effect of acoustic fields. *Advanced Powder Technology*, 22(2):174–183, 2011.

[110] Wim A Beverloo, Hendrik Antonie Leniger, and J Van de Velde. The flow of granular solids through orifices. *Chemical engineering science*, 15(3-4):260–269, 1961.

[111] CM Sinko. Granulation characterization: Methods and significance. *Drugs and the pharmaceutical sciences*, 81:419–470, 1997.

[112] Andrew W Jenike. Storage and flow of solids. *Bulletin No. 123, Utah State University*, 1964.

[113] Giovanna Bruni, Diego Barletta, Massimo Poletto, and Paola Lettieri. A rheological model for the flowability of aerated fine powders. *Chemical Engineering Science*, 62(1-2):397–407, 2007.

[114] Marco Lupo, Denis Schütz, Elke Riedl, Diego Barletta, and Massimo Poletto. Assessment of a powder rheometer equipped with a cylindrical impeller for the measurement of powder flow properties at low consolidation. *Powder Technology*, 357:281–290, 2019.

[115] Naïma Gaudel. *Rhéologie et contrôle des écoulements de dispersions granulaires par l'application de vibrations*. PhD thesis, Université de Lorraine, 2018.

[116] Lionel Choplin, Philippe Marchal, and Nadia Smirani. "system and method for rheological characterization of granular materials". *US Patent*, (6,971,262), Dec. 6 2005.

[117] Philippe Marchal. Viscoélasticité des milieux granulaires denses. 2013.

[118] Naïma Gaudel, Sébastien Kiesgen de Richter, Nicolas Louvet, Mathieu Jenny, and Salaheddine Skali-Lami. Bulk and local rheology in a dense and vibrated granular suspension. *Physical Review E*, 96(6):062905, 2017.

[119] Naïma Gaudel, Sébastien Kiesgen de Richter, Nicolas Louvet, Mathieu Jenny, and Salaheddine Skali-Lami. Granular avalanches down inclined and vibrated planes. *Physical Review E*, 94(3):032904, 2016.

[120] Caroline Hanotin. *Rhéophysique des suspensions granulaires vibrées*. PhD thesis, Université de Lorraine, 2014.

[121] R Freeman and Xiaowei Fu. Characterisation of powder bulk, dynamic flow and shear properties in relation to die filling. *Powder Metallurgy*, 51(3):196–201, 2008.

[122] Reg Freeman. Measuring the flow properties of consolidated, conditioned and aerated powders—a comparative study using a powder rheometer and a rotational shear cell. *Powder Technology*, 174(1-2):25–33, 2007.

[123] RE Freeman, JR Cooke, and LCR Schneider. Measuring shear properties and normal stresses generated within a rotational shear cell for consolidated and non-consolidated powders. *Powder Technology*, 190(1-2):65–69, 2009.

[124] Søren Søgaard, Mette Bryder, Morten Allesø, and Jukka Rantanen. Characterization of powder properties using a powder rheometer. In *Proceedings of Electronic Conference on Pharmaceutical Sciences*, volume 2, 2012.

[125] Faiz Mahdi, Ali Hassanpour, and Frans Muller. An investigation on the evolution of granule formation by in-process sampling of a high shear granulator. *Chemical Engineering Research and Design*, 129:403–411, 2018.

[126] Emmanuel YA Wornyoh, Venkat K Jasti, and C Fred Higgs. A review of dry particulate lubrication: Powder and granular materials. In *STLE/ASME 2006 International Joint Tribology Conference*, pages 1345–1360. American Society of Mechanical Engineers Digital Collection, 2006.

[127] Andrew W Jenike. Storage and flow of solids. bulletin no. 123 of the utah engineering experiment station; vol. 53, no. 26, november 1964. Technical report, Utah Univ., Salt Lake City (United

States), 1976.

[128] Paul C Johnson and Roy Jackson. Frictional–collisional constitutive relations for granular materials, with application to plane shearing. *Journal of fluid Mechanics*, 176:67–93, 1987.

[129] Albert W Alexander, Bodhisattwa Chaudhuri, AbdulMobeen Faqih, Fernando J Muzzio, Clive Davies, and M Silvina Tomassone. Avalanching flow of cohesive powders. *Powder Technology*, 164(1):13–21, 2006.

[130] Charles S Campbell. Granular shear flows at the elastic limit. *Journal of fluid mechanics*, 465:261–291, 2002.

[131] Jun Yang, Ales Sliva, Amit Banerjee, Rajesh N Dave, and Robert Pfeffer. Dry particle coating for improving the flowability of cohesive powders. *Powder technology*, 158(1-3):21–33, 2005.

[132] Adam M Stoklosa, Rebecca A Lipasek, Lynne S Taylor, and Lisa J Mauer. Effects of storage conditions, formulation, and particle size on moisture sorption and flowability of powders: A study of deliquescent ingredient blends. *Food research international*, 49(2):783–791, 2012.

[133] Yrjö H Roos. Importance of glass transition and water activity to spray drying and stability of dairy powders. *Le Lait*, 82(4):475–484, 2002.

[134] EH Gnagne, J Petit, C Gaiani, J Scher, and GN Amani. Characterisation of flow properties of foutou and foufou flours, staple foods in west africa, using the ft4 powder rheometer. *Journal of Food Measurement and Characterization*, 11(3):1128–1136, 2017.

[135] Z Kutelova, H Mainka, K Mader-Arndt, W Hintz, and J Tomas. Functionalization and surface modification of spherical glass beads. *Paper presented at the 7th International Conference for Conveying and Handling of Particulate Solids, Friedrichshafen, Germany*, 2011.

[136] Dieter Ameye, Eseldin Keleb, Chris Vervaet, Jean Paul Remon, Erwin Adams, and Desire L Massart. Scaling-up of a lactose wet granulation process in mi-pro high shear mixers. *European journal of pharmaceutical sciences*, 17(4-5):247–251, 2002.

[137] Xiaowei Fu, Deborah Huck, Lisa Makein, Brian Armstrong, Ulf Willen, and Tim Freeman. Effect of particle shape and size on flow properties of lactose powders. *Particuology*, 10(2):203–208, 2012.

[138] E Rondet, Thierry Ruiz, and Bernard Cuq. Rheological and mechanical characterization of wet agglomerates processed in low shear mixer. *Journal of food engineering*, 117(1):67–73, 2013.

[139] Ali Nokhodchi, Maryam Maghsoodi, Davood Hassan-Zadeh, and Mohammad Barzegar-Jalali. Preparation of agglomerated crystals for improving flowability and compactibility of poorly flowable and compactible drugs and excipients. *Powder technology*, 175(2):73–81, 2007.

[140] Dejan Lamešić, Odon Planinšek, Zoran Lavrič, and Ilija Ilić. Spherical agglomerates of lactose with enhanced mechanical properties. *International journal of pharmaceutics*, 516(1-2):247–257, 2017.

[141] SI Bulychev, VP Alekhin, M Kh Shorshorov, AP Ternovskij, and GD Shnyrev. Determination of young modulus by the hardness indentation diagram. *Zavodskaya Laboratoriya*, 41(9):1137–1140, 1975.

[142] JL Loubet, JM Georges, O Marchesini, and G Meille. Vickers indentation curves of magnesium

oxide (mgo). 1984.

[143] DMAHM Newey, MA Wilkins, and HM Pollock. An ultra-low-load penetration hardness tester. *Journal of Physics E: Scientific Instruments*, 15(1):119, 1982.

[144] B Poon, D Rittel, and G Ravichandran. An analysis of nanoindentation in linearly elastic solids. *International Journal of Solids and Structures*, 45(24):6018–6033, 2008.

[145] Atul Tiwari. Nanomechanical analysis of hybrid silicones and hybrid epoxy coatings—a brief review. 2011.

[146] Rafiqul A Tarefder and Hasan Faisal. Effects of dwell time and loading rate on the nanoindentation behavior of asphaltic materials. *Journal of Nanomechanics and Micromechanics*, 3(2):17–23, 2013.

[147] Sergiy Antonyuk, Stefan Heinrich, Jürgen Tomas, Niels G Deen, Maureen S van Buijtenen, and JAM Kuipers. Energy absorption during compression and impact of dry elastic-plastic spherical granules. *Granular Matter*, 12(1):15–47, 2010.

[148] Katja Mader-Arndt, Sergej Aman, Regina Fuchs, and Jürgen Tomas. Contact properties determination of macroscopic fine disperse glass particles via compression tests in normal direction. *Advanced Powder Technology*, 28(1):101–114, 2017.

[149] R Fuchs, J Meyer, T Staedler, and X Jiang. Sliding and rolling of individual micrometre sized glass particles on rough silicon surfaces. *Tribology-Materials, Surfaces & Interfaces*, 7(2):103–107, 2013.

[150] Gregory E Amidon. Physical and mechanical property characterization of powders. *DRUGS AND THE PHARMACEUTICAL SCIENCES*, 70:281–281, 1995.

[151] Everett N Hiestand. Mechanical properties of compacts and particles that control tableting success. *Journal of pharmaceutical sciences*, 86(9):985–990, 1997.

[152] Bruno C Hancock, Glenn T Carlson, Dauda D Ladipo, Beth A Langdon, and Matthew P Mullarney. The powder flow and compact mechanical properties of two recently developed matrix-forming polymers. *Journal of Pharmacy and Pharmacology*, 53(9):1193–1199, 2001.

[153] Changquan Sun and David JW Grant. Influence of crystal shape on the tableting performance of l-lysine monohydrochloride dihydrate. *Journal of pharmaceutical sciences*, 90(5):569–579, 2001.

[154] Xiaoping Cao, Mikayla Morganti, Bruno C Hancock, and Victoria M Masterson. Correlating particle hardness with powder compaction performance. *Journal of pharmaceutical sciences*, 99(10):4307–4316, 2010.

[155] Sowjanya Mannepalli and Kiran SRN Mangalampalli. Indentation plasticity and fracture studies of organic crystals. *Crystals*, 7(11):324, 2017.

[156] LJ Taylor, DG Papadopoulos, PJ Dunn, AC Bentham, JC Mitchell, and MJ Snowden. Mechanical characterisation of powders using nanoindentation. *Powder Technology*, 143:179–185, 2004.

[157] Victoria M Masterson and Xiaoping Cao. Evaluating particle hardness of pharmaceutical solids using afm nanoindentation. *International Journal of Pharmaceutics*, 362(1-2):163–171, 2008.

[158] Jennifer Burgain, Joël Scher, Jeremy Petit, Gregory Francius, and Claire Gaiani. Links between particle surface hardening and rehydration impairment during micellar casein powder storage. *Food*

Hydrocolloids, 61:277–285, 2016.

[159] Gerald Gold, Ronald N Duvall, Blaze T Palermo, and James G Slater. Powder flow studies ii: effect of glidants on flow rate and angle of repose. *Journal of pharmaceutical sciences*, 55(11):1291–1295, 1966.

[160] Adriaan B Spierings, Mark Voegtlin, T Bauer, and Konrad Wegener. Powder flowability characterisation methodology for powder-bed-based metal additive manufacturing. *Progress in Additive Manufacturing*, 1(1-2):9–20, 2016.

[161] MAS Quintanilla, JM Valverde, and A Castellanos. The transitional behaviour of avalanches in cohesive granular materials. *Journal of Statistical Mechanics: Theory and Experiment*, 2006(07):P07015, 2006.

[162] Karl Traina, Rudi Cloots, Sébastien Bontempi, Geoffroy Lumay, Nicolas Vandewalle, and Frédéric Boschini. Flow abilities of powders and granular materials evidenced from dynamical tap density measurement. *Powder technology*, 235:842–852, 2013.

[163] James B Knight, Christopher G Fandrich, Chun Ning Lau, Heinrich M Jaeger, and Sidney R Nagel. Density relaxation in a vibrated granular material. *Physical review E*, 51(5):3957, 1995.

[164] Geoffroy Lumay, Nicolas Vandewalle, C Bodson, L Delattre, and O Gerasimov. Linking compaction dynamics to the flow properties of powders. *Applied physics letters*, 89(9):093505, 2006.

[165] Janne Peltonen, Matti Murtomaa, and Jarno Salonen. Measuring electrostatic charging of powders on-line during surface adhesion. *Journal of Electrostatics*, 93:53–57, 2018.

[166] Antonella Rescaglio, Frederic De Smet, Luc Aerts, and Geoffoy Lumay. Tribo-electrification of pharmaceutical powder blends. *Particulate Science and Technology*, 37(8):1024–1031, 2019.

[167] Ganna Yablokova, Mathew Speirs, Jan Van Humbeeck, J-P Kruth, J Schrooten, Rudi Cloots, Frédéric Boschini, Geoffroy Lumay, and Jan Luyten. Rheological behavior of β-ti and niti powders produced by atomization for slm production of open porous orthopedic implants. *Powder Technology*, 283:199–209, 2015.

[168] G Lumay, S Pillitteri, M Marck, F Monsuur, T Pauly, Q Ribeyre, F Francqui, and N Vandewalle. Influence of mesoporous silica on powder flow and electrostatic properties on short and long term. *Journal of Drug Delivery Science and Technology*, 53:101192, 2019.

[169] Q Ribeyre, S Bocquet, F Francqui, and Geoffroy Lumay. Measuring the influence of talc on the properties of lactose powders. *ONdrugDelivery Magazine*, (89):74–77, 2018.

[170] Nicolas Vandewalle, Geoffroy Lumay, François Ludewig, and Jorgue Eduardo Fiscina. How relative humidity affects random packing experiments. *Physical Review E*, 85(3):031309, 2012.

[171] Frédéric Boschini, Vincent Delaval, Karl Traina, Nicolas Vandewalle, and Geoffroy Lumay. Linking flowability and granulometry of lactose powders. *International journal of pharmaceutics*, 494(1):312–320, 2015.

[172] Geoffroy Lumay and Nicolas Vandewalle. Compaction of anisotropic granular materials: experiments and simulations. *Physical Review E*, 70(5):051314, 2004.

[173] Ph Marchal, N Smirani, and L Choplin. Rheology of dense-phase vibrated powders and molecular analogies. *Journal of rheology*, 53(1):1–29, 2009.

[174] P Coussot and Ch Ancey. Rheophysical classification of concentrated suspensions and granular pastes. *Physical Review E*, 59(4):4445, 1999.

[175] Lionel CHOPLIN, Philippe MARCHAL, Christophe BARAVIAN, and Dominique LANGEVIN. Rhéologie et produits formulés complexes. 2010.

[176] Abdellatif Aït-Kadi, Philippe Marchal, Lionel Choplin, Anne-Sophie Chrissemant, and Mosto Bousmina. Quantitative analysis of mixer-type rheometers using the couette analogy. *The Canadian Journal of Chemical Engineering*, 80(6):1166–1174, 2002.

[177] Claire Gaiani, Pierre Schuck, Joël Scher, Jean-Jacques Ehrhardt, E Arab-Tehrany, M Jacquot, and Sylvie Banon. Native phosphocaseinate powder during storage: lipids released onto the surface. *Journal of Food Engineering*, 94(2):130–134, 2009.

[178] Ingrid Murrieta-Pazos, C Gaiani, Laurence Galet, Bernard Cuq, S Desobry, and J Scher. Comparative study of particle structure evolution during water sorption: Skim and whole milk powders. *Colloids and Surfaces B: Biointerfaces*, 87(1):1–10, 2011.

[179] Caroline Hanotin, S Kiesgen De Richter, Philippe Marchal, Laurent J Michot, and Christophe Baravian. Vibration-induced liquefaction of granular suspensions. *Physical Review Letters*, 108(19):198301, 2012.

[180] E Guerin, P Tchoreloff, B Leclerc, D Tanguy, M Deleuil, and G Couarraze. Rheological characterization of pharmaceutical powders using tap testing, shear cell and mercury porosimeter. *International journal of pharmaceutics*, 189(1):91–103, 1999.

[181] Jichun Xiang, Leping Liu, Xuemin Cui, Yan He, Guangjian Zheng, and Caijun Shi. Effect of fuller-fine sand on rheological, drying shrinkage, and microstructural properties of metakaolin-based geopolymer grouting materials. *Cement and Concrete Composites*, 104:103381, 2019.

[182] JA Grabowski, V-D Truong, and CR Daubert. Nutritional and rheological characterization of spray dried sweetpotato powder. *LWT-Food Science and Technology*, 41(2):206–216, 2008.

[183] Philippe Coussot. *Rheometry of pastes, suspensions, and granular materials: applications in industry and environment*. John Wiley & Sons, 2005.

[184] Christelle Salameh, Joel Scher, Jeremy Petit, Claire Gaiani, Chadi Hosri, and Sylvie Banon. Physico-chemical and rheological properties of lebanese kishk powder, a dried fermented milk-cereal mixture. *Powder Technology*, 292:307–313, 2016.

[185] *European pharmacopoeia 7.0, Powder flow Chapter **2.9.36***. 2010.

[186] Antonella Rescaglio, Julien Schockmel, Nicolas Vandewalle, and Geoffroy Lumay. Combined effect of moisture and electrostatic charges on powder flow. In *EPJ Web of Conferences*, volume 140, page 13009. EDP Sciences, 2017.

[187] Eric Mersch, Geoffroy Lumay, Frédéric Boschini, and Nicolas Vandewalle. Effect of an electric field on an intermittent granular flow. *Physical Review E*, 81(4):041309, 2010.

[188] Dan A Hays, James Mason, Peter J Mason, Robert Edward Zeman, and David Jackson. Fabrication of 3d objects via electrostatic powder deposition, April 30 2019. US Patent 10,272,618.

[189] Thomas Stichel, Tamara Brandl, Tobias Hauser, Bastian Geißler, and Stephan Roth. Electrophotographic multi-material powder deposition for additive manufacturing. *Procedia CIRP*, 74:249–253, 2018.

[190] Ali Hassanpour, Colin Hare, and Massih Pasha. *Powder Flow: Theory, Characterisation and Application*. Royal Society of Chemistry, 2019.

[191] EM Sloot and Nicolaas P Kruyt. Theoretical and experimental study of the transport of granular materials by inclined vibratory conveyors. *Powder Technology*, 87(3):203–210, 1996.

[192] G Lumay, K Traina, F Boschini, V Delaval, A Rescaglio, R Cloots, and N Vandewalle. Effect of relative air humidity on the flowability of lactose powders. *Journal of Drug Delivery Science and Technology*, 35:207–212, 2016.

[193] JE Fiscina, Geoffroy Lumay, François Ludewig, and Nicolas Vandewalle. Compaction dynamics of wet granular assemblies. *Physical review letters*, 105(4):048001, 2010.

[194] Shirin Enferad, Jérémy Petit, Claire Gaiani, Véronique Falk, Jennifer Burgain, Sébastien Kiesgen De Richter, and Mathieu Jenny. Effect of particle size and formulation on powder rheology. *Particulate Science and Technology*, pages 1–9, 2020.

[195] Nicolas Taberlet, Patrick Richard, and E John Hinch. S shape of a granular pile in a rotating drum. *Physical Review E*, 73(5):050301, 2006.

[196] Xiao Yan Liu, E Specht, and J Mellmann. Experimental study of the lower and upper angles of repose of granular materials in rotating drums. *Powder Technology*, 154(2-3):125–131, 2005.

[197] Jean Rajchenbach. Flow in powders: From discrete avalanches to continuous regime. *Physical review letters*, 65(18):2221, 1990.

[198] A Saker, M-G Cares-Pacheco, P Marchal, and V Falk. Powders flowability assessment in granular compaction: What about the consistency of hausner ratio? *Powder Technology*, 354:52–63, 2019.

Appendices

Taylor & Francis
Taylor & Francis Group

Particulate Science and Technology

An International Journal

ISSN: 0272-6351 (Print) 1548-0046 (Online) Journal homepage: https://www.tandfonline.com/loi/upst20

Effect of particle size and formulation on powder rheology

Shirin Enferad, Jérémy Petit, Claire Gaiani, Véronique Falk, Jennifer Burgain, Sébastien Kiesgen De Richter & Mathieu Jenny

To cite this article: Shirin Enferad, Jérémy Petit, Claire Gaiani, Véronique Falk, Jennifer Burgain, Sébastien Kiesgen De Richter & Mathieu Jenny (2020): Effect of particle size and formulation on powder rheology, Particulate Science and Technology, DOI: 10.1080/02726351.2020.1738605

To link to this article: https://doi.org/10.1080/02726351.2020.1738605

PARTICULATE SCIENCE AND TECHNOLOGY
https://doi.org/10.1080/02726351.2020.1738605

Taylor & Francis
Taylor & Francis Group

Effect of particle size and formulation on powder rheology

Shirin Enferad[a,b], Jérémy Petit[b], Claire Gaiani[b], Véronique Falk[c], Jennifer Burgain[b], Sébastien Kiesgen De Richter[a], and Mathieu Jenny[a]

[a]Université de Lorraine, Laboratoire d'Energetique et de Mécanique Théorique et Appliquée (LEMTA), CNRS, Vandoeuvre-lés-Nancy, France; [b]Université de Lorraine, Laboratoire d'Ingénierie des Biomolécules (LIBio), Vandoeuvre-lès-Nancy, France; [c]Université de Lorraine, Laboratoire Réactions et Génie des Procédés (LRGP), CNRS, Nancy, France

ABSTRACT

Links between flow properties and formulation of powders of 100 and 500 μm mean particle sizes were investigated. To determine the influence of surface treatment, the flow properties of glass beads were analyzed after various surface treatments leading to hydrophilic, hydrophobic, and lactose-coated surfaces. Furthermore, to investigate the influence of powder core composition, agglomerated lactose powders of circa 100 and 500 μm mean particle size were also produced by high-shear wet granulation and characterized. Hydrophilic and hydrophobic surface treatments did not alter surface topography and particle size distribution, whereas lactose-coated glass beads and agglomerated lactose powders presented noticeable changes of surface structure and particle size increase. Furthermore, all 100 μm powders were classified as easy flowing; hydrophobic glass beads and agglomerated lactose presented the highest and lowest powder flowability, respectively. For 500 μm powders, hydrophilic glass beads and agglomerated lactose powders had the highest and lowest flowability, respectively. The poorer flowability of agglomerated lactose may arise from their angular shape, their higher width of particle size distribution, the lower core density and the higher cohesion of lactose-coated particles. Last, no significant difference of powder compressibility was observed and all studied powders were hardly fluidizable, due to their high particle weight.

KEYWORDS

Mean particle size; formulation; surface composition; flow properties; glass beads; lactose

1. Introduction

Flow properties of powders are of great interest, particularly in pharmaceutics, food, cosmetics and ceramic industries. Indeed, the flow behavior of powders is crucial for product design, conveying, packing or transport. Recently, the flowability of hard granular material has been widely considered; dry particulate tribology (theory, experiments and numerical simulations) has been reviewed (Wornyoh, Jasti, and Higgs 2007). The effect of vibration on the flowability of granular materials in an idealized system has been studied by Gaudel et al. (2016): in this system, the glass beads flow down a 40-cm long and 10-cm wide plane that can be inclined up to $\theta = 35°$ and the flow is confined. It has been experimentally investigated that the flowability of spherical granular material on inclined plane is highly modified by the application of horizontal vibrations, especially in small angle declined plane where vibrations significantly improve powder flowability. Friction between particles is known to strongly influence the flowability of granular materials and dense suspensions (Jenike 1964; Johnson and Jackson 1987). Dry cohesion and consequently frictional forces can deeply affect flowability of cohesive particles, and thus, the triggering of the avalanching phenomenon which is known to have a prominent impact on granular flow behavior (Alexander et al. 2006). Also, as the Young's modulus of particles influences their collision behavior, thus an impact of particle core composition on flowability may be expected. Moreover, it is well-known that interparticle interactions are directly linked to particle surface structure and composition therefore the latter physicochemical characteristics may equally influence powder flowability (Campbell 2002).

The influence of formulation on powder flowability has often been investigated in the literature and it was evidenced that an hydrophobic particle surface enhances powder flowability (Yang et al. 2005). This is why the present study intended to investigate the influence of surface treatments (hydrophilic, hydrophobic) and lactose coating on the flowability of glass beads. The influence of core composition (related to particle Young's modulus) was also investigated by comparing flowability of lactose-coated glass beads and agglomerated lactose powders of similar particle size distribution.

Powder flowability is highly dependent on environmental conditions (i.e., temperature and relative humidity), as the macroscopic behavior of powders is determined by interparticle

CONTACT Shirin Enferad shirin.enferad@univ-lorraine.fr Université de Lorraine, Laboratoire d'Energetique et de Mécanique Théorique et Appliquée (LEMTA), CNRS, UMR 7563, Vandoeuvre-lés-Nancy, F-54500, France; Université de Lorraine, Laboratoire d'Ingénierie des Biomolécules (LIBio), 2 avenue de la Forêt de Haye, TSA 40602, 54518 Vandoeuvre-lès-Nancy, France.

Supplemental data for this article can be accessed here.

interactions. Thus, moisture content of particle surface is another factor to deal with in matter of powder flowability (Stoklosa et al. 2012). For instance, the phenomenon of interparticle liquid bridge formation due to moisture uptake from air humidity is known to decrease the flowability (Teunou and Fitzpatrick 1999). Therefore, hydrophilic and hydrophobic surface treatments as well as lactose coating are expected to interfere with moisture uptake by powders and thus modify powder flowability. Furthermore, particle size (more precisely, the surface-to-volume ratio of particles which generally decreases when increasing particle size) has a significant effect on moisture sorption and flowability of glass beads. In fact, small particles are more susceptible to moisture sorption, leading to poorer flow properties than large particles (Stoklosa et al. 2012).

The presence of lactose at particle surface may also increase powder cohesion and decrease its flowability, owing to the phenomenon of glass transition, occurring near ambient temperature for lactose powders containing 5% (*w/w*) moisture (Roos 2002). Indeed, when temperature is increased over the glass transition temperature of lactose, powders covered by amorphous lactose may become sticky, which can even result in powder caking (Alexander et al. 2006; Fitzpatrick et al. 2007).

The main objective of this article is to study the influence of particle surface composition and structure on powder flowability. With this aim, hydrophilic and hydrophobic treatments as well as lactose coating were performed on glass beads of two mean particle sizes (100 and 500 µm). Particle size distributions of samples were checked by laser granulometry. Then, powder flowability was characterized by four standard FT4 rheometer tests (stability, compressibility, aeration, and shear cell tests). FT4 powder rheometer (Freeman Technology; Freeman 2007; Freeman, Cooke, and Schneider 2009) is a universal powder rheometer which provides comprehensive series of methods that allows powder behavior to be characterized in various stress conditions. It has the capacity of providing classification of powder flowability by performing various standard tests (Freeman 2007; Freeman, Cooke, and Schneider 2009; Gnagne et al. 2017).

This experimental setup also permitted to investigate if the impact of surface treatment on powder flowability is size-dependent. To be able to uncouple the influence of particle surface and core on powder flowability, agglomerated lactose powders were produced by high-shear wet granulation and their granulometric characteristics and flow properties were compared to those of lactose-coated glass beads.

2. Materials and methods

2.1. Material: glass beads, lactose, and chemicals for surface treatment

Glass beads of types S 90–150 µm and S 400–600 µm, as well as monohydrate lactose powders of 32 µm mean size (Meggle group, Wasserburg, Germany) were used for this study. For surface treatments, sulfuric acid (H_2SO_4), 1H,1H,2H,2H-perfluorooctyltriethoxysilane (98%; Sigma-Aldrich, Germany), hydrogen peroxide (H_2O_2), and toluene (VWR International SAS, France) were employed.

2.2. Surface treatment of glass beads

Three types of glass bead surface modifications consisting of hydrophilic and hydrophobic treatments as well as lactose coating have been performed.

The hydrophilic treatment (Kutelova et al. 2011) was achieved with a 3:1 mixture of sulfuric acid and hydrogen peroxide. First, 50 g glass beads were put in a beaker and immersed in sulfuric acid then hydrogen peroxide was gently added. The mixture was kept 4 h at ambient temperature (circa 20 °C) under extractor hood. After that, glass beads were washed with distilled water and dried during 4 h at 70 °C.

For the hydrophobic treatment (Kutelova et al. 2011), the procedure of hydrophilic treatment was first followed, then hydrophilic glass beads were put in 500 mL toluene containing 2.5 g 1H,1H,2H,2H-perfluorooctyltriethoxysilane and the mixture was kept 72 h at ambient temperature under extractor hood. After that, the beads were washed twice with pure toluene, filtered with 125 mL Pro. 4 funnel and finally put 24 h at ambient temperature under extractor hood for drying purposes.

A saturated lactose solution (composed of 100 mL distilled water and 18 g lactose) was prepared for lactose coating. Lactose powder was rehydrated during about 30 min at 300 rpm with a magnetic stirrer (IKA RET basic IKAMAG, Sigma-Aldrich, Germany) at ambient temperature. Glass beads of 70 g were then put in the saturated lactose solution under stirring during 30 min. Finally, glass beads were recovered by filtering (125 mL Pro. 4 funnel), then dried in an air oven during 2 h at 70 °C.

2.3. Production of agglomerated lactose powder by high-shear wet granulation

Agglomeration of lactose powder (Ameye et al. 2002) was carried out with a 500 mL Mi-Pro granulator vacuum dryer (ProCepT, Zelate, Belgium) and operating parameters were selected with the objective of obtaining powders ranging from 100 to 500 µm mean particle sizes: 6 mL water, 50 g lactose powder, stirring at 1000 rpm, water addition at 2 mL/min during 3 min, and 2 min consolidation time at 3000 rpm chopper speed. Particles were kept in ambient conditions for 1 d for drying purposes. Obtained agglomerated lactose powder was then sieved with mesh sizes of 80 and 180 µm to obtain the 100 µm sample and with mesh sizes of 400 and 600 µm for the 500 µm sample.

2.4. Physical properties

The particle size distributions of investigated powders were determined by laser granulometry with a Mastersizer 3000 (Malvern Instruments Ltd., Worcestershire, UK) supplied with an Aero S dry dispersion unit. Dispersion conditions were as follows: 1 bar, 100% air pressure, 50% feed rate, and 4 mm hopper length. The size estimator was the equivalent diameter in volume. The median particle size (D_{50}) and the span were determined. D_{50} is defined as the diameter for

which half of the volume of particle population has a lower size. The span represents the width of the particle size distribution and was calculated with the following formula: Span $= (D_{90} - D_{10})/D_{50}$. D_{10} and D_{90} are defined as the diameters for which 10 and 90%, respectively, of the volume of particle population has a lower size.

To check the efficiency of surface treatment and lactose agglomeration protocols, particle microstructure was imaged with a scanning electron microscope (SEM; S-240 Rustat Road, Cambridge, United Kingdom) operating at 3 kV acceleration voltage. Before analysis, samples were deposited on a carbon adhesive tab (EMS® 77825-12) at ambient temperature and coated with a mixture of gold/palladium for 100 sec in a sputter coater (Polaron SC7640, Thermo VG Scientific, East Grinstead, UK). The images were obtained at two magnifications differing according to powder mean particle size: ×100 and ×600 for 100 µm powders and ×35 and ×120 for 500 µm powders.

2.5. Flow properties

Powder rheology was evaluated with a FT4 powder rheometer by performing stability, compressibility, shear cell and aeration tests using 25-mm accessories. In order to observe the influence of hydrophobic treatment on capillary interactions between powders, the shear cell and aeration tests have also been performed on control and hydrophobic glass beads in wet conditions, obtained by adding 1 mL = water to 25 mL = powder. Each test has been replicated three times at ambient temperature with air relative humidity ranging between 30 and 40%.

2.5.1. Stability test

The stability test performs a series of seven successive conditioning and test cycles (Freeman, Cooke, and Schneider 2009; Fu et al. 2012; Rondet, Ruiz, and Cuq 2013; Leturia et al. 2014). Conditioning was achieved by the gentle displacement of powder by the downward and upward moving of the rotating blade through the powder bed: it allowed erasing the previous stress history of the powder sample and removing entrapped air. Then, in each test cycle, the rotating blade moved faster through the powder bed contained in a 25 mL vessel and the total input energy required to make impeller flow in the powder bed was deduced from recorded axial force and torque. From these data, the software calculated basic flowability energy (BFE) and specific energy (SE). The BFE represents the total energy needed to displace the whole powder bed during the seventh test. The SE corresponds to the flow energy per mass of powder: it was calculated as the energy needed to displace the powder bed during the upward moving of the blade divided by the mass of analyzed powder sample.

2.5.2. Compressibility test

The compressibility test measures the evolution of powder bed density upon applied normal stress. In a single assay, the sampled powder mass is fixed, thus the evolution of density under compression can be evaluated by volume change. First, the powder was placed in the measurement vessel consisting of two overlaid glass cylinders of 25-mm diameter and 10-mL volume. Sample powder was conditioned, then vessel was split to obtain a precise volume (10 mL) of sampled powder which is compressed with a vented piston at 0.05 mm/sec from 0.50 to 15 kPa. Finally, the compressibility at x kPa was defined as the percentage change in sample volume after x kPa compression. Besides, the conditioned bulk density (CBD) was calculated as split mass of powder over split volume of powder.

2.5.3. Aeration test

The reduction of flow energy upon powder fluidization caused by air circulation through the powder bed can be measured with the aeration test. Before the aeration test begins, three conditioning cycles were performed with the powder sample placed in the measurement vessel fitted with a vented base.

Flow energy required to displace the powder bed with the blade moving at 100 mm/sec tip speed was recorded at air velocities from 0 to 50 mm/sec by 10 mm/sec steps for 100 µm powders and from 0 to 100 mm/sec by 20 mm/sec steps for 500 µm powders (maximal air velocity achievable by the FT4 apparatus is 161.2 mm/sec). Aerated energy (AE) corresponded to the flow energy at maximal investigating air velocity and aeration ratio (AR) was calculated as the ratio between BFE and AE.

Also, the minimum fluidization velocity was defined as the minimum air velocity required to fluidize the powder bed: it was determined graphically as the air velocity for which the measured flowability energy reached the AE.

2.5.4. Rotational shear cell test

By applying high shear stress with a rotational shear head, FT4 shear cell test evaluates the flowability of powders in confined environments. The shear cell itself was constituted by two overlaid glass cylinders of 10 mL volume. After conditioning, powder was preconsolidated at 9 kPa normal stress. Then, decreasing normal stresses from 7 to 3 kPa by 1 kPa steps were successively applied and the shear stresses (τ) required to make the powder flow (i.e. to induce preconsolidated powder bed failure) were recorded. Then, the software applied the yield locus approach to deduce the major principal stress (σ_1), the unconfined yield strength (σ_c) and powder cohesion (corresponding to the intercept of the yield locus, i.e. the equivalent shear stress causing powder bed failure at 0 kPa normal stress). The flowability index ff, characterizing powder flowability, was calculated with the following formula (Equation (1)):

$$ff = \sigma_1/\sigma_c \quad (1)$$

According to the Jenike classification (Jenike 1964), powders were considered as not flowing for $ff < 1$, very cohesive for $1 < ff < 2$, cohesive for $2 < ff < 4$, easy-flowing for $4 < ff < 10$ and free-flowing for $ff > 10$.

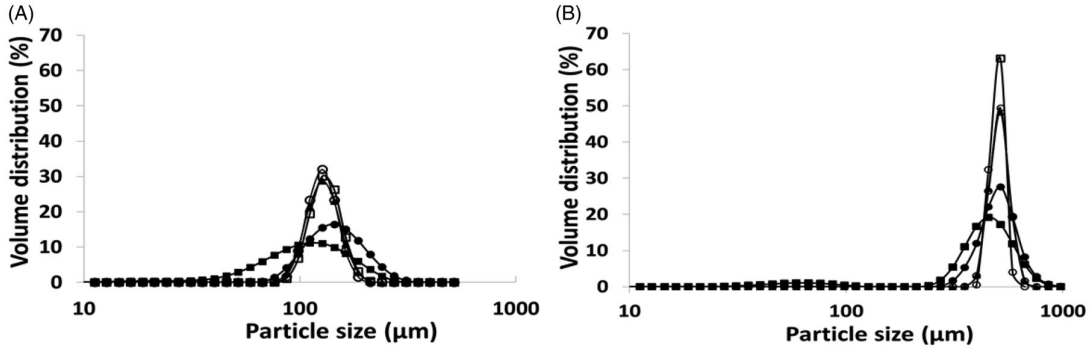

Figure 1. Particle size distributions of investigated powders with 100 (A) and 500 µm (B) mean sizes. Full triangles: control glass beads, empty circles: hydrophilic glass beads, empty squares: hydrophobic glass beads, full circles: lactose-coated glass beads, full squares: agglomerated lactose.

The shear cell test has just been carried out with 100 µm powder samples, as 500 µm powders contained too large particles to be measured with the 25-mm vessel.

2.5.5. Statistical analysis

All analyses were triplicated to ensure a good analytical repeatability and presented values correspond to means ± standard deviations. The presence of significant differences between results was checked by one-way ANOVA performed with Excel software version 2016 and means were separated by Tukey's HSD test at $p < 0.05$ significance level using the DSAASTAT add-on.

Table 1. Granulometric parameters of investigated powders.

Powders	D_{50} (µm)	Span (-)
100 µm		
Control glass beads	$136.66^{a} \pm 0.66$	$0.44^{b} \pm 0.02$
Hydrophilic glass beads	$135.00^{a} \pm 0.57$	$0.40^{ab} \pm 0.01$
Hydrophobic glass beads	$137.00^{a} \pm 1.00$	$0.41^{ab} \pm 0.01$
Lactose coated glass beads	$155.00^{a} \pm 3.05$	$0.92^{d} \pm 0.09$
Agglomerated lactose	$113.00^{a} \pm 1.00$	$1.18^{e} \pm 0.00$
500 µm		
Control glass beads	$543.00^{c} \pm 3.70$	$0.29^{ab} \pm 0.03$
Hydrophilic glass beads	$537.33^{c} \pm 1.27$	$0.23^{a} \pm 0.00$
Hydrophobic glass beads	$543.33^{c} \pm 2.67$	$0.29^{ab} \pm 0.00$
Lactose coated glass beads	$553.33^{c} \pm 29.50$	$0.45^{b} \pm 0.05$
Agglomerated lactose	$476.00^{b} \pm 4.01$	$0.73^{c} \pm 0.01$

Means with different superscripted letters in the same column were significantly different according to Tukey's HSD test ($p < 0.05$; $n = 3$).

3. Results and discussion

3.1. Physical properties

3.1.1. Granulometric characteristics

Figure 1 shows the particle size distributions of 100 (Figure 1(A)) and 500 µm (Figure 1(B)) powders. It shows that hydrophilic and hydrophobic surface treatments did not alter the particle size distributions of 100 and 500 µm powders, as granulometric characteristics of control, hydrophilic, and hydrophobic glass beads were similar (Table 1). However, agglomerated lactose powders and lactose-coated glass beads presented wider particle size distributions, which was reflected by their higher spans. Median particle size D_{50} of agglomerated lactose (113.0 ± 1.0 µm) was rather close to the target of about 136 µm (corresponding to the mean particle size of control glass beads of 100 µm) while being significantly lower, whereas lactose-coating induced a mean particle size increase up to 155.0 ± 3.0 µm owing to the addition of a lactose layer at the particle surface. It is similar for 500 µm powder samples. The refraction model used to deconvolute the light scattering in these measurements is Mie theory which assumes homogeneous materials characterized by a certain complex refractive index.

3.1.2. Particle appearance

Particle morphology and surface appearance after surface treatment were imaged by SEM (Figure 2). Whatever the mean particle size, surface structure of hydrophilic and hydrophobic glass beads was comparable to control glass beads meaning that chemical treatment did not modify surface structure, but lactose-coated glass beads were a little larger and their surface was wrinkled (similarly to agglomerated lactose).

SEM permitted to confirm the heterogeneity of particle sizes of lactose-coated and agglomerated lactose samples previously evidenced by laser granulometry. The increase in span induced by lactose-coating or wet granulation has been already reported in the literature (Nokhodchi et al. 2007; Fu et al. 2012; Lamesi et al. 2017).

3.2. Powder flow properties

3.2.1. Stability

Table 2 represents the mean flow parameters determined in stability and aeration tests for 100 and 500 µm powders. Based on BFE results, two groups of powders can be defined whatever the mean particle size: control, hydrophilic, and hydrophobic glass beads exhibited the lowest BFE, whereas lactose-coated glass beads and agglomerated lactose had the highest BFE. This denoted better flow properties of control, hydrophilic, and hydrophobic glass beads, which was logical owing to the spherical shape of these particles; indeed, lactose-coated glass beads and agglomerated lactose were composed of wrinkled spherical particles and angular particles, respectively (Fu et al. 2012). It is worth noting that BFE measures the energy required to put in motion a given volume of powder bed: it is informative of powder flowability

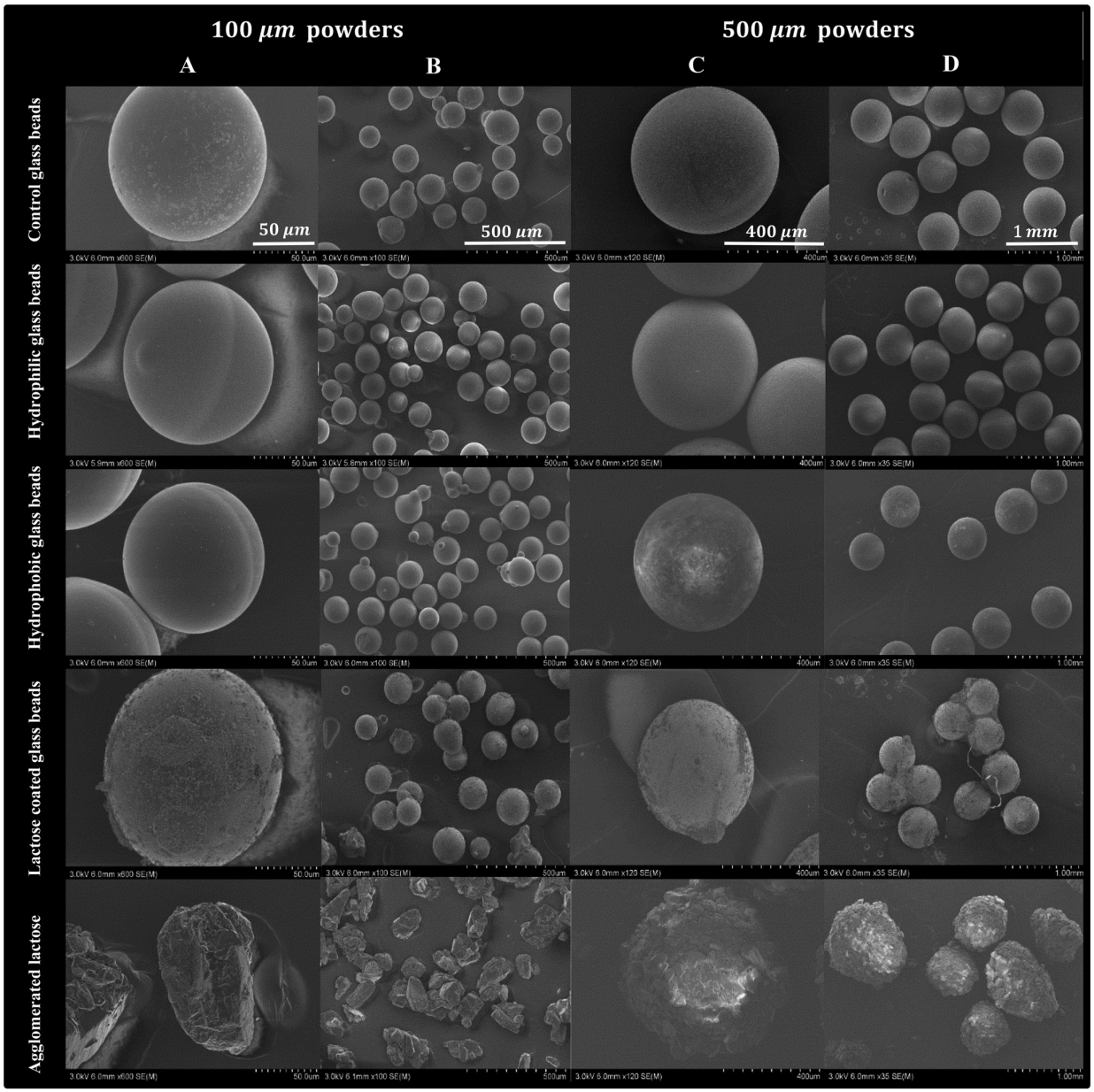

Figure 2. SEM images of investigated powders (magnification for 100 μm powders: ×100 (A) and ×600 (B); magnification for 500 μm powders: ×35 (C) and ×120 (D)).

Table 2. Stability and aeration test results of 100- and 500-μm mean size powders.

Particle size	Powders	BFE (mJ)	SE (mJ/g)	AE (mJ)	AR (−)	Minimum fluidization velocity (mm/sec)*	CBD (g/mL)
100 μm	Control glass beads	$171.52^{ab} \pm 5.63$	$1.95^{a} \pm 0.00$	$1.75^{a} \pm 0.14$	$129.92^{c} \pm 4.36$	$16.86^{a} \pm 0.02$	$1.46^{d} \pm 0.00$
	Hydrophilic glass beads	$217.76^{bc} \pm 11.22$	$1.92^{a} \pm 0.01$	$1.60^{a} \pm 0.04$	$100.25^{b} \pm 3.10$	$20.47^{ab} \pm 3.15$	$1.46^{de} \pm 0.00$
	Hydrophobic glass beads	$234.06^{bc} \pm 2.75$	$3.03^{b} \pm 0.05$	$1.45^{a} \pm 0.66$	$89.63^{b} \pm 1.35$	$17.67^{a} \pm 0.04$	$1.46^{de} \pm 0.00$
	Lactose-coated glass beads	$372.20^{d} \pm 6.88$	$3.13^{b} \pm 0.06$	$2.26^{a} \pm 0.23$	$160.63^{d} \pm 5.28$	$31.71^{b} \pm 0.82$	$1.29^{c} \pm 0.00$
	Agglomerated lactose	$295.52^{cd} \pm 14.48$	$5.05^{c} \pm 0.18$	$0.89^{a} \pm 0.00$	$248.68^{e} \pm 0.75$	$22.98^{ab} \pm 0.26$	$0.59^{a} \pm 0.00$
500 μm	Control glass beads	$158.76^{ab} \pm 5.13$	$1.82^{a} \pm 0.10$	$106.33^{b} \pm 4.55$	$1.60^{a} \pm 0.05$	n.a.	$1.49^{ef} \pm 0.00$
	Hydrophilic glass beads	$99.16^{a} \pm 2.24$	$1.25^{a} \pm 0.00$	$106.73^{b} \pm 7.26$	$1.09^{a} \pm 0.10$	n.a.	$1.50^{f} \pm 0.00$
	Hydrophobic glass beads	$191.20^{b} \pm 12.61$	$2.10^{a} \pm 0.10$	$236.33^{d} \pm 29.05$	$1.15^{a} \pm 0.03$	n.a.	$1.47^{def} \pm 0.00$
	Lactose-coated glass beads	$353.39^{d} \pm 31.43$	$3.56^{b} \pm 0.16$	$172.00^{c} \pm 7.22$	$1.23^{a} \pm 0.02$	n.a.	$1.28^{c} \pm 0.00$
	Agglomerated lactose	$351.62^{d} \pm 33.57$	$4.64^{c} \pm 0.50$	$107.00^{b} \pm 1.89$	$4.70^{b} \pm 0.41$	$125.56^{c} \pm 5.50$*	$0.67^{b} \pm 0.00$

n.a.: not applicable.
*Estimated by linear regression of corresponding curve in Figure 4(B).
Means with different superscripted letters in the same column were significantly different according to Tukey's HSD test ($p < 0.05$; $n = 3$).

in low-stress conditions, but powder density has an important impact on BFE values. SE is generally more efficient to sort powders according to their flowability, as it corresponds to flow energy per mass of powder sample and it is a good indication of powder cohesion in low-stress conditions (Fu et al. 2012). For 100 µm powders, three groups can be formed from SE results: first, control and hydrophilic glass beads had very low SE (under 2 mJ/g) indicating very good flowability, then hydrophobic and lactose-coated glass beads had low SE around 3 mJ/g showing a good flowability, last, agglomerated lactose had higher SE (about 5 mJ/g) which can be interpreted as correct powder flowability. For 500 µm powders, the same classification was obtained, except that hydrophobic glass beads had closer SE to control and hydrophilic glass beads (i.e. SE values led to the same powder classification as BFE for 500 µm powders). Then, hydrophobic surface treatment decreased flowability of 100 µm glass beads but not the one of 500 µm glass beads. This may due to the fact that the relative importance of cohesive forces was decreased when increasing the particle size.

It should also be noticed that BFE and SE of 500 µm powders were generally lower than those of 100 µm powders, which was logical as large particles have less contact points, then interparticle friction is decreased and powder flowability improved, in comparison with powder samples composed of small and/or irregular particles. The poorer flowability of lactose-coated glass beads and agglomerated lactose powder may be explained by their more irregular particle shape (Fu et al. 2012). Similar results have been reported in the literature (Freeman 2007; Freeman and Fu 2008; Lamesi et al. 2017). Also Table 2 displays the CBD values of all tested particles. All the particles with glass core logically showed higher density than agglomerated lactose. In general, a lower powder density is detrimental to powder flowability and CBD results were consistent with the lower flowability of agglomerated lactose in comparison with lactose-coated glass beads.

3.2.2. Aeration

Figure 3 shows the evolution of flow energy with air velocity: it appeared that 100 µm powders reached a fluidized state in the conditions of the aeration test, whereas 500 µm powders were not fluidized even when increasing the air velocity up to 100 mm/sec (the standard FT4 aeration test has a maximal air velocity of 10 mm/sec). This can easily be explained by the fact that 500 µm particles had a well higher weight than 100 µm particles, then making it more difficult to suspend them in the air. For 500 µm powders, only agglomerated lactose seemed significantly sensitive to aeration, as its flow energy markedly decreased with air velocity. This is in accordance with the fact that agglomerated lactose had the lowest density of studied powders. These observations were confirmed by AR and AE values reported in Table 2. 100 µm powders had well lower AE and higher AR than 500 µm powders. Generally, powders with low AR values are cohesive and/or have a high weight; consequently, they require a higher air velocity for fluidization (Fu et al. 2012; Gnagne et al. 2017). Thus, according to the classification of powders based on AR values proposed by Freeman Technology, studied 100 µm powders fall in the category of average sensitivity to aeration.

Minimal fluidization velocities obtained for 100 µm powders ranged from about 16 to 31 mm/sec, which is rather high and can be explained both by the large size of 100 µm powders and the elevated true density of particles (close to glass density, i.e. about 2.5 g/cm^3, for control, hydrophilic, hydrophobic, and lactose-coated powders and close to lactose specific density, i.e. about 1.5 g/cm^3, for agglomerated lactose), leading to high particle mass. Minimal fluidization velocity of 500 µm agglomerated lactose was estimated at circa 126.5 ± 5.5 mm/sec by linear regression of the curve presented in Figure 3(B); this value is huge which illustrates the difficulty to fluidize 500 µm particles.

Minimal fluidization velocities permitted to draw the general classification of 100 µm powders sensitivity to aeration as follow: control glass beads > hydrophobic glass beads > hydrophilic glass beads > agglomerated lactose powders > lactose-coated glass beads.

3.2.3. Compressibility

The evolution of compressibility according to applied normal stress is displayed in Figure 4 for 100 and 500 µm powders. Compressibility of 100 µm powders increased from 1−2% to 2−4%, while for 500 µm powders it evolved from

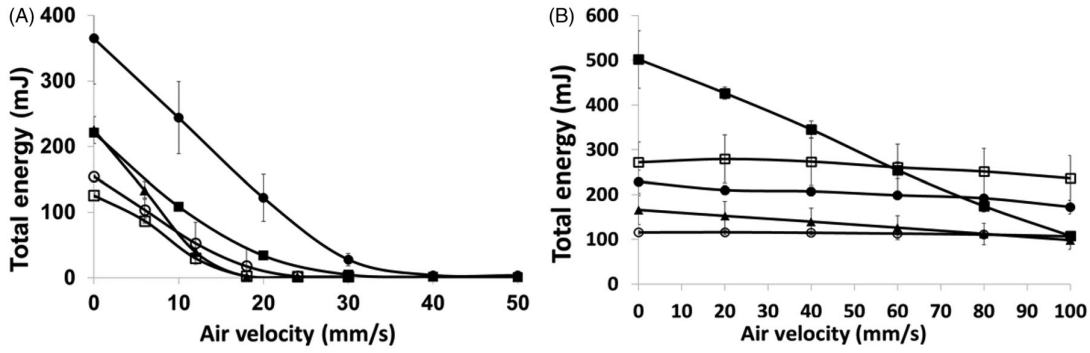

Figures 3. Evolution of flowability energy of the powder bed with air velocity during the aeration test for studied powders of 100 (A) and 500 (B) µm mean sizes. Error bars represent standard errors; some were not visible as their size was inferior to the marker size. Full triangles: control glass beads, empty circles: hydrophilic glass beads, empty squares: hydrophobic glass beads, full circles: lactose-coated glass beads, full squares: agglomerated lactose.

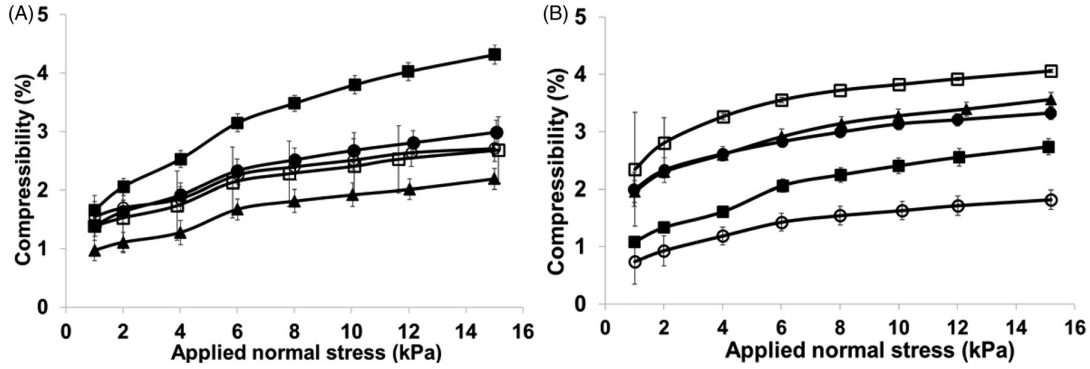

Figure 4. Evolution of powder compressibility with applied normal stress for studied powders of 100 (A) and 500 (B) µm mean sizes. Error bars represent standard errors; some were not visible as their size was inferior to the marker size. Full triangles: control glass beads, empty circles: hydrophilic glass beads, empty squares: hydrophobic glass beads, full circles: lactose-coated glass beads, full squares: agglomerated lactose.

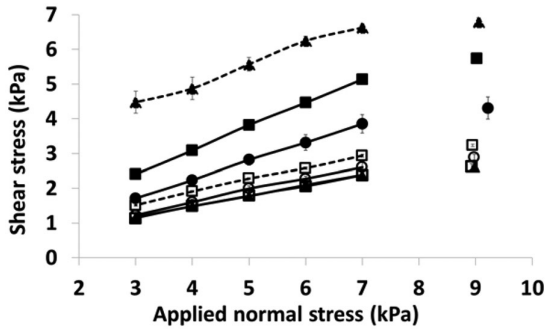

Figure 5. Evolution of shear stress with applied normal stress after preshear at 9 kPa for 100 µm powders. Error bars represent standard errors; some were not visible as their size was inferior to the marker size. Solid lines: dry powders, dashed lines: wet powders, full triangles: control glass beads, empty circles: hydrophilic glass beads, empty squares: hydrophobic glass beads, full circles: lactose-coated glass beads, full squares: agglomerated lactose.

Table 3. Flow parameters derived from shear cell test for 100 µm mean size powders.

Powders	Cohesion (kPa)	*ff* (-)
Control glass beads	$0.20^{a} \pm 0.00$	$19.70^{d} \pm 0.81$
Hydrophilic glass beads	$0.27^{ab} \pm 0.02$	$17.27^{cd} \pm 0.40$
Hydrophobic glass beads	$0.20^{a} \pm 0.01$	$19.74^{d} \pm 1.66$
Lactose-coated glass beads	$0.31^{ab} \pm 0.03$	$13.44^{bc} \pm 1.21$
Agglomerated lactose	$0.42^{b} \pm 0.06$	$10.01^{b} \pm 1.44$
Wet control glass beads	$2.05^{c} \pm 0.06$	$2.43^{a} \pm 0.07$
Wet hydrophobic glass beads	$0.30^{ab} \pm 0.00$	$14.96^{bcd} \pm 0.44$

Means with different superscripted letters in the same column were significantly different according to Tukey's HSD test ($p < 0.05$; $n = 3$).

0.5−2.5% to 1−4%, showing that the range of compressibility of investigated powders was not dependent on mean particle size.

Compressibilities at 15 kPa were very low (inferior than 5%), meaning that very good flow properties may be expected for investigated powders, consistently with BFE and SE results. Indeed, compressible powders require higher flowability energy to be put in motion; when trying to displace them, the powder bed first undergoes compaction before it could move (Ameye et al. 2002; Freeman, Cooke, and Schneider 2009).

3.2.4. Shear cell

Shear stress versus applied normal stress curves obtained during the shear cell test for 100 µm powders are presented in Figure 5 and flow characteristics (cohesion and flow factor) deduced from these curves following the yield locus approach which are listed in Table 3. A higher shear stress at a given applied normal stress denotes poorer powder flowability in high-stress conditions, as shear stress represents the force needed to induce consolidate powder bed failure, i.e. relative motion of particles within the powder bed. Following this, powder flowability in high-stress conditions increased in the following order: agglomerated lactose < lactose-coated glass beads < hydrophilic glass beads ≈ control glass beads ≈ hydrophobic glass beads. This is globally consistent with stability and compressibility results.

Flow parameters deduced from the yield locus approach for 100 µm powders confirmed these observations (Table 3). All powders exhibited low cohesion ranging from 0.20 to 0.42 kPa, in agreement with the good flowing and aeration properties previously evidenced. Cohesion of investigated powders increased in the following order: hydrophobic glass beads ≈ control glass beads ≈< hydrophilic glass beads ≈ lactose-coated glass beads < agglomerated lactose. Also, *ff* values were found over 10 for all 100 µm powders, indicating that they were "free-flowing." Such excellent flow properties were expected for powders composed of large particles. On the basis of *ff* values, powder flowability in high-stress conditions increased as follows: agglomerated lactose < lactose-coated glass beads < hydrophilic glass beads ≈< hydrophobic glass beads ≈ control glass beads. The higher density and sphericity of lactose-coated glass beads in comparison with agglomerated lactose may explain the better flowability of the former. In order to clarify the influence of hydrophobic treatment on glass beads, the shear cell test was performed on control and hydrophobic glass beads after water addition. In wet conditions, control glass beads flowability was markedly decreased, as denoted by the increase in cohesion from 0.20 to 2.05 kPa and the decrease in flow factor from 19.70 to 2.43, whereas flowability of hydrophobic glass beads remained correct (cohesion increased from 0.20 to 0.30 kPa and flow factor decreased from 17.27 to 14.96). This "protecting" effect of the hydrophobic treatment against cohesion increase in wet state was also evidenced by the strong decrease of fluidizability of control glass beads, to be compared to the small decrease of

fluidizability of hydrophobic glass beads (see Supporting Information presenting aeration test results for wet control and hydrophobic glass beads).

The shear cell test could not be carried out on 500 µm powders, because some particles of 500 µm powder samples may be too large to be correctly analyzed with the FT4 25-mm vessel. Indeed, according to Freeman Technology support, the clearance gap (distance between blade and vessel wall) for 25-mm vessel is 750 µm. Consequently, particle trapping may occur for investigated samples (especially for lactose-coated glass beads and agglomeration lactose that have maximal particle size of circa 900 µm), thus impairing result accuracy and reliability.

4. Conclusion

The objective of this study was to evaluate the influence of particle size, chemical surface treatment, and core composition on powder flowability. Therefore, control glass beads were compared with surface-treated glass beads (hydrophilic, hydrophobic, lactose-coated) and agglomerated lactose powders with mean particle sizes of 100 and 500 µm. Whatever the mean particle size, the particle size distribution of investigated powders was not modified by hydrophobic and hydrophilic surface-treatments, whereas agglomerated lactose and lactose-coated glass beads had close mean particle sizes and wider particle size distributions. These results were confirmed by SEM which showed that surface of hydrophilic, hydrophobic, and control glass beads had the same appearance. Lactose-coated glass beads were a little larger and less monodisperse and presented a more wrinkled surface, whereas agglomerated lactose particles were a little smaller and had a rather irregular and angular shape.

Furthermore, FT4 rheological tests permitted to obtain a general classification of powders according to flowability: in decreasing order, hydrophobic glass beads $\approx$ control glass beads $\approx$ hydrophilic glass beads $>$ lactose-coated glass beads $>$ agglomerated lactose. The higher cohesion and wider spans of lactose-coated glass beads and agglomerated lactose, as well as the more irregular shape and lower density of agglomerated lactose particles were likely responsible for their poorer flowability. All powders were hardly fluidized, owing to their high weight (resulting from their high density and/or size): 100 µm powders only reached a fluidized state between 16 and 31 mm/sec air velocity. For 100 µm powders, the hydrophobic treatment was rather effective in preserving the fluidisability of wet hydrophobic glass beads, whereas wet control glass beads became hardly fluidizable, as denoted by the minimum fluidization velocities of wet control and hydrophobic glass beads: 523 and 41 mm/sec, respectively.

Acknowledgments

This study was conducted in the framework of the "PowderReg" project, funded by the European program Interreg VA GR within the priority axis 4 "Strengthen the competitiveness and the attractiveness of the Grande Région / Groβregion".

ORCID

Shirin Enferad http://orcid.org/0000-0002-9925-6270
Claire Gaiani http://orcid.org/0000-0003-0434-8453
Véronique Falk http://orcid.org/0000-0001-9780-3480
Jennifer Burgain http://orcid.org/0000-0002-9573-4052
Sébastien Kiesgen De Richter http://orcid.org/0000-0002-7513-6709
Mathieu Jenny http://orcid.org/0000-0001-5932-2117

References

Alexander, A. W., B. Chaudhuri, A. Faqih, F. J. Muzzio, C. Davies, and M. S. Tomassone. 2006. Avalanching flow of cohesive powders. *Powder Technology* 164 (1):13–21. doi: 10.1016/j.powtec.2006.01.017.

Ameye, D., E. Keleb, C. Vervaet, J. F. Remon, E. Adams, and D. L. Massart. 2002. Scaling-up of a lactose wet granulation process in Mi-Pro high shear mixers. *European Journal of Pharmaceutical Sciences* 17 (4–5):247–51. doi: 10.1016/S0928-0987(02)00218-X.

Campbell, C. S. 2002. Granular shear flows at the elastic limit. *Journal of Fluid Mechanics* 465:261–91. doi: 10.1017/S002211200200109X.

Fitzpatrick, J. J., M. Hodnett, M. Twomey, P. S. M. Cerqueira, J. O'Flynn, and Y. H. Roos. 2007. Glass transition and the flowability and caking of powders containing amorphous lactose. *Powder Technology* 178 (2):119–28. doi: 10.1016/j.powtec.2007.04.017.

Freeman, R. A. 2007. Measuring the flow properties of consolidated, conditioned and aerated powders - A comparative study using a powder rheometer and a rotational shear cell. *Powder Technology* 174 (1–2):25–33. doi: 10.1016/j.powtec.2006.10.016.

Freeman, R. E., J. R. Cooke, and L. C. R. Schneider. 2009. Measuring shear properties and normal stresses generated within a rotational shear cell for consolidated and non-consolidated powders. *Powder Technology* 190 (1–2):65–9. doi: 10.1016/j.powtec.2008.04.084.

Freeman, R., and X. Fu. 2008. Characterisation of powder bulk, dynamic flow and shear properties in relation to die filling. *Powder Metallurgy* 51 (3):196–201. doi: 10.1179/174329008x324115.

Fu, X., D. Huck, L. Makein, B. Armstrong, U. Willen, and T. Freeman. 2012. Effect of particle shape and size on flow properties of lactose powders. *Particuology* 10 (2):203–8. doi: 10.1016/j.partic.2011.11.003.

Gaudel, N., S. K. de Richter, N. Louvet, M. Jenny, and S. Skali-Lami. 2016. Granular avalanches down inclined and vibrated planes. *Physical Review E* 94 (3):032904. doi: 10.1103/PhysRevE.94.032904.

Gnagne, E. H., J. Petit, C. Gaiani, J. Scher, and G. N. Amani. 2017. Characterisation of flow properties of foutou and foufou flours, staple foods in West Africa, using the FT4 powder rheometer. *Journal of Food Measurement and Characterization* 11 (3):1128–36. doi: 10.1007/s11694-017-9489-2.

Jenike, A. W. 1964. *Storage and flow of solids*, Bulletin No. 123. Salt Lake City, Utah: University of Utah. https://trove.nla.gov.au/version/21252833.

Johnson, P. C., and R. Jackson. 1987. Frictional–collisional constitutive relations for granular materials, with application to plane shearing. *Journal of Fluid Mechanics* 176 (1):67–93. doi: 10.1017/S0022112087000570.

Kutelova, Z., H. Mainka, K. Mader-Arndt, W. Hintz, and J. Tomas. 2011. Functionalization and surface modification of spherical glass beads. Paper presented at the 7th International Conference for Conveying and Handling of Particulate Solids, Friedrichshafen, Germany.

Lamesi, D., O. Planinsek, Z. Lavri, and L. Ilic. 2017. Spherical agglomerates of lactose with enhanced mechanical properties. *International Journal of Pharmaceutics* 516 (1–2):247–57. doi: 10.1016/j.ijpharm.2016.11.040.

Leturia, M., M. Benali, S. Lagarde, I. Ronga, and K. Saleh. 2014. Characterization of flow properties of cohesive powders: A comparative study of traditional and new testing methods. *Powder Technology* 253:406–23. doi: 10.1016/j.powtec.2013.11.045.

Nokhodchi, A., M. Maghsoodi, D. Hassan-Zadeh, and M. Barzegar-Jalali. 2007. Preparation of agglomerated crystals for improving flowability and compactibility of poorly flowable and compactible

drugs and excipients. *Powder Technology* 175 (2):73–81. doi: 10.1016/j.powtec.2007.01.030.

Rondet, E., T. Ruiz, and B. Cuq. 2013. Rheological and mechanical characterization of wet agglomerates processed in low shear mixer. *Journal of Food Engineering* 117 (1):67–73. doi: 10.1016/j.jfoodeng.2013.02.006.

Roos, Y. H. 2002. Importance of glass transition and water activity to spray drying and stability of dairy powders. *Le Lait* 82 (4):475–84. doi: 10.1051/lait:2002025.

Stoklosa, A. M., R. A. Lipasek, L. S. Taylor, and L. J. Mauer. 2012. Effects of storage conditions, formulation, and particle size on moisture sorption and flowability of powders: A study of deliquescent ingredient blends. *Food Research International* 49 (2):783–91. doi: 10.1016/j.foodres.2012.09.034.

Teunou, E., and J. J. Fitzpatrick. 1999. Effect of relative humidity and temperature on food powder flowability. *Journal of Food Engineering* 42 (2):109–16. doi: 10.1016/S0260-8774(99)00087-4.

Wornyoh, E. Y., V. K. Jasti, and C. F. Higgs. 2007. A review of dry particulate lubrication: Powder and granular materials. *Journal of Tribology* 129 (2):438–49. doi: 10.1115/1.2647859.

Yang, J., A. Sliva, A. Banerjee, R. N. Dave, and R. Pfeffer. 2005. Dry particle coating for improving the flowability of cohesive powders. *Powder Technology* 158 (1–3):21–33. doi: 10.1016/j.powtec.2005.04.032.

Abstract: Compacting and aging of powders: influence of the formulation

This study is conducted in the framework of the "PowderReg" project, funded by the European program Interreg VA GR within the priority axis 4 "Strengthen the competitiveness and the attractiveness of the Grande Région / Groβregion". Understanding the link between microscopic organization and powders flow behavior is a major step forward in establishing criteria for optimizing their transport, storage and processing properties. Whereby, better understating of powder flow behavior saves the industries from huge economic loss. Therefore, it is essential to evaluate their flowability. This work consists in experimentally studying the influence of powder formulation, particle size, as well as influence of environmental condition such as humidity on flow behaviors of powders.

Five types of formulations have been analyzed : control glass bead has been used as reference powder and three types of surface formulations consisting of hydrophilic, hydrophobic and lactose coating as well as agglomerated lactose powder have been prepared. First, influence of two different sizes 100 and 500 µm on flow behavior of powders has been analyzed.

Then, the powders flow behavior has been considered with different experimental equipements: FT4, Granutools and Rheometer Discover HR3. Including different techniques, such as shear cell, compressibility, rotating angle of repose, etc. The objective was to figure out the behavior of powders under different processing conditions. The, results reported that the transition from one technique to another can modify the classification of the powder flowability. Since the powders were experiencing different mechanical stresses.

At the last part of this thesis, we observed the impressive influence of humidity after 80 % on flow behavior of two different size of control glass beads (40 and 100 µm). Small diameter glass bead showed lower flowability which is due to the more surface contacts of these particles. Furthermore, the comparison of flow behavior of control and hydrophobic glass beads with 100 µm size at high shear rate reported the same flowability for both samples. While at low shear rate measurements by vibrational rheology revealed higher flowability in control glass bead. The flowability of control glass bead decreased dramatically after 80 % of humid control, however hydrophobic formulated glass bead kept its flow behavior like as before with very low sensitivity to humidity. Finally, influence of addition of small quantity of water on flow behavior of control glass bead has been investigated.

Key words: Flowability, Vibrational rheology, Glass bead, Agglomerated lactose, Surface formulation, Humid control, Different size.

Résumé: Compactage et vieillissement des poudres: influence de la formulation

Cette étude est menée dans le cadre du projet "PowderReg", financé par le programme européen Interreg VA GR dans le cadre de l'axe prioritaire 4 "Renforcer la compétitivité et l'attractivité de la Grande Région / Groβregion". La compréhension du lien entre l'organisation microscopique et le comportement de l'écoulement des poudres est une avancée majeure dans l'établissement de critères pour optimiser leurs propriétés de transport, de stockage et de traitement. Ainsi, une meilleure compréhension du comportement de l'écoulement des poudres évite aux industries d'énormes pertes économiques. Il est donc essentiel d'évaluer leur aptitude à l'écoulement. Ce travail consiste à étudier expérimentalement l'influence de la formulation des poudres, de la taille des particules, ainsi que l'influence des conditions environnementales telles que l'humidité sur les comportements d'écoulement des poudres.

Cinq types de formulations ont été analysés: la bille de verre témoin a été utilisée comme poudre de référence et trois types de formulations de surface consistant en un enrobage hydrophile, hydrophobe et de lactose ainsi qu'une poudre de lactose agglomérée ont été préparés. Tout d'abord, l'influence de deux tailles différentes, 100 et 500 µm, sur le comportement d'écoulement des poudres a été analysée.

Ensuite, le comportement de l'écoulement des poudres a été étudié avec différents équipements expérimentaux: FT4, Granutools et rhéomètre Discover HR3. Y compris différentes techniques, telles que la cellule de cisaillement, la compressibilité, l'angle de rotation du repos, etc. L'objectif était de déterminer le comportement des poudres dans différentes conditions de traitement. Les résultats ont montré que le passage d'une technique à l'autre peut modifier la classification de la fluidité des poudres. Comme les poudres subissaient des contraintes mécaniques différentes.

Dans la dernière partie de cette thèse, nous avons observé l'influence impressionnante de l'humidité après 80 % sur le comportement d'écoulement de deux tailles différentes de billes de verre de contrôle (40 et 100 µm). Les perles de verre de petit diamètre ont montré une fluidité plus faible qui est due au plus grand nombre de contacts de surface de ces particules. De plus, la comparaison du comportement d'écoulement des billes de verre de contrôle et hydrophobes de taille 100 µm à un taux de cisaillement élevé a révélé la même fluidité pour les deux échantillons. Alors qu'à faible taux de cisaillement, les mesures par rhéologie vibratoire ont révélé une fluidité plus élevée dans les billes de verre de contrôle. La fluidité de la perle de verre témoin a diminué de façon spectaculaire après 80 % de contrôle de l'humidité, mais la perle de verre hydrophobe a conservé son comportement d'écoulement comme auparavant avec une très faible sensibilité à l'humidité. Enfin, l'influence de l'ajout d'une petite quantité d'eau sur le comportement d'écoulement de la bille de verre de contrôle a été étudiée.

Mots clés: Coulabilité, Rhéologie vibratoire, billes de verre, Lactose aggloméré, Formulation de surface, Contrôle de l'humidité, Taille différente.